Technische Universität München
TUM School of Life Sciences

Pulsed and alternating flow conditions for the cleaning-in-place (CIP) of membranes

Christian Kürzl

Vollständiger Abdruck der von der TUM School of Life Sciences der Technischen Universität München zur Erlangung eines

Doktors der Ingenieurwissenschaften (Dr.-Ing.)

genehmigten Dissertation.

Vorsitz: Prof. Dr.-Ing. Petra Först

Prüfende der Dissertation:

1. Prof. Dr.-Ing. Ulrich Kulozik
2. Prof. Dr. rer. nat. Sonja Berensmeier
3. Prof. Dr.-Ing. Stefan Panglisch

Die Dissertation wurde am 19.10.2023 bei der Technischen Universität München eingereicht und durch die TUM School of Life Sciences am 18.05.2024 angenommen.

Meiner Familie

„To infinity and beyond!“

– Buzz Lightyear in Toy Story[1]

[1] Lasseter, J. (1995). *Toy Story*. Buena Vista Pictures.

Acknowledgements

This thesis resulted from my work at the Chair of Food and Bioprocess Engineering (later Professorship Food Process Engineering) of the Technical University of Munich between February 2019 and October 2023.

During this time, so many people supported me on this journey in one way or another that it is impossible to do justice to each of them. Nonetheless, there are some people whom I would like to thank in particular.

My special thanks go to Prof. Dr.-Ing. Ulrich Kulozik for encouraging and initiating this thesis and the related project. I also want to thank him for granting me maximum scientific freedom to conduct research with nearly unlimited resources, excellent facilities and a wonderful team.

I am also very grateful to all the institute members who supported my thesis with knowledge, scientific discussions, technical support, a supportive environment, and various free time activities. In particular, I want to acknowledge the workshop team consisting of Christian Ederer, Franz Fraunhofer and Erich Schneider for always having a helping hand, which, in many cases, was crucial to the success of this thesis. The analytical and technical experts, namely Claudia Hengst, Annette Brümmer-Rolf, Heidi Wohlschläger, Hermine Roßgoderer, Günther Unterbuchberger, Andreas Matyssek, Franz Kuhnert and Martin Hilz are gratefully acknowledged for their support with analytical questions and the realisation of experiments and ideas. In this regard, special thanks go to Heidi Wohlschläger for her never-ending support and expertise towards method development and troubleshooting. Sabine Becker and Frederike Schöpflin are acknowledged for their organisational support, and Sabine Grabbe for her support in all IT-related questions.

Moreover, I want to acknowledge my students, Thomas Tran, Marcel Comes, Carina Malescha, Carolin Modesto, Diana Kellhammer, Anne Wenigmann, Lina Dohm, Elen Neureiter, Ramona Kammertöns, Nora Biesenthal and Patrick Ong, for providing theoretical and practical work, fresh ideas, and a substantial contribution to this thesis.

Many thanks also go to Siegfried Tuchborn from SIMA-tec GmbH for a great collaboration and unlimited support with new ideas, troubleshooting and equipment. Prof. Dr.-Ing. Petra Först is thanked for enabling me to finish my research and thesis in her new Professorship after the retirement of Prof. Kulozik.

Furthermore, I would like to express my sincerest gratitude to the new friends and colleagues I met on the way. These are in particular: my “office mates” Martin Hartinger, Hans-Jürgen Heidebrecht and Michael Reitmaier for being wandering encyclopaedias never running out of relevant literature or bad jokes; the “Filtration boys” Martin Hartinger, Hans-Jürgen

Heidebrecht, Simon Schiffer, Roland Schopf, Andreas Matyssek and Maria Weinberger for never-ending discussions about filtration-related topics and those about the similarities between membranes and elephants, as well as countless fun activities; the “remaining ones” Isabel Kalinke and Marius Reiter for keeping our spirits up and sticking together during times of uncertain academic future. It wouldn’t have been such an unforgettable and incredible time of my life without all of you.

For saving my work-life balance with joint holiday trips, gaming nights or simple things as changing tires together, and always cheering me up during Covid19-lockdowns or other times needed, I want to thank my dear friends, especially Leonhard Mayrhofer, Tristan Rebischke, Fabian Pohlmann, Moritz Meier and Marco Weiß.

Lastly and most importantly, my greatest thanks go to my family, especially my parents Christine and Klaus Kürzl for their tireless support through every hurdle on my path, and Danielle Bräunig for always being there for me and making me laugh.

Contents

Abbreviations

Latin symbols

Latin	Unit	Description
A	m^2	Active membrane area
AB		Lewis acid-base interactions
ACN		Acetonitrile
A_{cross}	m^2	Free cross-section
AFM		Atomic force microscopy
ANOVA		One-way analysis of variance
ATD		Anti-telescoping device
BCA		Bicinchoninic acid
BSA		Bovine serum albumin
bw		Backward
CF	-	Concentration factor
CFD		Computational fluid dynamics
CF_{req}	-	Required concentration factor to process a quantification with RP-HPLC
cFRR	%	Flux recovery achieved during cleaning
$c_{i,\,p}$	g L^{-1}	Concentration of component i in the permeate
$c_{i,\,r}$	g L^{-1}	Concentration of component i in the retentate
CIP		Cleaning-in-place
$c_{min,\,RP\text{-}HPLC}$	g L^{-1}	Lowest quantifiable protein concentration of the RP-HPLC method
CN		Casein
c_{NaOH}	%	NaOH concentration during cleaning
CP		Concentration polarisation
$c_{Protein,\,applied}$	g L^{-1}	Applied protein concentration of the initial sample solution without SPE
$c_{Protein,\,applied,\,RP\text{-}HPLC}$	g L^{-1}	Protein concentration applied to RP-HPLC
$c_{Protein,\,detected}$	g L^{-1}	Detected protein concentration after SPE
$c_{Protein,\,detected,\,RP\text{-}HPLC}$	g L^{-1}	Protein concentration detected in RP-HPLC
$c_{Protein,\,initial\,sample}$	g L^{-1}	Protein concentration in the initial sample
CTM		Ceramic tubular membrane
DF	-	Dilution factor
$DF_{RP\text{-}HPLC}$	-	Dilution factor of the sample with GdnHCl buffer
d_H	m	Hydraulic diameter

d_i	m	Inner diameter of a hollow fibre
DI		Deionised
d_p	m	Particle diameter
DTT		Dithiothreitol
EL		Electrostatic interactions
$E_{norm, spec, pulsed}$	-	Specific energy consumption of pulsed flow during filtration normalised for steady flow consumption
E_{pulsed}	W	Energy consumption of pulsed flow
$E_{spec, pulsed}$	W g^{-1} m^2 h	Specific energy consumption of pulsed flow during filtration
$E_{spec, steady-avg}$	W g^{-1} m^2 h	Specific energy consumption of steady average flow during filtration
f	Hz	Frequency
F_F	N	Friction forces
F_L	N	Lift forces
FRR	%	Flux recovery ratio
FSM		Flat-sheet membrane
FTIR		Fourier-transform infrared spectroscopy
fw		Forward
F_y	N	Drag forces
GdnHCl		Guanidine hydrochloride
HFM		Hollow fibre membrane
i		Component i
IEP		Isoelectric point
IgA		Immunoglobulin A
IgG		Immunoglobulin G
IgM		Immunoglobulin M
J	L m^{-2} h^{-1}	Flux
$J_{after\ cleaning}$	L m^{-2} h^{-1}	Water flux of the membrane after experimental cleaning
$J_{cleaning}$	L m^{-2} h^{-1}	Flux achieved during cleaning
$J_{initial}$	L m^{-2} h^{-1}	Initial water flux of the clean membrane
L	m	Membrane length
LF		Lactoferrin
LW		Lifshitz-Van der Waals interactions
MF		Microfiltration
m_i	g m^{-2} h^{-1}	Mass flow of a component i
$m_{Protein, applied, SPE}$	g	Protein mass of the sample applied to the SPE cartridge

MPS	m	Maximum pore size
NaOH		Sodium hydroxide
NF		Nanofiltration
NPS	m	Nominal pore size
P&I		Piping and instrumentation
p_1	bar	Pressure at the membrane inlet
p_2	bar	Pressure at the membrane outlet
p_3	bar	Pressure at the permeate outlet
PAGE		Polyacrylamide gel electrophoresis
PES		Polyethersulfone
P_i	%	Permeation of component i
protein recovery $rate_{CF}$	%	Protein recovery rate specific for a certain CF during SPE
PVDF		Polyvinylidene fluoride
Re	-	Reynolds number
Re_{crit}	-	Critical Reynolds number
R_f	m^{-1}	Fouling resistance
$R_{f, irrev}$	m^{-1}	Irreversible Fouling resistance
$R_{f, rev}$	m^{-1}	Reversible Fouling resistance
R_m	m^{-1}	Membrane resistance
RO		Reverse osmosis
RP-HPLC		Reversed-phase high-performance liquid chromatography
SEM		Scanning electron microscopy
SPE		Solid-phase extraction
$steady_{avg}$		Steady flow with average v and Δp_{TM}
$steady_{max}$		Steady flow with maximum v and Δp_{TM}
$steady_{v\text{-}max}$		Steady flow with average Δp_{TM} and maximum v
SWM		Spiral-wound membrane
T	°C	Temperature
t	min	Time
TFA		Trifluoric acid
UF		Ultrafiltration
UTP		Uniform transmembrane pressure
UV		Ultraviolet
v	$m\ s^{-1}$	Flow velocity
v_{avg}	$m\ s^{-1}$	Average flow velocity

$V_{elution}$	mL	Concentrated sample volume obtained after SPE
$\dot{V}_{feed}$	L h^{-1}	Feed flow rate
$V_{inj, actual}$	mL	Actual injection volume for RP-HPLC
$V_{inj, cal}$	mL	Calibrated injection volume for RP-HPLC
v_{max}	m s^{-1}	Maximum flow velocity
v_{min}	m s^{-1}	Minimum flow velocity
$\dot{V}_{per}$	L h^{-1}	Permeate flow rate
V_{sample}	mL	Sample volume applied to SPE
$V_{sample, req}$	mL	Required sample volume to enable concentration and quantifaction
WP		Whey protein
xDLVO		Extended Derjaguin-Landau-Verwey-Overbeek
XPS		X-ray photoelectron spectroscopy

Greek Symbols

Greek	**Unit**	**Description**
ΔFRR	%	Improvement in FRR by pulsed or alternating flow
Δp_L	bar	Axial pressure loss over the membrane length
ΔProtein removal	%	Improvement in protein removal by pulsed or alternating flow
Δp_{TM}	bar	Transmembrane pressure
$\Delta p_{TM, after\ cleaning}$	bar	Transmembrane pressure during water flux measurement after experimental cleaning
$\Delta p_{TM, avg}$	bar	Average transmembrane pressure
$\Delta p_{TM, cleaning}$	bar	Transmembrane pressure during cleaning
$\Delta p_{TM, cycle}$	bar	Transmembrane pressure amplitude
$\Delta p_{TM, Filtration}$	bar	Transmembrane pressure during filtration
$\Delta p_{TM, initial}$	bar	Transmembrane pressure during initial water flux measurement
$\Delta p_{TM, max}$	bar	Transmembrane pressure at maximum pump capacity
$\Delta p_{TM, min}$	bar	Transmembrane pressure at minimum pump capacity
$\Delta p_{TM, inlet}$	bar	Transmembrane pressure at the membrane inlet
Δt_{max}	s	Phase duration with maximum flow velocity
Δt_{min}	s	Phase duration with minimum flow velocity
Δv	m s^{-1}	Flow velocity amplitude
α-La		α-lactalbumin
β-Lg		β-lactoglobulin

δ_{lam}	m	Height of the laminar sublayer
$\Delta\tau_w$	Pa	Shear stress amplitude
η	Pa s	Dynamic viscosity
λ	-	Friction factor
ρ	kg m^{-3}	Density
τ_{pulse}	%	Increase in wall shear stress by pulsed flow compared to steady flow
τ_W	Pa	Wall shear stress
$\tau_{W,max}$	Pa	Maximum occurring wall shear stress
$\tau_{W,min}$	Pa	Minimum occurring wall shear stress
ϕ	-	Correction factor to the Stokes drag force

Summary & Zusammenfassung

Summary

Pressure-driven filtration processes are a major operation unit in processing, e.g., liquid food, beverages, pharmaceuticals and wastewater treatment. The exemplary fractionation task assessed in this study is the separation of skim milk into casein micelles and whey proteins by microfiltration. Overall, the fundamental limitations of the filtration process are fouling, biofouling and subsequent cleaning. Fouling causes reductions in the filtration performance, i.e. a decrease in permeate flux and the permeation of solutes smaller than the membrane pore size. The temperature-dependent biofouling, relevant for longer filtration runs, causes an increase in the bacterial count and microbial activity, leading to negative consequences regarding plant hygiene, pH development and filtration performance. Hence, for typical filtration temperatures of 55 °C, the filtration time is limited to around 7 h. Furthermore, the subsequent cleaning cycle required to remove accumulated fouling is a time-, energy- and chemicals-intensive process, consisting of several chemical cleaning and rinsing steps taking up to 4 h. Hence, optimising the filtration and cleaning processes is of utmost ecological and economic interest.

One approach to process optimisation is by creating an unsteady flow. This can be either pulsed flow, defined by constantly switching between high and low flow rates and respective pressure conditions, or alternating flow, characterised by an additional change in the feed-side flow direction with each pulsed flow cycle. The resulting fluid instabilities and turbulences were beneficial to flux during the filtration of simple model systems such as yeast suspensions but not for skim milk, presumably due to the extensive cross-linking of milk proteins. Regarding cleaning, this concept has also been proven beneficial for the removal of whey proteins in complex stainless steel geometries, but no studies on membrane cleaning after skim milk MF have been conducted, where the cross-linking between milk proteins are loosened or cleaved by chemical cleaning agents such as NaOH. Since the geometry and flow characteristics between membranes and steel geometries also differ significantly, the behaviour in membranes with an additional vertical flow towards and through the wall has to be investigated separately.

Hence, this thesis aimed at systematically investigating the effects of pulsed and alternating flow on cleaning success and shed light on the underlying modes of action. The impact of varying frequency, amplitude, concentration of cleaning agent, membrane length, and module geometry on the efficiency of pulsed and alternating flow cleaning were assessed to encompass relevant influencing factors fully. Afterwards, the newly gained knowledge from cleaning experiments was conveyed to pulsed/alternating flow filtration. Finally, a concept for

plant modification was developed that allows the utilisation of pulsed flow in existing filtration plants using membrane modules of an industrial scale.

To study the effects of flow variations on cleaning efficiency not only hydrodynamically but also chemically, and due to a high ratio of plant volume to active membrane area being present in lab-scale studies, a new approach allowing the separate quantification of milk proteins at very low concentrations had to be developed. Here, a combination of pre-concentration by solid-phase extraction (SPE) and quantification by reversed-phase high-performance liquid chromatography (RP-HPLC) allowed a selective binding of milk proteins to a C18 SPE cartridge with subsequent elution from the cartridge and quantification by RP-HPLC. This novel approach enabled a high recovery rate of proteins (>94 %), a high reproducibility, and a flexible adjustment of required concentration factors (≤ 500), enabling the quantification of singular proteins with concentrations < 10 ng ml^{-1}. The method's robustness, with results not significantly affected by NaOH concentrations between 0 – 0.3 % in the cleaning sample, enabled widely varying the cleaning agent concentration. As the correlation between hydraulic and chemical cleanliness is unknown, a combination of methods should be used. Hence, the additional chemical cleaning evaluation was vital for validating the interpretation of the following cleaning results.

Regarding the main variables of unsteady flow, i.e. frequency and amplitude, both pulsed and alternating flow showed similar results during cleaning in hollow fibre modules (HFM). The highest protein removal was observed for increasing amplitudes and the highest frequency possible with the lab-scale setup (0.5 Hz) for both flow types. At the same time, the flux recovery rate (FRR) also improved with pulsed flow in HFM (+11 %). Still, the remaining FRR results for alternating flow and varying frequency and amplitude were inconclusive. The underlying reason for the discrepancy between chemical and hydraulic cleaning evaluation was presumed to be due to different levels of cleanliness on the membrane surface primarily affecting chemical cleanliness and internal fouling, e.g. pore blocking, mainly affecting flux. The critical aspect determining the efficiency of flow reversal during cleaning after filtration was found to be the change in the local ratio of $v/\Delta p_{TM,\,inlet}$ as it translates to high shear forces with a simultaneous low Δp_{TM} at the previous module inlet, where the deposition was most pronounced during filtration. Due to the length dependency, this ratio and, thus, the efficiency of flow reversal increased with membrane length causing improvements of +30 % in protein removal with alternating flow at 1.0 m membrane length. Interestingly, no differences between permanent, i.e. steady backward flow, and cyclic flow reversal, i.e. alternating flow, could be observed. Despite the significant improvement in protein removal in membranes of industrial length, no significant benefits of alternating flow over pulsed flow, with a gain of up to 32 % in protein removal in HFM, could be detected. Hence, due to the additional effort of requiring controlled valves and additional piping to enable alternating flow not providing a clear benefit

over pulsed flow, this thesis focused on pulsed flow as it can be considered the superior unsteady flow type in the given scenario.

One major factor affecting the efficiency of pulsed flow cleaning is membrane geometry. While HFM mainly consist of a free-flow section, other popular membrane geometries used in the dairy industry, such as flat sheet membranes (FSM) and spiral-wound membranes (SWM), contain spacers that secure a defined flow channel between membrane layers. These spacers promote turbulence but also the formation of flow shadows behind spacer filaments, thus limiting the filtration performance and cleanability. In FSM, pulsed flow was more beneficial than in HFM (protein removal +48 % instead of +32 %) due to pulsed flow improving access to former flow shadows, as confirmed by scanning electron microscopy (SEM) imaging. Besides a synergistic effect between pulsed flow and low NaOH concentrations (0.03 %) found, pulsed flow also improved protein removal in FSM when no NaOH was present (+36 %), which implies positive effects of pulsed flow also applying to rinsing steps. However, it is to be noted that no positive effects of pulsed flow could be observed for either membrane geometry at higher NaOH concentrations (0.30 %).

While an impaired filtration performance was reported for the fractionation of skim milk with MF due to the protein cross-linking in combination with pressure peaks causing increased deposit compaction in HFM at 10 °C (Weinberger and Kulozik 2021a), pulsed flow improved cleaning success in FSM without a cleaning agent present, and thus for an intact deposit without any loosening by NaOH. As this resembles comparable conditions as during the filtration process, this implied positive effects of pulsed flow on skim milk microfiltration (MF), contrary to the results obtained under different experimental conditions by Weinberger and Kulozik (2021a) in HFM. A further study on the MF of skim milk at 50 °C with different flow types confirmed the hypothesis that synergistic effects between alternative flow types and a filtration system containing spacers could overcome the adverse effects of pressure peaks by distinctly improving access to former flow shadows, increasing the active membrane area, more evenly distributing shear forces across the flow channel and, thus, improving filtration efficiency. Coomassie-colouring of proteins deposited in an FSM revealed pulsed and alternating flow significantly reducing deposit amounts and homogenising the overall deposition by removing deposit peaks, particularly behind spacer filaments. Regarding filtration performance, pulsed flow was superior to alternating and steady flow. With starting values of flux and permeation being higher and diminishing slower and less pronounced, this emphasises the improved deposit control. Overall, pulsed flow improved the whey protein mass flow by > 37 % over any steady flow filtration conditions.

In addition to the mechanistic findings, this thesis also proposes a novel approach to pulsation-creation on industrial-scale modules, as the previous procedure using pumps with rapid flow velocity ramps is not feasible at the industrial scale. It comprises a bypass controlled

by a pneumatic valve and manual throttle, enabling pulsed flow with a defined frequency, amplitude, and similar flow profile as in lab-scale trials but at a constant pump capacity. The positive effects of pulsed flow on filtration performance and cleaning success could be confirmed for SWM. However, improvements were less distinct than in FSM, presumably due to geometric module differences.

Besides improvements in process efficiency, the results obtained in this thesis also translate to significant improvements in the sustainability of the filtration and cleaning process. While pulsed and alternating flow require more pump energy than the average steady flow conditions, this drawback is exceeded by the improvements achieved with these alternative flow types. In particular, applying e.g. pulsed flow led to more significant gains in filtration performance and cleaning success than a more than doubled wall shear stress under steady flow conditions. Accordingly, in terms of the specific pump energy related to the amount of protein removed during cleaning and WP mass flow achieved during filtration, pulsed flow led to significant reductions in the specific pump energy consumption by > 58 % during cleaning and > 69 % during filtration in comparison to the optimum steady flow conditions. In scale-up to an industrial-scale module, the proposed bypass system for pulsation creation poses an energetic drawback for singular modules, as parts of the pump energy are returned unused to the feed tank. However, with many modules installed in most industrial applications, this bypass could instead be used to feed a second membrane filtration stage. As the proposed approach would then feed two filtration stages alternatingly with pulsed flow phases, no energy remained unused.

In conclusion, pulsed and alternating flow lead to significant improvements in filtration performance and cleaning success, particularly for membranes geometries suffering from flow shadows, whereas pulsed flow can be considered the superior flow type in the given scenario due to the lower effort required for implementation. With significant improvements during filtration, chemical cleaning, and rinsing steps, pulsed flow could improve the whole process unit of membrane filtration in terms of process efficiency and, thus, its economic and ecological sustainability.

Zusammenfassung

Druckbetriebene Filtrationsverfahren sind ein wichtiger Prozessschritt zur Verarbeitung z. B. von flüssigen Lebensmitteln, Getränken, Arzneimitteln und der Abwasseraufbereitung. Die in dieser Studie beispielhaft untersuchte Fraktionierungsaufgabe ist die Trennung von Magermilch in Kaseinmizellen und Molkenproteine mittels Mikrofiltration. Die Haupt-Limitationen des Filtrationsprozesses sind Fouling, Biofouling und die anschließende Reinigung. Fouling führt zu einer Verringerung der Filtrationsleistung, d. h. zu einer Abnahme des Permeatflusses und der Permeation von gelösten Stoffen, die kleiner als die Porengröße der Membran sind. Das temperaturabhängige Biofouling, das bei längeren Filtrationsläufen relevant wird, führt zu einem Anstieg der Keimzahl und der mikrobiellen Aktivität, was negative Folgen für die Anlagenhygiene, die pH-Entwicklung und die Filtrationsleistung hat. Bei typischen Filtrationstemperaturen von 55 °C ist die Filtrationszeit daher auf ca. 7 h begrenzt. Darüber hinaus ist der anschließende Reinigungszyklus zur Entfernung des akkumulierten Foulings zeit-, energie- und chemikalienintensiv, da er aus mehreren chemischen Reinigungs- und Spülschritten besteht, die bis zu 4 h dauern können. Die Optimierung der Filtrations- und Reinigungsprozesse ist daher von höchstem ökologischen und ökonomischen Interesse.

Ein Ansatz zur Optimierung des Filtrationsergebnisses sind instationäre Strömungen. Dabei kann es sich entweder um eine pulsierende Strömung handeln, bei der ständig zwischen hohen und niedrigen Durchflussraten und entsprechenden Druckverhältnissen gewechselt wird, oder um eine alternierende Strömung, bei der sich bei jedem Pulsations-Zyklus zusätzlich die feed-seitige Anströmrichtung ändert. Die daraus resultierenden Strömungsinstabilitäten und -turbulenzen waren bei der Filtration von einfachen Modellsystemen wie Hefesuspensionen vorteilhaft für den Flux, nicht aber bei Magermilch, vermutlich aufgrund der starken Vernetzung der Milchprotein-Deckschicht. In Bezug auf die Reinigung, so hat sich dieses Konzept auch für die Entfernung von Molkenproteinen in komplexen Edelstahlanlagen ohne permeable Wände als vorteilhaft erwiesen. Es wurden jedoch keine Studien über die Membranreinigung nach Magermilch-MF durchgeführt, bei der die Vernetzungen zwischen den Milchproteinen durch chemische Reinigungsmittel wie NaOH gelockert oder aufgespalten werden. Da sich auch die Geometrie und die Strömungseigenschaften zwischen Membranen und Edelstahlgeometrien deutlich unterscheiden, muss das Verhalten in Membranen mit einer zusätzlichen vertikalen Strömung zur und durch die Wand separat untersucht werden.

Ziel dieser Arbeit war es daher, die Auswirkungen von pulsierender und alternierender Strömung auf den Reinigungserfolg systematisch zu untersuchen und die zugrundeliegenden Wirkungsweisen aufzuklären. Um die relevanten Einflussfaktoren vollständig zu erfassen, wurden die Auswirkungen der Variation von Frequenz, Amplitude, Reinigungsmittelkonzentration, Membranlänge und Modulgeometrie auf die Effizienz der Reinigung mit pulsierender und alternierender Strömung untersucht. Anschließend wurden die

neu gewonnenen Erkenntnisse aus Reinigungsversuchen auf die Filtration übertragen. Zusätzlich wurde ein Konzept zur Anlagenmodifikation entwickelt, das die Nutzung der pulsierenden Strömung in bestehenden Filtrationsanlagen mit Membranmodulen im industriellen Maßstab ermöglicht.

Um die Auswirkungen verschiedener Strömungstypen auf die Reinigungseffizienz nicht nur hydrodynamisch, sondern auch chemisch zu untersuchen, musste aufgrund des hohen Verhältnisses von Anlagenvolumen zu aktiver Membranfläche bei Untersuchungen im Labormaßstab ein neuer Ansatz entwickelt werden, der die separate Quantifizierung von Milchproteinen bei sehr niedrigen Konzentrationen ermöglicht. Hier ermöglichte eine Kombination aus Vorkonzentration mittels Festphasenextraktion (SPE) und Quantifizierung durch Umkehrphasen-Hochleistungsflüssigkeitschromatographie (RP-HPLC) eine selektive Bindung der Milchproteine an eine C18-SPE-Kartusche mit anschließender Elution von der Kartusche und Quantifizierung durch RP-HPLC. Dieser neuartige Ansatz ermöglichte eine hohe Wiederfindungsrate der Proteine (>94 %), eine hohe Reproduzierbarkeit und eine flexible Anpassung der erforderlichen Konzentrationsfaktoren (≤ 500), wodurch die Quantifizierung einzelner Proteine mit Konzentrationen < 10 ng ml^{-1} ermöglicht wurde. Die Robustheit der Methode, deren Ergebnisse durch NaOH-Konzentrationen zwischen 0 und 0,3 % in der Reinigungsprobe nicht signifikant beeinflusst wurden, ermöglichte zudem eine breite Variation der Reinigungsmittelkonzentration. Da die Korrelation zwischen hydraulischer und chemischer Sauberkeit nicht bekannt ist, sollte eine Kombination von Methoden verwendet werden. Daher war die zusätzliche Bewertung der chemischen Reinigung von entscheidender Bedeutung für die Validität der Interpretation der folgenden Reinigungsergebnisse.

In Bezug auf die Hauptvariablen der instationären Strömung, d. h. Frequenz und Amplitude, zeigten sowohl die pulsierende als auch die alternierende Strömung ähnliche Ergebnisse bei der Reinigung im Hohlfasermodulen (HFM). Der höchste Proteinabtrag wurde bei zunehmenden Amplituden und der höchsten im Labormaßstab möglichen Frequenz (0,5 Hz) für beide Strömungsarten beobachtet. Gleichzeitig zeigte sich auch bei der sogenannten flux recovery rate (FRR) eine Verbesserung mit pulsierender Strömung in HFM (+11 %), die übrigen FRR-Ergebnisse für alternierende Strömung sowie Variation von Frequenz und Amplitude waren jedoch inkonklusiv. Der Grund für die Diskrepanz zwischen den Ergebnissen der chemischen und hydraulischen Reinigungsevaluierung wird darin vermutet, dass der unterschiedliche Sauberkeitsgrad der Membranoberfläche hauptsächlich die chemische Sauberkeit, und das interne Fouling, z. B. die Porenverblockung, hauptsächlich den Flux beeinflusst. Als kritischer Aspekt, der die Effizienz der Strömungsumkehr während der Reinigung nach der Filtration bestimmt, erwies sich die Änderung des lokalen Verhältnisses von $v/\Delta p_{TM}$ am Einlass, da dies hohe Scherkräfte bei gleichzeitig niedrigem Δp_{TM} am vorherigen Moduleinlass, wo Fouling während der Filtration am stärksten ausgeprägt war,

bedeutet. Aufgrund der Längenabhängigkeit nahm dieses Verhältnis und damit die Effizienz der Strömungsumkehr mit der Membranlänge zu, was zu einer Verbesserung des Proteinabtrages um +30 % mit alternierender Strömung bei 1,0 m Membranlänge führte. Interessanterweise konnten keine Unterschiede zwischen permanenter, d.h. stetiger Rückwärtsströmung, und zyklischer Strömungsumkehr, d.h. alternierender Strömung, festgestellt werden. Trotz der signifikanten Verbesserung des Proteinabtrages in Membranen industrieller Länge konnte kein signifikanter Vorteil der alternierenden Strömung gegenüber der pulsierenden Strömung mit einer Verbesserung des Proteinabtrages von bis zu 32 % in HFM festgestellt werden. Da der zusätzliche Aufwand, der durch die Notwendigkeit von gesteuerten Ventilen und zusätzlichen Rohrleitungen entsteht, um die alternierende Strömung zu ermöglichen, keinen eindeutigen Vorteil gegenüber der pulsierenden Strömung bietet, konzentrierte sich diese Arbeit auf die pulsierende Strömung, da sie in dem gegebenen Szenario als die überlegene instationäre Strömungsart angesehen werden kann.

Ein wichtiger Faktor, der die Effizienz der pulsierenden Strömung beeinflusst, ist die Membrangeometrie. Während HFM hauptsächlich aus einen freien Strömungskanal bestehen, enthalten andere in der Milchindustrie gängige Membrangeometrien wie Flachmembranen (FSM) und Spiralwickelmembranen (SWM) Abstandshalter (sog. Spacer), die einen definierten Strömungskanal zwischen den Membranschichten sicherstellen. Diese Spacer fördern Turbulenzen, aber auch die Bildung von Strömungsschatten hinter den Spacer-Filamenten, wodurch die Filtrationsleistung und die Reinigungsfähigkeit eingeschränkt werden. Bei FSM war die gepulste Strömung vorteilhafter als bei HFM (Proteinabtrag +48 % statt +32 %), da die pulsierende Strömung den Zugang zu den ehemaligen Strömungsschatten verbessert, was durch rasterelektronenmikroskopische (SEM) Aufnahmen bestätigt wurde. Neben einem synergistischen Effekt zwischen pulsierender Strömung und niedrigen NaOH-Konzentrationen (0,03 %) verbesserte die pulsierende Strömung den Proteinabtrag in FSM, auch wenn keine NaOH vorhanden war (+36 %). Dies deute darauf hin, dass die positiven Auswirkungen der pulsierenden Strömung auch für Spülschritte gelten. Es ist jedoch anzumerken, dass bei höheren NaOH-Konzentrationen (0,30 %) bei keiner der beiden Membrangeometrien positive Auswirkungen der pulsierenden Strömung beobachtet werden konnten.

Während bei der Fraktionierung von Magermilch mittels MF aufgrund der Proteinvernetzung in Kombination mit Druckspitzen, die zu einer verstärkten Deckschichtkompaktierung in HFM bei 10 °C führen, eine verschlechterte Filtrationsleistung berichtet wurde (Weinberger and Kulozik 2021a), verbesserte die pulsierende Strömung den Reinigungserfolg in FSM ohne vorhandenes Reinigungsmittel und damit für eine intakte Deckschicht ohne Auflockerung durch NaOH. Da dies vergleichbaren Bedingungen wie während des Filtrationsprozesses entspricht, impliziert dies positive Effekte der pulsierenden Strömung auf die Mikrofiltration (MF) von Magermilch, konträr zu den Ergebnissen von

Weinberger and Kulozik (2021a) in HFM. Eine weitere Studie zur MF von Magermilch bei 50 °C mit verschiedenen Strömungsarten bestätigte die Hypothese, dass die Synergieeffekte zwischen alternativen Strömungsarten und einem Filtrationssystem mit Spacern die nachteiligen Auswirkungen von Druckspitzen überwinden könnten, indem der Zugang zu ehemaligen Strömungsschatten deutlich verbessert, die aktive Membranfläche vergrößert, die Scherkräfte gleichmäßiger über den Strömungskanal verteilt und somit die Filtrationseffizienz verbessert wird. Die Coomassie-Färbung von Proteinen, die sich in einem FSM abgelagert haben, zeigte, dass die pulsierende und die alternierende Strömung das Fouling deutlich reduzierten und die Gesamtablagerung durch die Entfernung von Peaks in der Ablagerungsmenge, insbesondere hinter Spacer-Filamenten, homogenisierten. Hinsichtlich der Filtrationsleistung war die pulsierende Strömung der alternierenden und der stetigen Strömung überlegen. Die Anfangswerte von Fluss und Permeation waren höher und nahmen langsamer und weniger ausgeprägt ab, was die verbesserte Fouling-Kontrolle unterstreicht. Insgesamt verbesserte die pulsierende Strömung den Molkenproteinmassenstrom um > 37 % gegenüber allen Filtrationsbedingungen mit stetiger Strömung.

Zusätzlich zu den mechanistischen Erkenntnissen wird in dieser Arbeit auch ein neuartiger Ansatz zur Erzeugung von Pulsation auf Modulen im industriellen Maßstab vorgestellt, da der bisherige Ansatz über Pumpen mit schnellen Strömungsgeschwindigkeitsrampen im industriellen Maßstab nicht realisierbar ist. Dieser neuartige Ansatz besteht aus einem Bypass, der durch ein pneumatisches Ventil und eine manuelle Drossel gesteuert wird und eine pulsierende Strömung mit definierter Frequenz und Amplitude sowie einem ähnlichen Durchflussprofil wie bei Versuchen im Labormaßstab ermöglicht, jedoch bei konstanter Pumpenleistung. Die positiven Auswirkungen der pulsierenden Strömung auf die Filtrationsleistung und den Reinigungserfolg konnten für SWM bestätigt werden. Allerdings waren die Verbesserungen weniger ausgeprägt als in FSM, was vermutlich auf die geometrischen Unterschiede in den Modulen zurückzuführen ist. Neben der Verbesserung der Prozesseffizienz führen die in dieser Arbeit erzielten Ergebnisse auch zu erheblichen Verbesserungen der Nachhaltigkeit des Filtrations- und Reinigungsprozesses. Pulsierende und alternierende Strömung erfordern zwar mehr Pumpenenergie als die mittlere stetige Strömung, doch wird dieser Nachteil durch die mit alternativen Strömungsarten erzielten Verbesserungen übertroffen. Insbesondere die Anwendung von pulsierender Strömung führte zu deutlicheren Verbesserungen der Filtrationsleistung und des Reinigungserfolgs als eine mehr als verdoppelte Wandschubspannung unter stetiger Strömung. Dementsprechend führte die pulsierende Strömung in Bezug auf die spezifische Pumpenenergie, bezogen auf die während der Reinigung entfernte Proteinmenge und den während der Filtration erzielten Molkenproteinmassenstrom, zu einer signifikanten Verringerung des spezifischen Pumpenenergieverbrauchs um > 58 % während der Reinigung

und >69 % während der Filtration im Vergleich zu den optimalen stetigen Strömungsbedingungen. Beim Scale-up auf ein Modul im industriellen Maßstab stellt das vorgeschlagene Bypass-System zur Pulsationserzeugung bei einzelnen Modulen einen energetischen Nachteil dar, da ein Teil der Pumpenenergie ungenutzt in den Vorlaufbehälter zurückgeführt wird. Bei mehreren Modulen, wie sie in den meisten industriellen Anwendungen installiert sind, könnte dieser Bypass jedoch zur Speisung einer zweiten Filtrationsstufe verwendet werden. Da der vorgeschlagene Ansatz somit zwei Filtrationsstufen gleichzeitig mit verschiedenen pulsierenden Strömungsphasen versorgen würde, bliebe keine Energie ungenutzt.

Zusammenfassend lässt sich sagen, dass die pulsierende und alternierende Durchströmung zu erheblichen Verbesserungen der Filtrationsleistung und des Reinigungserfolgs führen, insbesondere bei Membran- bzw. Modulgeometrien, in denen Strömungsschatten entstehen, wobei die gepulste Durchströmung in dem gegebenen Szenario aufgrund des geringeren Implementierungsaufwands als die überlegene Durchflussart angesehen werden kann. Mit signifikanten Verbesserungen während Filtration, chemischer Reinigung und Spülschritten könnte die pulsierende Strömung die gesamte Prozesskette der Membranfiltration im Hinblick auf die Prozesseffizienz und damit ihre wirtschaftliche und ökologische Nachhaltigkeit verbessern.

1 General introduction

Membrane filtration is a non-thermal separation process and important unit operation in several industrial areas ranging from water treatment to pharmaceuticals and food production. Due to the retention of particles larger than the pore size and the simultaneous convective transport of these particles towards the membrane, an accumulation of various macromolecules on and in the membrane occurs, depending on the composition and complexity of the feed solution. This leads to the blocking of membrane pores and the formation of a deposit layer (Bartlett et al. 1995; Bird and Bartlett 2002) which causes a reduction in flux and protein permeation (Ripperger and Altmann 2002; Ng et al. 2018), thus impairing filtration performance. While high crossflow velocities are often used to reduce fouling (Hartinger et al. 2020c; Altmann and Ripperger 1997), it cannot be completely avoided and remains the main limitation of membrane processes. In combination with biofouling, irreversible deposits, that cannot be removed by rinsing steps, generate the need for regular chemical cleaning cycles. They consist of several rinsing and chemical cleaning steps and are thus a chemical- and energy-intensive process causing several hours of downtime per day.

One approach to improve fouling control and cleaning success is by inducing an unsteady flow, i.e. pulsed or alternating flow. While pulsed flow refers to a constant fluctuation between high and low flow rate phases with related changes in pressure conditions, alternating flow additionally induces a cyclic feed-side flow reversal. To a limited extent, these concepts of pulsed/alternating flow have previously been shown to improve filtration performance for model feed systems (Weinberger and Kulozik 2021c, 2022, 2021b; Howell et al. 1993; Hadzismajlovic and Bertram 1999, 1998), consisting of e.g. yeast and BSA. However, for complex feed systems such as skim milk, no such improvements were reported, arguably due to the extensive cross-linking of milk proteins causing stronger irreversible fouling when subjected to temporary pressure peaks (Weinberger and Kulozik 2021a). Regarding cleaning, pulsed and alternating flow have been shown beneficial for various media, but only for the cleaning of smooth steel surfaces (Gillham et al. 2000; Blel et al. 2009a; Blel et al. 2009b; Yang et al. 2019; Föste et al. 2013; Bode et al. 2007; Augustin and Bohnet 1999), which differ significantly from membrane surfaces in terms of surface roughness, surface porosity as well as the related flow characteristics due to the additional vertical flow through the wall/membrane structure.

Accordingly, this study aims at investigating the effects of pulsed and alternating flow on the membrane cleaning process following skim milk microfiltration as well as to establish a deeper understanding of the interplay between alternative flow types and other process characteristics, such as the frequency and amplitude of pulsed/alternating flow, the membrane geometry, the membrane length, the concentration of the cleaning agent and the transferability

of these flow types to industrial-scale membrane modules. Therefore, the effects of pulsed and alternating flow on cleaning success were evaluated by monitoring flux recovery, protein removal and performing a surface analysis via scanning electron microscopy. Lastly, the newly found optimum process conditions were used to re-assess the effect of alternative flow types on the filtration performance of skim milk via flux, permeation, and surface characterisation.

1.1 Composition and characteristics of bovine skim milk

Bovine milk is a complex, nutrient-rich liquid food consisting of water, fat, proteins, lipids, sugars and salts (Table 1-1), where skim milk comprises the fat-free fraction of whole milk obtained by removing the fat phase via centrifugation. The main components are water (88 %), lactose (4.8 %) and milk proteins (3.5 %). It is to be noted that the composition can vary depending on the season, breed, fodder and other factors.

Table 1-1. Composition of bovine milk (Töpel 2016).

Organic constituents	**Concentration [g kg^{-1}]**	**Inorganic constituents**	**Concentration [g kg^{-1}]**
Lipids	30-45	Water	860-880
Protein	32-36	Ions	6.0-7-5
Caseins	26-30	*Cations*	2.8-3.7
α_{S1}	10.3-11.9	Calcium	1.00-1.40
α_{S2}	2.6-3.1	Magnesium	0.10-0.15
β	9.9-11.9	Sodium	0.35-0.60
κ	3.3-3.5	Potassium	1.35-1.55
Whey proteins	6.0-6.2	*Anions*	3.2-3.8
α-lactalbumin	1.2-1.3	Carbonate	0.2
β-lactoglobulin	3.1-3.5	Chloride	0.8-1.4
Serum albumin	0.4	Sulfate	0.1
Others	1.9-2.3	Phosphate	2.1
Carbohydrates	46-48		
α-lactose-hydrate	17.7-18.0		
β-lactose	29-30		
Others	0.07		

The milk proteins can be further divided based on the insolubility of caseins and the solubility of native whey proteins at pH 4.6 and T = 20 °C (Fox et al. 2015; Toro-Sierra et al. 2013). The latter comprise around 20 % of the total protein concentration and are spherical, globular and highly hydrophobic proteins (Walstra 1999) with a particle size ranging from 2 nm to 8 nm (see Figure 1-1) (Heidebrecht and Kulozik 2019). Whey proteins mainly comprise α-Lactalbumin (α-La) with 2 – 5 % of the total protein concentration (Töpel 2016) and a molecular weight of 14.2 kDa (Calderone et al. 1996) and β-Lactoglobulin (β-Lg) with 7 – 12 % (Töpel 2016) and 18.3 kDa (Farrell et al. 2004). α-La contains four disulfide bridges but no free thiol group and is a calcium-binding protein with an isoelectric point (IEP) of 4.2 – 4.5 (Töpel 2016). β-Lg contains two stabilising internal disulfide bridges and a free thiol group available for interactions with e.g. other proteins, with an IEP of 5.2 (Töpel 2016). Furthermore, its genetic variants β-Lg A and B have different tertiary and quaternary structures depending on temperature and pH (Belitz et al. 2008; Tolkach and Kulozik 2007; Cheison et al. 2011), leading

to different sizes that could affect separation efficiency and reactivity with other proteins, depending on the exposure of the free thiol group. Other aspects, such as forces induced by filtration (Steinhauer et al. 2014) or concentration effects in the filtration-induced deposit (Ng et al. 2017) might also lead to exposure of the free thiol group and thus, affect deposit characteristics during filtration. Additionally, there are some minor fractions, such as bovine serum albumin (BSA), lactoferrin (LF) and immunoglobulins (IgG, IgA and IgM), that do not play a decisive role in fouling due to their low concentration.

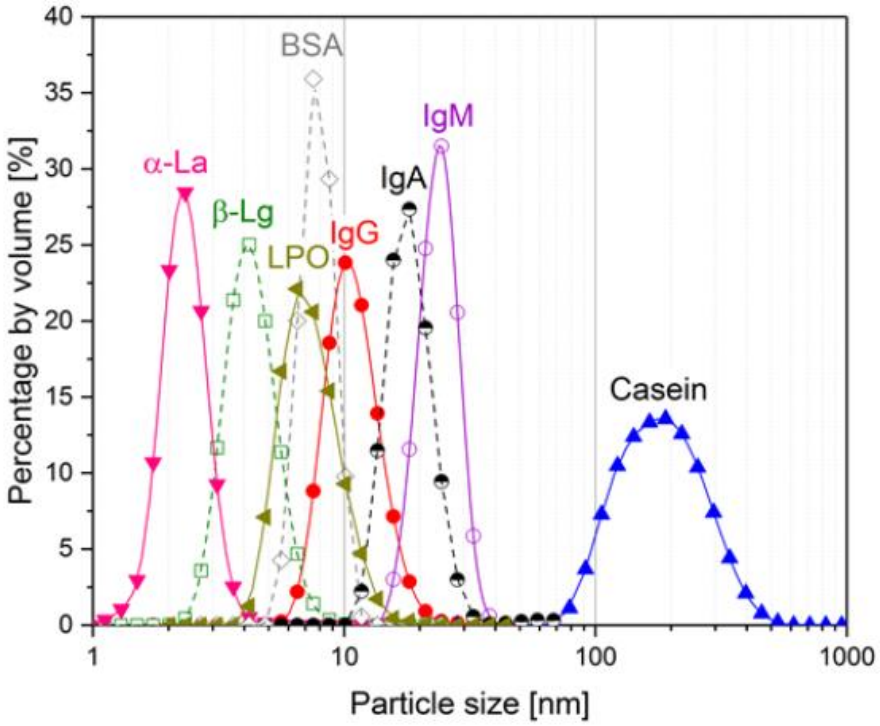

Figure 1-1. Particle size distribution of native whey proteins and casein micelles (Heidebrecht and Kulozik 2019).

Caseins comprise the remaining 80 % of the total protein concentration in milk. In contrast to whey proteins, they tend to self-aggregate and form large structural complexes with sizes from 20 – 300 nm (Brans et al. 2004), namely casein micelles (see Figure 1-2), in which up to 95 % of native casein is bound (Töpel 2016). The main casein monomers α_{S1}-, α_{S2}-, β- and κ-Casein have molecular weights ranging from 19.0 kDa to 25.2 kDa and also differ in terms of cysteine residues, calcium sensitivity, phosphoserine binding sites and hydrophobicity (Töpel 2016). Accordingly, they fulfil different roles within the casein micelle.

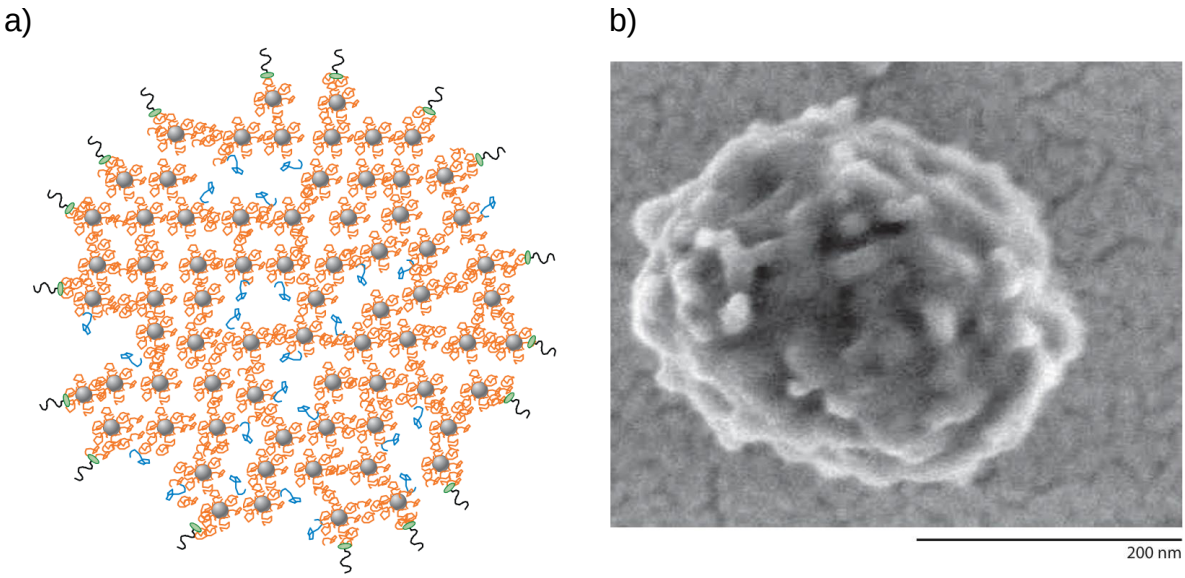

Figure 1-2. a): Schematic image of a casein micelle containing α_S- and β-caseins (orange) attached to calcium phosphate nanoclusters (grey circles), β-caseins (blue) hydrophobically bound to other caseins and κ-caseins (green with grey tail) on the micelle surface forming a hairy layer (Dalgleish and Corredig 2012). b): Field-emission scanning electron microscopy image of a casein micelle (Dalgleish and Corredig 2012).

While the casein micelle's exact structure is still controversial among researchers (Horne 2020; Dalgleish and Corredig 2012; Holt et al. 2013), the most widely agreed model is the so-called nanocluster model. Overall, phosphorylated caseins (α_{S1}-, α_{S2}- and β-casein) associated with calcium phosphate accumulated in nanoclusters form the casein micelle's main body (Holt 2004), presumably cross-linked by their phosphoserine pairs (Horne 2020) and stabilised by hydrophobic interactions (Horne 2003), calcium bridging, hydrogen bonding and Van der Waals interactions (Dalgleish 2011). κ-casein, due to its amphoteric nature and lack of phosphoserine clusters, cannot be incorporated into the micelle's structure but instead accumulates at the micelle's surface, forming a so-called hairy layer. It plays a vital role in stabilising micelles against aggregation due to steric repulsion (Kruif and Zhulina 1996). However, it is not fully covering the micelle surface, making it an open and porous structure accessible to smaller particles. This leads to casein micelles being highly hydrated (Fox and Brodkorb 2008), compressible and sponge-like structures (Dalgleish and Corredig 2012). However, it is to be noted that for casein concentrations > 178 g L^{-1}, as they can occur during filtration within the deposit layer, aggregation and, thus, the formation of a gel-like structure can be induced by high osmotic stress (Bouchoux et al. 2010). It is to be noted that changes in the milk serum, particularly the salt equilibrium such as the content of soluble calcium, can also significantly affect the cross-linking of casein micelles and thus the deposit formation and filtration performance (Jimenez-Lopez et al. 2008; Rabiller-Baudry et al. 2005; Adams et al. 2015).

1.2 Pressure-driven membrane processes

1.2.1 Basic principles of the membrane-based separation

Filtration is a membrane process driven by the pressure difference between the feed p_1 or retentate p_2 and permeate side p_3, i.e. the transmembrane pressure Δp_{TM} (eq. (1-1)). Due to the friction-induced pressure loss along the membrane module Δp_L (eq. (1-2)), the average of pressures at the inlet and outlet must be considered for this calculation. Δp_{TM} causes the transport of permeable feed solutes through the membrane pores as so-called flux J according to Darcy's Law (see eq. (1-3)). Additional influencing factors are the permeate viscosity η, the membrane resistance R_m resulting from membrane characteristics such as the pore size and distribution, and the fouling resistance R_f resulting from the accumulation of retained particles on the membrane surface. Overall, flux is a key performance indicator that can also be calculated by dividing the permeate flow rate $\dot{V}_{permeate}$ by the active membrane area A.

$$\Delta p_{TM} = \frac{p_1 + p_2}{2} - p_3 \tag{1-1}$$

$$\Delta p_L = p_1 - p_2 \tag{1-2}$$

$$J = \frac{\dot{V}_{permeate}}{A} = \frac{\Delta p_{TM}}{\eta \cdot (R_m + R_f)} \tag{1-3}$$

The separation mechanism for microfiltration (MF), ultrafiltration (UF) and nanofiltration (NF) is based on size exclusion, where the retention of solutes depends on their particle size and the related nominal pore size (NPS) of the membrane. For reverse osmosis (RO), the membrane is considered free of pores, and the separation mechanism is based on the solution-diffusion model instead.

Due to the pore size being variable between > 100 µm and < 1 Å, membrane-based separation is widely used across various industries with many applications ranging from e.g. water treatment to removal of microorganisms, purification of biopharmaceuticals, clarifying and concentrating beverages, cell harvesting, blood purification, milk protein fractionation and many more. The latter, i.e. the fractionation of skim milk by MF into the micellar assembled caseins and whey proteins, poses an essential process in the dairy industry, enabling the valorisation of single fractions for various functionalities and applications. An overview of the milk solutes that can be separated by different pore sizes is given in Figure 1-3.

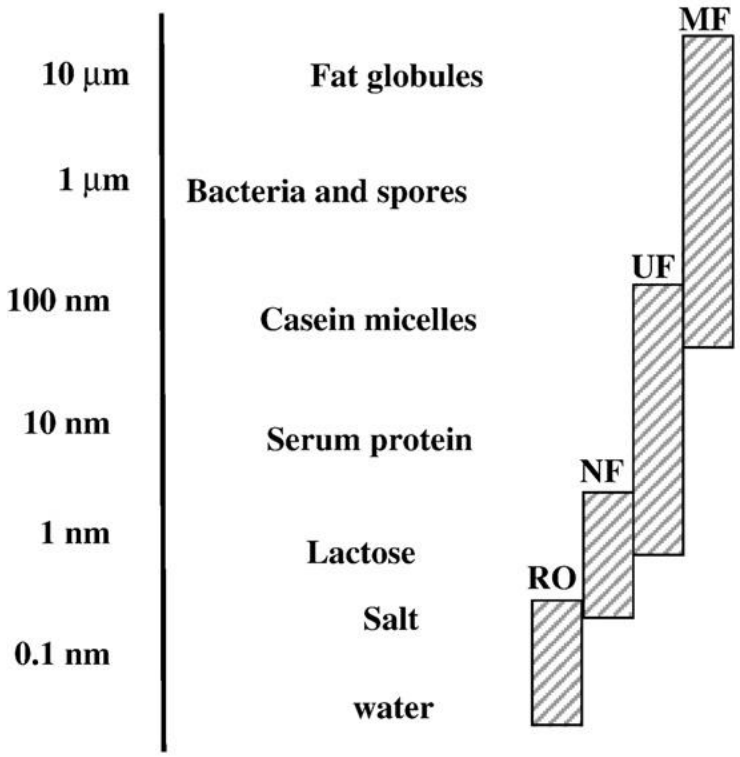

Figure 1-3. Separation and retention of different milk ingredients by membranes with different pore sizes (Saxena et al. 2009).

Hence, in fractionation tasks where two or more components are to be separated from each other, the capability of a membrane to separate these fractions poses another critical indicator that needs to be considered when evaluating filtration performance. This can be done by assessing the permeation P_i (eq. (1-4)) of a target component i by measuring its concentration in the permeate $c_{i,p}$ and retentate $c_{i,r}$. Combining flux and permeation, the mass flow, according to equation (1-5), can be calculated as an additional quality criterion.

$$P_i = \frac{c_{i,p}}{c_{i,r}} \tag{1-4}$$

$$\dot{m}_i = J \cdot c_{i,p} \tag{1-5}$$

It is to be noted that the prioritisation of flux, permeation or mass flow depends on whether the fractionation aims to concentrate retained particles, separate two components or harvest a target component in the permeate.

1.2.2 Operating modes

The main modes of operation are dead-end filtration and crossflow filtration. For dead-end filtration, the feed flows perpendicular to the membrane surface and particles either permeate or are retained and then accumulate on the membrane surface. Over time, the deposited amount continuously increases, creating an additional filtration resistance (compare R_f in eq. (1-3)) and reducing permeate flow. Hence, filtration quickly becomes inefficient, and the membrane subsequently must be cleaned in equally short intervals. Besides its main

limitation, dead-end filtration can be preferred or necessary, e.g. when the particle content is low (van Reis and Zydney 2007). The industrially more common alternative is crossflow filtration, where the feed flows along the membrane surface. Due to enhanced shear forces, friction and lift forces, deposition can be significantly reduced and deposit layer height limited, which enables more stable filtration performance and, thus, prolonged filtration intervals and reduced cleaning intervals (Kraume 2012).

1.3 Fouling phenomena and deposit layer formation

1.3.1 Forces determining deposition/removal of particles

During crossflow filtration and cleaning, several forces simultaneously act on a particle. An overview is given in Figure 1-4. Accordingly, the balance or ratio between those forces determines whether a particle deposits onto or into the membrane and whether an already deposited particle gets removed from the deposit layer.

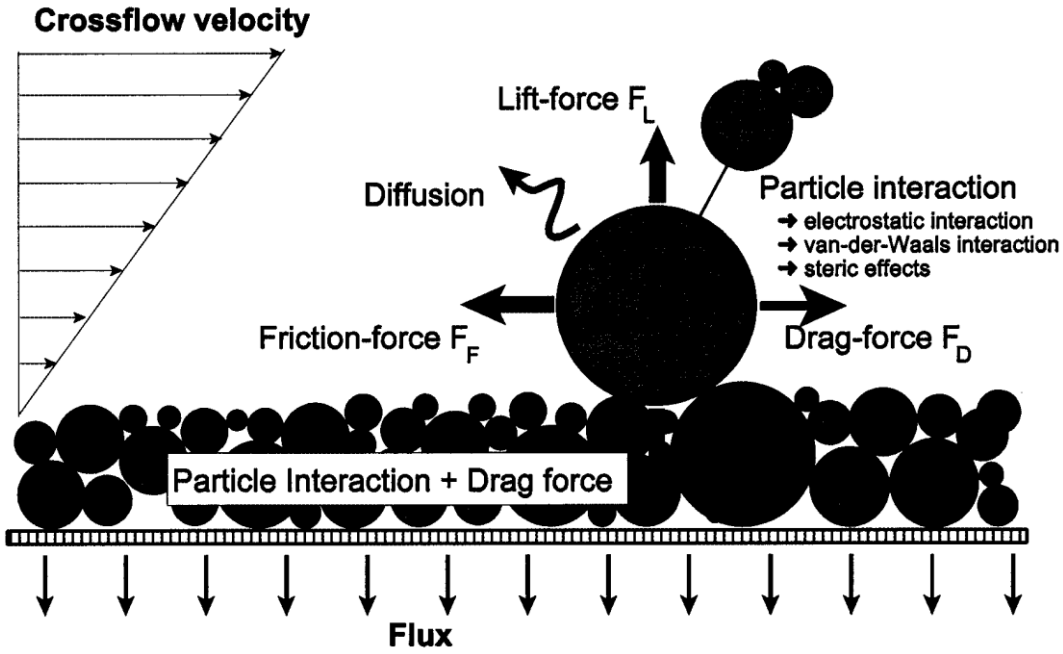

Figure 1-4. Forces acting on a particle during crossflow filtration (Ripperger and Altmann (2002).

The extended Derjaguin-Landau-Verwey-Overbeek-Theory (xDLVO) compares the occurring non-covalent colloidal forces, e.g. between proteins as well as between proteins and the membrane, and summarises whether repulsive or attractive forces prevail at a given distance (van Oss 1993; Derjaguin and Landau 1993; Verwey and Overbeek 1948). A schematic overview is depicted in Figure 1-5.

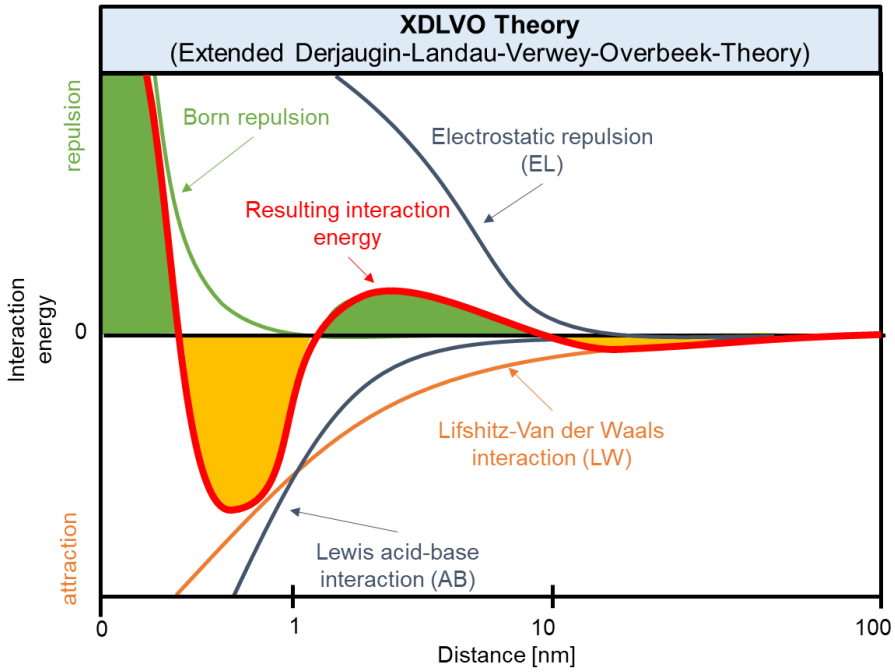

Figure 1-5. Schematic xDLVO diagram summarising the interaction energies between two particles as a function of their distance.

Involved forces include the Born repulsion, Lifshitz-Van der Waals interactions (LW), electrostatic interactions (EL), and Lewis acid-base interactions (AB). Born repulsion occurs only for very low distances due to overlapping electron hulls and ensures a minimum distance d_0 = 0.157 nm. LW and EL interactions prevail in the classic DLVO theory for larger distances. Hence, the resulting interaction energy depends on various physicochemical (e.g. particle size, geometry, zeta potential) and chemical (e.g. pH, ionic strength) aspects. Due to DLVO's unprecise predictions for complex systems and biogenic material such as proteins, it was extended by solvation forces, i.e., the short-range polar electron-acceptor/-donor (AB) interactions (van Oss 2006). It is particularly relevant for e.g. membrane-colloid interactions in polar media with small separation distances of a few nanometres and high ionic strengths (Kühnl et al. 2010). During filtration, different interactions dominate different filtration stages (Huisman et al. 2000), and the dominance of different interactions can significantly affect the occurrence of different fouling types (see chapter 1.3.2) (Han et al. 2018a), the deposit layer homogeneity (Han et al. 2018a), thickness, porosity and permeability (Han et al. 2021; Faibish et al. 1998). For complex systems, additional interactions such as covalent disulfide bonds can occur, e.g. between proteins tightly packed in a deposit (Qu et al. 2015; Bouchoux et al. 2010; Roche and Royer 2018; Weinberger et al. 2021). Overall, these interactions can also be affected by hydrodynamic forces, as the permeate flux, resulting from Δp_{TM}, leads to a compaction of the deposit layer and, thus, changes in the particle distance and, possibly, changes in the dominance of attractive or repulsive interactions.

In terms of hydrodynamic forces, the present shear forces, i.e. wall shear stress τ_w (eq. (1-6)), depend on the friction-induced pressure loss Δp_L (eq. (1-2) and (1-6)) along the membrane.

$$\Delta p_L = \frac{1}{2} \cdot \lambda \cdot \frac{L}{d_H} \cdot \rho \cdot v^2 = \frac{4 \cdot L \cdot \tau_w}{d_H} \tag{1-6}$$

where λ is the friction factor, L is the membrane length, d_H is the hydraulic diameter of the membrane channel, ρ is the feed density, and v is the flow velocity.

The latter can be calculated by the feed flow rate $\dot{V}_{feed}$ and the cross-section of the membrane channel A_{cross} (eq. (1-7)).

$$v = \frac{\dot{V}_{feed}}{A_{cross}} \tag{1-7}$$

The resulting turbulence can be characterised by the Reynolds number Re (eq. (1-8)). For low Re in a laminar regime, the fluid mostly flows in layers with little lateral mixing leading to the local flow velocity highly depending on the radial position. In contrast, for high Re with turbulent flow, vortices induce lateral mixing making the local flow velocity increasingly independent of the radial position. However, identical Re can represent different turbulences depending on the geometry of the flow channel. As an example, baffles such as membrane spacers cause disruptions in the flow profile leading to reductions in the critical Reynolds number Re_{crit}, where turbulent flow occurs, from $Re_{crit} \approx 2300$ in regular channels (Rott 1990) down to ranges of $35 < Re_{crit} < 1000$ (Geraldes 2002; Han et al. 2018b; Koutsou et al. 2007). Details will be discussed in chapter 1.4.

$$Re = \frac{\rho \cdot v \cdot d_H}{\eta} \tag{1-8}$$

Even for turbulent flow, due to the friction effects between the membrane and feed flow, the feed velocity reduces towards the membrane surface, leading to a laminar sublayer with a height δ_{lam} (eq. (1-9)) in its close vicinity.

$$\delta_{lam} = \frac{5 \cdot \eta}{\sqrt{\tau_w \cdot \rho}} \tag{1-9}$$

Drag forces F_y towards the membrane, induced by the flow towards the membrane and depending on the particle diameter d_p, are the leading cause for particle deposition. For low Re and no particle interaction, F_y can be estimated with the Stokes equation (eq. (1-10)).

$$F_y = F_{Stokes} = 3 \cdot \pi \cdot \eta \cdot d_p \cdot J \cdot \phi \tag{1-10}$$

where ϕ is a correction factor to the Stokes drag force. The opposing forces are diffusive and inertial lift forces F_L, strongly depending on the particle size. F_L of a deposited particle can be calculated according to (Ripperger and Grein 2007) (eq. (1-11)).

$$F_L = 0.761 \cdot \frac{\tau_w^{1.5} \cdot d_p^3 \cdot \rho^{0.5}}{\eta} \quad (1\text{-}11)$$

The particle size also determines whether Brownian diffusion (for d_p < 0.1 µm) or hydrodynamic forces (for d_p > 1.0 µm) for inert particles can prevail over drag forces, as shown in Figure 1-6.

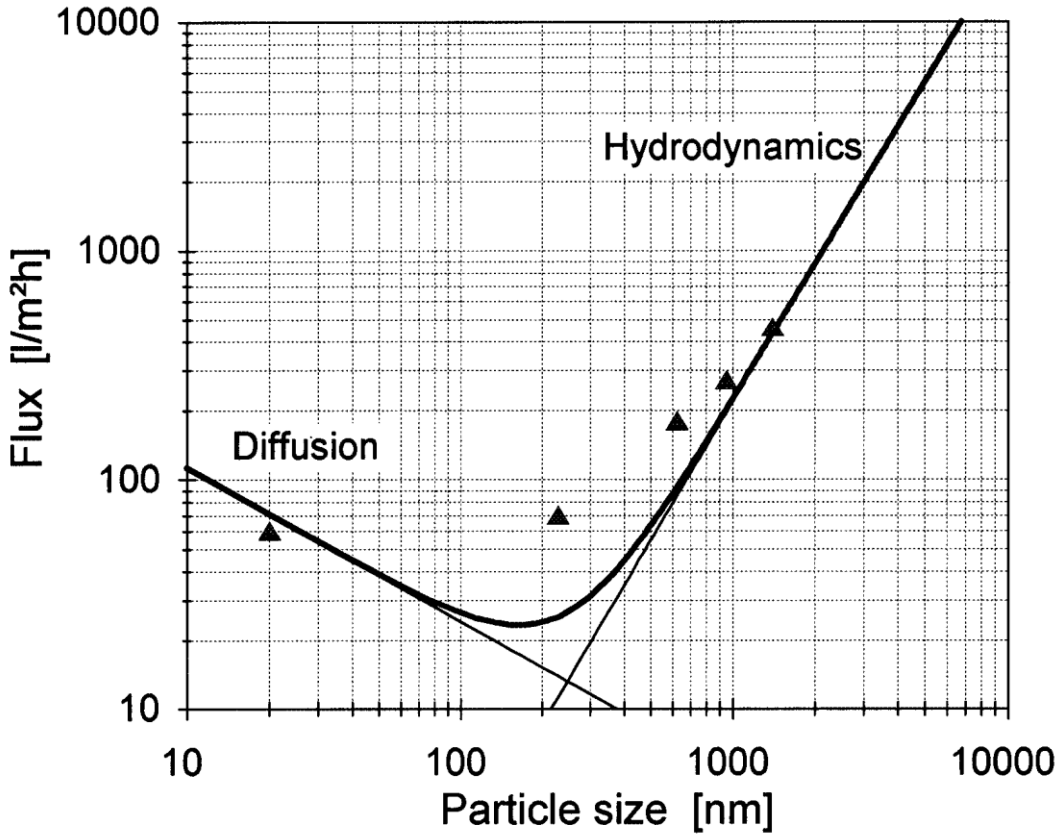

Figure 1-6. Susceptibility of particles to diffusive and hydrodynamic forces depending on their particle size according to the resulting flux at two different flow velocities (Ripperger and Altmann 2002).

While diffusion prevails for small particles and lift forces prevail for large particles, a minimum in flux and, thus, susceptibility to diffusion or hydrodynamics occurs for particles in the range 0.1 µm < d_p < 1.0 µm. Hence, e.g. casein micelles with a particle size distribution between 20 – 300 nm are likely to deposit during skim milk microfiltration and difficult to control by processing conditions such as flow velocity, as they are in a size range neither strongly affected by diffusion nor hydrodynamics.

1.3.2 Fouling mechanisms

The occurrence of different fouling mechanisms (see Figure 1-7) depends on particle properties, such as size and charge, and membrane properties, such as the material characteristics, pore size distribution and geometry (Cui et al. 2010).

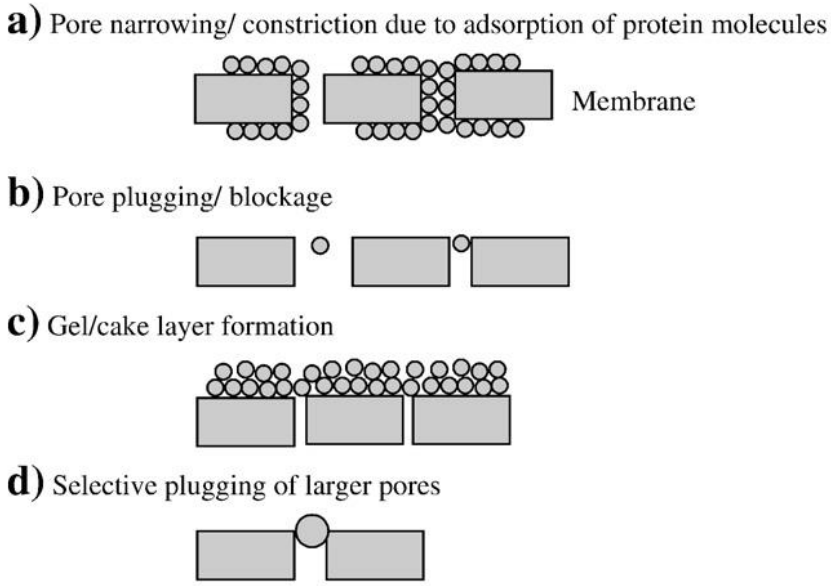

Figure 1-7. Overview of the main fouling mechanisms during protein fractionation by MF (Saxena et al. 2009).

In-pore fouling mainly occurs at the start of filtration (Ho and Zydney 2000), when the membrane is clean, and its surface is free of deposited particles. It can further be divided into pore constriction and pore blockage. The former occurs when smaller/permeable proteins adsorb to the inner pore surface, constricting flow channels with a subsequent reduction in flux. While it could be shown that pore-narrowing by whey proteins is no primary driver of fouling during the MF of milk (Zulewska and Barbano 2013), the effects of smaller casein micelles on internal fouling have not been investigated so far to the author's knowledge. The underlying cause can be e.g. hydrophobic interactions between proteins and the membrane, as shown by Hashino et al. (2011) for polyvinylidene fluoride (PVDF) membranes. During MF of skim milk, a complete reduction in flux and permeation caused by a blocked pore is not to be expected due to casein micelles being penetrable by solutes and small proteins (Qu et al. 2012). Pore blockage can be both externally and internally. While external blockage is due to particles larger than the pore size blocking the pore inlet (Saxena et al. 2009), the non-uniform pore size along the pore channel also allows internal pore blockage for particles slightly smaller than the effective pore size.

With progressing filtration time, the fouling mechanisms shift to external deposit formation. First, the retention of particles too large to permeate combined with the drag forces towards the membrane (see eq. (1-10)) leads to an accumulation of retained particles on the membrane surface. A deposit layer can form when the concentration within this so-called

concentration polarisation (CP) layer (Zydney and Colton 1986) becomes too high. In terms of removability, deposits and related filtration resistances R_f (see eq. (1-12)) can be separated into reversible fouling $R_{f,\,rev}$ that can be addressed by hydrodynamic forces, and irreversible fouling $R_{f,\,irrev}$ that can only be removed by chemical cleaning. However, with flow velocities used to determine the reversible and irreversible fouling shares varying widely (Qu et al. 2012; Wemsy Diagne et al. 2013; Rabiller-Baudry et al. 2006), as no uniform hydrodynamic forces are defined for its determination, this concept and related results should be treated with caution. Despite deposit formation being the dominant fouling mechanism throughout most of the filtration time, internal fouling can nonetheless have a higher impact on filtration resistance (Ng et al. 2017).

$$R_f = R_{f,rev} + R_{f,irrev} \tag{1-12}$$

For skim milk, due to the compressibility of casein micelles, an elongational deformation of the micelles caused by the flow through the deposit was reported (Gebhardt 2014). However, no significant interactions between casein micelles were reported below a critical concentration of 125 g L^{-1} (Bouchoux et al. 2009). For even higher concentrations above 200 g L^{-1}, the formation of an irreversible gel was reported (Bouchoux et al. 2010; Gebhardt et al. 2012), stabilised by extensive cross-linking including hydrophobic and electrostatic interactions. Hence, compaction and concentration reached levels where attractive interactions between micelles overcame the repulsive forces (compare xDLVO theory in chapter 1.3.1) of the micelle's κ-CN hairy layer. Further consequences of increased pressures, compaction and thus concentrations reported besides forming a dense network are dewatering of the micelles (Bouchoux et al. 2009) and a collapse of the micellar structure (Bouchoux et al. 2010). It is also worth noting that for casein micelle deposits, Qu et al. (2012) reported the deposit's retention properties to being more determined by the micelle's internal channels and porosity than the voids between individual micelles. It is to be noted that for milk filtration, besides proteins, the precipitation of minerals on the membrane can also cause mineral fouling, so-called scaling. Its relevance in a given scenario depends on similar characteristics as protein fouling, such as the pore size (Ng et al. 2017).

From a hygienic perspective, biofouling poses the most crucial fouling type. To enable sufficient shelf-life while preserving valuable nutrients and vitamins, milk is often gently heat treated with high-temperature short-time heat treatment, e.g. at 74 °C for 28 s. Hence, pasteurised skim milk is not free of microorganisms, which can then accumulate in the feed and concentrate during filtration due to size-induced retention. Filtration at the growth optimum of 40 – 65 °C (Burgess et al. 2010) for thermostable microorganisms, such as *Pseudomonas* (Porcellato et al. 2018), *Geobacillus* spp. and *Bacillus* spp., supports rapid metabolisation of the nutrient-rich milk components and thus, increasing bacterial count until eventually

surpassing the critical concentration of 10^5 per mL according to regulations of some national laws. Hence, maximum filtration times before a cleaning cycle becomes necessary can vary between > 24 h at low temperatures (10 °C) and ≤ 7 h at elevated temperatures (55°C) (Schiffer and Kulozik 2020). In the case of improper handling or processing, the problems of undisturbed biofouling can be manifold as it supports the formation of a highly resistant biofilm. From a processing perspective, biofilms are very hard to clean (Frank and Koffi 1990; Flint et al. 2002; Carrascosa et al. 2021), leading to decreased production times, increased cleaning times, product losses and costs (Seale et al. 2015). Furthermore, the adherence of biofouling to e.g. heat exchangers reduces heat transfer to the actual product and fluid flow, thus causing increased energy consumption to ensure sufficient heat treatment. Additionally, microorganisms can leave an established biofilm to contaminate other parts of the processing line and, thus, spread cleaning issues within the whole plant. From a hygienic perspective, the main issue arising from biofouling is food safety, as the contamination of foods will lead to accelerated spoilage and potentially cause severe or even fatal health issues for consumers (Seale et al. 2015; Carrascosa et al. 2021).

Another important aspect related to fouling mechanisms is the length dependency of fouling. Imposed by the friction-induced energy dissipation and, thus, pressure loss along the membrane channel (see eq. (1-6)), the local Δp_{TM} decreases along the membrane module. Accordingly, the fouling intensity is most pronounced at the module inlet (Gésan et al. 1993) and decreases along the module (Piry et al. 2008; Hartinger et al. 2020c), as shown in Figure 1-8.

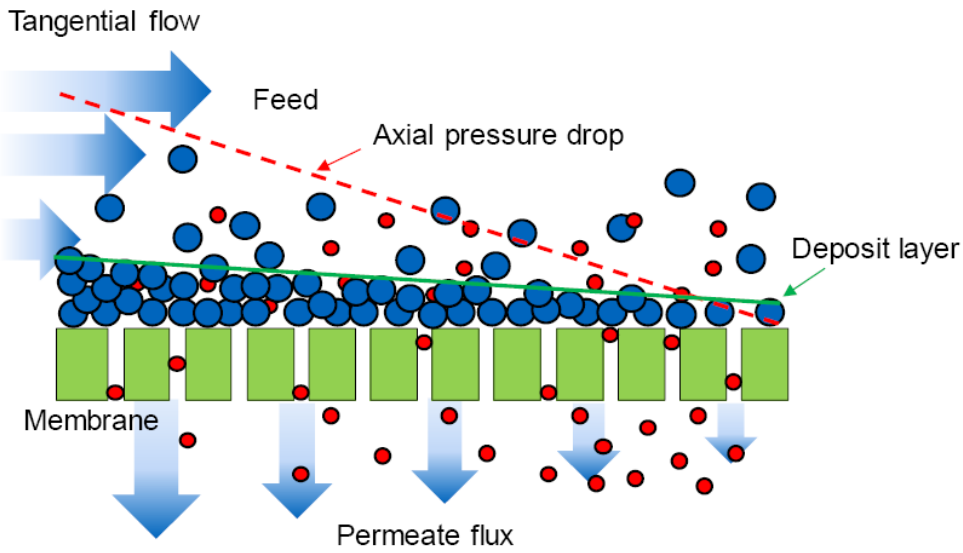

Figure 1-8. Schematic depiction of deposit layer formation along a membrane module with most pronounced fouling at the inlet and least pronounced fouling at the module outlet (Schopf 2022).

As this length dependency also transfers to the filtration performance (Piry et al. 2008), i.e. not the whole membrane can be operated at the optimum Δp_{TM}, length dependency effects

negatively affect process control and filtration performance. Consequently, a recent study by Schopf et al. (2021a), assessing the length-dependent filtration performance of skim milk MF in HFM, concluded a reduction in membrane length of industrial modules from typically 1.0 m to 0.6 m to be of advantage. According to the authors, this length provided the best combination of high flux, high permeation and improved control over deposit formation due to the decreased Δp_L enabling operation at lower Δp_{TM} without inducing back-pressure in the rear parts of the module.

1.3.3 Effects of deposit layer formation on filtration performance

For the filtration of e.g. pure water, where no fouling can occur, flux increases according to Darcy's Law (eq. (1-3)) proportionally to any increase in Δp_{TM}. Here, the flux level mainly depends on the membrane resistance, determined by its material, pore size distribution and other properties (Melin and Rautenbach 2007). For other feed solutions where fouling can occur, the additional fouling resistance leads to reductions in flux and permeation and a non-linear behaviour for increasing Δp_{TM} compared to water filtration (see Figure 1-9).

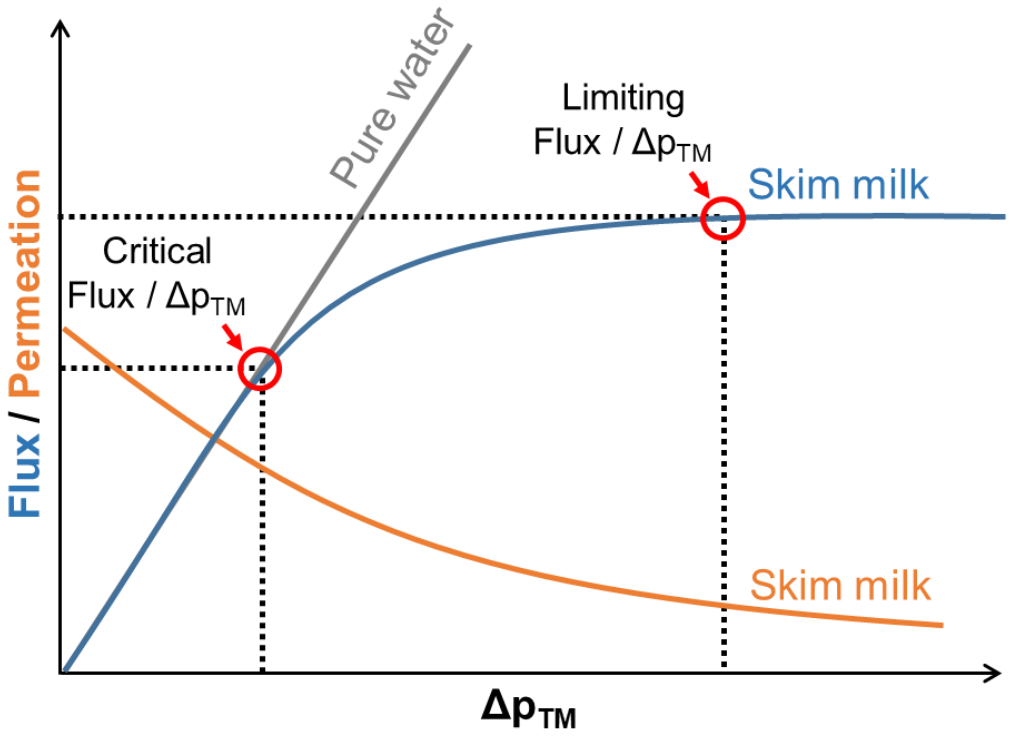

Figure 1-9. Schematic depiction of flux (blue) and whey protein permeation (orange) as a function of Δp_{TM} during the MF of skim milk based on results from Bacchin et al. (2006) and Schopf and Kulozik (2021). The linear flux increase of water (dashed line) is given as a reference. Dotted lines and red circles mark the critical and limiting flux and Δp_{TM}.

During the MF of e.g. skim milk, flux initially increases linearly with Δp_{TM} until reaching the critical flux, or critical Δp_{TM}. Within this initial Δp_{TM}-range, convective transport towards the membrane, and thus fouling, remains negligibly small. Afterwards, filtration behaviour switches

from membrane-based to fouling-based filtration behaviour due to the increased Δp_{TM} causing increased drag and, thus, deposit formation and compaction leading to additional fouling resistance. The deposit layers acting as a second selective layer now mainly govern filtration performance. For further increases in Δp_{TM}, the flux levels off until it reaches the limiting flux, or limiting Δp_{TM} (Field et al. 1995), where any further increase in Δp_{TM} leads to an equivalent increase in fouling resistance without any further changes in flux. Besides flux, the increasing formation and compaction of the deposit also negatively affects protein permeation. The balance between high flux at high Δp_{TM} and high permeation at low Δp_{TM} translates to an optimum protein mass flow at medium Δp_{TM}, e.g. at 0.5 bar for HFM (Schopf and Kulozik 2021).

It is worth noting that high Δp_{TM} can induce the previously mentioned formation of a gel layer at high protein concentrations. Additionally, experiments using Δp_{TM}-ramps (low – high – low Δp_{TM}) found a hysteresis in flux between the pressure increase and decrease, meaning that the intrinsic deposit structure changes irreversibly at high Δp_{TM} (Schiffer et al. 2020; Hartinger et al. 2019a; Gésan-Guiziou et al. 1999). Hence, the filtration performance is governed by the maximum applied Δp_{TM} and deposit characteristics cannot be reverted by decreasing Δp_{TM}.

1.3.4 Fouling mitigation

Besides carefully considering the optimum Δp_{TM} to balance flux and permeation, as discussed in the previous chapter, the flow velocity and the related τ_w poses the main process condition to mitigate fouling. An increase in flow velocity leads to an increase in turbulence (eq. (1-8)), a decrease in the laminar sublayer thickness (eq. (1-9)), an increase in τ_w (eq. (1-6)), and an increase in lift forces (eq. (1-11)), which all support particle removal and exacerbate particle deposition. The consequence should be improvements in flux and protein permeation. Indeed, a comparison of studies with different flow velocities found improved flux at higher crossflow velocities (Brans et al. 2004). Other studies also investigated the impact of increasing flow velocities on flux and permeation during skim milk MF. The authors found increasing flux for increasing shear stress up to a critical τ_w where further increases would lead to a decrease in flux (Schiffer et al. 2020; Kulozik and Kersten 2002b; Hartinger et al. 2019c), presumably due a shift of the deposit's particle size (Altmann and Ripperger 1997), protein deformation (Gebhardt et al. 2012) or a shift in transport mechanism through the micelles (Qu et al. 2012). However, regarding whey protein permeation, no influence of varying flow velocities on the average whey protein permeation of the module could be found (Schiffer et al. 2020), only locally when comparing axial membrane sections (Hartinger et al. 2020c). It is to be noted that increasing flow velocities also cause increased $\Delta p_{L.}$ This induces an enhanced length dependency of Δp_{TM}, fouling intensity and filtration performance, meaning that its respective

distribution becomes increasingly inhomogeneous along the membrane module. Consequently, the local fouling control becomes impeded despite the advantages of high flow velocities. Hence, with the benefits of high flow velocities being limited by length dependency, fouling mechanisms and mechanical stability of certain module types (see chapter 1.4), flow velocity poses no universal answer to fouling mitigation.

Another important aspect is the filtration temperature. Besides the previously mentioned hygienic issues of increased biofouling at elevated temperatures, the related metabolisation of milk components also leads to a drop in pH (Schiffer and Kulozik 2020), a loss of product quality (Deeth et al. 2002), an increase in fouling intensity and, thus, a substantial decrease in filtration performance (Schiffer and Kulozik 2020; Chamberland et al. 2019; France et al. 2021b; France et al. 2021a). Despite the increased fouling and biofouling at elevated temperatures of 55 °C compared to low temperatures of 10 °C, the filtration performance is still increased at elevated temperatures due to the reduced permeate viscosity, even when considering the reduction in annual production time due to additional cleaning cycles to prevent biofouling (Schiffer and Kulozik 2020).

Besides process conditions, several novel approaches to enhance filtration performance or cleaning efficiency were reported and will be reviewed in detail in chapter 1.6. The module design choice, discussed in the following chapter, can also strongly affect fouling intensity and filtration performance (Schopf et al. 2021b).

1.4 Membrane modules and flow properties

While there are several different membrane geometries and modules, CTM and SWM are most commonly used for the fractionation of skim milk by MF. Another membrane type, HFM, which is already extensively used across various industries and applications (Lehmkuhl et al. 2018; Yamamoto et al. 2005; Ebrahimi et al. 2018), is an emerging membrane type for milk protein fractionation (Schopf and Kulozik 2021; Schopf et al. 2021a; Weinberger and Kulozik 2021a). Due to the consequences of geometry- and manufacturing-related aspects, these module types vary widely regarding their separation characteristics, manufacturing and operational costs, packing density, flow characteristics, friction-induced pressure losses, cleanability, and their chemical, thermal and mechanical stability (Melin and Rautenbach 2007; Schopf et al. 2021b; Hartinger et al. 2020a; Kavianipour et al. 2017).

1.4.1 Hollow fibre membranes (HFM)

HFM, first developed by Mahon (1966), consist of polymeric fibres that are obtained by solution spinning or melt spinning (Luelf et al. 2016) of a polymeric material, typically polyether sulfone (PES) or PVDF. As the membrane characteristics are achieved during the polymerisation process, different additives and solvents can be added to improve particle size distribution or flux (Díez and Rosal 2020). Afterwards, the single fibres are bundled and glued into a pressure tube at both ends via a potting (see Figure 1-10a and b).

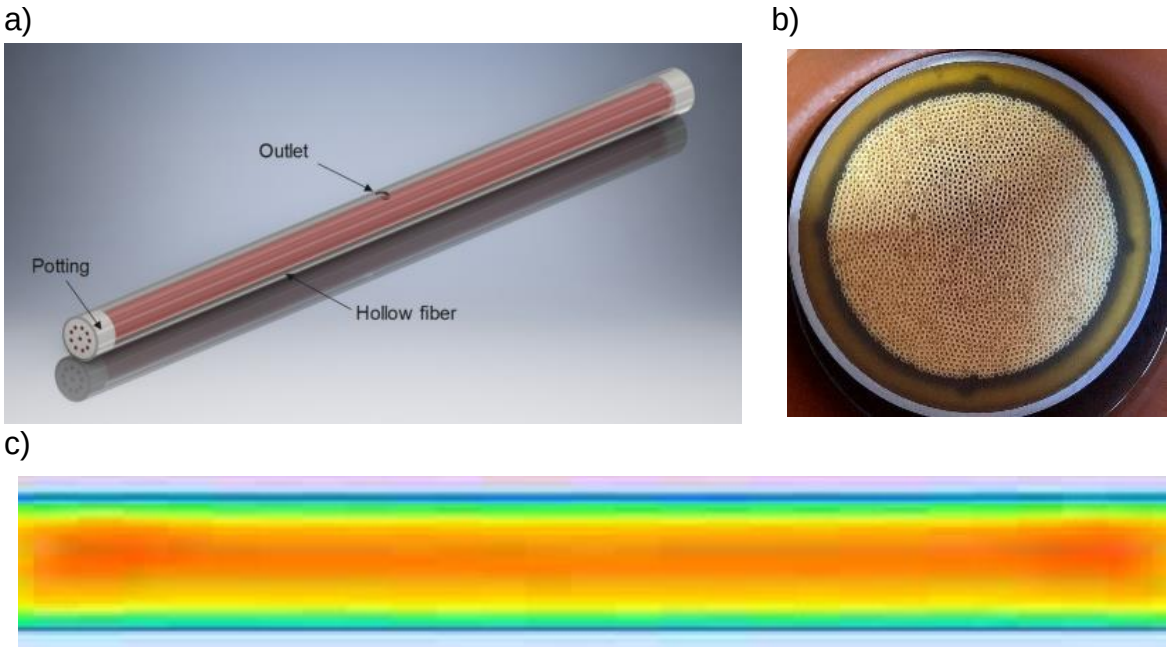

Figure 1-10. Illustration of an inside-out lab-scale HFM with ten hollow fibres (a) (Schopf 2022), the front-view of an industrial-scale HFM (b), and the flow properties within a channel with open cross-section visualised by computational fluid dynamics (CFD) simulations (Kavianipour et al. 2017).

The fibres and resulting modules can either be constructed for outside-in filtration, where the feed permeates from the outside into the fibre, or inside-out filtration, where the feed flows through the fibre and permeates outwards. While the former leads to a high active membrane area and suitability for high particle concentrations, the latter causes an improved fouling control due to the defined open cross-section (Xu et al. 2017). Regardless of the filtration mode, the fibres consist of a selective layer on the respective feed side, responsible for the separation characteristics, and a supporting layer on the respective permeate side, responsible for the fibre stability.

Resulting from the simple geometry and open cross-section, particularly for inside-out filtration, flow velocities are homogeneously distributed along the flow channel (see Figure 1-10c) with the typical pattern of decreasing flow velocities towards the channel wall (Kavianipour et al. 2017). Hence, HFM are not subject to flow shadows, meaning deposit formation can be somewhat controlled and deposits removed during cleaning. Nonetheless, fouling remains an issue for all feed systems (Laksono et al. 2021) and can be optimised by various aspects.

Influencing factors include the arrangement of a single fibre within a module due to hydrodynamics (Yeo and Fane 2005), the fibre diameter (Chang and Fane 2001) and the fibre wall thickness (Armbruster et al. 2018; Xu et al. 2017). A novel approach is varying the inner fibre geometry towards a sinusoidal/helical shape (Luelf et al. 2017; Tepper et al. 2022; Roth et al. 2019; Wiese et al. 2019) to increase turbulence and reduce fouling.

Regarding performance characteristics, Schopf et al. (2021b) comparatively assessed the three main module types CTM, SWM and HFM. Here, HFM was found to have a good packing density, filtration performance and low manufacturing costs (Schopf et al. 2021b; Baker 2012).

CTM is an alternative to HFM, which might be more suitable for certain applications and related processing demands. CTM has similar flow characteristics but typically uses multi-channel membranes. Hence, its filtration performance strongly depends on channel cross-sectional shapes (Springer et al. 2010), channel numbers and the local channel positions (Schopf et al. 2022; Hurt et al. 2015). Due to the ceramic material, CTM are more durable and robust against chemical and mechanical filtration or cleaning conditions, but are expensive during manufacturing, have a low packing density and the lowest whey protein mass flow per module (Schopf et al. 2021b; Baker 2012).

1.4.2 Spiral-wound membranes (SWM)

SWM are widely used in the dairy industry due to their low manufacturing cost, very high packing density and high whey protein mass flow per module (Schopf et al. 2021b). SWM consist of membrane pockets obtained by glueing together two flat-sheet membranes at their outer rims. These membrane pockets are connected to a central permeate collection tube (see Figure 1-11).

a) b)

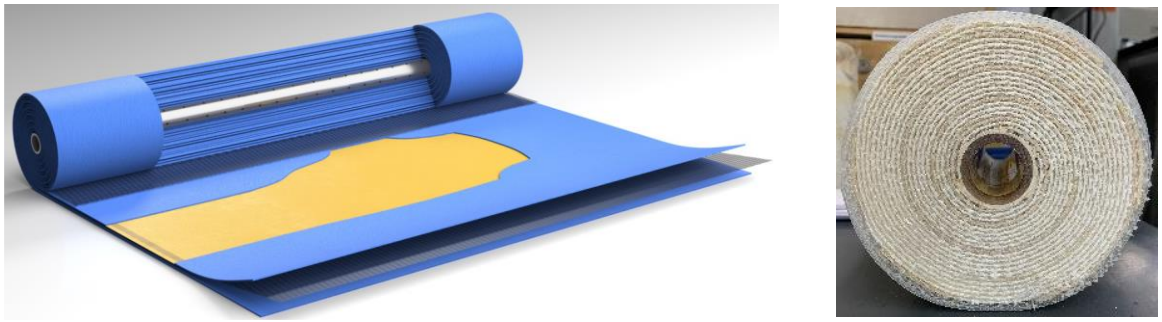

Figure 1-11. Illustration of an industrial-scale SWM (a) (Hartinger et al. 2019b) and its front-view (b).

To ensure defined flow channels, the membrane sheets form a membrane pocket, and each membrane pocket is separated by a feed spacer. The alternatingly stacked membrane

pockets and spacers are then wrapped around the permeate collection tube and fixed by an outer spacer wrap.

It is to be noted that the feed spacer is not connected or glued to the membrane sheets or permeate collection tube. Instead, it is only held in place by the friction induced by the compacting wrapping pressure and maintained by the outer spacer wrap. While an increased wrapping strength would increase friction and, thus, improve module stability, it would simultaneously reduce the active membrane area and could even disrupt the membrane's selective layer (Karabelas et al. 2018). Due to this tradeoff between performance, stability and potential membrane damage, wrapping strength is limited, and module stability mainly depends on the glue connections. Their stability depends on various construction- and process-related aspects. The former aspects mainly include the glue composition (Habenicht 2008) and geometry of glue connections, i.e. their design (Dilger 2010), overlapping length (Grote et al. 2018) and thickness (Althof 1984). The process-related aspects mainly include the process temperature (Habenicht 2008) and stress characteristics, i.e. its speed, intensity, kind and duration (Habenicht 2008; Althof 1984).

Two main membrane failure mechanisms arise from the construction, geometry and related stability limitations, namely rupture of membrane pockets and telescoping. The membrane/permeate pockets are particularly susceptible to negative Δp_{TM}, as this stresses the bond joints via peeling and can cause a rupture of the permeate pockets. Hence, manufacturers often state a maximum negative Δp_{TM}, usually 0.3 bar, to prevent this membrane failure mechanism. Negative Δp_{TM} can occur in the rear membrane parts during processing at high Δp_{TM} with high Δp_L or due to plant configuration, e.g. a height difference between the membrane and permeate tank. Lastly, pressure surges or water hammer could be induced by e.g. the sudden closing of a valve. A recent study by Avlonitis et al. (2010) confirmed that rapidly closing a valve in an RO membrane can lead to a short-time pressure increase of up to 6.0 bar, enough to damage the membrane modules severely.

The second primary failure mechanism, telescoping, describes an axial displacement of membrane sheets relative to the fixed permeate collection tube towards the retentate side as a result of frictional losses along the membrane module (Δp_L) surpassing the frictional stability of the module wrapping. Telescoping can also include a displacement of the feed spacer, leaving the channel width of related feed channels undefined and affecting the local fouling intensity as the flow velocities also change depending on the altered channel geometry. As a side effect of the axial displacements, membrane pockets can deform and rupture, and the shear of the spacer displacement along the membrane surface could also cause damage to the selective layer. Configurational measures to add stability are anti-telescoping devices (ATD), disk-shaped retainers in different configurations added to the module inlet and outlet. While this stabilises the membrane sheets, membrane manufacturers nonetheless limited the

maximum axial friction and Δp_L to 1.3 bar m^{-1} to prevent the consequences of telescoping. However, this restriction in Δp_L, v and τ_w strongly limits process-related options to control deposit formation or improve cleaning success with conventional cross-flow in SWM.

While spacers are necessary to ensure defined flow channels, spacers can also act as baffles and, thus, lead to reductions in Re_{crit}, as discussed in chapter 1.3.1, but also increased Δp_L (Hartinger et al. 2020a). Hence, they enable turbulent flow and improve flux (Howell et al. 1993; Neal et al. 2003) but also further limit the maximum applicable flow rates due to the increased Δp_L. Spacers consist of polymeric filaments that can have different geometric dimensions, i.e. shape and thickness, and arrangements, i.e. the angle and distance between filaments and the grid orientation towards the feed flow. A common spacer geometry is the diamond spacer (see Figure 1-12) which consists of spacer filaments perpendicular to each other. It can further be distinguished by whether the perpendicular filaments cross each other alternatingly or form two separate layers, namely woven or non-woven spacer grids.

a) b)

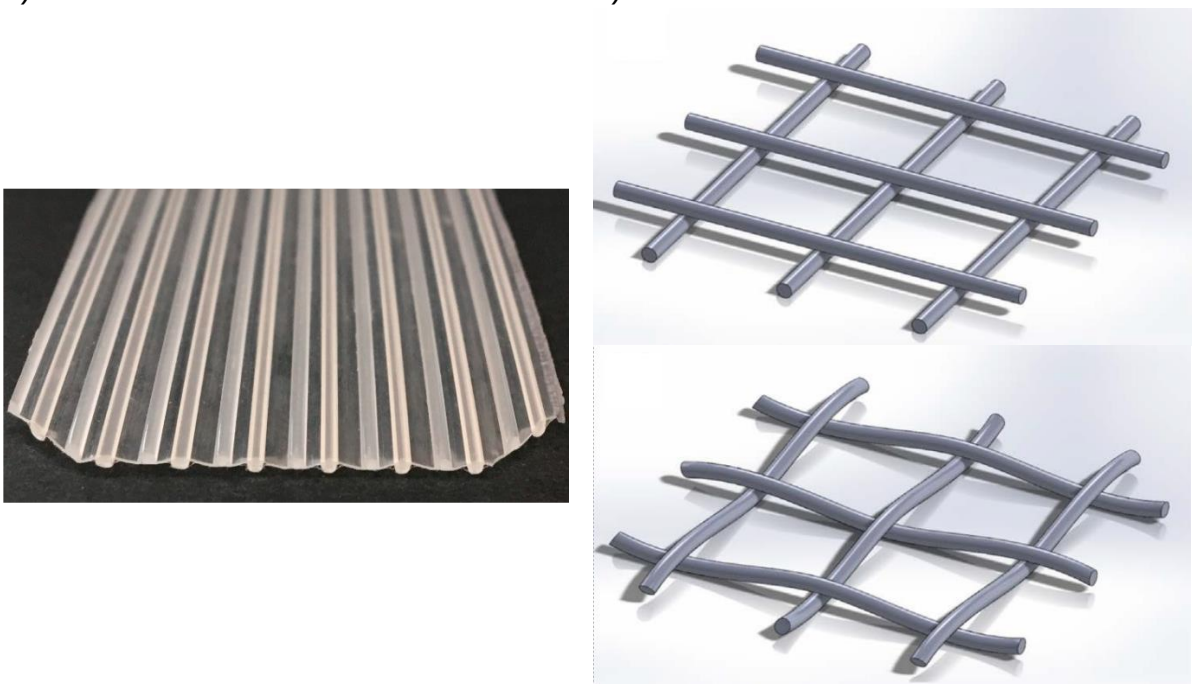

Figure 1-12. Parallel (a) (Hartinger et al. 2020a) and diamond spacer (b) in a non-woven (top) and woven (bottom) configuration (Gu et al. 2017).

Depending on the chosen geometry, such as parallel (Figure 1-12a) or diamond spacer (Figure 1-12b), not only the related improvements in process performance can vary widely (Hartinger et al. 2020a), but spacers can also induce significant flow shadows (see Figure 1-13a and b) and thereby cause severe issues with fouling (see Figure 1-13c) and cleanability.

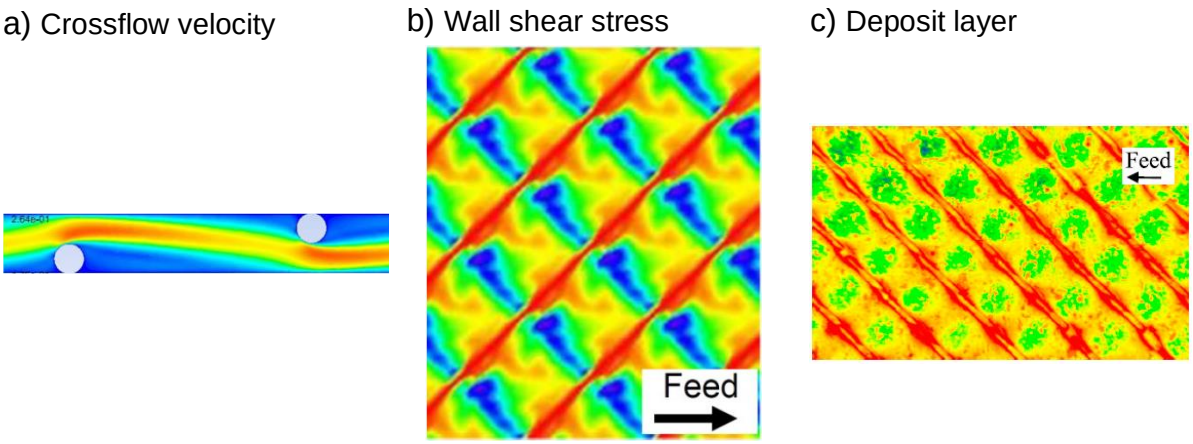

Figure 1-13. Flow properties within a channel containing a diamond spacer (grey circles) visualised by CFD simulations (a) (Kavianipour et al. 2017), the wall shear stress distribution of a channel containing a diamond spacer visualised by CFD simulations (b) (Koutsou et al. 2009), and the resulting local deposited protein amounts visualised by a false colour image of a Coomassie-stained membrane piece (c) (Hartinger et al. 2020a). Blue colour refers to a low value in the respective flow velocity, shear stress or protein deposition, while red refers to high values. Grey circles mark the crossing of a spacer filament.

Several CFD simulations (Koutsou et al. 2009; Kavianipour et al. 2017; Geraldes 2002; Gu et al. 2017; Han et al. 2018b; Schwinge et al. 2002; Fischer et al. 2020) examined the profiles of flow velocity (see Figure 1-13a) and shear stress (see Figure 1-13b) around different spacer geometries. Regardless of the examined Re number, all simulations showed distinct flow shadows, particularly in the close vicinity of the spacer filaments close to the membrane. Consequently, experimental works (Hartinger et al. 2020a) found an inhomogeneous fouling distribution with increased fouling accumulation in areas subject to flow shadows. A study investigating the rinsing behaviour of SWM found the rinsing duration to be dependent on the spacer dimensions, thus underlining the practical implications and issues related to spacer-induced flow shadows (Kieferle and Kulozik 2021).

Overall, it can be summarised that fouling is of particular importance in SWM, as the incorporated spacers create flow shadows with intense fouling. At the same time, this issue cannot be tackled by increasing flow velocities due to the limited mechanical module stability. Besides the fouling accumulation during filtration, the fouling control issues in SWM also extend to the subsequent cleaning process. Again, the limited mechanical stability limits the application of high shear forces for efficient fouling removal, particularly in areas subject to flow shadows. Additionally, the limited chemical stability induced by the polymeric material and glue connections exacerbates efficient chemical cleaning as the viable pH values are restricted. Depending on the fouling intensity and irreversible fouling share occurring during the filtration of a feed solution, intensive chemical cleaning might be a crucial step to enabling long-term stable membrane performance and ensuring plant and food safety. Hence, novel concepts to improve fouling control and cleaning performance, particularly by improving access to flow shadows, could significantly reduce the limitations of the established and otherwise very advantageous module type SWM.

1.5 Membrane cleaning

Overall, membrane cleaning aims to remove foulants by overcoming the attractive forces between foulants and the membrane formed during the filtration process and fully restoring the filtration performance. Different combinations of foulant, the surface to be cleaned, and processing parameters require different cleaning procedures and intensities. Despite fouling unfolding in numerous ways, some general principles regarding cleaning processes can be stated. Figure 1-14 provides an overview of the factors influencing cleaning efficiency and intensity.

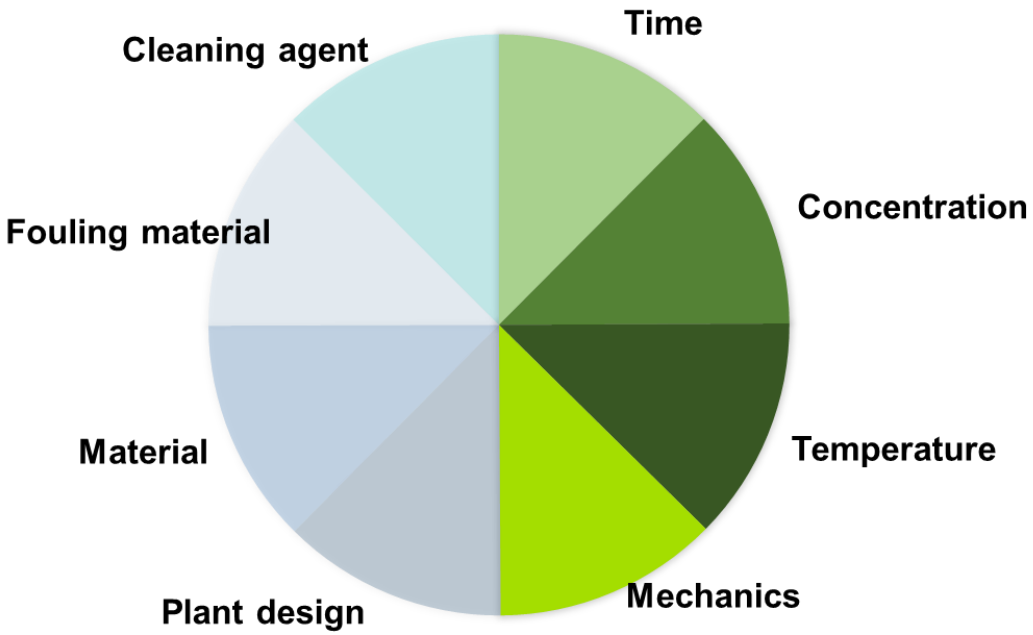

Figure 1-14. Overview of the factors influencing cleaning success.

Firstly, the plant design should follow the rules of hygienic design, meaning that it should be easy to clean without e.g. any flow shadows, sharp corners, limited drainability and many more (EHEDG 2018). The used materials and their characteristics, such as surface roughness or corrosivity, also affect the hygienic design and cleanability of the plant. Furthermore, the materials used also define the mechanical and chemical stability of the plant and, thus, its cleanability, as the weakest point defines the limiting fluid forces and pH values applicable during cleaning. While the fouling material is also a crucial aspect of cleaning efficiency, this aspect, combined with the plant materials and design, is usually fixed and not easily adjustable for improving cleaning success. The remaining factors can be attributed to mechanical and chemical aspects, i.e. the cleaning agent with its concentration, and the temperature and time supporting the cleaning agent's efficiency in removing foulants. While there are manifold cleaning agents with diverse functionalities and fields of applications, the main cleaning agents are alkalis for removing organic fouling, such as proteins, and acids for

removing inorganic foulants, such as minerals. Details on mechanical and chemical cleaning aspects will be discussed in the following chapters: 1.5.3 and 1.5.2.

For complex fouling, such as during skim milk MF, a typical cleaning cycle consists of several chemical cleaning steps accompanied by preceding and subsequent rinsing steps. An example is illustrated in Figure 1-15.

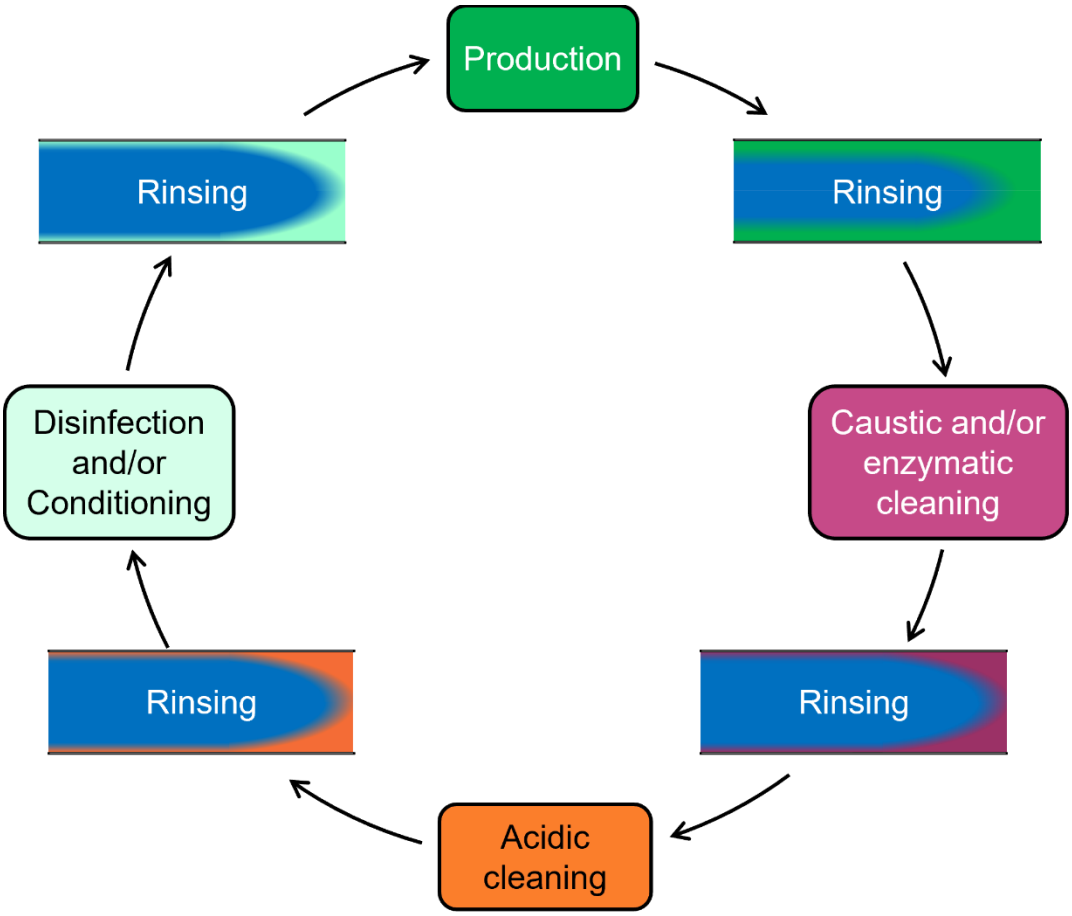

Figure 1-15. Schematic illustration of the steps included in a typical dairy cleaning cycle.

After the filtration of skim milk, a first rinsing step is needed to remove the bulk product from the filtration plant and loosely bound reversible fouling. The following chemical cleaning step and the order of chemical cleaning steps depend on the distribution of organic and inorganic fouling as well as specific interactions or possible detrimental effects between foulants and cleaning agents. Accordingly, with proteins dominating dairy fouling, the first chemical cleaning step is usually alkaline, often supported by enzymes or surfactants. However, acidic cleaning was recommended for some cases as a first step (Daufin et al. 1991; D'Souza and Mawson 2005), presumably due to a scenario-specific dominance of mineral fouling. In some cases, no effect of the chemical cleaning order on the cleaning success was found (Bartlett et al. 1995). After an intermediate rinsing step, an acidic cleaning removes any remaining inorganic fouling, which is important in whey applications (Trägårdh 1989). After another rinsing step, the cleaning cycle can be concluded by a disinfecting step, potentially necessary depending on the product and microbial load, a conditioning step to prepare the

membrane for the next filtration cycle (Trägårdh 1989), or another caustic cleaning step supplemented with chlorine (Bohner and Bradley 1992; D'Souza and Mawson 2005). While the necessary cleaning times of each step can vary depending on the dimensions of the filtration plant (D'Souza and Mawson 2005) and fouling intensity, chemical cleaning steps are usually run for 15 – 60 min (Regula et al. 2014) while rinsing steps are usually run for 5 – 20 min (D'Souza and Mawson 2005). In summary, this equals a time consumption of 2 – 4 h for a complete cleaning cycle.

In summary, the cleaning process is a very cost, chemical, energy and time-intensive process, making up around 30 % of the total environmental impact of the process unit filtration (including equipment, production and logistics) in the dairy industry (Gésan-Guiziou et al. 2019) and around 15 – 20 % of the operating costs (Regula et al. 2014). With dairy cleaning cycles of several hours to be performed for every 7 h of production time at 50 °C (Rabiller-Baudry et al. 2008; Schiffer and Kulozik 2020), cleaning also consumes a large share of potential production time. Hence, even minor improvements in cleaning efficiency can positively affect the process unit's ecological and economic sustainability.

1.5.1 Cleaning evaluation

While many hydraulic, physical-chemical and microbiological methods are available to evaluate cleaning success, the most commonly used one in industry and literature is the flux recovery rate (FRR). The reason is its easy accessibility, as this value can be obtained by measuring permeate flow. Normalising the permeate flux for Δp_{TM} gives the membrane permeability and allows a comparison of flux values independently of variations in Δp_{TM} (see eq. (1-13)).

$$Membrane\ permeability = \frac{J}{\Delta p_{TM}} \tag{1-13}$$

Division of the pure water membrane permeability after cleaning ($water\ permeability_{after\ cleaning}$) by the initial water permeability before filtration ($water\ permeability_{initial}$) then gives the FRR (see eq. (1-14)). The membrane is assumed to be hydraulically clean when the FRR surpasses 90 %.

$$FRR = \frac{water\ permeability_{after\ cleaning}}{water\ permeability_{initial}} \tag{1-14}$$

However, it is not free of flaws since flux measurements cannot reflect the chemical cleanliness (Rabiller-Baudry et al. 2008) as there might be proteins between pores or in the support layer of the membrane where they barely affect Flux (Trägårdh 1989; Blanpain-Avet et al. 2009). Contrary to cleaning results from studies investigating the UF of skim milk (Rabiller-Baudry et al. 2002; Rabiller-Baudry et al. 2008), Blanpain-Avet et al. (2009) found no

simple correlation between the hydraulic and chemical cleanliness for studies investigating the MF of whey protein concentrates. The authors attributed the differing results to the fouling scenario in MF being more complex, precisely due to internal fouling playing a major role only in MF systems. Another flaw is that flux measurements were found particularly unreliable when cleaning agents (e.g. surfactants or chlorine) interact with the foulant or the membrane, thus altering the membrane permeability regardless of its actual chemical cleanliness (Rabiller-Baudry et al. 2021; Daufin et al. 1991; Rabiller-Baudry et al. 2008; Trägårdh 1989).

Instead, several methods focus on chemical cleanliness using surface analyses such as Fourier-transform infrared spectroscopy (FTIR) (Daufin et al. 1991; Rabiller-Baudry et al. 2021; Väisänen et al. 2002; Berg et al. 2014), atomic force microscopy (AFM) (Väisänen et al. 2002; Ang et al. 2006; Li and Elimelech 2004), x-ray photoelectron spectroscopy (XPS) (Argüello et al. 2005; Daufin et al. 1991) or scanning electron microscope (SEM) (Rabiller-Baudry et al. 2021; Väisänen et al. 2002; Kim et al. 1993; Bird and Bartlett 2002) that evaluate the chemical composition of the membrane after cleaning compared to virgin and fouled membranes. However, most of these methods are destructive and thus do not monitor the temporal cleaning progression (Argüello et al. 2005; Daufin et al. 1991; Väisänen et al. 2002; Rabiller-Baudry et al. 2008) or only enable qualitative comparisons (Bird and Bartlett 2002; Berg et al. 2014; Partridge and Furtado 1990).

Other approaches to assess chemical cleanliness are the quantification of residual proteins on the membrane surface (Partridge and Furtado 1990; Allie et al. 2003), which is also destructive, or a quantification of the removed foulants in the cleaning solution (Kim et al. 1993; Matzinos and Álvarez 2002; Bansal et al. 2006; Nigam et al. 2008; Field et al. 2008). However, standard assays (Bobe et al. 1998; Dumpler et al. 2017; Bradford 1976; Smith et al. 1985; Lowry et al. 1951; Holzmüller and Kulozik 2016) are often limited by their sensitivity and provide no information on residual fouling.

Nonetheless, both FRR and protein removal allow quantitative comparisons between different flow types for an invariable cleaning agent. With contrasting results on the presence or absence of a correlation between hydraulic and chemical cleanliness reported (Blanpain-Avet et al. 2009; Rabiller-Baudry et al. 2002; Rabiller-Baudry et al. 2008; Wemsy Diagne et al. 2013), a combination of hydraulic and chemical cleaning evaluation methods should be used.

1.5.2 Chemical cleaning aspects

Besides the actual cleaning agents, water plays a unique role as it has several functions: It transports chemicals to the fouling layer, removes foulants and chemicals away from the membrane and conveys the mechanical forces of fluid dynamics to the foulants on and in the membrane. Depending on the severity of fouling and thus the distribution of

reversible and irreversible fouling, flushing steps (without additional chemicals) can be sufficient to remove large portions of the fouling layer. This helps reduce the dirt load for subsequent chemical cleaning steps and, thus, can enable reductions in the required concentration of cleaning agents. Despite the large amounts consumed during cleaning, high water quality is necessary. Otherwise, microorganisms, organic matter, suspended solids, or minerals could cause additional fouling (Rabiller-Baudry et al. 2002) or reduce the activity of cleaning agents (Trägårdh 1989) and, thus, reduce the cleaning efficiency. Hence, using high-quality water, i.e. deionized water, is an important aspect not to be neglected.

In terms of organic and inorganic fouling removal, this section focuses on alkaline cleaning as organic proteins are the dominant foulants during the MF of skim milk. Sodium hydroxide (NaOH) is the most used and researched alkaline cleaning agent and the working principle for removing proteins is as follows. In the first phase, NaOH diffuses into the protein matrix (see Figure 1-16a) (Gillham et al. 1999). This step is presumed to proceed rapidly as the caustic can easily penetrate the large membrane pores of an MF or UF, particularly for a non-zero Δp_{TM}, and thus, quickly diffuse into the thin deposit layers (Mercadé-Prieto and Chen 2005). The proteins react, swell and solubilize on contact with hydroxyl anions for pH-values >10 (Mercadé-Prieto et al. 2008; Gillham et al. 1999). Here, swelling describes a pH-induced charge increase leading to the unfolding of the protein structure, which translates to an increased size and swollen state. Additionally, particle distances change, which affects the prevailing forces according to xDLVO theory (see chapter 1.3.1), and the deposit becomes looser. During the uniform stage (see Figure 1-16b) for pH-values >11.2, NaOH breaks down the non-covalent crosslinks between the loosened protein aggregates and destroys the gel structure (Mercadé-Prieto et al. 2008; Gillham et al. 1999). For whey protein hydrogels, this was found to be the rate-limiting step of NaOH cleaning (Fan et al. 2019). The solubilised and loosened aggregates can then be removed via erosive forces. During this phase, the flux increases strongly as the bulk fouling progressively gets removed at a uniform cleaning rate (Gillham et al. 1999). While the first two phases are mainly governed by temperature and NaOH-concentration (c_{NaOH}), the removal of residual deposits in the final decay phase (see Figure 1-16c) is mainly governed by shear forces and the most time-consuming phase (Gillham et al. 1999). Here, the cleaning rate decreases until a steady flux value is reached.

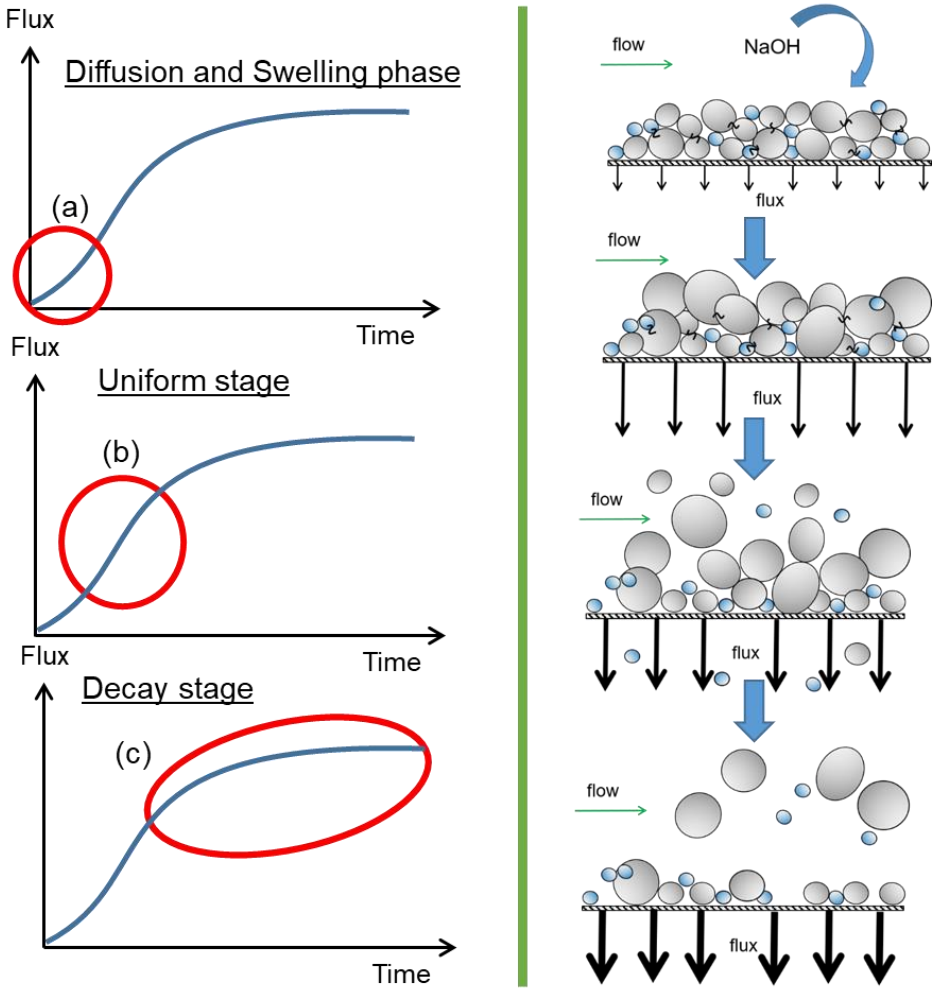

Figure 1-16. Overview of the three main cleaning phases according to Gillham et al. (1999) regarding flux progression (left) and schematic deposit removal (right).

Regarding cleaning times, it is to be considered that longer cleaning times do not necessarily provide improved cleaning results. Several studies cleaning membranes with different pore sizes, cleaning agents, cleaning concentrations, temperatures and foulants all found an optimum cleaning time, varying around 15 – 60 min, beyond which cleaning success does not further increase but eventually even decreases (Blanpain-Avet et al. 2009; Makardij et al. 1999; Bird and Bartlett 2002; Bartlett et al. 1995; Ang et al. 2006; Muñoz-Aguado et al. 1996). Exemplary, for the cleaning of an MF CTM membrane at 50 °C fouled with whey protein concentrate, an optimum cleaning time of 20 min was found (Blanpain-Avet et al. 2009).

One explanation for the flux decrease after e.g. 20 min is that foulants previously released into the cleaning solution redeposit onto the membrane surface (Field et al. 2008; Blanpain-Avet et al. 2009). Interestingly, whether flux reaches a steady-state value (Bird and Bartlett 2002; Matzinos and Álvarez 2002; Bansal et al. 2006) or decreases after reaching the maximum flux (Bartlett et al. 1995; Bird and Bartlett 2002; Makardij et al. 1999; Nigam et al. 2008) might, among others, be related to c_{NaOH} and only occur above a threshold concentration. Overall, the pH resulting from the chosen concentration poses the critical factor for the

effectiveness of chemicals (Trägårdh 1989), with the optimum being at pH 11 – 12 (Berg et al. 2014; D'Souza and Mawson 2005). However, for high c_{NaOH}, different mechanisms have been reported to affect cleaning success negatively. One theory is that at high pH for membrane-foulant combinations susceptible to internal fouling, gelation of the deposited proteins is more rapid than the dissolution and removal, leading to pore blockage and deteriorated removal (Mercadé-Prieto and Chen 2005; Mercadé-Prieto et al. 2008). Another study investigating the cleaning of whey protein aggregates concluded that for too high c_{NaOH} (> 0.2 mol L^{-1}), the swelling and subsequent cleavage of non-covalent interactions is hindered and, thus, slowed down due to screening effects of counter ions caused by the high ionic strengths (Fan et al. 2019). The observed decrease in cleaning efficiency at high pH is particularly interesting as hydrolysis only occurs for very high c_{NaOH} but not in the optimum pH range around 11.5 at 50 °C for 1 h (Berg et al. 2014; Wemsy Diagne et al. 2013; Paugam et al. 2010; Griggs 1921; Hou et al. 2017). This translates to either covalent interactions being somewhat irrelevant in fouling removal compared to non-covalent interactions or the benefits of hydrolysis being compensated by the accompanying disadvantages at high pH.

The optimum cleaning temperature for enzymatic cleaning agents (Regula et al. 2014) and NaOH (Bird and Bartlett 2002; Bartlett et al. 1995; Rabiller-Baudry et al. 2002; Väisänen et al. 2002; Kazemimoghadam and Mohammadi 2007; Kim and Fane 1995; Zhang et al. 2004) was reported to be at 50 °C but can differ for other cleaning agents. Although the time to reach the maximum flux was reduced for increasing temperatures up to 70 °C due to sped-up chemical reactions (Bartlett et al. 1995; Bird and Bartlett 2002), the maximum flux was reduced compared to 50 °C. This could be due to the inverse solubility of calcium phosphate causing stronger mineral fouling at elevated temperatures or, similar to the effects at high pH, due to rapid gelation causing intensified pore blockage (Bird and Bartlett 2002).

For cleaning with NaOH alone, several authors reported incomplete cleaning reaching no hydraulic cleanliness but only FRRs of 60 – 80 % (Blanpain-Avet et al. 2009; Bartlett et al. 1995; Bird and Bartlett 2002; Berg et al. 2014; Wemsy Diagne et al. 2013) and no complete removal of proteinaceous material (Blanpain-Avet et al. 2009; Paugam et al. 2010). Hence, industrial cleaning solutions often contain chemical additives such as enzymes, wetting agents, chlorines or surfactants to enhance cleaning power. The related benefits can include increased wettability, solubilisation, prevention of re-fouling, modification of the surface charge or enzymatic cleavage of foulants (D'Souza and Mawson 2005; Regula et al. 2014). However, adding supporting chemicals increases the environmental impact, wastewater pollution, and cost. Additionally, residual cleaning agents, which are a particular issue for surfactants due to their adsorption to (Byhlin and Jönsson 2003) and desorption from the membrane, could impair product quality and safety.

Furthermore, the frequency and harshness of cleaning conditions can even lead to membrane damage or a reduced lifetime, which cannot be ignored, considering that the replacement of membranes makes up 25-40 % of the total membrane plant cost (Maartens et al. 2002). Not only oxidative (Gitis et al. 2006; Yadav and Morison 2010; Causserand et al. 2006; Rouaix et al. 2006; Puspitasari et al. 2010; Rabiller-Baudry et al. 2021) but also alkaline cleaning (Bégoin et al. 2006; Hashim et al. 2011) were found to affect the chemical structure and morphology of polymeric membranes and their active layer (Porcelli and Judd 2010) in the long term. A detailed review of the causes and consequences of ageing was conducted by Regula et al. (2014). In short, the degradation leads to increased pore size, resulting in increased water flux and a deteriorated separation efficiency, and a modification of the membrane surface, resulting in reduced product flux due to increased fouling (Yadav and Morison 2010; Rabiller-Baudry et al. 2021).

Overall, NaOH cleaning has much optimisation potential, particularly in the decay phase, with the longest portion of necessary cleaning time being governed by fluid forces. While chemical additives could improve cleaning success, efficient cleaning and the avoidance of over-dosage of chemicals are critical to ensure long membrane lifetime, product quality, product safety and maximising production times by reducing cleaning times.

1.5.3 Mechanical cleaning aspects

Analogous to fouling during filtration, where the balance of prevailing forces decides over deposition, these forces govern the removal of deposits during rinsing and cleaning. While the previously discussed chemical cleaning aspects mainly help reduce the attractive force between the foulants and membrane by various mechanisms, mechanical forces govern the actual removal. The main factors governing deposit removal are the wall shear stress, determined by the flow velocity and flow channel geometry, and Δp_{TM}, which governs the fluid flow ratio along and towards/ through the membrane and, consequently, the compression of remaining deposits. Hence, following hydrodynamic principles, high flow velocities and low Δp_{TM} allow high shear rates and Reynolds numbers whilst only mildly compressing the deposit and generating the best cleaning results. However, some exceptions must be considered for both flow velocity and Δp_{TM}.

Regarding Δp_{TM}, it is commonly known that the FRR decreases with increasing Δp_{TM} (Blanpain-Avet et al. 2009; Wemsy Diagne et al. 2013; Bartlett et al. 1995; Mercadé-Prieto and Chen 2005). Nonetheless, so far it is unclear whether the optimum is at low Δp_{TM} or zero Δp_{TM}, meaning a closed permeate valve. Some authors found a Δp_{TM} = 0.0 bar to provide the best cleaning results in terms of FRR (Bartlett et al. 1995; Bird and Bartlett 2002; Blanpain-Avet et al. 2009) as this omits fluid forces pushing deposit further into/against the membrane surface.

However, while agreeing on zero Δp_{TM} providing the best FRR, one of those studies found a low non-zero Δp_{TM} = 0.25 bar to be superior in terms of protein removal (Blanpain-Avet et al. 2009). The authors attributed this to an applied Δp_{TM} mainly affecting the internal fouling, considerably present in the MF of whey protein. Consequently, manufacturers of cleaning agents often recommend starting MF membrane cleaning with the lowest possible Δp_{TM} to remove external deposits and then increasing Δp_{TM} to tackle internal fouling (D'Souza and Mawson 2005; Bartlett et al. 1995; Bird and Bartlett 2002). Ultimately, the present research findings cannot conclusively answer the question of the best Δp_{TM} for membrane cleaning, particularly as no studies investigated the effects of those differences in hydraulic and chemical cleanliness on filtration performance and as the answer might depend on the extent of internal fouling resulting from the membrane-foulant combination. Nonetheless, those findings emphasise the importance of assessing hydraulic and chemical cleanliness simultaneously and not isolated.

Regarding flow velocity, the effect of increased flow velocities on improving cleaning success is still under debate. Several studies on various foulants have shown removal kinetics to being a function of the flow velocity (Bird and Bartlett 2002; Jennings et al. 1957; Gallot-Lavallee et al. 1984; Kim et al. 2002) and wall shear stress (Visser 1970; Sharma et al. 1992), with removal times decreasing for increasing flow velocities (Gillham et al. 1999). However, several studies also found little to no effect of flow velocity on cleaning success (Bartlett et al. 1995; Daufin et al. 1991; Shorrock and Bird 1998; D'Souza and Mawson 2005; Cabero et al. 1999) without this effect depending on the prevailing flow regime (Bartlett et al. 1995). Some studies demonstrated that the impact of increasing flow velocities on cleaning success depends on the efficiency of the cleaning agent (Ang et al. 2006; Lee and Elimelech 2007; Lee et al. 2001). Hence, the interplay between mechanical and chemical cleaning should not be neglected when assessing the effects of either cleaning aspect. Again, another discrepancy between hydraulic and chemical cleanliness was found by Blanpain-Avet et al. (2009) for the MF of whey, as they observed positive effects of flow velocity only on hydraulic but not chemical cleanliness. One explanation could be that removing residual proteins blocking whole membrane pores strongly affects flux but is barely detected as additional protein removal. This would also translate to high flow velocities being beneficial to unblock pores and non-zero Δp_{TMs} being necessary for membrane-foulant combinations susceptible to internal fouling. Also, some authors pointed out that, especially for complex geometries with significant local differences in flow characteristics, removal mechanisms not only depend on the average wall shear stress but also on the fluctuation rate, i.e. local turbulence (Lelièvre et al. 2002). This means that even if the flow rate and thus the mean wall shear stress are low, high turbulence and thus high fluctuation of the wall shear rate can achieve good deposit removal (Lelièvre et al. 2002).

Generally, it can be concluded that, as a rule of thumb, low Δp_{TM} and high flow velocities benefit cleaning success. Nevertheless, because fouling and cleaning scenarios are very complex, several other factors of a given cleaning scenario must be considered. These include the intensity of deposit formation, the chemical cleaning efficiency affecting mechanical removability and the flow channel geometry.

1.6 Novel concepts to improve filtration and cleaning efficiency

In industrial plants, material or pump characteristics can limit applied pressures and flow velocities. Hence, in existing setups, cleaning efficiency might not be sufficient. Chemical and mechanical cleaning enhancement methods can aim to increase or accelerate fouling removal by using the capacities of the existing setup more efficiently or by adding additional equipment or chemicals.

1.6.1 Chemical approaches

Chemical approaches to reduce fouling during filtration include changes in the physico-chemical environment by adjusting e.g. the pH or calcium content to affect deposit characteristics (Adams et al. 2015; Jimenez-Lopez et al. 2008; Rabiller-Baudry et al. 2005) or adding a conditioning step prior to filtration to prime the membrane charge towards repelling particles (Schiffer et al. 2021). However, these approaches are commonly limited by only applying to one specific application. Another way to reduce fouling is by studying new ways, such as polymer blending, and new materials for membrane fabrication (Yin et al. 2023; Liao et al. 2013; Anvari et al. 2019; Rehan et al. 2016) or chemically modifying the membrane surface via e.g. surface grafting (Kumar and Ismail 2015; Igbinigun et al. 2016), plasma-induced grafting (Jaleh et al. 2019; Siow et al. 2006; Wang et al. 2018), UV-induced grafting (Abdul Rahman and Abu Seman 2018; Kaneda et al. 2019) or membrane surface coating (Li et al. 2014; Kasemset et al. 2016; Efome et al. 2016). Individual limitations include instability of coating layers or requiring energy-intensive and thus costly procedures (Díez and Rosal 2020). Also, as they represent lab-scale trials, most studies cannot provide insights into the long-term stability and performance or the scale-up and associated costs.

During cleaning, chemical approaches mostly comprise adding novel cleaning agents or assessing different combinations and orders of cleaning agents. Ng et al. (2017) compiled an extensive overview of those studies. While adding supporting cleaning agents can significantly enhance cleaning success, the related drawbacks of intense chemical cleaning leading to membranes ageing faster or even being damaged should not be neglected (compare chapter 1.5.2).

1.6.2 Mechanical approaches

While technical/mechanic approaches usually have the potential to improve every step in the process chain, i.e. filtration, rinsing and chemical cleaning, most of the following approaches have only been evaluated for one of those process steps. Besides other concepts to e.g. reducing length dependency by applying pressure gradients or generating uniform Δp_{TM} (UTP) by recirculating permeate to create a similar pressure loss on the permeate side (Kulozik and Kersten 2002b), most concepts aim to induce turbulence and fluid instabilities on the flow channel.

Concepts using external turbulence generation include vibrating modules (Al-Akoum et al. 2002), rotating discs (Meyer et al. 2015; Engler 2000; Ding et al. 2002), air slugs (Cui and Wright 1996; Cui and Taha 2003), scouring particles (Noordman et al. 2002), submersion of membranes in ultrasonic baths (Jin et al. 2014; Duriyabunleng et al. 2001) or electric fields (Visvanathan and Aim 1989; Wakeman 1998). These approaches utilise different ways of inducing an increased shear rate on the system and thus improving particle removal from the system. One of the most common limitations is the scale-up, as e.g. the application of ultrasound requires the membrane module to be submersed in an ultrasonic bath, which is challenging for the implementation in large industrial systems. Related drawbacks are the costs of implementing such concepts and the increased operation costs due to additional power consumption of the external turbulence generator. Also, no long-term studies on the effects of those concepts on membrane performance or the wear of membranes or pumps have been conducted, as e.g. applying vibration on membrane modules and surrounding plant components will require extensive plant robustness.

Another option to induce turbulence is by using static inserts, which can be spacers in FSM or SWM (Hartinger et al. 2020a; Winzeler and Belfort 1993) (see chapter 1.4.2), other inserts in open channels (Howell et al. 1993; Krstić et al. 2002) or membrane modifications e.g. in HFM leading to a coiled/ sinusoidal/ helical shape (Luelf et al. 2017; Tepper et al. 2022; Roth et al. 2019; Wiese et al. 2019) (see chapter 1.4.1). While the latter approach currently leads to higher-priced membranes, spacers and other inserts often also create flow shadows, thus generating issues with cleanability and plant hygiene (Hartinger et al. 2020a; Gu et al. 2017; Kavianipour et al. 2017).

The third option is to use forms of unsteady flow, i.e. a flow that constantly changes velocity or direction. One common approach is to invert Δp_{TM} and generate an inflow from the permeate side to actively push deposited material away from the membrane surface with different durations and intervals, thus called backpulse/backshock (frequent short cycles) or backwash/backflush (few long cycles) (Redkar et al. 1996; Mores and Davis 2003, 2002; Amar et al. 1990; Rodgers and Sparks 1992). As these approaches appear to be most beneficial for

applications with little fouling intensity (Kuberkar and Davis 1999), they are mostly used in the water treatment filtration process, where cleaning cycles can be omitted particularly long (Chang et al. 2017), to prolong filtration times further (Matsumoto et al. 1988). While this concept could be proven very beneficial in several studies, it can be challenging in scale-up as it is difficult to control the pressure in large systems. Additionally, some membrane types, particularly SWM, are incompatible with distinct negative Δp_{TM} and, thus, incompatible with applying concepts such as backflow from the permeate side.

Two more approaches towards unsteady flow are pulsed and alternating flow, which will be the focus of this thesis. Pulsed flow describes a flow constantly fluctuating between minimum (v_{min}) and maximum flow velocity (v_{max}) and related pressure conditions (see Figure 1-17). Hereby, the range between minimum and maximum flow rate (and pressure) defines the amplitude Δv (eq. (1-15)), while the summed duration of each one phase of low (Δt_{min}) and high flow velocity (Δt_{max}) defines the frequency f (eq. (1-16)). Alternating flow refers to a pulsed flow with additional feed-side cyclic flow reversal, i.e. a change of feed and retentate side but no backflow from the permeate side.

$$\Delta v = v_{max} - v_{min} \tag{1-15}$$

$$f = \frac{1}{\Delta t_{max} + \Delta t_{min}} \tag{1-16}$$

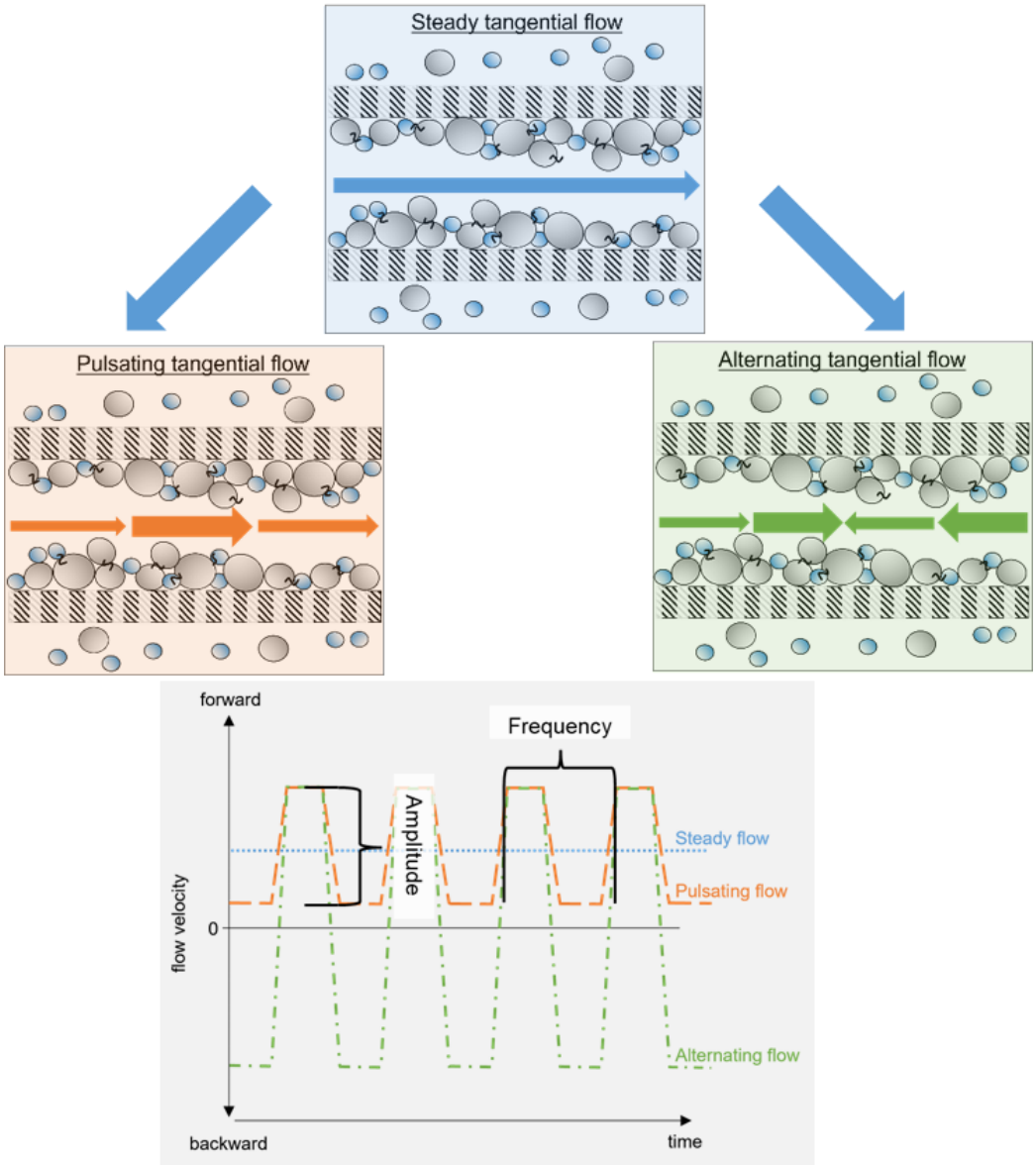

Figure 1-17. Comparison of steady (blue), pulsed (orange) and alternating flow (green) in terms of flow velocity. Curved braces define the range of flow velocity fluctuations (amplitude) and summed cycle time of each a high and low flow velocity phase (frequency), which are the most critical characteristics of pulsed and alternating flow.

Pulsed flow can be generated by e.g. pumps allowing rapid pump capacity ramps (Weinberger and Kulozik 2021a, 2021c, 2021b), which enable precise simultaneous control of flow and pressure conditions. Other types, such as bellows or piston pumps (Gillham et al. 2000; Bode et al. 2007) do not enable precise control as the intensity of piston/bellows strokes defines flow, pressure and time conditions dependently. Also, some studies using those pump units reported negative Δp_{TM} and, thus, flow velocities during the backwards-stroke phases (Gillham et al. 2000; Bode et al. 2007). Hence, an alternating flow was induced, which makes this type of pulsation creation unsuitable for examining pulsed flow in e.g. SWM systems. However, for more defined alternating flow conditions, e.g. with a pump system allowing rapid pump capacity ramps, the necessary plant modifications are more sophisticated and expensive as additional piping and precisely controlled valves are required to enable a defined change of

flow direction with identical flow and pressure conditions in both forward and backward flow phases. Nonetheless, studies utilising pulsed flow for cleaning pipes, i.e. non-permeable walls fouled with whey protein residues, found particularly distinct improvements when flow reversal, i.e. alternating flow, occurred (Blel et al. 2009a; Föste et al. 2013; Bode et al. 2007; Weidemann et al. 2014; Augustin et al. 2010).

Besides frequency (Gillham et al. 2000; Blel et al. 2009a; Blel et al. 2009b; Yang et al. 2019; Weidemann et al. 2014), amplitude (Gillham et al. 2000; Blel et al. 2009a; Blel et al. 2009b; Augustin et al. 2010) and flow regime (Gillham et al. 2000; Weidemann et al. 2014) as important influencing factors, modes of action including induced turbulence (Blel et al. 2009a; Blel et al. 2009b; Bode et al. 2007; Augustin et al. 2010), near-wall flow reversal (Blel et al. 2009a; Föste et al. 2013; Bode et al. 2007; Weidemann et al. 2014; Augustin et al. 2010), enhanced mass transfer (Gillham et al. 2000; Blel et al. 2009a; Blel et al. 2009b), deposit fatigue due to pressure fluctuations (Gillham et al. 2000) and the annular effect (Richardson and Tyler 1929; Schlichting and Gersten 2006) could be identified. The latter is characteristic of pulsed flow and, for laminar flow, describes a shift in the maximum flow velocity from the channel centre towards the channel wall, depending on the pulsed flow frequency (Richardson and Tyler 1929; Schlichting and Gersten 2006). Another theory is that improved removal is the cause of the combined phases of low flow and pressure, with relaxation and destabilisation of the deposit, followed by phases of flow and pressure, where the high shear stress causes enhanced removal of the destabilised deposits (Gupta et al. 1992). This would also explain the importance of frequency and amplitude as they define the intensity and frequency of fluctuations and, thus, the intensity of destabilisation during low flow phases followed by the intensity of shear stress during high flow phases.

Pulsed flow could already be shown to be beneficial for the cleaning of stainless steel geometries fouled with bacteria (Blel et al. 2009a; Blel et al. 2009b), egg yolk (Yang et al. 2019), starch matrices (Föste et al. 2013) or whey protein solution (Gillham et al. 2000; Bode et al. 2007), and for the filtration of silica particles (Bertram et al. 1993; Hadzismajlovic and Bertram 1998; Li et al. 1998), clay suspensions (Boonthanon et al. 1991), bentonite (Spiazzi et al. 1993), yeast suspensions (Hadzismajlovic and Bertram 1999; Howell et al. 1993; Weinberger and Kulozik 2021b, 2021c; Olayiwola and Walzel 2009) and different beverages (Gupta et al. 1992; Blanpain-Avet et al. 1999; Jaffrin et al. 1994). Similarly, alternating flow could improve the filtration performance for BSA solutions (Hargrove and Ilias 1999; Hargrove et al. 2003), yeast suspensions (Weinberger and Kulozik 2021c, 2021b, 2022) and perfusion processes (Pollock et al. 2013). To our knowledge, no systematic study on alternating flow cleaning has been conducted yet.

However, no general advantageousness can be stated. Instead, some important exceptions and distinctions, namely the feed system or chemical environment and the surface geometry, have to be noted.

No studies have been reported on pulsed/alternating flow membrane cleaning under crossflow conditions, e.g. after skim milk MF. The only study on pulsed flow membrane cleaning, conducted by Weidemann et al. (2014), was performed in dead-end mode with spray nozzles of perpendicular flow towards the membrane fouled with large (5 and 10 µm) inert model particles. The main differences between flow in steel geometries and membranes are the surface roughness and porosity. In contrast to steel geometries, membranes have a rough surface of open porous structure, allowing flow through the wall/membrane. Compared to closed and non-porous walls, where the flow velocity near the wall is assumed to be zero, fluid transport towards and through a porous wall causes a shift of the maximum flow velocities towards the wall and, thus, flow velocities above zero (Richardson and Tyler 1929; Camacho et al. 2012; Falade et al. 2017). Due to this enhanced friction near the wall/membrane, the flow velocity and shear stress profiles can be assumed to also differ significantly between open porous and non-porous surface geometries.

The chosen feed system could also be found to be of significant impact. While during the pulsed filtration of many different model feed systems, improvements in filtration performance could be observed, this was not the case during the MF of skim milk in HFM (Weinberger and Kulozik 2021a). The authors attributed the absence of positive effects to the specific fouling scenario of skim milk with smaller particles of different sizes, intensive cross-linking between proteins and the membrane and a resulting cohesive deposit. Additionally, during the cleaning of whey protein fouled steel piping (Bode et al. 2007), benefits of pulsed flow could only be observed in the presence of a cleaning agent (NaOH), but not for cleaning without NaOH, where the deposit is still intact. Hence, for complex and irreversible deposits, a chemical loosening of the deposit structure might be a prerequisite for the benefits with pulsed flow. The necessity of an additional chemical cleaning agent for efficient pulsed flow cleaning raises the question of whether the cleaning agent itself and its concentration also affect pulsation efficiency.

In summary, pulsed and alternating flow pose promising concepts to improve process efficiency as it has already been shown to be beneficial during filtration and cleaning processes. However, thus far, no studies on pulsed/alternating flow membrane cleaning have been conducted with complex feed solutions such as skim milk, and a systematic study on the effects of the cleaning agent on pulsation efficiency is also missing. Furthermore, scale-up could be an issue that remains to be solved as pumps enabling rapid pump capacity ramps are currently not available at an industrial scale.

2 Objective and outline

Crossflow microfiltration is a vital unit operation across many industries and applications. However, fouling remains a critical issue, decreasing filtration performance and requiring frequent cleaning cycles. While there are numerous approaches to decreasing fouling during filtration or improving fouling removal during cleaning, most of them have not been adapted to industrial scale yet and, besides scale-up, share other limitations such as hygienic issues, high cost or difficult control. Among the most promising approaches are pulsed and alternating flow, defined by flow velocity and related pressure conditions fluctuating between maximum and minimum values with a defined frequency and amplitude. One of the presumed modes of action is that fluctuation induces turbulence that loosens the deposits on the membrane. For alternating flow, which is a pulsed flow with an additional cyclic feed-side flow reversal, the enhanced fluctuation and change in stress direction might induce fatigue on the deposits.

Regarding cleaning, positive effects were reported only for cleaning whey protein-fouled stainless-steel geometries that significantly differ from membranes due to the roughness and open-pored structure with additional flow through the wall/membrane, causing fundamental differences in flow characteristics. While positive effects of those unsteady flow types could be shown for the filtration of simple one-component model solutions or suspensions, no positive effects could be shown for complex biogenic feed solutions such as skim milk. Interestingly, as one study during the cleaning of whey protein-fouled steel surfaces also found positive effects of pulsed flow only in the presence of a cleaning agent, the chemical environment and state of the deposit seem to be affecting unsteady flow efficacy. No studies on the cleaning and filtration of complex biogenic solutions have been conducted regarding alternating flow.

Hence, this work focused on investigating the effects and related influencing factors of pulsed and alternating flow on cleaning success after skim milk MF to enhance process efficiency and, thus, its economic and ecological sustainability. Following this goal, the present thesis aims to contribute to the following aspects.

A novel method must be developed to complement hydraulic cleaning evaluation via FRR by a chemical cleaning evaluation technique, allowing reproducible and highly sensitive detection and quantification of even traces of individual milk protein residues in cleaning solutions. This way, cleaning success can be determined both hydraulically and chemically in a non-destructive way.

In a second step, the efficiency of pulsed flow cleaning after skim milk MF should be evaluated for a low-concentrated NaOH within the presumed pH optimum range, precisely pH 11.3, at a typical industrial cleaning temperature of 50 °C. Here, the relationship between FRR,

protein removal and flux progression are to be comparatively assessed and optimum conditions in terms of pulsed flow frequency and amplitude for both v and Δp_{TM} identified. The increase in energy consumption resulting from pulsed flow should be weighed against possible improvements in cleaning efficiency to determine changes in the cleaning process's specific energy consumption or mechanical energy input efficiency and the resulting sustainability.

Based on these results, the identified optimum cleaning conditions are used to assess the influence of membrane geometry on pulsed flow cleaning efficiency. As SWM suffer from flow shadows and extensive fouling, it was hypothesised that pulsed flow inducing additional turbulence might be particularly useful in this membrane type. As SWM do not allow direct access to surface characterisation after cleaning, a test cell containing an FSM must be used, and results compared to those obtained in HFM. Additionally, as the chemical environment was shown to be of relevance, the effect of varying c_{NaOH} on pulsed flow efficiency should be investigated.

For alternating flow cleaning, the influences of frequency and amplitude on hydraulic and chemical cleanliness in HFM after skim milk MF need to be investigated for the first time. Then, the influence of length dependency can be assessed by varying membrane length and steady flow direction to distinguish between the effects of a permanent flow reversal for steady backwards flow cleaning and the cyclic fluctuation of shear stress, Δp_{TM} and flow direction for alternating flow cleaning.

Furthermore, the results and knowledge obtained during cleaning studies should be transferred to the pulsed/alternating flow microfiltration of skim milk at optimum settings and conditions. This assesses whether unsteady flow can enhance filtration performance even for complex biogenic solutions with intensive fouling when choosing optimum conditions. Again, energy consumption should be considered to assess the effects of pulsed/alternating flow on mechanical energy input efficiency.

Lastly, to tackle scale-up issues, a novel concept should be developed, enabling the utilisation of pulsed flow on industrial-scale membrane systems and pumps. The results obtained during lab-scale filtration and cleaning studies on HFM and FSM can then be compared to those of industrial-scale HFM and SWM.

The following chapters are organised along six peer-reviewed publications. The contributions of the doctoral candidate are described in front of each chapter.

3 Concentration, purification and quantification of milk protein residues following cleaning processes using a combination of SPE and RP-HPLC[2]

Christian Kürzl*, Heidi Wohlschläger, Simon Schiffer, and Ulrich Kulozik

Chair of Food and Bioprocess Engineering, TUM School of Life Sciences, Technical University of Munich, Weihenstephaner Berg 1, Freising, Germany

* Corresponding author

Summary and contribution of the doctoral candidate

The availability of reliable and informative methods is crucial to evaluating the success of cleaning membrane cleaning. However, single methods for cleaning evaluation are limited in their validity. Hydrodynamic methods, i.e. flux measurements, for example, cannot detect proteins between pores or in the support layer of the membrane and are affected by e.g. the chemical cleaning conditions. With the correlation between hydraulic and chemical cleanliness also unknown, a combination of methods should be used. Hence, a complementary chemical evaluation of cleanliness is vital for the validity of the interpretation of results. While standard assays provide easy-to-use approaches to protein quantification, they are limited in their applicability to evaluating cleaning success. This is due to their often absent capability of distinguishing and separately quantifying specific proteins and their restricted sensitivity. This is particularly challenging in lab-scale studies, where a high ratio of plant volume to active membrane area is present, as this causes cleaning samples to contain low protein concentrations. Hence, a novel method allowing the separate quantification of milk proteins at very low concentrations had to be developed.

The chosen approach comprised a pre-concentration via solid-phase extraction (SPE) and a protein quantification by reversed-phase high-performance liquid chromatography (RP-HPLC). Here, SPE allowed a selective hydrophobic binding of the milk proteins to a modified C18 silica gel-containing cartridge while other sample substances could pass the cartridge unhindered. Combined with the subsequent elution by a solution with a higher affinity to the cartridge, the concentrated proteins could be collected for quantification by RP-HPLC. Again

[2] Original publication: Kürzl et al. (2022b): Kürzl, C.; Wohlschläger, H.; Schiffer, S.; Kulozik, U. 2022. Concentration, purification and quantification of milk protein residues following cleaning processes using a combination of SPE and RP-HPLC. MethodsX 9, 101695. doi: 10.1016/j.mex.2022.101695. Adapted original manuscript. Adaptations of the manuscript refer to enumeration type, citation style, spelling, notation of units, format, and merging of all lists of references into one at the end of the dissertation. No special permission is required to reuse all or part of the article published by Elsevier Limited.

based on hydrophobic interactions, a solvent gradient with increasing hydrophobicity enabled the separate UV-detection and subsequent quantification of the four major caseins (κ-CN, α_{S2}-CN, α_{S1}-CN and β-CN) and the two major whey proteins (α-LA and β-LG).

Overall, the developed approach enabled a high recovery rate of proteins (> 94%), a high reproducibility (coefficient of variation < 3.0%), and a flexible adjustment of required concentration factors (≤ 500) without comprising the recovery rate of proteins. Regarding robustness, the method and its results were not significantly affected by NaOH concentrations between 0 – 0.3% in the cleaning sample.

The doctoral candidate designed the experimental concept and approach based on a critical literature review with support from Heidi Wohlschläger. Furthermore, the doctoral candidate conducted experimental work, data analysis, interpretation, calculation and plotting. The doctoral candidate also wrote and revised the manuscript. The co-authors contributed to the project outline, the discussion of results, the execution of experiments, and the revision of the manuscript.

Abstract

Detection and quantification of milk protein residues can be of utmost importance for validation of cleaning process efficiency in removing even traces of residues as well as quality assurance and product safety. However, currently available assays cannot provide a combination of high sensitivity and a simultaneous quantification of the individual milk proteins. Furthermore, a low protein-to-protein-variability and high compatibility with other reagents such as residual cleaning agents (e.g. surfactants) cannot be ensured. Therefore, a new method was developed comprised of a pre-concentration of proteins by solid-phase extraction and optimisation of the sensitivity of an existing reversed-phase high performance liquid chromatography method for the separate quantification of bovine milk proteins κ-Casein, α_{S2}-Casein, α_{S1}-Casein, β-Casein, α-Lactalbumin, and β-Lactoglobulin. Hereby, solid-phase extraction enables robust and reproducible purification and concentration of protein residues with a high protein recovery rate and flexible adjustment of concentration factors. The increased sensitivity of the reversed-phase high performance liquid chromatography method was achieved by changes in the measurement wavelength and guanidine buffer concentration. This new method enables reproducible concentration, purification and quantification of protein concentrations below 7 ng mL^{-1} and thus can be used to detect milk protein residues in highly diluted aqueous systems.

Highlights:

- Concentration, purification and quantification of milk protein residues with a high recovery rate of proteins (> 94%) and high reproducibility (coefficient of variation (CV) < 3.0%)
- Flexible adjustment of sample volumes allows the utilisation of high concentration factors (≤ 500) without compromising the recovery rate of proteins (recovery rate of proteins decreases by 2.74% per 100 CF)

Keywords: skim milk, casein, whey protein, cleaning validation, beta-lactoglobulin, low protein concentration, quality assurance, quality control, product safety

Graphical abstract:

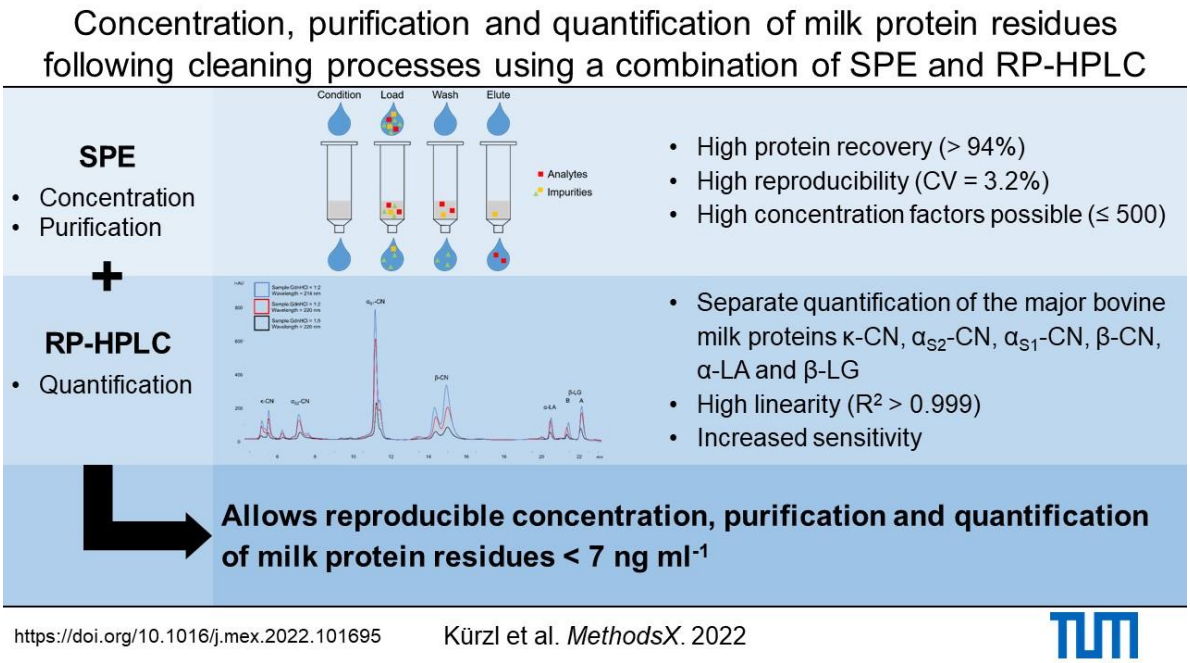

3.1 Method details

Background information and applicability of the method

The analysis of milk protein residues in highly diluted systems, as in cleaning validation or quality control, still poses a major challenge. Standard assays such as Bradford (Bradford 1976; Compton and Jones 1985), bicinchoninic acid (BCA) (Smith et al. 1985), Coomassie-staining (Congdon et al. 1993), Lowry (Lowry et al. 1951), Dumas (Wiles et al. 1998), or ultraviolet (UV) absorption provide easy-to-use approaches for protein concentrations in the range of 0.5 – 2,000 µg mL^{-1} (without taking the assay-specific sample dilutions into account). Therefore, they are limited in their applicability for the validation of cleaning processes or the detection of allergens such as β-Lactoglobulin (β-LG) in production plants where significantly lower concentrations can be relevant and specific proteins need to be identified. In contrast to the firstly mentioned methods, polyacrylamide gel electrophoresis (PAGE) (Holzmüller and Kulozik 2016) and RP-HPLC (Bobe et al. 1998; Bonfatti et al. 2008; Dumpler et al. 2017) allow a simultaneous detection and quantification of individual milk proteins. For this method, RP-HPLC was chosen due to being a reproducible and well-established method for protein quantification of bovine milk samples.

However, the sensitivity of commonly used RP-HPLC methods for milk protein quantification is limited to a protein concentration of 6.25 µg mL^{-1} (Bonfatti et al. 2008; Bobe et al. 1998), which is insufficient in determining traces of milk proteins on surfaces of technical equipment in highly diluted aqueous cleaning solutions after cleaning-in-place (CIP) processes. Therefore, a solid-phase extraction (SPE) was established in this work as a concentration method prior to RP-HPLC analysis.

The working principle of the applied SPE approach is based on a hydrophobic binding of proteins onto a modified C18 silica gel embedded into a cartridge while other substances in the sample solution pass unhindered (Hennion 1999; Poole and Poole 2002). Besides hydrophobic binding as the main binding mechanism, remaining free silanol groups also allow for polar secondary interactions such as hydrogen bonding. Due to the working principle of SPE, it is possible to adjust the concentration factor freely by increasing the applied sample volume. Even highly diluted solutions can be concentrated to such an extent that they fall within the detection range of the quantification method with regard to the specific analyte. A limitation of the concentration by SPE is given by the loading capacity of the chosen cartridge size (Hennion 1999). Compared to this approach, other concentration methods such as centrifugal filters or acetone precipitation can only achieve high concentration factors with larger centrifuges or several repetitions of the centrifugation step due to large volumes to process.

With regard to the protein binding onto the SPE material, the sample flow rate must be controlled and cannot exceed a certain limit, without a decrease in the dynamic binding

capacity (Hennion 1999; Poole and Poole 2002). Hence, the applied sample volume determines the time required to bind the proteins in an initial phase of the concentration process on the SPE material. After hydrophobically binding the proteins on the SPE material, a washing step with ultrapure water was conducted in order to remove unbound as well as other weakly bound substances, e.g. residual cleaning agents or other sample components such as salts and lactose. Subsequently, the analytes were eluted with a low volume of a more hydrophobic solvent – containing acetonitrile (ACN), trifluoroacetic acid (TFA) and ultrapure water – from the cartridge. Hereby, the extent of hydrophobic and polar regions in the analyte as well as the amount of remaining free silanol groups determine the required hydrophobicity of the eluent. Thus, it is possible to reduce the sample volume. Due to hydrophobic regions in the structure of milk proteins, this method shows a high recovery rate of proteins over the concentration process. Due to the binding mechanisms being mainly based on hydrophobic interactions and to some extent on polar secondary interactions, the binding strength depends on the protein's structure, size and state. Hence, a change in analyte always necessitates new calibration and validation. Details will be discussed in the Method validation section.

In summary, the SPE-based method can be conducted to purify and concentrate analyte and to remove substances that might interfere with a quantification of the individual milk proteins by RP-HPLC. Since the applied sample volume and initial protein concentration determine the processing time of the concentration step by SPE, the available sample volume and protein concentration could restrict the applicability of this method. Therefore, an increase in the sensitivity of the subsequent RP-HPLC quantification step was investigated to reduce the necessary concentration factor, the required sample volume and the SPE time.

With regard to the protein analysis in skim milk by RP-HPLC, Bobe et al. (1998) developed a method which enables the quantification of the four major caseins (CN) (κ-CN, α_{S2}-CN, α_{S1}-CN and β-CN) as well as the two major whey proteins (α-LA, and β-LG) in bovine milk. In this method, the milk proteins are diluted in a guanidine (GdnHCl) buffer and bind by hydrophobic interactions onto a silica-based C-18 RP-HPLC column. Afterwards, the proteins are gradually removed by an ACN based solvent gradient with increasing hydrophobicity, which allows a quantification of the individual bovine milk proteins by UV-detection. Hereby, the applied wavelength of the UV-detector determines the detected component in the sample. At a wavelength of 260 – 290 nm mostly the aromatic amino acids Tryptophan, Tyrosine, Histidine and Phenylalanine are detected, whereas peptide bond absorption is detected at wavelengths of 190 – 230 nm, respectively (Scopes 1974; Nielsen and Schellman 1967; Pace et al. 1995). Thus, at low wavelength the absorption is dominated by peptide bonds. At these wavelengths, aromatic side chains show only a slight absorption which induces a lower protein-protein variability due to the reduced impact of the content of specific amino acids. However, technical difficulties were reported for detection at wavelengths below 200 nm, such as an

increasing signal noise induced by the absorption of air (Scopes 1974). Furthermore, absorption maxima shift for different proteins and their different molecular states, depending on pre-treatment, degree of nativity as well as present solvents and their concentrations (Scopes 1974; Grimsley and Pace 2004; Pace et al. 1995; Nielsen and Schellman 1967). Therefore, depending on the sample matrix and the aim of the analysis, different wavelengths might be required, which is an unknown, thus limiting the reliability of the results for samples with different protein states.

Due to the impact of changes in solvents and sample composition, different observations regarding the performance optima at different wavelengths were made by several authors (Bobe et al. 1998; Bonfatti et al. 2008; Bonizzi et al. 2009; Dumpler et al. 2017). Bobe et al. (1998) used a wavelength of 220 nm instead of 210 nm within the UV-detection during RP-HPLC, in order to reduce baseline noise as well as to enhance the peak resolution. In contrast to that, Bonfatti et al. (2008) applied a wavelength of 214 nm instead of 220 nm for the same reasons. However, in a subsequent study, Dumpler et al. (2017) showed a high resolution with a detection wavelength of 220 nm, similar to the observations made by Bobe et al. (1998). Besides wavelength, the RP-HPLC method for milk protein quantification as established by Bobe et al. (1998) has been further adapted by Bonfatti et al. (2008), Bonizzi et al. (2009) and Dumpler et al. (2017) regarding the optimisation criteria of higher resolution, increased simplicity of sample preparation and quantification of protein concentrates. The lowest detectable protein amount for an individual protein was reported to be approximately 0.5 µg for α-LA (6.25 µg mL^{-1}) (Bonfatti et al. 2008; Bobe et al. 1998). In the latest modification of the method, as reported by Dumpler et al. (2017), a minimum quantifiable individual protein concentration of approximately 25 µg mL^{-1} in the initial sample can be determined. This is due to the maximum injection volume of most HPLC setups being limited to 100 µl, as well as the 5-fold dilution with guanidine buffer as part of the sample preparation prior to the analysis. The most recent modification of the method, conducted by Dumpler et al. (2017) enables a reduction of the sample analysis time, as well as a high resolution by an optimisation of the applied solvent gradient. Additionally, the buffering capacity was enhanced by an increased sodium citrate amount and furthermore, the storage stability at room temperature was increased by an enhanced guanidine concentration (5.1 M) during sample preparation. The guanidine concentration was increased in order to counterbalance the instability of whey proteins at room temperature as observed by Bonfatti et al. (2008). The instability of whey proteins was assumed to be caused by a guanidine concentration insufficient to completely denature the present whey proteins and thus leading to a refolding of the proteins in the buffer solution as a function of the storage time explaining the decreased detection of proteins during RP-HPLC after storage of samples for several hours at room temperature (Greene and Pace

1974; Dumpler et al. 2017). With this increased GdnHCl concentration (5.1 M) in the sample, proteins in concentrated skim milk with up to 27% total solids could be quantified.

However, the dilution of milk samples with GdnHCl buffer as shown by Dumpler et al. (2017) was calculated for concentrated samples, whereas the approach investigated in this study focuses on the quantification of protein residues in diluted aqueous systems and thus protein concentrations lower than a third of that in milk after pre-concentration with SPE. The concentration by SPE, as explained above, produces a purified aqueous protein system with low protein content. Therefore, lower buffering capacity and lower GdnHCl concentrations are required in comparison to the concentrations used by Dumpler et al. (2017). Hence, the sample dilution in GdnHCl buffer could be reduced to 1:2 leading to a final GdnHCl concentration of 3 M in the sample. Furthermore, due to the reduced dilution of the initial sample, the detection limit is decreased. Additionally, a wavelength of 214 nm was applied to increase signal response and thus decrease the detection limit.

The combined improvement of SPE and RP-HPLC methods, as targeted in this study, allows to concentrate, to purify and to quantify proteins in diluted test samples containing extremely low amounts of milk protein residues. The developed method enables a flexible adjustment of required concentration factors according to the target analyte under consideration. In this regard, the increase of applied sample volume and thus concentration factor is only limited by the loading/binding capacity of the SPE cartridge, which must not be exceeded. Furthermore, the specific binding mechanism of proteins onto the SPE material reduces the appearance of interfering substances, e.g. of polar substances such as residual cleaning agents, in the produced concentrate. The developed SPE method is likely to be applicable to other protein systems apart from diluted aqueous solutions derived from removing milk protein deposits on solid surfaces or similar applications, possibly with slight adjustments to the procedure or sample state. A main limitation of the method is that higher concentration factors (CF) and volumes are accompanied by longer processing times of up to 11 h. In future studies, a significant reduction of processing times might be achieved by using larger cartridges that allow higher flow rates or pre-concentrating the sample with e.g. a rotary evaporator.

Preparation of solvents

Solvent A (0.1% TFA, 90% ultrapure water and 10% ACN) and solvent B (0.07%TFA, 90% ACN and 10% ultrapure water) are prepared according to Dumpler et al. (2017) and used for the RP-HPLC analysis. Furthermore, the solvents A and B are also used during the elution step of the SPE concentration. The guanidine buffer is prepared according to Dumpler et al.

(2017) containing 6 M guanidine hydrochloride, 21.5 mM trisodium citrate, 19.5 mM dithiothreitol (DTT) and 0.1 M BisTris buffer (pH 6.8).

Concentration and purification of sample solution by SPE

The assessment criteria for the applicability of the developed SPE method is determined by the recovery rate of proteins (see equation (3-1)). The recovery rate of proteins is defined as the quotient of the detected protein concentration after SPE ($c_{protein,\ detected}$) and the applied protein concentration of the initial sample solution without SPE ($c_{protein,\ applied}$), measured by RP-HPLC. Hereby, it can be differentiated between the total protein concentration and the concentration of an individual milk protein.

$$\text{Recovery rate of protein} = \frac{c_{protein,\ detected}}{c_{protein,\ applied}} \tag{3-1}$$

The CF produced by SPE, is defined as the quotient of the applied initial sample volume V_{sample} and the elution volume $V_{elution}$ during protein desorption (see equation (3-2)).

$$CF = \frac{V_{sample}}{V_{elution}} \tag{3-2}$$

The applied concentration factor achievable by SPE depends on the availability of sample volume as well as the protein concentration in the sample. If the protein concentration in the sample is known or can reliably at least roughly be estimated, the required CF and sample volume can be calculated with the following equations (3-3) – (3-4):

$$CF_{req} = \frac{c_{min,\ RP\text{-}HPLC}}{c_{protein,\ applied}} \cdot \frac{1}{\text{protein recovery rate}} \tag{3-3}$$

with $c_{min,\ RP\text{-}HPLC}$ as the lowest quantifiable protein concentration of the RP-HPLC method (see Method validation section) and CF_{req} as the required concentration factor to process a quantification with RP-HPLC. Combining equations (3-2) and (3-3), the required sample volume ($V_{sample,\ req.}$) critical for a concentration with SPE in order to conduct a protein quantification with the modified RP-HPLC method, can be calculated by the following equation (3-4):

$$V_{sample,\ req.} = \frac{c_{min,\ RP\text{-}HPLC}}{c_{protein,\ applied}} \cdot \frac{V_{elution}}{\text{protein recovery}} = CF_{req.} \cdot V_{elution} \tag{3-4}$$

Here, $V_{elution}$ = 3 mL and values for $c_{min,\ RP\text{-}HPLC}$ can be seen in Table 3-2.

If the sample volume is limited or contains various proteins, the required sample volume for the concentration factor must be calculated for the protein with the lowest concentration or a certain target protein. If the sample volume is not limited, it is recommended to aim for a $V_{sample} > 1.1 \cdot V_{sample,\ req}$.

Procedure of the SPE method

Sample preparation

1 If applicable: filter particulates from sample with a sterile filter (0.45 µm)

2 Add 22.67% of a 3 mM $Ca(OH)_2$ solution and 8% solvent B to the sample

3 Adjust pH with 1 M HCl and 1 M NaOH to 7.0 ± 0.03

Note: The increase in hydrophobicity, achieved by addition of solvent B, was necessary to improve protein binding onto the sorbent. Low binding with pure water as a medium could be due to proteins assembling into more hydrophilic complexes or insufficient wetting of the silica surface. $Ca(OH)_2$ was added to reduce negative charges in the calcium-sensitive proteins α_{S2}-CN, α_{S1}-CN and β-CN (Horne and Dalgleish 1980; Horne 2020) and thus improve their binding onto the hydrophobic sorbent.

SPE cartridge preparation

1 Connect the cartridge to the vacuum chamber and open the connection between cartridge and vacuum chamber (outlet)

2 Condition the sorbent with 6 mL ACN (slight vacuum can be applied; flow rate < 3.0 mL min^{-1})

3 Equilibrate the sorbent with 6 mL ultrapure water (slight vacuum can be applied; flow rate < 3.0 mL min^{-1})

Note: The flow rate should be <3.0 mL min^{-1} for all steps except the washing step (< 6.0 mL min^{-1}) and can be adjusted by partially closing the outlet or applying a slight vacuum. In case the next step (sample application) is not executed immediately afterwards, leave ~1 mL ultrapure water in the cartridge and close the outlet until continuation of the process to avoid a drying of the SPE sorbent.

Sample application

1 Apply the desired amount of prepared sample volume (at least the minimum required volume calculated with equation (3-4)) before the ultrapure water from the equilibration step has completely run through, to avoid a drying of the cartridge (slight vacuum can be applied; flow rate < 3.0 mL min^{-1})

2 Rinse the cartridge with 6 mL ultrapure water

Note: Avoid drying of the SPE material and the entrapment of air bubbles. In case the next step (washing application) is not executed immediately afterwards, leave ~1 mL ultrapure water in the cartridge and close the outlet until continuation of the process to avoid a drying of the SPE sorbent.

Washing step

1 Wash with 100 mL ultrapure water (slight vacuum can be applied), with a flow rate of < 6.0 mL min^{-1}

2 Apply vacuum and let the cartridge run dry for 5 min to remove any leftover water

3 Close the outlet

Elution step

1 Apply 1.5 mL of elution agent containing 61.6% solvent A and 38.4% solvent B and let it soak for 3 min to ensure diffusion of the elution agent into the sorbent matrix and to enhance the removal of analytes from the sorbent

2 Open the outlet (no vacuum applied; flow rate < 3.0 mL min^{-1})

3 After the passage, apply a vacuum for 15 s to recover the elution agent and thus enable a reproducible quantification of the protein amount of the initial sample

4 Repeat steps 1 – 3 once

Note: The optimum solvent composition and thus hydrophobicity depends on sample characteristics, cartridge characteristics and interactions between the two. The chosen composition showed the highest recovery for diluted milk samples compared to more polar or more hydrophobic eluents. It is known that a repeated elution with low volumes leads to an enhanced protein recovery rate compared to a single elution with a higher volume. For diluted skim milk samples, a 2-fold elution with 1.5 mL each showed a protein recovery rate of 94.2%, while keeping the elution volume low and therefore enabling concentration factors of up to 500 (see Method validation section for details). Due to the incomplete recovery, SPE cartridges should not be re-used. Complete recovery of the elution agent can be validated with a 100 µl pipette.

Calculation

Calculate the protein mass of the sample applied to the SPE cartridge $m_{protein,\ applied,\ SPE}$ by RP-HPLC measurement (see equation (3-5)) and the inclusion of the additional SPE terms (see equations (3-1) and (3-2)).

$$m_{protein,\ applied,\ SPE} = c_{protein,\ initial\ sample} \cdot V_{sample} = c_{protein,\ applied,\ RP\text{-}HPLC} \cdot V_{elution} \cdot \frac{1}{\text{protein recovery rate}} \quad (3\text{-}5)$$

with $c_{protein,\ applied,\ RP\text{-}HPLC}$ as the protein concentration detected in RP-HPLC and $c_{protein,\ initial\ sample}$ as the protein concentration in the initial sample.

To calculate whether a selected sample volume is within the compatible range of RP-HPLC and SPE, the protein recovery rate should be omitted since proteins that bind only weakly and are washed out or bind too strong to be eluted, must still be counted towards the loading capacity.

Validation

1 Process a RP-HPLC of a skim milk sample in order to obtain the protein concentration for the following validation

2 Dilute skim milk 1:120, 1:900, 1:3,000, 1:6,000 and 1:9,000 with ultrapure water, conduct a concentration by SPE (as described above), dilute the SPE eluate 1:2 in GdnHCl buffer and process a RP-HPLC with a detection wavelength of 214 nm

3 Evaluate results according to equation (3-6) and calculate the protein recovery rate according to equation (3-1).

Note: If this method is to be applied to other protein systems, the concentration step by SPE might require an adjustment. If the protein recovery rate is low, analyse the sample volume that passed the SPE column in the loading step with RP-HPLC to obtain if protein can be found in this passed sample (in this case, the binding strength is too low). If not, binding strength might be too high or elution strength too low. In this case, the elution agent, elution mode and pre-treatment might require further adjustments.

Quantification with RP-HPLC

General procedure:

1 Prepare a 1:2 mixture of the eluted sample from the SPE in the guanidine buffer

2 Let the solution react at room temperature (RT) for 30 min

3 Conduct a RP-HPLC analysis as described by Dumpler et al. (2017). Set the detection wavelength to 214 nm and the injection volume to 100 µl

Note: After incubation with GdnHCl-buffer for 30 min, conduct RP-HPLC within 24 h to exclude decreasing protein detection due to refolding of proteins (see Method validation section)

Calibration of the RP-HPLC method:

1 Dilute protein standards κ-CN, α-CN and β-CN 1:9, α-LA 1:5, β-LG B and β-LG A 1:3 separately in GdnHCl buffer

2 Process a RP-HPLC measurement with an applied wavelength of 214 nm in the UV detector for each individual standard, with an injection volume of 5 µl, 10 µl and 20 µl. Subsequently, correlate the obtained peak areas with applied protein amounts (taking purity of purchased standards into account).

Quantification:

1 Separate and integrate RP-HPLC-peaks of the different milk proteins κ-CN, α_{S2}-CN, α_{S1}-CN, β-CN, α-LA and β-LG as shown by Dumpler et al. (2017).

2 Calculate the applied protein concentration according to equation (3-6):

$$c_{protein,\ applied,\ RP\text{-}HPLC} = c_{protein,\ detected,\ RP\text{-}HPLC} \cdot DF_{RP\text{-}HPLC} \cdot \frac{V_{inj,cal}}{V_{inj,\ actual}} \qquad (3\text{-}6)$$

with $c_{protein,\ detected,\ RP\text{-}HPLC}$ as the protein concentration detected in RP-HPLC, $DF_{RP\text{-}HPLC}$ as the dilution factor (DF) of the sample with GdnHCl buffer (DF = 2), $V_{inj,cal}$ as the calibrated injection volume (20 µL) and $V_{inj,\ actual}$ as the applied injection volume (100 µL).

Validation:

1 Dilute skim milk 1:7.5, 1:10, 1:15, 1:20, 1:30, 1:50, 1:75, 1:100, 1:250, 1:400, 1:600, 1:750, 1:1,000 in ultrapure water. Dilute the obtained solutions 1:2 in GdnHCl buffer.

2 Conduct a RP-HPLC measurement (with a detection wavelength of 214 nm) with an injection volume of 50 µl and 100 µl. and compare detected RP-HPLC amounts with applied protein amounts.

3.2 Method validation

SPE procedure

Reproducibility and protein recovery rates of the SPE method

Protein concentration with the described protocol for SPE results in a total protein recovery of 94.2 ± 3.0% (n = 8). A high reproducibility of the applied SPE method could be proven by a calculation of the standard deviation (3.0%) and the CV (3.2%) of the total protein recovery rate between experiments. Furthermore, the protein recovery rates of the individual milk proteins were calculated and are shown in Figure 3-1. Compared to the recovery rate of the total protein concentration, α_{S1}-CN, β-CN, β-LG B and β-LG A achieved higher recovery rates with 102.4 ± 4.3%, 101.9 ± 7.3%, 99.8 ± 9.5% and 97.2± 5.0% respectively. In contrast to that, the recoveries of κ-CN, α_{S2}-CN and α-LA were lower, with 62.5 ± 2.3%, 75.4 ± 8.6% and 85.2 ± 5.8% respectively.

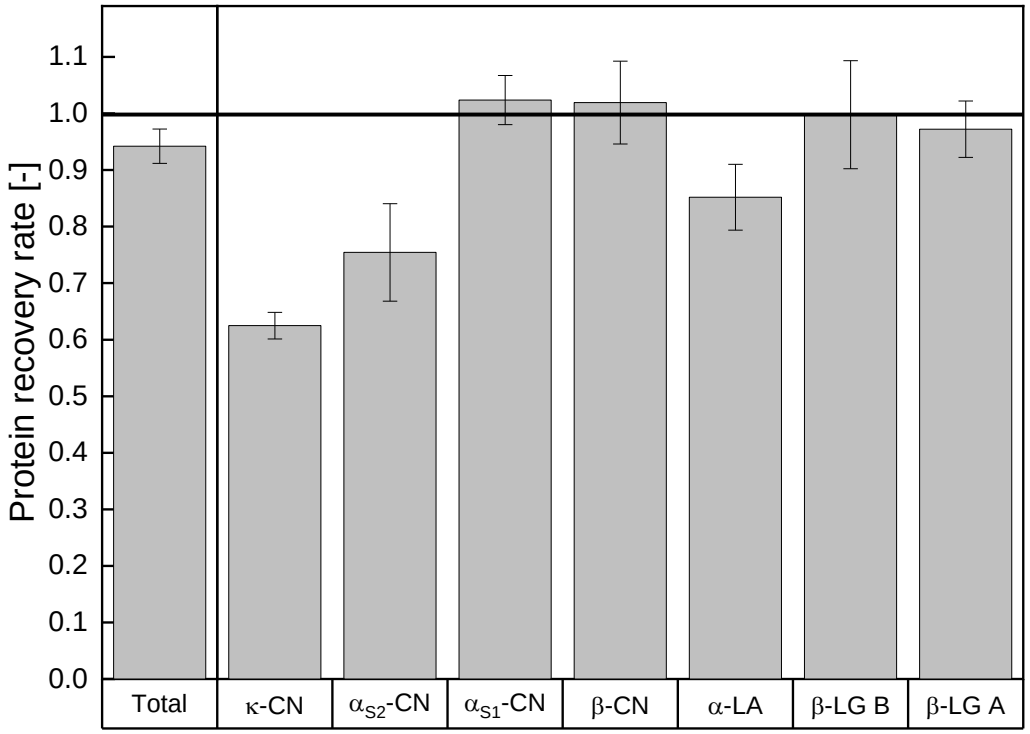

Figure 3-1. Protein recovery rates after SPE and RP-HPLC for the total protein as well as for the individual milk proteins (κ-CN, α_{S2}-CN, α_{S1}-CN, β-CN, α-LA, β-LG B and β-LG A) (n = 8).

Influence of residual cleaning agents on protein recovery rate

Furthermore, it was investigated whether residual cleaning agents in the sample can affect the affinity of proteins to the SPE sorbent. It should be noted, that for cleaning validation and thus the detection of protein residues after cleaning and rinsing steps, concentrations of residual cleaning agents are nonetheless expected to be low. To examine the influence of cleaning agents on protein recovery and thus the robustness of the method, different

concentrations were added to diluted milk samples (1:200 in water) for 20 min at 50°C to resemble common cleaning conditions. Afterwards, pH was neutralized, and SPE followed by RP-HPLC was processed. The resulting influence of chemical concentrations on protein recovery is depicted in Figure 3-2. This study validated the robustness of the method for NaOH (A) and a common combination of an industrial alkaline NaOH-based cleaner (Ultrasil 120) with a surfactant-based additive (Ultrasil 08) (B). No clear trend can be observed for protein recoveries with NaOH concentrations up to 0.3%, and no significant differences from NaOH-free samples were detected. Hence, NaOH-induced changes in protein charge or denaturation do not deteriorate the protein recovery for NaOH concentrations up to 0.3%. On the contrary, for industrial cleaning agents with an alkaline cleaner and a surfactant-based additive, three different levels of protein recovery can be observed. No difference to chemical-free samples can be noted for low concentrations up to 0.1%/0.16% (of Ultrasil 08 and Ultrasil 120). For medium concentrations of 0.2%/0.32% - 0.3%/0.48%, protein recovery increases to 98.7% and 97.9% respectively. At higher concentrations of 0.4%/0.64% - 0.5%/0.8%, protein recovery decreases to 82.5% and 84.1% respectively. Consequently, it can be concluded that the SPE method is more susceptible to influences on the binding affinity when using industrial cleaners that, next to NaOH, contain additives such as surfactants. Accordingly, separate validation needs to be conducted for different cleaning agents and concentrations.

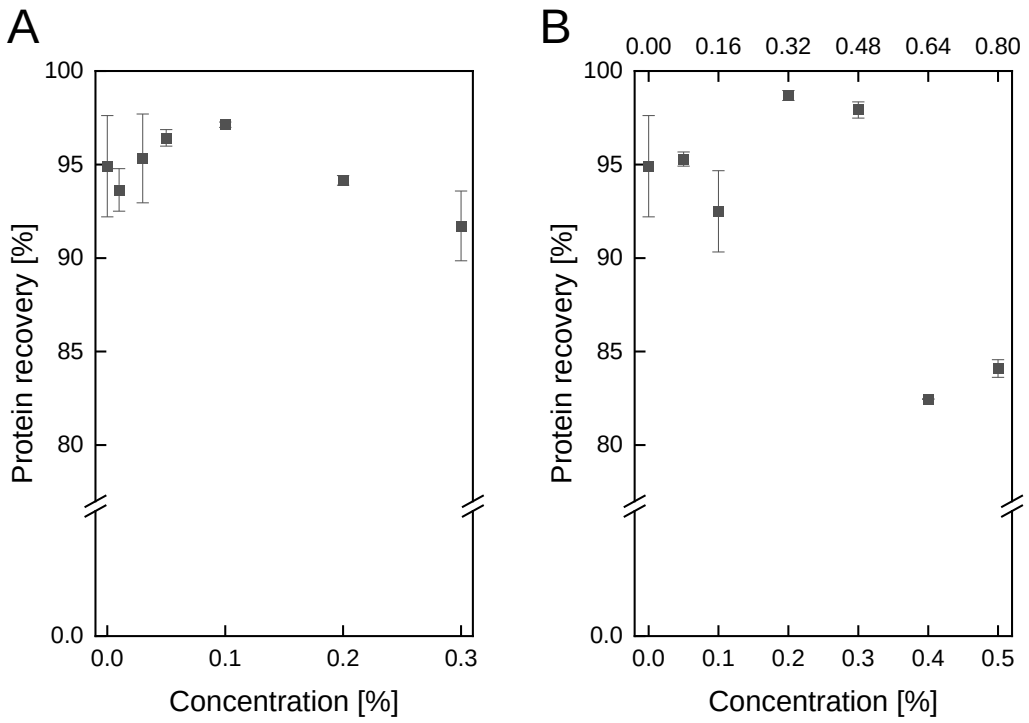

Figure 3-2. Protein recovery of total milk proteins for varying residual concentrations of cleaning agents NaOH (A) and a combination of industrial cleaning agents Ultrasil 120 (upper x-axis) as an alkaline NaOH-based cleaning agent and Ultrasil 08 (lower x-axis) as a surfactant-based additive (B).

Influence of sample volume and protein concentration

In order to validate the applicability of the described method to different sample volumes and protein concentrations, the effect of the protein concentration in the sample as well as sample volume or process time on protein recovery rate was investigated. Therefore, skim milk was diluted with ultrapure water and processed by SPE (applied protein concentrations of 294.97 µg mL^{-1}, 38.03 µg mL^{-1}, 11.41 µg mL^{-1}, 5.71 µg mL^{-1} and 3.80 µg mL^{-1} in the SPE sample). To compensate the different protein concentrations, the applied sample volumes have been adjusted accordingly to recover identical protein amounts (5.7 mg in total) after SPE and RP-HPLC. With constant flow rates of 3 mL min^{-1}, the changes in sample volume induce longer sample process times on the one hand and higher CFs on the other hand. An overview of the influence of skim milk dilution on sample volume, protein concentration and thus CF and sample processing time can be seen in Table 3-1.

Table 3-1. Influence of different dilution factors of skim milk (1:120, 1:900, 1:3,000, 1:6,000 and 1:9,000; details see Method details section) on resulting sample volume, SPE volume, protein concentration, CF and sample processing time

Sample number	Sample volume [mL]	SPE volume[a] [mL]	Protein concentration[b] [µg mL^{-1}]	CF[c] [-]	Sample processing time[d] [min]
1	20	26.1	294.97	6.7	8.7
2	150	196.1	38.03	50.0	65.4
3	500	653.6	11.41	166.7	217.8
4	1000	1307.3	5.71	333.3	435.7
5	1500	1960.9	3.80	500.0	653.5

[a] sample volume after addition of SPE ingredients. [b] total protein concentration in the sample after addition of SPE ingredients. [c] calculated based on the initial sample volume without SPE additives and the elution volume of 3.0 mL. [d] calculated with a flow rate of 3.0 mL min^{-1} only refers to the process time of the applied sample, no preceding or succeeding SPE steps included

In addition to the process time of samples with different protein concentrations and thus volumes, the protein recovery rates of the different samples in dependence of the CF were calculated (see Figure 3-3 and equation (3-7)). The protein recovery for a CF = 50 corresponds to the results shown in Figure 3-1. In Figure 3-3 it can be seen that a significant linear decrease ($p < 0.05$) occurs with increasing CF and thus the sample volume. Hereby, the correlation coefficient $R^2 = 0.89$ indicates a linear correlation between the protein recovery rate and the CF of the sample, and one-way ANOVA confirms the significance of the slope ($p < 0.05$).

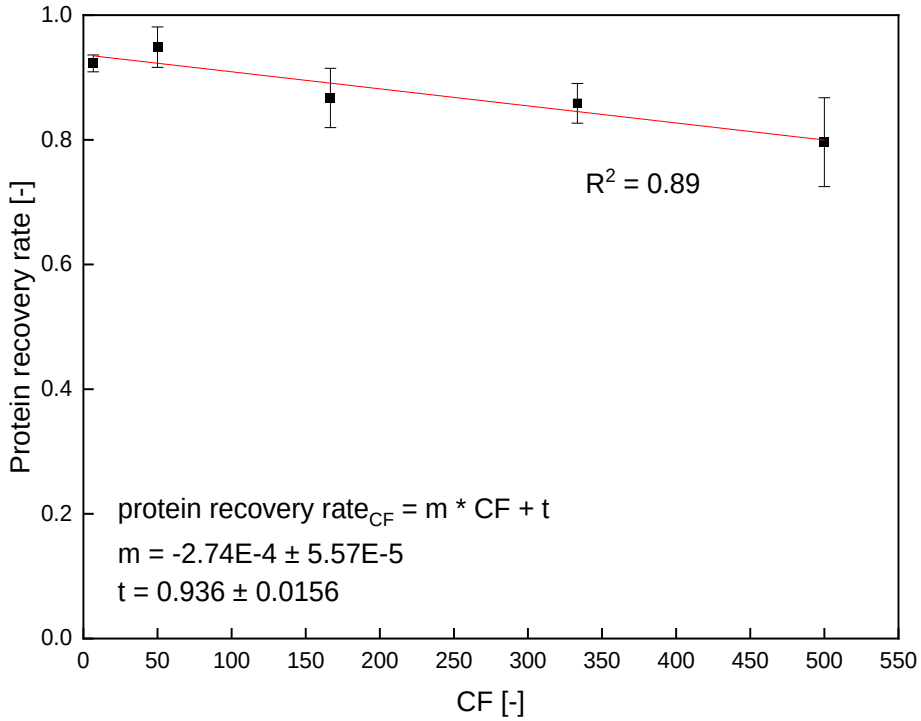

Figure 3-3. Protein recovery rate of the total protein for skim milk samples diluted 1:120, 1:900, 1:3000, 1:6000 and 1:9000 after concentration by SPE and quantification by RP-HPLC.

Furthermore, the linear equation (3-7) shows that the negative slope and thus decrease in protein recovery rate with increasing sample volume equals 2.74% per 100 CF or 9.12% per 1000 mL sample volume.

$$\text{protein recovery rate}_{CF} = -2.74\text{E-}4 \cdot CF + 0.936 \quad (3\text{-}7)$$

Therefore, the protein recovery rate remains high for large values of CF. This allows flexible scalability of sample volume and CF. While CF is not limited to 500, using equation (3-3) with an exemplary CF of 500, the corresponding protein recovery rate of 79.6% and the minimum quantifiable protein concentration with RP-HPLC for e.g. the allergen β-LG B of 3.30 µg mL^{-1} shows that protein concentrations $c_{\beta\text{-LG B}} < 0.0083$ µg mL^{-1} can be quantified with this approach.

Validation of the modified RP-HPLC method

In order to examine the effects of wavelength changes on peak separation and base line noise, diluted skim milk was diluted 1:2 in GdnHCl buffer and analysed by RP-HPLC with a UV-detector wavelength of 214 nm and 220 nm. Furthermore, the effect of changes in the GdnHCl concentration in skim milk samples was investigated by a comparison of diluted skim milk diluted 1:2 and 1:5 in GdnHCl and measured by RP-HPLC (detector wavelength = 214 nm).

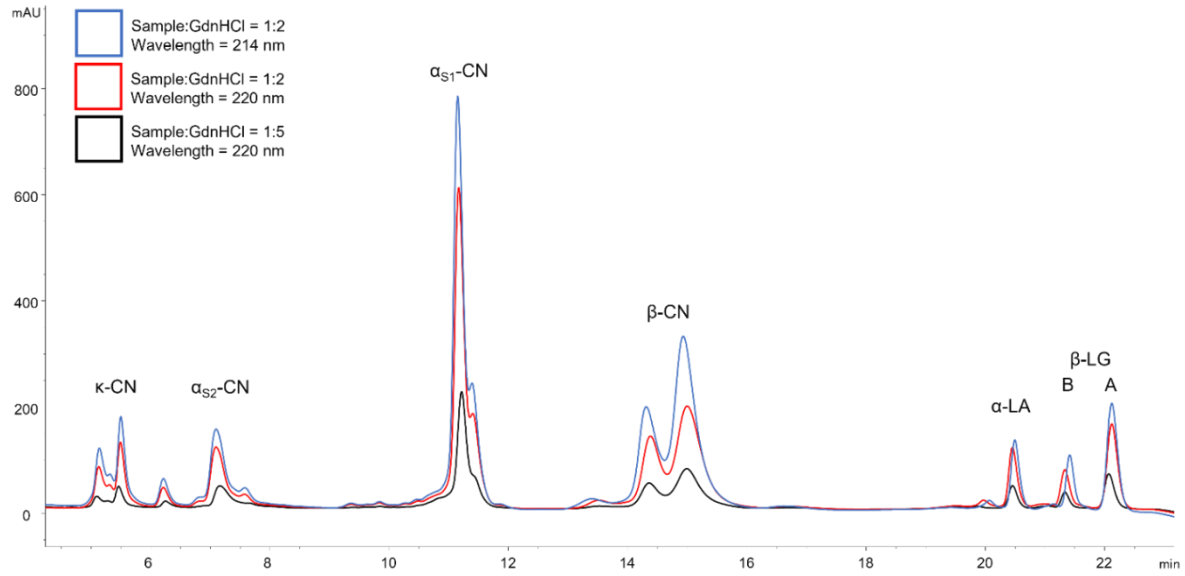

Figure 3-4. UV signal of a RP-HPLC analysis with a 1:5 sample dilution in GdnHCl-buffer and a detection wavelength of 220 nm as postulated by Dumpler et al. (2017) (black); a 1:2 sample dilution in GdnHCl-buffer and a detection wavelength of 220 nm (red); a 1:2 sample dilution in GdnHCl-buffer and a detection wavelength of 214 nm (blue).

In Figure 3-4 it can be seen that a reduction in the GdnHCl buffer concentration from 1:5 to 1:2 increases the detected peak areas by 126%. Additionally, it could be shown that a change of the detection wavelength from 220 nm, as applied by Dumpler et al. (2017), to 214 nm does not affect baseline noise or peak resolution but increases the signal response and thus the peak area by 37% for diluted skim milk samples. In summary, the applied changes in wavelength and GdnHCl buffer concentration can improve the method postulated by Dumpler et al. (2017) regarding the detected peak area by 209%. Therefore, the applied changes facilitate peak identification and integration of low protein content samples and thus enable a lowering of the detection limit which reduces sample volumes required in SPE. Total protein amounts in skim milk were found to be 34.70 ± 1.18 mg mL^{-1} (n = 14) which is in accordance with literature values (Swaisgood 2003; Bobe et al. 1998; Bijl et al. 2013). Thus, it can be concluded that the changes applied to the RP-HPLC method are not affected by additional noise or protein loss due to incomplete denaturation followed by refolding, as it was observed by Bonfatti et al. (2008), and yields correct protein values.

Furthermore, a refolding and thus decreased detection during RP-HPLC due to incomplete denaturation had to be excluded. For this purpose, the storage stability of samples was analysed. After 30 min incubation of diluted milk samples (1:200 in water) with GdnHCl buffer, samples were stored at RT and repeatedly analysed with RP-HPLC for 70 Figure 3-5Hence, it can be concluded that the reduced GdnHCl-buffer concentration in the sample does lead to incomplete denaturation and thus refolding over time. Nevertheless, the refolding-related decrease in detected protein amounts is less than 2% after 24 h and less than 5% after 48 h allowing sufficient analysis time.

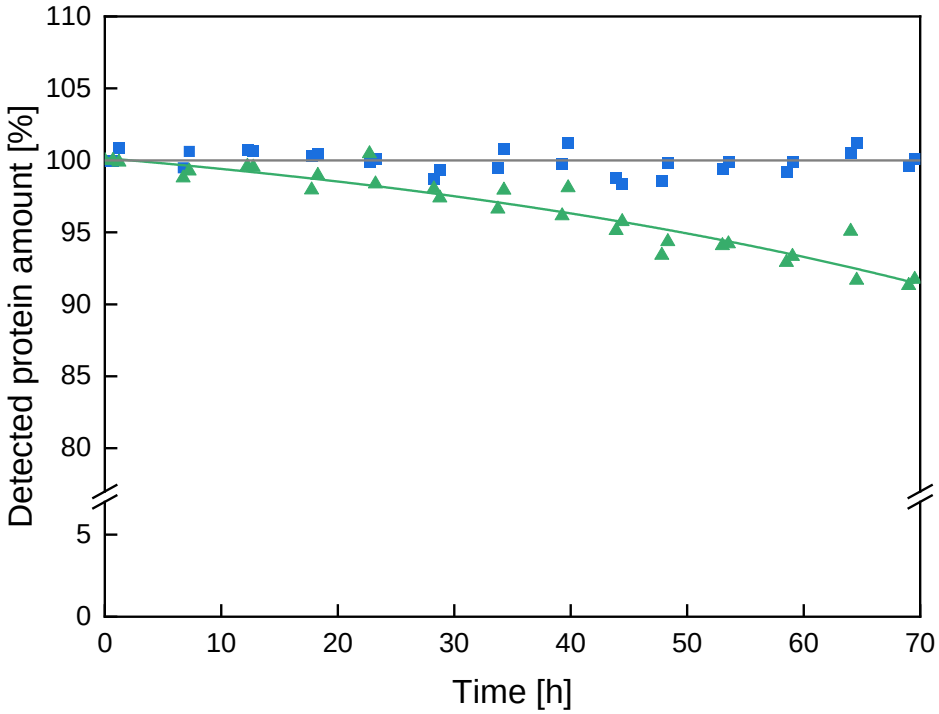

Figure 3-5. Detected amount (with RP-HPLC) of whey proteins (green triangles) and caseins (blue squares) as a function of the storage time at RT relative to the initial protein amount detected after 30 min incubation with GdnHCl buffer. The grey line highlights the reference point of 100% detected protein.

To examine the linear working range of the method, pasteurised skim milk was diluted to different extents (1:7.5 – 1:1,000; for details see Method details section), mixed with GdnHCl buffer and analysed by RP-HPLC. The detected total protein concentration $c_{Protein,\ detected}$ in skim milk as a function of the applied protein concentration $c_{Protein,\ applied}$ was used to investigate the linearity of the slope with the correlation coefficient as well as the significance of the slope by ANOVA (see Figure 3-6).

Within the examined range of protein concentrations of up to 11.57 mg mL^{-1} total protein, a slope significantly different from zero ($p < 0.05$) could be confirmed by ANOVA. Furthermore, the correlation coefficient was determined to be $R^2 > 0.999$ confirming linearity within this range. The linear equation (3-8) shows that the slope m = 1.00021 ± 0.00545 is close to one, implying that any increase in $c_{Protein,\ applied}$ causes an equivalent increase in $c_{Protein,\ detected}$.

$$c_{Protein,\ detected} = 1.00021 \cdot c_{Protein,\ applied} \quad (3\text{-}8)$$

Besides the linear range for the total protein concentration in skim milk (see Figure 3-6), the individual milk proteins (κ-CN, α_{S2}-CN, α_{S1}-CN, β-CN, α-LA, β-LG B and β-LG A) were also analysed for linearity within the examined range of diluted skim milk concentrations (see Table 3-2). Here, α-LA showed the lowest R^2 value of 0.991 while κ-CN and α_{S1}-CN showed the highest R^2 values of 0.998. In addition to R^2 values exceeding 0.99 for each milk protein,

ANOVA confirmed a slope significantly different from zero ($p < 0.05$) for each milk protein. Linearity can therefore be assumed in the given range for individual milk proteins as well as the total protein.

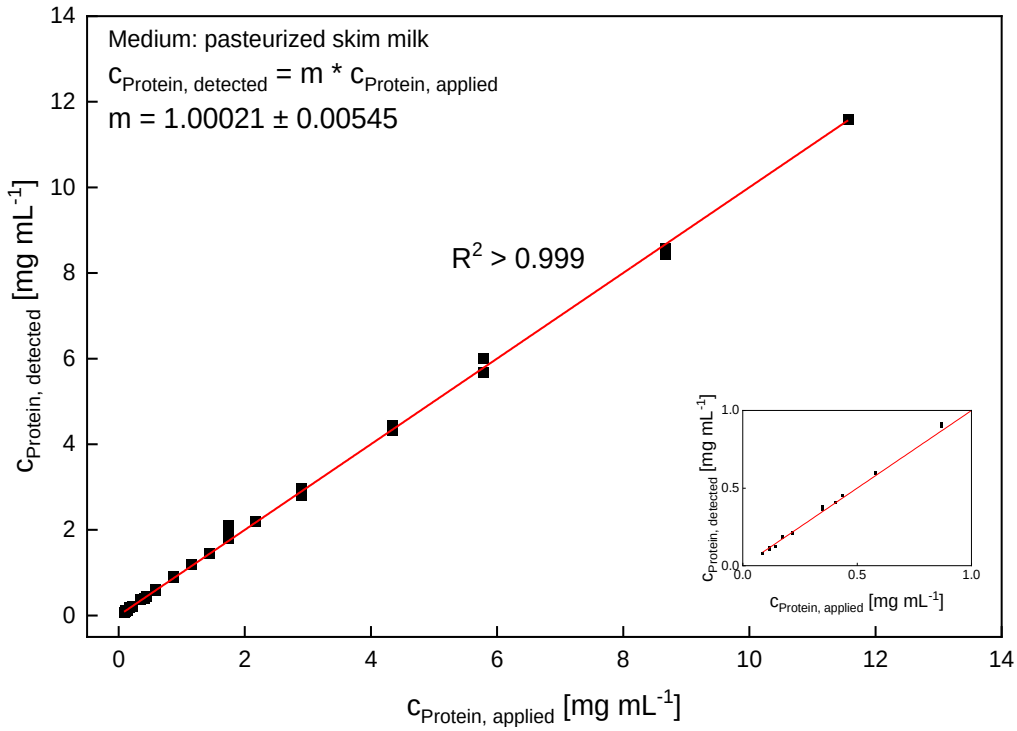

Figure 3-6. Detected protein concentration (with RP-HPLC) as a function of the applied protein concentration (0.09 mg mL^{-1} – 11.57 mg mL^{-1}). The applied concentration was calculated according to equation (3-6).

Table 3-2. Test for linearity of RP-HPLC method with pasteurised skim milk

Milk protein	Range of concentrations [µg mL^{-1}]	Range of amounts[a] [µg]	$R^{2\,b}$
κ-CN	9.6 – 1283.9	0.96 – 128.39	0.998
α_{S2}-CN	8.8 – 1179.8	0.88 – 117.98	0.995
α_{S1}-CN	27.5 – 3666.6	2.75 – 366.66	0.998
β-CN	27.0 –3597.2	2.70 – 359.72	0.997
α-LA	2.9 – 393.3	0.29 – 39.33	0.991
β-LG B	3.3 – 439.5	0.33 – 43.95	0.996
β-LG A	7.6 – 1017.9	0.76 – 101.79	0.997
Total	**86.8 – 11566.7**	**8.68 – 1156.67**	**> 0.999**

[a] applies for an injection volume of 100 µl. [b] R^2, correlation coefficient: high values indicate linear correlation. probability for zero slope of line all < 0.001

Overall, the performed approach enables robust and reproducible concentration, purification and concentration of bovine milk proteins in aqueous diluted skim milk samples and in presence of cleaning agents. The developed SPE method allows high protein recovery rates with flexible scalability of the CF while improvements towards the RP-HPLC method provide additional sensitivity reducing the necessary CFs and thus processing time. However,

changes in sample composition, analyte of interest or protein state will necessitate new calibration, validation and possibly adjustments to the method procedure.

Acknowledgements:

We gratefully thank Nora Biesenthal, Martin Hilz and Hermine Roßgoderer for their assistance concerning SPE execution and RP-HPLC analysis of skim milk samples. David Andlinger and Roland Schopf are thanked for valuable discussions.

This IGF Project of the FEI (AiF 57 EWN) was supported by AiF within the program for promoting the Industrial Collective Research (IGF) of the German Ministry of Economic Affairs and Energy (BMWi), based on a resolution of the German Parliament. This work was supported by the German Research Foundation (DFG) and the Technical University of Munich (TUM) in the framework of the Open Access Publishing Program.

Declaration of interests:

The authors declare that they have no known competing financial interests or personal relationships that could have appeared to influence the work reported in this paper.

4 Application of a pulsed crossflow to improve chemical cleaning efficiency in hollow fibre membranes following skim milk microfiltration[3]

Christian Kürzl*, Thomas Tran, and Ulrich Kulozik

Chair of Food and Bioprocess Engineering, TUM School of Life Sciences, Technical University of Munich, Weihenstephaner Berg 1, Freising, Germany

* Corresponding author

Summary and contribution of the doctoral candidate

Due to the retained casein micelles forming gel-like, compressible and strongly cross-linked fouling layers during skim milk MF, the subsequent efficient fouling removal by chemical cleaning remains challenging. Chemical approaches or additives to improving cleaning efficiency bear the limitations of being restricted to supporting only specific cleaning scenarios such as removing milk proteins, increasing the environmental impact, wastewater pollution and costs of the cleaning process, and possibly being detrimental to the life span of membranes. On the contrary, physical approaches could benefit the whole process chain of cleaning, i.e., chemical and rinsing steps. One of these concepts is pulsed flow, which rapidly and regularly switches with a defined frequency and amplitude between the minimum and maximum flow velocity and related pressure conditions. While this concept has been proven beneficial for cleaning complex stainless steel geometries, no studies on membrane cleaning after skim milk MF have been conducted. Since the geometry and flow characteristics differ significantly between these systems, the behaviour in membranes with an additional vertical flow towards and through the wall has to be investigated separately.

Hence, this study systematically examined the influence of pulsed flow on cleaning efficiency after skim milk MF in HFM by varying the pulsed flow amplitude and frequency at a fixed concentration of cleaning agent (c_{NaOH} = 0.03%). During cleaning, the flux and protein removal were constantly monitored to observe the time-resolved effects of the variation in flow type.

[3] Original publication: Kürzl et al. (2022a): Kürzl, C.; Tran, T.; Kulozik, U. 2022. Application of a pulsed crossflow to improve chemical cleaning efficiency in hollow fibre membranes following skim milk microfiltration. Separation and Purification Technology 302, 122123. doi: 10.1016/j.seppur.2022.122123. Adapted original manuscript. Adaptations of the manuscript refer to enumeration type, citation style, spelling, notation of units, format, and merging of all lists of references into one at the end of the dissertation. Permission for the reuse of the article is granted by by Elsevier Limited.

It could be shown that both FRR and protein removal benefit from the highest frequency possible with the current setup and increased amplitudes. Overall, the cleaning success in terms of protein removal and FRR could be improved by up to 32% and 11%, respectively, due to the enhanced mechanical cleaning effect caused by the pulsation-induced turbulence and annular effect. Also, pulsed flow demonstrated to allow reductions in energy consumption as its application posed a more efficient way to enhance mechanical cleaning power than increasing flow velocity under steady flow.

The doctoral candidate designed the experimental approach for this study based on a critical review of the literature. Data acquisition was mainly done by the doctoral candidate. Also, the doctoral candidate developed the experimental concept, analysed, interpreted and plotted data. The manuscript was written and reviewed by the doctoral candidate. The co-authors contributed to the project outline, the discussion of results, the execution of experiments, and the revision of the manuscript.

Abstract

As the efficient cleaning of membrane systems used for milk protein fractionation remains a challenge, more efficient concepts are required to reduce cleaning times and chemicals consumption. This study examined the so far not commonly applied concept of pulsed flow, characterised by a cyclic transition between high/low flow rates and high/low-pressure phases. To determine its effects on protein fouled polymeric microfiltration membranes, pulsed crossflow conditions were varied in frequency and amplitude during a cleaning step with NaOH as a chemical cleaning agent. The cleaning efficiency was characterised by protein removal and flux recovery. It could be shown that both increasing frequency and flow velocity amplitude can increase protein removal and flux recovery, provided extreme transmembrane pressures are avoided. With pulsed flow, the protein removal could be increased by up to 32% and the flux recovery by 11% compared to a conventionally used steady flow cleaning, thus confirming an increased mechanical cleaning effect when applying pulsed flow. Furthermore, the application of pulsed flow poses a more efficient way to enhance mechanical cleaning power than by increasing the flow velocity under steady flow. Hence, it allows a reduction of energy consumption and thus improves sustainability of the cleaning process. The results indicate a mode of action involving a combination of pulsation induced turbulence and fluctuating relaxation and compaction of the deposit, altogether weakening forces stabilising deposited layer material.

Keywords: alternative flow types; pulsed flow; fouling; protein removal; flux recovery

Graphical abstract:

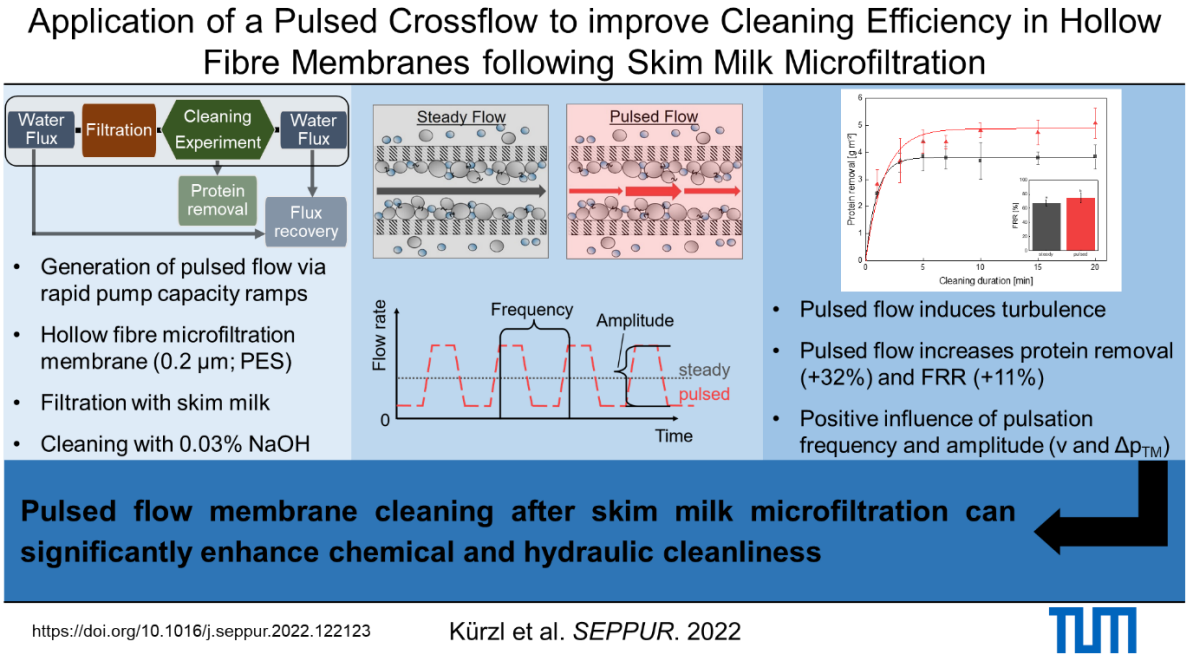

4.1 Introduction

The separation of milk proteins in whey proteins and casein micelles using microfiltration (MF) membranes is evolving as a major operation in the dairy industry. However, the accumulation of retained components (mainly casein micelles (Jimenez-Lopez et al. 2008)) on and in the membrane impairs flux and protein permeation, as well as causing the necessity of regular, more or less frequent cleaning cycles. The latter consist of several rinsing and chemical cleaning steps, making them chemicals- and energy-intensive and causing significant down-time of the filtration plant. The membrane fouling and cleaning mechanisms shall be introduced in the following paragraph as a base for a better understanding of the concept of this study.

The retained micelles as the main fouling material are highly hydrated, sponge-like structures with internal porosity, which can be reversibly or partially irreversibly compressed, thus forming gel-like structures under higher transmembrane pressures with extensive cross-linking (Bouchoux et al. 2010; Gebhardt et al. 2012; Qu et al. 2015). Fouling can occur as a deposit on the membrane surface and thus act as a secondary selective layer or adsorb onto or into the membrane, leading to pore constriction and pore blockage (Bartlett et al. 1995; Bird and Bartlett 2002), e.g. by smaller casein micelles. Accordingly, milk protein fractionation by MF retaining casein micelles is characterised by a complex fouling situation within and on the membrane surface, requiring a thorough cleaning process.

For the removal of protein fouling, NaOH is one of the most used cleaning agents (D'Souza and Mawson 2005; Ng et al. 2017). Different cleaning effects prevail during the three phases of NaOH-cleaning of protein fouling. These phases include the swelling phase (at pH > 10) with diffusion of NaOH into the protein matrix and little protein removal, the erosion phase with weakening of non-covalent bonds (at pH > 11.2) and thus high removal rates, and the decay phase with shear forces mainly governing residual protein removal until a steady-state is reached (Mercadé-Prieto et al. 2008; Gillham et al. 2000). In terms of chemical cleaning agent composition, NaOH alone is usually considered insufficient (Blanpain-Avet et al. 2009; Bartlett et al. 1995; Berg et al. 2014). Hence, compounded industrial cleaning agents commonly contain chemical additives such as enzymes, wetting agents, chlorines or surfactants to enhance cleaning power. However, this increases the environmental impact, wastewater pollution, and costs. Also, excessive chemical cleaning causing oxidation is detrimental to the life span of polymeric membranes (D'Souza and Mawson 2005; Rabiller-Baudry et al. 2021).

Therefore, besides chemical enhancement of cleaning efficiency, several studies were conducted on enhancing mechanical cleaning power by applying hydrodynamic forces, as this has the potential to optimise cleaning success while improving the environmental and

ecological sustainability of the membrane filtration process. Potential approaches include backflushing (Amar et al. 1990), backpulsing (Mores and Davis 2002; Redkar et al. 1996; Rodgers and Sparks 1992) or turbulence promoters (Howell et al. 1993; Hartinger et al. 2020a). Another not commonly applied hydrodynamic concept is pulsed flow with a defined frequency and amplitude between the minimum and maximum flow velocity and related pressure conditions. For the NaOH cleaning of stainless steel pipes/geometries fouled with bacteria (Blel et al. 2009a; Blel et al. 2009b), egg yolk (Yang et al. 2019), starch matrices (Föste et al. 2013) or whey protein solution (Gillham et al. 2000; Bode et al. 2007), pulsed flow was found to enhance the removal of fouling material. Notably, temporary negative pressures were observed under certain conditions of generating pulsed flow, indicating that flow reversal occurred (Gillham et al. 2000). Nonetheless, positive results were confirmed for forward-only pulsed flow (Gillham et al. 2000). Gillham et al. (2000) also found that forward-pulsed flow increases the cleaning rate compared to steady flow exclusively during the shear-sensitive decay phase. Furthermore, critical pulsation features such as frequency (Blel et al. 2009a; Blel et al. 2009b; Gillham et al. 2000; Yang et al. 2019; Weidemann et al. 2014), amplitude (Augustin et al. 2010; Blel et al. 2009a; Blel et al. 2009b; Gillham et al. 2000) and turbulent/laminar flow regime (Gillham et al. 2000; Weidemann et al. 2014) could be identified, and modes of action including increased turbulence (Augustin et al. 2010; Blel et al. 2009a; Blel et al. 2009b; Bode et al. 2007), enhanced mass transfer (Blel et al. 2009a; Blel et al. 2009b; Gillham et al. 2000), fatigue of material upon pressure fluctuation (Gillham et al. 2000) as well as the annular effect (Richardson and Tyler 1929; Schlichting and Gersten 2006) and near-wall flow reversal (Augustin et al. 2010; Blel et al. 2009a; Bode et al. 2007; Föste et al. 2013; Weidemann et al. 2014) were proposed. The annular effect, characteristic for pulsed flow, describes a shift in the maximum velocity from the channel centre towards the channel wall for laminar flow and depends on the pulsation frequency (Richardson and Tyler 1929; Schlichting and Gersten 2006). Other studies also observed the propagation of transverse velocity waves (Camacho et al. 2012) and the onset of turbulence under laminar pulsed flow conditions close to surfaces (Zhao and Cheng 1996). It was also hypothesised that the low-pressure phase causes destabilisation of the deposit, while during the following peak-pressure phase, the accompanying high shear causes enhanced particle removal (Gupta et al. 1992).

Regarding membrane cleaning, there are significant differences compared to these already well-studied systems. Firstly, compared to the smooth steel piping surfaces used in previous works, membranes are characterised by a rougher and, importantly, porous surface with an additional vertical flow towards and through the wall/membrane. As it occurs in membrane processes, fluid flow towards and through porous walls is known to significantly change the flow field, heat and mass transfer rates and shear stress distributions (Jha and Ajibade 2009; Ishak et al. 2008). While fluid injection into the boundary layer along aeroplane

wings is used in aerodynamics to reduce friction and fuel consumption (Singh 1984; Shojaefar et al. 2005), permeate flow in membrane processes resembles the opposite, a fluid transport from the feed side towards the open porous wall, i.e. the membrane. Compared to non-porous walls, where flow velocity near the wall is assumed to be zero, fluid transport towards a porous wall causes a shift of maximum flow velocities towards the wall/membrane and thus near-wall velocities above zero (Falade et al. 2017; Richardson and Tyler 1929). This effect causes increased friction, i.e. higher wall shear stresses. This led to the hypothesis that this effect, in combination with the propagation of transverse velocity waves under pulsed flow conditions (Camacho et al. 2012), should result in an enhanced hydrodynamic effect removing deposited material from membrane surfaces during cleaning procedures, further synergistically supported by chemical agents, weakening the cohesive forces between deposited material. Accordingly, flow profiles and local wall shear stress distributions – to which the proposed mechanism of improved cleaning efficiency by pulsed flow is mainly attributed– can be assumed to differ significantly between porous and non-porous systems.

To the best of our knowledge, no work has so far been reported on the effects of pulsed flow on the cleaning of membranes operated under cross-flow conditions, e.g. after skim milk microfiltration. The only study on membrane cleaning under pulsed flow conditions was conducted by Weidemann et al. (2014). However, this was performed in dead-end filtration mode with spray nozzles (Weidemann et al. 2014), where perpendicular flow towards the membrane causes different fouling and fluid behaviours than in tangential cross-flow mode (van der Bruggen 2018). Also, this study was conducted with larger inert model particles (5 and 10 µm) (Weidemann et al. 2014), whereas compared to more complex systems such as defatted milk, no cross-linking occurs or the addition of cleaning agents is necessary. As a result of this complex situation, the effect of pulsed flow on the removal of different foulants from different surfaces/geometries with different flow characteristics cannot be predicted for chemical cleaning in tangential cross-flow membrane systems fouled by skim milk.

The impact of the chosen feed system on the efficiency of pulsed flow was also shown for filtration of milk and other products prior to membrane cleaning (Howell et al. 1993; Weinberger and Kulozik 2021c; Bertram et al. 1993; Gupta et al. 1992; Hadzismajlovic and Bertram 1999). While pulsed flow significantly reduced fouling during filtration of several single-component suspensions (Weinberger and Kulozik 2021c; Howell et al. 1993; Hadzismajlovic and Bertram 1999), no strong positive effects were observed for the MF of skim milk in hollow fibre membranes (HFM), an emerging membrane type for various applications providing a free flow cross-section. The absence of positive effects of pulsed flow was attributed to specific deposit characteristics, e.g. the small size of casein micelles and intense cross-linking and resulting cohesion (Weinberger and Kulozik 2021a). This indicates that pulsed flow might

particularly support the mechanical effect in chemical cross-flow membrane cleaning, where NaOH helps to loosen the deposit.

We hypothesise that pulsed flow, supported by NaOH at low concentration, can improve the mechanical cleaning power and, thus, membrane cleaning efficiency after milk MF in HFM. This is based on the assumption that pulsed flow induces fluctuating stress on the deposit layer and additional turbulence, thus causing high local and time-dependent wall shear stresses along the membrane surface and improving the removal of deposited material on the membrane surface. To prove or disprove this hypothesis, we applied pulsed flow for the cleaning of MF membranes fouled by the retained casein protein fraction by fast-reacting, inductively driven centrifugal pumps able to rapidly generate pulsed flow in a specifically designed pilot plant. The influencing factors systematically studied in this work were frequency and amplitude.

The assessment criteria in this study were flux recovery ratio (FRR) using water flux of the clean membrane as standard condition and protein removal using a specifically developed highly sensitive analytical method (Kürzl et al. 2022b) to quantify protein removal. Both methods allow for a quantitative cleaning evaluation of different flow types, with only NaOH as a cleaning agent at low concentration. The aim was to assess the effectiveness of pulsed flow in membrane cleaning and to understand the influence of the pulsed flow conditions on the removal of fouling material and the related kinetics in terms of hydraulic and chemical cleanliness. If pulsed flow was successful in terms of faster or more complete mechanical removal of fouling material, the idea was that the industrially applied compounded complex cleaning agents with various chemical building blocks could potentially be reduced in concentration or be made less complex to lower the environmental burden of cleaning solutions finally released into wastewater treatment plants.

4.2 Material and methods

4.2.1 Skim milk

Pasteurised skim milk (74 °C, 28 s) was purchased from the local dairy Molkerei Weihenstephan (Freising, Germany) and used in all experiments for deposit formation. Before usage, skim milk was stored at 4 °C for up to five days. Protein content determined with reversed-phase high-performance liquid chromatography (RP-HPLC) (Kürzl et al. 2022b) was 34.70 ± 1.18 mg/mL, which is in accordance with literature values (Walstra and Jenness 1984; Swaisgood 2003; Bijl et al. 2013; Bobe et al. 1998).

4.2.2 Filtration plant

The experimental filtration and cleaning trials were conducted with a custom-designed lab-scale filtration plant (SIMA-tec GmbH, Schwalmtal, Germany), as shown in Figure 4-1.

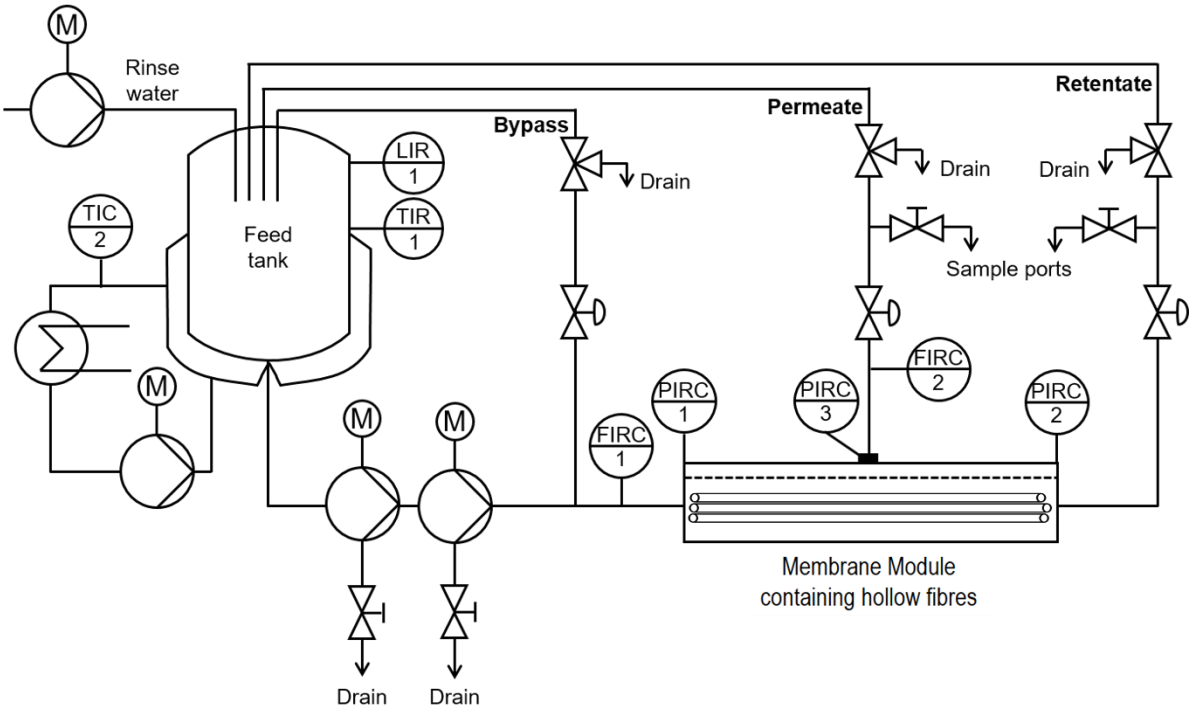

Figure 4-1. Piping and instrumentation (P&I) diagram of the membrane filtration plant. The two centrifugal feed pumps operated in series allowed for a broader spectrum of transmembrane pressures.

Hollow fibre membranes (HFM) made from polyethersulfone (PES) with an inner fibre diameter of 1.5 mm, a maximum pore size of 0.2 µm, and a nominal water flux of 700 L m^{-2} h^{-1} at Δp_{TM} = 0.10 bar were used (Pentair X-Flow BV, Enschede, Netherlands). The resulting membrane module with a length of 540 mm has an active membrane area of 0.0233 m^2.

The feed tank was equipped with a double jacket and temperature sensor WIKA TR30 (WIKA Alexander Wiegand SE & Co. KG, Klingenberg, Germany) for temperature control. Two serially connected PuraLev-200MU (Levitronix GmbH, Zurich, Switzerland) centrifugal pumps with a contact-free impeller bearing were a plant's centrepiece. Combined with the pump control via magnetic fields, the pumps can be rapidly started up and shut down. This allows a uniform flow during steady cross-flow experiments and steep pump flow ramps with defined high and low pump flow phases during pulsed flow. Transmembrane pressure Δp_{TM} and specific flux J were calculated by equations (4-1) and (4-2).

$$\Delta p_{TM} = \frac{p_1 + p_2}{2} - p_3 \tag{4-1}$$

$$J = \frac{\dot{V}_{per}}{A} \tag{4-2}$$

where p_1 is the feed inlet pressure, p_2 is the retentate outlet pressure, p_3 is the permeate pressure (usually atmospheric pressure) measured by WIKA A-10 pressure sensors (WIKA Alexander Wiegand SE & Co. KG, Klingenberg, Germany; response time < 4ms; Error 0.15%), $\dot{V}_{per}$ is the permeate flow rate measured by ABB FEH511 (ABB Automation Products GmbH, Göttingen, Germany; damping time 0.05 s; Error 0.3%) and A is the active membrane area. Furthermore, the pressure drop Δp_L along the membrane length between inlet p_1 and outlet p_2 can be used to calculate the wall shear stress τ_W according to equation (4-3):

$$\Delta p_L = p_1 - p_2 = \frac{1}{2} \cdot \lambda \cdot \frac{L}{d_i} \cdot \rho \cdot v^2 = \frac{4 \cdot L \cdot \tau_W}{d_i} \tag{4-3}$$

where λ is the friction factor, L is the membrane length, d_i is the inner diameter of a hollow fibre capillary, ρ is the density, and v is the flow velocity at the membrane inlet.

4.2.3 Pulsation profile

With pulsed flow being created by varying target volumetric flow rates with transition ramps, a distinct flow profile is created, as depicted in Figure 4-2. It shows the set target values versus the obtained cross-flow velocity profile during pulsed flow. Due to rapid acceleration and deceleration ramps, the phase durations of high (Δt_{max}) and low (Δt_{min}) pump capacity define the full cycle duration, and thus the frequency f, as equation (4-4) shows.

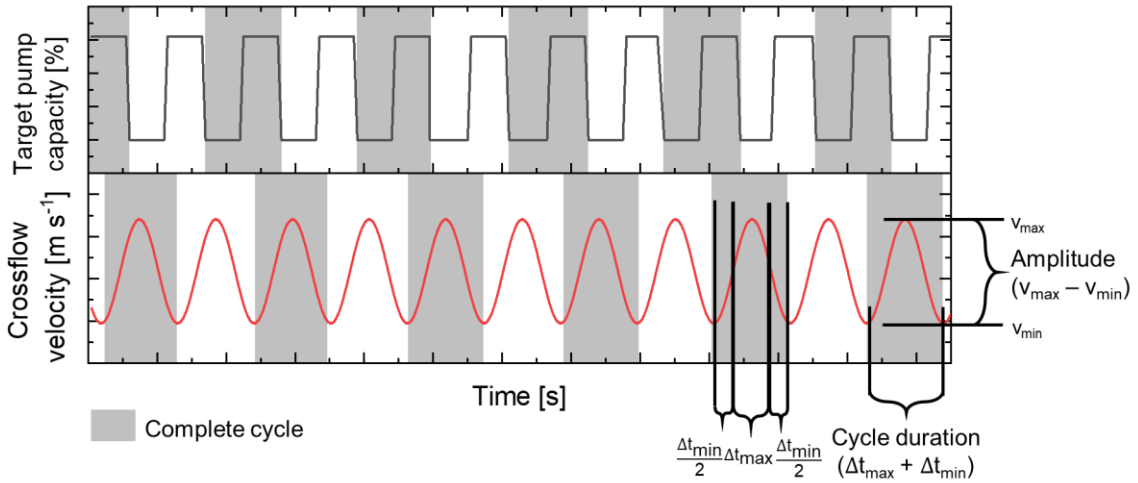

Figure 4-2. Theoretical stepwise flow profile (black) according to set target values versus the resulting sinusoidal flow profile of the cross-flow velocity (red).

$$f = \frac{1}{\Delta t_{max} + \Delta t_{min}} \tag{4-4}$$

Next to frequency, the pulsation amplitude is the second main variable connected to the cyclic changes in pump capacity. This describes the difference between flow velocities in

high and low pump capacity phases (eq. (4-5)). It is to be noted that Δp_{TM} also underlies similar sinusoidal fluctuations like the flow velocity between a maximum and minimum value, denoted as $\Delta p_{TM,cycle}$. With the present membrane system and the chosen approach to generating pulsation, a maximum frequency of 0.5 Hz with a maximum amplitude of 2.5 m s^{-1} could be achieved. Higher values were not feasible as the transition speed for pump capacity changes was technically limited. Details of all conducted cleaning experiments can be found in chapter 4.2.4.

$$\Delta v = v_{max} - v_{min} \tag{4-5}$$

Values of the volumetric flow rate, flow velocity v, and Δp_{TM} were averaged over one minute for better comparison with steady flow experiments (see eq. (4-6)) as an example for flow velocity):

$$v_{avg} = \frac{\sum_{x-1\,min}^{x} v}{t_x - t_{x-1\,min}} \tag{4-6}$$

where v_{avg} is the flow velocity v averaged over one minute, namely between t_x and $t_{x-1\,min}$.

4.2.4 Experimental procedure

An overview of the separate processing steps of the experimental procedure is given in Figure 4-3, and details are presented in the following section. All steps were performed at 50 °C. Deionised (DI) water was used in all steps except filtration and either pure during rinsing or in combination with NaOH during cleaning.

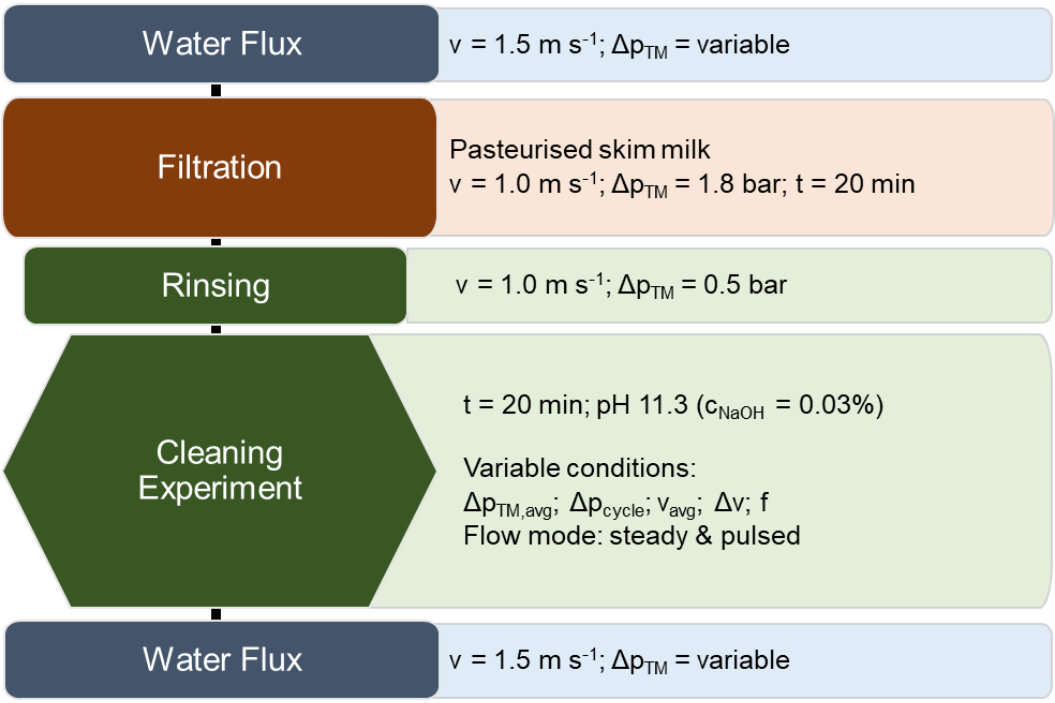

Figure 4-3. Overview of the separate processing steps in the experimental procedure.

Initial water flux measurement

Water flux measurements are a means for evaluating hydraulic membrane cleanliness. Calculating the membrane permeability, the Flux normalised for Δp_{TM} (see eq. (4-7)), allows comparisons of flux values regardless of variations in Δp_{TM}.

$$Membrane\ permeability = \frac{J}{\Delta p_{TM}} \quad (4\text{-}7)$$

An averaged membrane permeability was calculated after steady flow water flux measurement at three Δp_{TM} levels. This approach applies to both the initial water flux measurement of the clean membrane and the water flux measurement after the cleaning experiment.

Filtration

Steady flow skim milk MF was carried out with a flow velocity v = 1 m s^{-1} (Re = 2386) and a Δp_{TM} = 1.80 bar to create a standardised fouling layer for the subsequent cleaning experiment. Filtration was performed for 20 min in circulation mode to establish steady state conditions and completed fouling. Hereby, Flux reached a steady state after 5 min with low standard deviations between all runs (Figure 4-11).

Rinsing

After filtration, milk was drained and the system carefully rinsed with water at v = 1 m s^{-1} of steady flow (Re = 2386) and Δp_{TM} = 0.5 bar for 90 s to remove bulk milk from the module, connecting tubes and the feed vessel and loosely bound material at the membrane walls.

Cleaning experiments

Subsequently, cleaning experiments were performed for 20 min with 0.03% NaOH at pH 11.3 in circulation under steady and pulsed flow mode. This chemically simple cleaning fluid, with its low NaOH concentration and absence of other cleaning enhancing agents like sequestering agents, enzymes and surfactants was deliberately chosen to allow for a sensitive measurement of the effect of pulsed flow, which was not superimposed by other dominating factors. The NaOH solution volume was high compared to the membrane area to be cleaned (yielding a specific cleaning volume of 214.6 L per square meter of membrane surface area) and therefore, an excess of cleaning agent compared to the amount of protein to be removed, which also explains why the study was performed with this low NaOH concentration. For a direct comparison with initial pure water flux during the cleaning progression, the cleaning flux

recovery ratio (cFRR) was obtained by dividing the membrane permeability during cleaning by the initial pure water membrane permeability (see eq. (4-7) & (4-8)) and continuously monitored.

$$cFRR = \frac{J_{Cleaning}}{\Delta p_{TM.\,Cleaning}} \Big/ \frac{J_{Initial}}{\Delta p_{TM,\,Initial}} \tag{4-8}$$

Flow conditions during the cleaning experiments were either applied as pulsed or steady flow. The pulsation parameters frequency and amplitude were varied in this step for pulsed flow. For comparison, steady flow experiments were performed at the same average flow rate and Δp_{TM} as the pulsed flow experiments. Conditions were controlled during experiments by monitoring pump capacity and flow rate of the pumps at maximum and minimum values of v by the control software and manually adjusting the Δp_{TM} with permeate and retentate side throttles. An overview of the set of cleaning experiments is given in Table 4-1. Samples for protein analysis were collected from the feed tank after 1, 3, 5, 7, 10, 15 and 20 min of the cleaning process. The processing data for pulsed flow with f = 0.5 Hz and Δv = 2.5 m s^{-1} corresponds to the maximum achievable combination of frequency and amplitude. As the speed of pump capacity increasing and decreasing was limited, higher frequencies would require reduced amplitudes. Also, phase durations can only be set in increments of whole seconds, which limits the variation of the frequency in a wider range.

Table 4-1. Conducted cleaning experiments with associated levels of the variables.

Flow mode [-]	Frequency [Hz]	v [m s^{-1}]				Re [-]			Δp_{TM} [bar]			
	f	max	min	Δ	avg	max	min	avg	max	min	Δ	avg
steady	0.00	n.a.	n.a.	n.a.	2.2	n.a.	n.a.	5250	n.a.	n.a.	n.a.	0.35
pulsed	0.10	3.5	0.9	2.5	2.2	8256	2250	5250	0.60	0.10	0.50	0.35
pulsed	0.25	3.5	0.9	2.5	2.2	8256	2250	5250	0.60	0.10	0.50	0.35
pulsed	0.50	3.5	0.9	2.5	2.2	8256	2250	5250	0.60	0.10	0.50	0.35
pulsed	0.50	2.8	1.7	1.1	2.2	6562	3937	5250	0.47	0.23	0.24	0.35
steady	0.00	n.a.	n.a.	n.a.	2.2	n.a.	n.a.	5250	n.a.	n.a.	n.a.	0.00
pulsed	0.50	3.5	0.9	2.5	2.2	8256	2250	5250	0.00	0.00	0.00	0.00
steady	0.00	n.a.	n.a.	n.a.	2.2	n.a.	n.a.	5250	n.a.	n.a.	n.a.	0.50
pulsed	0.50	3.5	0.9	2.5	2.2	8256	2250	5250	0.87	0.13	0.74	0.50

Water flux measurement after cleaning experiment

At first, the cleaning solution was drained, and then the system was rinsed with water for 10 min at v = 1 m s^{-1} of steady flow (Re = 2386) and Δp_{TM} = 0.5 bar to remove any residues of detached protein and cleaning agent.

Then, the water flux was again measured. The relation of water flux after cleaning ($water\ permeability_{after\ cleaning}$) to the initial clean water flux ($water\ permeability_{initial}$) provides the water flux recovery ratio (FRR) (see eq. (4-9)), an indicator for hydraulic

cleanliness. If the cleaning evaluation indicated incomplete cleaning (i.e. FRR < 90%), an additional industrial cleaning step was conducted to completely recover the initial water flux.

$$FRR = \frac{water\ permeability_{after\ cleaning}}{water\ permeability_{initial}} = \frac{J_{after\ cleaning}}{\Delta p_{TM.\,after\ cleaning}} \Big/ \frac{J_{initial}}{\Delta p_{TM,\,initial}} \tag{4-9}$$

This experimental procedure allowed high reproducibility with no significant influence of increasing membrane age on FRR (Figure 4-12a) and protein removal (Figure 4-12b).

4.2.5 Evaluation of the removed protein amount

Concentration, purification, and quantification of proteins in the cleaning solution were performed by applying a highly sensitive method to determine even low residual amounts of protein, according to Kürzl et al. (2022b). The evaluation of protein data for experiments with time-resolved sampling had to be adjusted toward the changing volumes during each sample collection. Hence, concentration changes should only refer to the reduced feed volume (see eq. (4-10)). Accordingly, the accumulated protein removal over cleaning time was calculated.

$$m_{Protein,y} = m_{Protein,x,y-1} + \left(\frac{(c_{Protein,y} - c_{Protein,y-1}) \cdot V_{elution} \cdot DF_{GdnHCl} \cdot \frac{V_{inj,cal}}{V_{inj,actual}}}{V_{SPE} \cdot \left(V_{feed,y=0} - (n-1) \cdot V_{sample}\right)} \right) \tag{4-10}$$

where y represents a specific time point during cleaning. $c_{Protein,y}$ and $c_{Protein,y-1}$ are the protein concentrations determined by RP-HPLC after solid-phase extraction (SPE) of the current and previous sample, respectively. V_{SPE} is the sample volume applied to the SPE cartridge, $V_{elution}$ is the elution volume used to recover protein from the SPE cartridge, DF_{GuHCl} is the dilution factor caused by the addition of guanidine buffer, $V_{inj,cal}$ is the calibrated injection volume of the RP-HPLC method and $V_{inj,actual}$ is the injection volume used for the current sample. With regard to the cleaning experiment and sampling, $V_{feed,y=0}$ is the initial volume of cleaning solution (5 L), n is the number of samples collected so far and V_{sample} is the amount of sample collected from the feed tank. $m_{Protein,y}$ and $m_{Protein,y-1}$ are the calculated protein masses in the cleaning solution according to the current and previous sample, respectively.

4.2.6 Data evaluation

The energy consumption of the pump impeller was logged with the accompanying service software (V1.0.107) and corrected by loss factors provided by the manufacturer to obtain the overall energy consumption of the pump. For analysis of RP-HPLC chromatograms, Agilent ChemStation software (Rev. B.04.03) was used. Data was plotted, fitted, and statistically evaluated using OriginPro 2021 (OriginLab Corporation, Northampton, MA, USA). All experiments were done at least in triplicates. Error bars depict the standard deviation of the

replicates. Statistical significance between data sets was evaluated using a one-way analysis of variance (ANOVA) at the significance level of 5% ($p < 0.05$).

4.3 Results and discussion

4.3.1 Influence of pulsed flow on cleaning success

First, it was examined whether the pulsed flow can benefit the cleaning success in the custom-designed filtration system. As the strongest effects were expected for maximum frequency and amplitude, pulsed cleaning with f = 0.5 Hz, $\Delta p_{TM,cycle}$ = 0.50 bar and Δv =2.5 m s^{-1} was conducted and compared to steady crossflow cleaning conditions of v_{avg} = 2.2 m s^{-1} and Δp_{TM} = 0.35 bar. The results for the progression of cleaning rate, cumulative protein removal and thus chemical cleanliness are depicted in Figure 4-4.

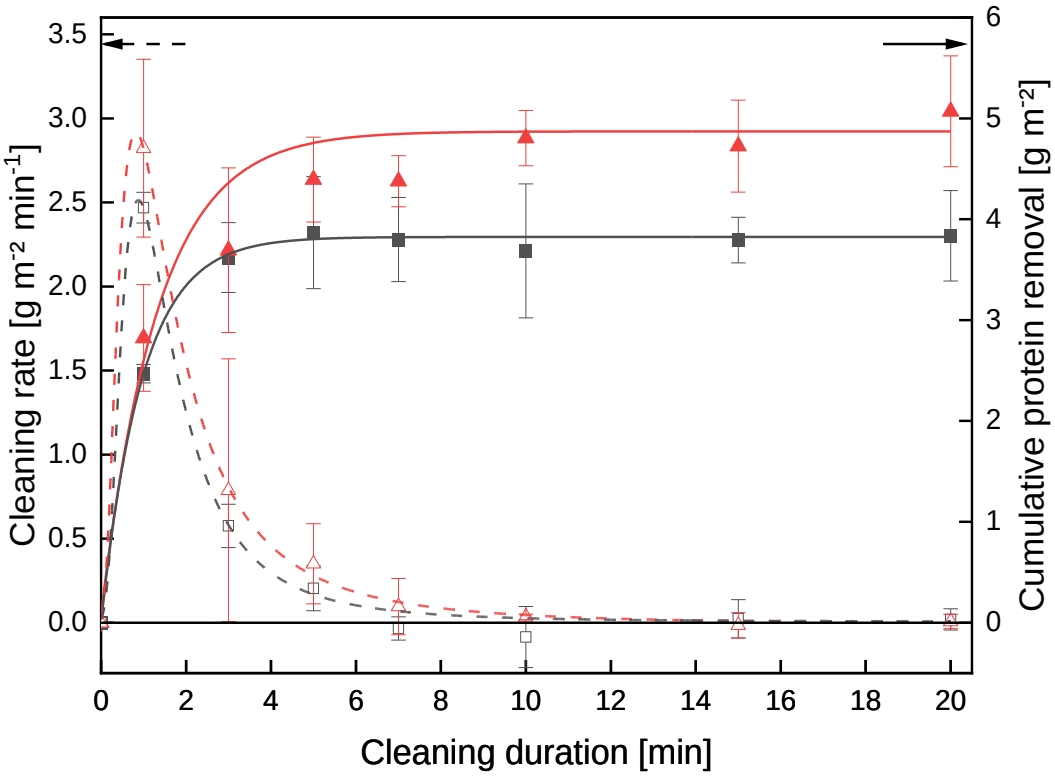

Figure 4-4. Influence of pulsed flow (red triangles) in comparison to steady flow (black squares) on cleaning progression in terms of cleaning rate (open symbols, dashed lines) and cumulative protein removal (filled symbols, solid lines). Cleaning conditions: f = 0.5 Hz, v_{avg} = 2.2 m s^{-1}, Δv =2.5 m s^{-1}, $\Delta p_{TM,avg}$ = 0.35 bar, $\Delta p_{TM,\ cycle}$ = 0.50 bar. Steady flow cleaning was conducted at identical v_{avg} and $\Delta p_{TM,avg}$.

The curve for cumulative protein removal representing steady flow cleaning conditions is characterised by a sharp increase in protein removal within the first 3 min, which then levelled off and finally asymptotically reached a stable value. This is also observable within the curve of the cleaning rate, which reached its peak value after one minute and then steeply

declined until reaching zero cleaning rate after 10 min. An initial lag phase, during which swelling but little protein removal often occurs, as described by Gillham et al. (2000) for instance, could not be observed. It can be explained by differences in the composition and the condition of the fouling layer, which mainly consisted of caseins instead of whey proteins and had not been affected by intense thermal effects, which would be typical for fouling layers on heat exchanger surfaces. In this case, a chemical enhancement of protein removal by NaOH also occurred, but the swelling phase was negligibly short. The rapid increase without lag phase could also be attributed to the open-pored structure of an MF-membrane compared to a stainless steel pipe, allowing faster access of NaOH passing through the entire deposited layer, thus removing deposited material not only at the surface of the fouling layer.

The accumulated protein removal as a function of cleaning time under pulsed flow conditions also underwent a sharp increase with a steeper slope than steady cross-flow within the first 3 min. The steady-state reached after 10 min was at a higher level than the steady forward cross-flow. Besides also reaching its peak cleaning rate after one minute, the cleaning rate was constantly higher with pulsed flow during the whole cleaning duration. While the increases in cleaning rate were not significant, after a cleaning time of 20 min, pulsed cleaning reached an accumulated protein removal of 5.07 ± 0.55 g m^{-2}, which was significantly higher (+32.0%) than that of steady flow cleaning (3.84 ± 0.45 g m^{-2}). The removed proteins had a casein/whey protein ratio of CN:WP = 3.74 ± 0.83, confirming that the deposit mainly consisted of caseins. This could be one explanation for the susceptibility of the deposit to increased erosive forces, as the casein micelles are two magnitudes larger than whey proteins (Brans et al. 2004), making them more susceptible to shear forces (Ripperger and Altmann 2002). Also, there is no difference in the CN:WP-ratio between steady and pulsed flow, meaning that the enhanced removal is evenly distributed between caseins and whey proteins.

Besides pulsed and steady experiments run with the identical flow and pressure conditions, the average wall shear stress was increased for pulsed flow due to the exponential increase of pressure loss and the related wall shear stress upon cyclic change of the flow velocity (see eq. (4-3) in chapter 4.2.2) at v_{max} compared to v_{avg} and v_{min}. In this example, the average wall shear stress of pulsed flow cleaning was indeed 31% higher compared to that of the steady flow cleaning with v_{avg} = 2.2 m s^{-1}, where pulsed flow caused the observed increase in protein removal by 32.0% (see Table 4-2).

Table 4-2. Influence wall shear stress (τ_w) on protein removal for steady and pulsed flow

Flow mode	v				τ_w	τ_{pulse}	Protein removal	ΔProtein removal	ΔFRR
[-]	[m s^{-1}]				[Pa]	[%]	[g m^{-2}]	[%]	[%]
	max	min	Δ	avg					
steady$_{avg}$*	n.a.	n.a.	n.a.	2.2	22.9	n.a.	3.84 ± 0.45	n.a.	67.4 ± 4.8
steady$_{max}$	n.a.	n.a.	n.a.	3.5	53.7	+134.5	3.67 ± 0.09	-4.4	64.7 ± 6.7
pulsed	3.5	0.9	2.5	2.2	30.0	+30.9	5.07 ± 0.55	+32.0	75.0 ± 7.0

*steady reference cleaning condition, which τ_{pulse}, Δprotein removal and ΔFRR refer to.

To compare the effects of increased shear stress in steady and pulsed flow, a steady cleaning experiment with the maximum conditions (steady$_{max}$) occurring in pulsed flow (v_{max} = 3.5 m s^{-1}, $\Delta p_{TM,max}$ = 0.60 bar) was conducted. This induced an increase in shear stress by 135% compared to previous steady cleaning experiments (v_{avg} = 2.2 m s^{-1}, $\Delta p_{TM,avg}$ = 0.35 bar). However, despite the theoretical increase in shear stress by 135%, no increase in protein removal (-4.4%; 3.67 ± 0.09 g m^{-2}) was observed. Several authors also reported only slight or no increase of FRR (Blanpain-Avet et al. 2009; Ang et al. 2006; Bird and Bartlett 2002; Bartlett et al. 1995) and protein removal (Blanpain-Avet et al. 2009) at increasing flow rates and related wall shear stresses. Therefore, it can be concluded that the increased protein removal for pulsed flow was not or not only due to an increase in the average shear stress, thus confirming the starting hypothesis. Rather, it seems to be due to the annular effect in pulsed flow leading to a shift of maximum flow velocities and related shear forces from the membrane centre towards the membrane surface, with additional turbulences occurring due to the high frequency of velocity fluctuations. This results in a more efficient distribution of local fluid forces in the vicinity of the membrane surface.

Another consequence of pulsed flow and increased turbulence is an increased local velocity gradient, reducing the laminar boundary layer thickness with thus increased shear stress in membrane surface vicinity as well as enhanced mass transfer. Both increased removal due to increased local and temporal shear stress peaks near the membrane surface and enhanced mass transfer could be responsible for the improved cleaning success. However, previous studies indicated that enhanced heat/mass transfer is mostly relevant in laminar flow regimes (Gillham et al. 2000; Pérez-Herranz et al. 1999). Additionally, Gillham et al. (2000) indicated that the increase in cleaning efficiency was more linked to the physical deposit structure than intensified transport processes. This would also indicate a temporal dependency of the relevance of transport processes and shear forces, determined by the remaining cross-linking and binding forces.

Besides chemical cleanliness, hydraulic cleanliness was also investigated in terms of the progression of relative membrane permeability and FRR (Figure 4-5). The progression of the relative membrane permeability shows that the values of steady flow were consistently

higher than pulsed flow during the progression of cleaning. After 20 min cleaning time, both flow types reached a steady state. The observed discrepancy of times required to reach a steady-state between the progression of permeability and protein removal indicates an opening of previously blocked pores and, thus, the removal of internal fouling. Removing proteins from blocked pores caused a further increase in membrane permeability but not a detectable increase in protein removal. Hence, besides the progression of protein removal indicating a steady state after 5 – 10 min, cleaning with neither flow type should be terminated earlier since hydraulic permeability still increased further up to 10 – 20 min cleaning time.

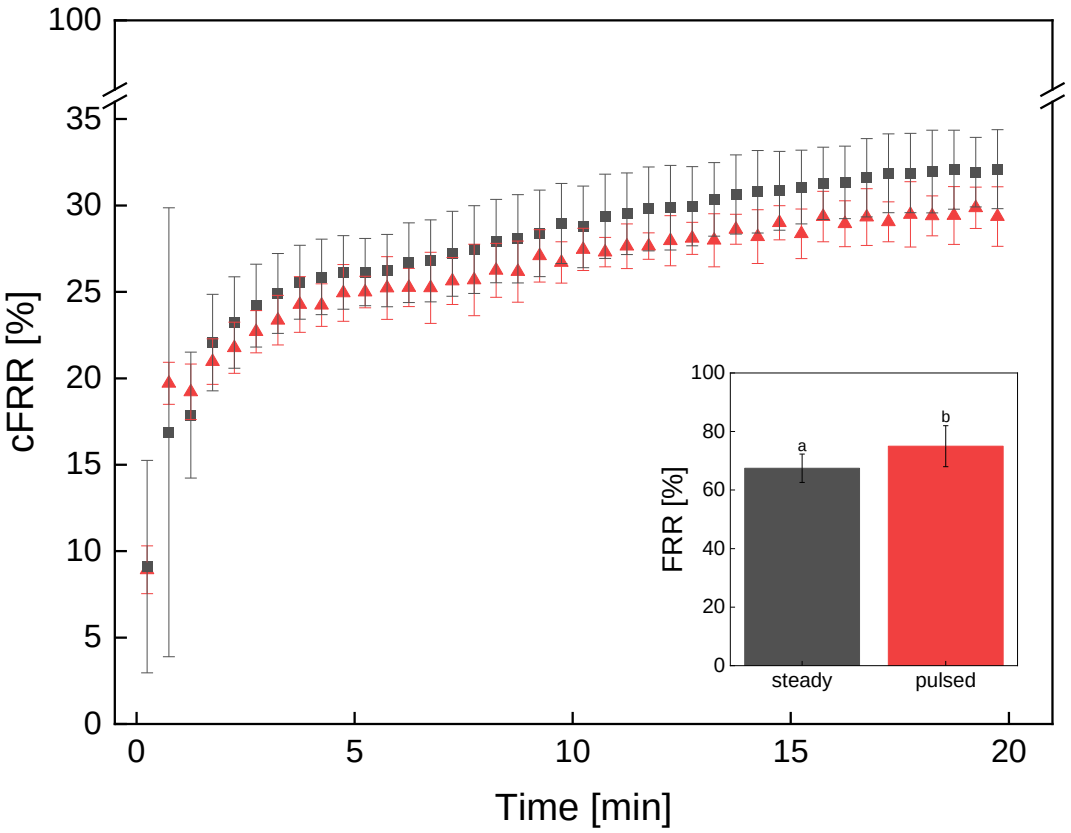

Figure 4-5. Influence of pulsed flow (red triangles) on cFRR and FRR in comparison to steady flow (black squares) during cleaning. Cleaning conditions: f = 0.5 Hz, v_{avg} = 2.2 m s^{-1}, Δv =2.5 m s^{-1}, $\Delta p_{TM,avg}$ = 0.35 bar, $\Delta p_{TM,cycle}$ = 0.50 bar. Steady flow cleaning was conducted at identical v_{avg} and $\Delta p_{TM,avg}$. $^{a-b}$ different letters indicate significant differences between flow modes ($p < 0.05$).

After 20 min cleaning time, the relative permeability of steady flow reached a slightly higher value than pulsed flow, which can be explained as follows.

Figure 4-6 shows the flux curves of skim milk, cleaning solution and pure water permeation. While the water flux curve increases linearly with Δp_{TM}, the MF of milk hardly reacts to Δp_{TM} due to intense membrane fouling. Compared to that, the Flux during cleaning increased, but underproportionally due to the recirculation of the cleaning solution, which does not take the removed protein out of the system. A medium Δp_{TM} = 0.35 bar (black circle) as a mean pressure condition for both pulsed and steady cross-flow means that this condition is a permanent one for steady cross-flow only, while for pulsed flow Δp_{TM} fluctuated between 0.1

and 0.6 bar (red circles). Since the removed protein was still present in the cleaning solution and thus reversible redeposition during the cleaning could be expected, the permeability at 0.6 bar should be lower than that at 0.35 bar. Hence, if pulsation did not positively affect Flux during a pulsation cycle, the average of a high membrane permeability during $\Delta p_{TM,min}$ and low membrane permeability during $\Delta p_{TM,max}$ would lead to a significantly lower average mean permeability compared to steady flow. Therefore, both curves presenting similar flux progressions indicate that pulsed flow benefits cleaning success.

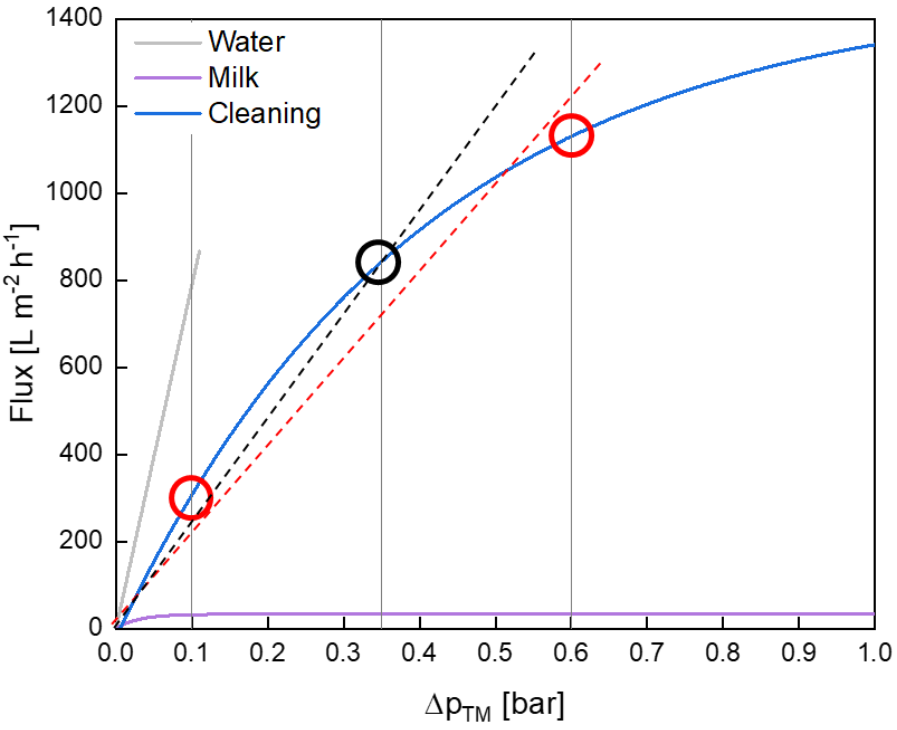

Figure 4-6. Flux increase with Δp_{TM} for skim milk (purple), pure water (grey) and cleaning (blue). The black circle shows $\Delta p_{TM,\,avg}$ for steady cleaning and the red circles show $\Delta p_{TM,\,max}$ and $\Delta p_{TM,\,min}$ for pulsed cleaning. The dotted lines indicate the resulting average membrane permeability of steady and pulsed flow.

The results for FRR (Figure 4-5), measured with pure water after the cleaning cycle, i.e. without protein redeposition, underline the results of the progression of protein removal. Steady flow reaches an FRR of 67.4 ± 4.8% for average flow conditions and an FRR of 64.7 ± 6.7% under maximum flow and pressure conditions. This is in accordance with other studies reporting a range of 60 – 80% for cleaning of protein fouling in membranes at roughly tenfold higher NaOH concentrations (Blanpain-Avet et al. 2009; Bird and Bartlett 2002; Rabiller-Baudry et al. 2002; Berg et al. 2014). In contrast, cleaning with pulsed flow reaches an FRR of 75.0 ± 7.0%, significantly higher than steady flow under average flow conditions (+11%) and maximum flow conditions (+15.9%), despite the low NaOH concentration.

The discrepancy between the increase in FRR (+11%) and protein removal (+32%) between pulsed and steady forward flow can be explained by a non-linear correlation or pulsed

flow mainly enhancing deposit removal at the membrane surface, but not the removal of internal fouling material. To further assess the effect of pulsed flow on external and internal fouling removal, further studies comparing the open-pored MF membranes, affected by a mix of external and internal fouling, with less porous membranes (UF, NF, UO) that should be more dominated by surface fouling. Hence, this could provide further insights regarding the underlying mode of action of the cleaning improvement with pulsed flow.

The comparison of pulsed flow cleaning with steady flow cleaning under maximum pump capacity ($steady_{max}$) is also interesting from an energetic point of view, as shown in Table 4-3. It depicts the wall shear stress, protein removal and energy consumption, normalised for $steady_{max}$ cleaning and relatively compared to $steady_{avg}$ and pulsed flow cleaning. Indeed, pulsed flow requires more pump energy than steady flow under average conditions ($steady_{avg}$) due to the constant changes in pump capacity (+25%). Nonetheless, the increased energy consumption is over-proportionally compensated by increased protein removal (+32%). Furthermore, from the industrial application perspective, pulsed flow cleaning would need to be compared to $steady_{max}$, where steady flow cleaning utilises the maximum possible flow conditions. Here, pulsed flow requires less pump energy than $steady_{max}$ (-58%) due to the lower average pump capacity and thus shear stress while still achieving significantly higher cleaning success (+38%) in terms of hydraulic and chemical cleanliness.

Table 4-3. Comparison of pump energy consumption with resulting wall shear stress and protein removal for different flow conditions

Flow type*	τ_w*	Energy consumption*	Protein removal*
[-]	[-]	[-]	[-]
$steady_{max}$	1.00	1.00	1.00
$steady_{avg}$	0.43	0.34	1.04
pulsed	0.43	0.42	1.38

*Results of wall shear stress, protein removal and energy consumption were normalised for $steady_{max}$ cleaning and compared to $steady_{avg}$ and pulsed flow cleaning. This was done by dividing all values of shear stress, energy consumption and protein removal by the one of $steady_{max}$ cleaning.

4.3.2 Analysis of pulse characteristics

As reported above, pulsed flow can significantly improve chemical and hydraulic cleanliness. To gain further insights into the action mechanism of pulsed flow and its main variables that lead to increased cleanliness, an excerpt of the time-resolved pulsation characteristics from the results analysed in chapter 4.3.1 is given in Figure 4-7. It depicts the cross-flow velocity v, Δp_{TM}, and flux progression over several pulsation cycles. While both Δp_{TM} and v are high during the high pump capacity phase, the Flux reaches its peak value delayed by 0.6 s during the downwards ramp, where Δp_{TM} and cross-flow velocity sharply decrease. This indicates that deposit relaxation outweighs the decreasing flow velocity and average shear stress during the starting relaxation phase. This could be either due to the relaxing deposit becoming more accessible and thus increasingly removable by shear forces or the deposit simply becoming more porous and thus permeable.

During the low-pressure phase, the Flux slowly decreased due to a relaxing deposit with low flow velocities. During the upwards ramp, the Flux reached its minimum due to the increasing compaction of the deposit, outweighing the increasing shear forces. This suggests that – inversely similar to the downwards ramp – deposit relaxation/compaction mainly governs the flux development, which indicates that besides the amplitude of shear forces, the amplitude of the Δp_{TM} might play a crucial role in pulsation efficacy.

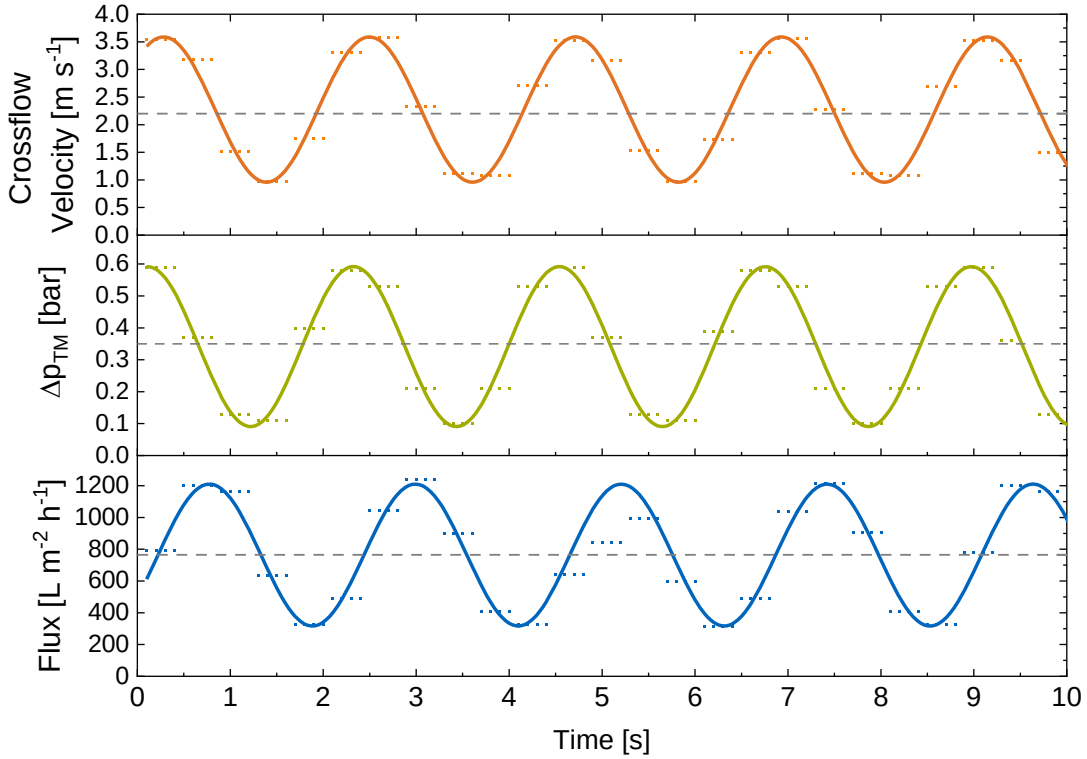

Figure 4-7. Time-resolved progression of crossflow velocity (orange), Δp_{TM} (green) and flux (blue) over several cycles during cleaning with f = 0.5 Hz and Δv = 2.5 m s^{-1}. The dotted lines (grey) indicate averaged values of each variable.

The flux maximum occurring during the relaxation phase implies that high frequencies and amplitudes are beneficial: The frequency correlates with the number of pulsation cycles and thus relaxation phases, and the amplitude correlates with the intensity of deposit relaxation.

The occurrence of maximum Flux during the relaxation phase could also be attributed to the annular effect, which describes a phase delay of radially channel-centred flow layers and thus v_{avg} compared to near-wall flow layers and the pressure gradient. A slight phase delay of v_{avg} and flux compared to Δp_{TM} of 0.2 s and 0.7 s, respectively, can be observed in Figure 4-7, which is due to fluid inertia for rapid pressure ramps. This translates into high local flow velocities and thus turbulences during both the starting relaxation and compaction phases, despite decreasing/increasing Δp_{TM} and v_{avg}, and also explains the flux peak occurring within the starting relaxation phase. Underlined by other studies observing an additional onset of turbulence due to pulsed flow mainly during the deceleration phase (Zhao and Cheng 1996), it can be assumed that strong turbulence persists throughout the full cycle due to the high local and temporal variations of flow velocities. The amount of added turbulence and thus the gain in protein removal induced by pulsed flow should then increase with pulsation frequency and amplitude as they define the intensity and frequency of flow velocity fluctuations. However, the high Δp_{TM} during the compaction phase might also impair the removability of the remaining deposit.

Accordingly, the interplay between high amplitudes of shear forces and Δp_{TM} with their effect on pulsation efficacy and the pulsation frequency will be discussed in detail in the following chapters 4.3.4 and 4.3.3, respectively.

4.3.3 Influence of pulsation frequency on cleaning efficiency

In order to assess the effect of the pulsation frequency, defined by the duration of a combined cycle of a high flow rate and a low flow rate phase (or related pressure conditions), the cleaning success was analysed for different pulsation frequencies. Pulsation amplitudes of flow velocity and pressure remained unchanged. Figure 4-8 shows the resulting FRR and accumulated protein removal after cleaning for 20 min with NaOH at pH 11.3. Results shown for a frequency of 0.0 Hz correspond to steady cross-flow cleaning results. Besides the pulsation frequency discussed in chapter 4.3.1, additional lower frequencies of 0.1 Hz (5 s of each high and low flow rate) and 0.25 Hz (2 s of each high and low flow rate) were considered. As Figure 4-8a shows, there was no increase in FRR for a frequency of 0.1 Hz (FRR = 67.7 ± 8.6%) and a decrease for 0.25 Hz (FRR = 52.8 ± 6.1%) compared to steady cross-flow cleaning. No clear trend can be observed. Compared to steady flow cleaning, pulsed flow led to a significantly increased FRR only for 0.5 Hz.

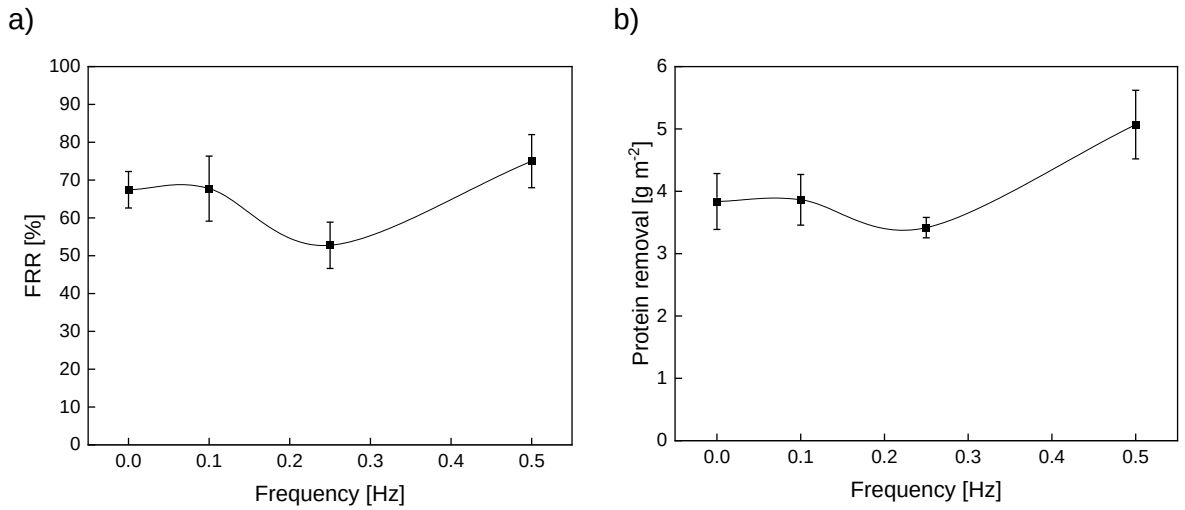

Figure 4-8. Influence of pulsation frequency on FRR (a) and protein removal (b). Data points for 0.0 Hz correspond to steady cleaning results. Lines are a guide to the eye. Cleaning conditions: v_{avg} = 2.2 m s^{-1}, Δv = 2.5 m s^{-1}, $\Delta p_{TM,avg}$ = 0.35 bar, $\Delta p_{TM,cycle}$ = 0.5 bar. Steady flow cleaning was conducted at identical v_{avg} and $\Delta p_{TM,avg}$.

A similar trend was observed for protein removal, as shown in Figure 8b. Here, neither a frequency of f = 0.1 Hz (3.86 ± 0.41 g m^{-2}) nor f = 0.25 Hz (3.42 ± 0.16 g m^{-2}) did increase protein removal compared to the steady cross-flow condition. For decreasing frequencies, holding times during each pulsation phase increase, cycle numbers decrease, and the rate of velocity changes decreases. The observed lack of increase at 0.1 Hz and 0.25 Hz compared to the significant improvements at 0.5 Hz suggest that a particular threshold frequency seems to be required for efficient pulsation. This could be explained in terms of reduced heat (and mass) transfer. Gbadebo et al. (1999) found heat (and mass) transfer to be enhanced at medium frequencies and decreased at lower and higher frequencies within their studied range. This behaviour also depended on Re-numbers and will presumably differ between studied systems. The decreased cleaning success at low frequencies could also be based on an unfavourable combination of the relaxation/ low shear and compaction/ high shear phase durations, as both the annular effect (Schlichting and Gersten 2006; Camacho et al. 2012) and shear stress enhancement (Blel et al. 2009a) depend on pulsation frequency. This supports the hypothesis that pulsed flow acts as a turbulence promoter since preventing the formation of distinct flow profiles and causing additional turbulence might depend on a particular frequency of velocity changes. Hence, a part of the pulsed flow mechanism most probably lies in the temporal component of the cyclic stress or flow disruption, which supposedly adds turbulence and thus improves protein removal during the decay phase (compare Figure 4-4).

The necessity of a certain threshold frequency could also be correlated to avoiding the redeposition of detached proteins. Other studies investigating the use of pulsed dead-end flow to avoid clogging of sieve pores (Dincau et al. 2022) or deposition of minerals onto heat exchanger surfaces (Augustin and Bohnet 1999) also found a threshold frequency to be critical due to the undisturbed flow time necessary to allow clogging or redeposition. Concerning

proteins, this would correspond to the time necessary in laminar/undisturbed flow to develop attractive bonds with the remaining deposit or membrane leading to redeposition.

4.3.4 Influence of pulsation amplitude on cleaning efficiency

In addition to the temporal component of pulsation-related flow and pressure fluctuations, the influence of their intensity – i.e. the pulsation amplitude – was investigated while frequency conditions (0.5 Hz) remained unchanged. Steady forward flow cleaning (amplitude of 0.0 m s^{-1}) was compared to pulsed flow cleaning with amplitudes of 2.5 m s^{-1} (see chapter 4.3.1) and 1.1 m s^{-1}.

As depicted in Figure 4-9a, a change in the flow type and the higher pulsation amplitude led to a linear increase in the FRR. Regarding protein removal, as shown in Figure 4-9b, there was a significant linear increase with increasing amplitudes in the examined range with both amplitudes of 1.1 m s^{-1} and 2.5 m $s^{-1,}$ achieving significant increases in protein removal compared to steady flow cleaning. Hence, the efficiency of pulsed flow increased with the intensity of stress fluctuations. In analogy to Table 4-2 in chapter 4.3.1, a potential correlation between the increase in protein removal with pulsed flow and the increased average shear rate was measured for the amplitude of 1.1 m s^{-1}. Hereby, the increase in protein removal was 14.3%, whereas the calculated increase of the average shear stress was 5.8% only. It supports the view that the increase in protein removal is not primarily due to an increase in average shear stress and that this value alone is insufficient to explain the effects of pulsed flow. Instead, it seems to support the hypothesis stated in chapter 4.3.1, i.e. that the increased removal is due to the formation of highly time-dependent shear force peaks near the membrane surface. This is assumed to be the result of pulsation-induced turbulence due to rapid and intense velocity fluctuations as well as the annular effect causing a shift in maximum flow rates towards the membrane surface.

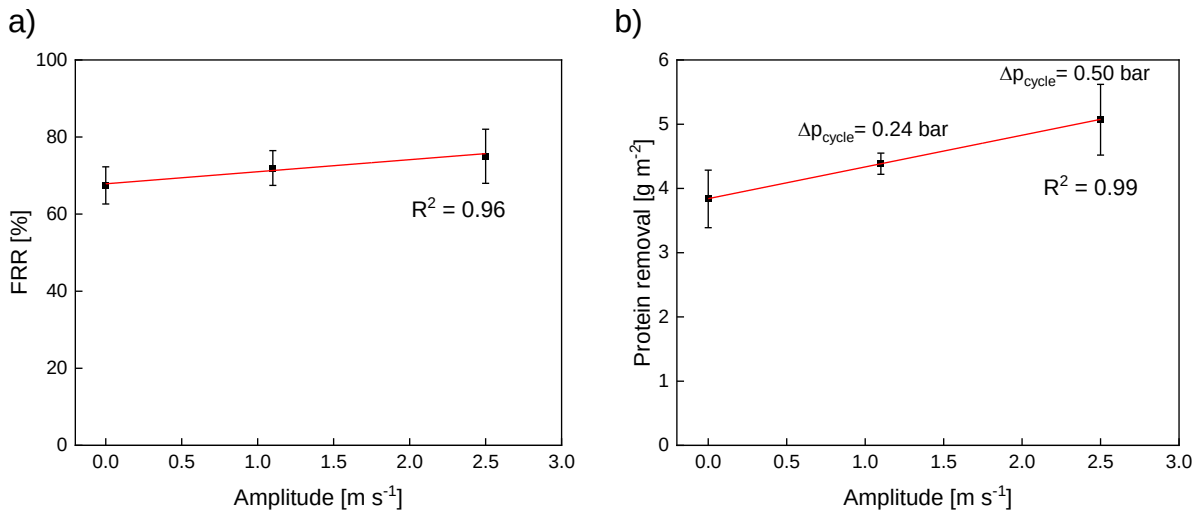

Figure 4-9. Influence of pulsation amplitude on FRR (a) and protein removal (b). Data points for 0.0 Hz correspond to steady cleaning results. Cleaning conditions: f = 0.5 Hz, v_{avg} = 2.2 m s^{-1} (v_{max} = 2.8 m s^{-1} and v_{min} = 1.7 m s^{-1} for Δv = 1.1 m s^{-1}; v_{max} = 3.5 m s^{-1} and v_{min} = 0.9 m s^{-1} for Δv = 2.5 m s^{-1}), $\Delta p_{TM,avg}$ = 0.35 bar ($\Delta p_{TM,max}$ = 0.47 bar and $\Delta p_{TM,min}$ = 0.23 bar for Δv = 1.1 m s^{-1}; $\Delta p_{TM,max}$ = 0.6 bar and $\Delta p_{TM,min}$ = 0.1 bar for Δv = 2.5 m s^{-1}). Steady flow cleaning was conducted at identical v_{avg} and $\Delta p_{TM,avg}$.

It should further be noted that besides an increase in the flow rate amplitude, increasing the intensity of shear stress fluctuations also increases the intensity of relaxation and compaction of the deposit in terms of $\Delta p_{TM.cycle}$. A distinction should be therefore made between the effects of Δv or $\Delta\tau_w$, respectively, and $\Delta p_{TM,cycle}$. This was assessed by selectively throttling of the pressure and pump capacity allowing variations of the $\Delta p_{TM,cycle}$ while keeping the amplitude of the flow velocity at the same level. Figure 4-10 shows the influence of varying Δp_{TM}-regimes on the difference in protein removal between steady and pulsed cleaning. The steady flow cleaning results used as reference correspond to cleaning with identical $\Delta p_{TM,avg}$ and flow velocity levels. Data points at $\Delta p_{TM,avg}$ = 0.35 bar represent previously discussed results (see chapter 4.3.1).

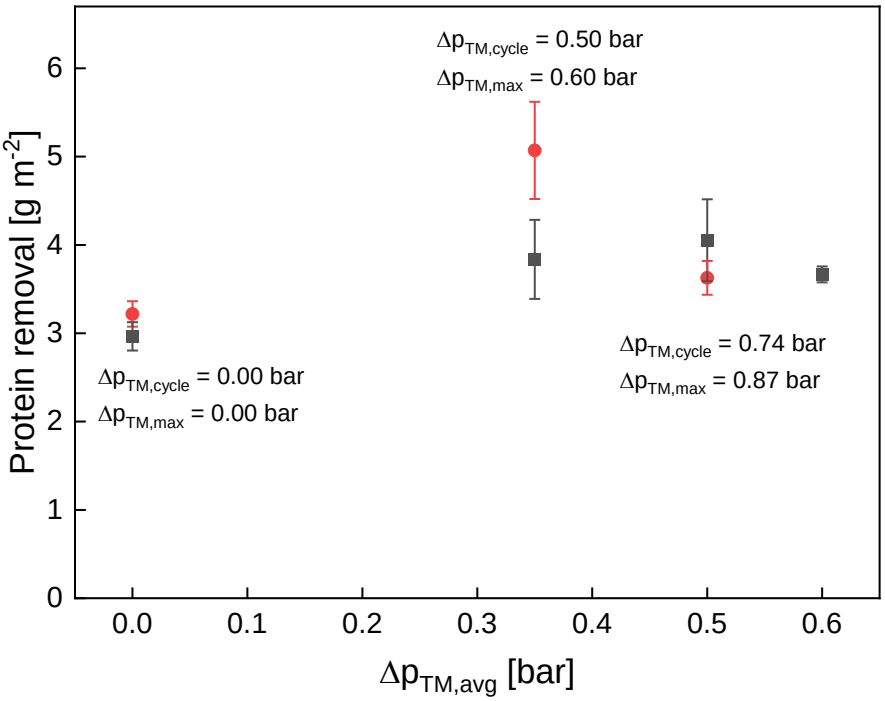

Figure 4-10. Influence of varying Δp_{TM} regimes on the efficacy of pulsed flow (red circles) for protein removal in comparison to steady flow (black squares) during cleaning. Cleaning conditions: f = 0.5 Hz, v_{avg} = 2.2 m s^{-1}, Δv = 2.5 m s^{-1}. Steady flow cleaning was conducted at identical v_{avg} and $\Delta p_{TM,avg}$.

Closure of the permeate side led to a $\Delta p_{TM,avg}$ of 0.0 bar with a $\Delta p_{TM,cycle}$ of 0.0 bar since no permeation could occur. Hence, there was only a fluctuation in pressure on the feed/retentate side but no fluctuation of Δp_{TM} while maintaining a flow velocity amplitude of Δv = 2.5 m s^{-1}. Besides these cleaning conditions resembling the most comparable ones to the cleaning of steel pipes, and regardless of the flow velocity amplitude, the omittance of a Δp_{TM} or $\Delta p_{TM,cycle}$ restricts the overall cleaning effect and that of pulsed flow such that it does not significantly increase protein removal compared to steady flow cleaning.

A study by Blanpain-Avet et al. (2009) on cleaning MF membranes also found that a medium Δp_{TM}, in this case 0.25 bar, achieved a higher protein removal than an absent Δp_{TM} (or higher Δp_{TM} levels of 0.50 – 0.84 bar). One consequence of the closure of the permeate side is that fluid flow has restricted access to internal fouling due to the lack of permeate flow. It can be assumed that a considerable amount of compressible micelles is removed from the surface deposit and membrane pores through the open-pored MF membrane and not exclusively along the membrane, which explains the overall reduced cleaning effect at zero Δp_{TM} in MF membranes.

With pulsed flow not benefitting cleaning efficiency without permeate flow, this also means that pulsed flow requires access of fluid flow to both the deposit at the membrane surface and the inner membrane fouling for improved protein removal. This could be because of the cyclic relaxation/compaction of the deposit combined with local shear stress peaks

leading to additional pulsation effects within the membrane, especially at later stages of cleaning where large parts of the deposit are already removed.

In contrast to the improved protein removal at Δp_{TM} = 0.50 bar, a further increase in the Δp_{TM} amplitude to $\Delta p_{TM,cycle}$ = 0.74 bar leads to another convergence of steady and pulsed flow cleaning results. This could be due to the increased $\Delta p_{TM,cycle}$, accompanied by an increased $\Delta p_{TM,max}$= 0.87 bar. It could lead to irreversible fouling layer compaction resulting in gel formation, which was reported to occur above a critical transmembrane pressure level (Qu et al. 2012), or increased transport of proteins into the membrane's pores, thus leading to impaired pulsation efficiency and reduced cleaning success.

Overall, it can be stated that there is an optimum in protein removal both under steady and pulsed flow conditions in MF for a medium Δp_{TM} = 0.35 bar and a minimum in protein removal for zero Δp_{TM} and large Δp_{TM} levels. Obviously, the overall removal mechanism in open porous MF membranes benefits from access of the fluid flow to the internal membrane structure, but this is impaired at high Δp_{TM} levels due to irreversible gel formation or increased internal fouling. This hypothesis is also supported by pulsed flow achieving the highest cleaning success compared to steady cleaning for a medium Δp_{TM} of 0.35 bar. A moderate Δp_{TM} ($\Delta p_{TM,avg}$ = 0.35 bar; $\Delta p_{TM,min}$ = 0.10 bar; $\Delta p_{TM,max}$ = 0.60 bar) provides a balance between sufficient access of fluid flow to the inner pore structure and intense fluctuations in shear stress and deposit compaction/relaxation without impairing cleaning efficiency by too high $\Delta p_{TM,max}$ levels.

4.4 Conclusion

This study demonstrated the usefulness of the concept of pulsed flow in membrane cleaning after milk 0.1 µm MF for protein fractionation as it can significantly enhance chemical and hydraulic cleanliness compared to steady flow cleaning under constant flow conditions. Here, the importance of the pulsation variables, frequency and amplitude, could be confirmed for membrane cleaning. This study also showed that pulsed flow could increase the mechanical cleaning power more efficiently than increased flow velocities during steady flow. Compared to the maximum flow conditions of steady flow, pulsed flow with a lower average flow velocity still achieved significant increases in protein removal (+38.1%) and FRR (+15.9%) while requiring 57.8% less pump energy due to the lower average pump capacity. Hence, pulsed flow poses a more efficient way to enhance mechanical cleaning power than increasing the flow velocity in steady flow and thus contributes to making cleaning processes more efficient and sustainable.

However, for the cleaning with only NaOH, as examined in this study, cleaning efficiency remains incomplete according to the hydraulic cleanliness criterion (FRR < 90%). It

remains to be investigated how pulsed flow affects cleaning efficiency with compounded cleaning agents and how this enhanced mechanical cleaning power can be utilised to reduce chemical agent consumption by reducing its concentration or cleaning time, thus increasing the process sustainability further.

It should be noted that the results presented in this study are valid for the hollow fibre membrane system investigated. In further ongoing work in our group, the usefulness and applicability of pulsed flow in other membrane systems with different pore sizes, e.g. in the ultrafiltration range, and geometries, such as spiral-wound and flat sheet membranes, which suffer from enhanced fouling due to flow shades behind spacer net filaments (Hartinger et al. 2020a; Han et al. 2018b), will be addressed, and more gains could result in these systems. Furthermore, the generation of pulsed flow in industrial membrane systems remains to be investigated. Here, pulsation creation will require other technical means than pulsation generation via rapid changes in the pump capacity.

Author Contributions

Conceptualisation, C.K.; methodology, C.K.; software, C.K.; validation, C.K. and T.T.; formal analysis, C.K.; investigation, C.K. and T.T.; resources, U.K.; data curation, C.K.; writing—original draft preparation, C.K.; writing—review and editing, C.K. and U.K.; visualisation, C.K.; supervision, U.K.; project administration, C.K.; funding acquisition, U.K. All authors have read and agreed to the published version of the manuscript.

Funding

This IGF Project of the FEI was supported via AiF to promote the Industrial Collective Research (IGF) of the German Ministry of Economic Affairs and Energy (BMWi), based on a resolution of the German Parliament. Project: AiF 57 EWN.

Acknowledgements

We gratefully thank Heidi Wohlschläger, Hermine Roßgoderer and Nora Biesenthal for their assistance with the RP-HPLC analysis of cleaning samples, as well as Dirk Weber from Pentair X-Flow BV for providing hollow fibre membranes. Furthermore, we want to thank Siegfried Tuchborn from SIMA-tec GmbH and Christian Ederer, Erich Schneider, and Franz Fraunhofer in our workshop for technical support. We also want to thank Lina Dohm for her experimental support. Finally, we want to thank Simon Schiffer, Roland Schopf, Thomas Bühler (Ecolab GmbH), Maria Weinberger, and Martin Hartinger for fruitful discussions.

Conflicts of interests

The authors declare no conflict of interest. The authors declare no conflict of interest. The authors declare that they have no known competing financial interests or personal relationships that could have influenced the work reported in this paper. The funders had no role in the design of the study, in the collection, analyses, or interpretation of data, in the writing of the manuscript, or in the decision to publish the results.

Supplementary

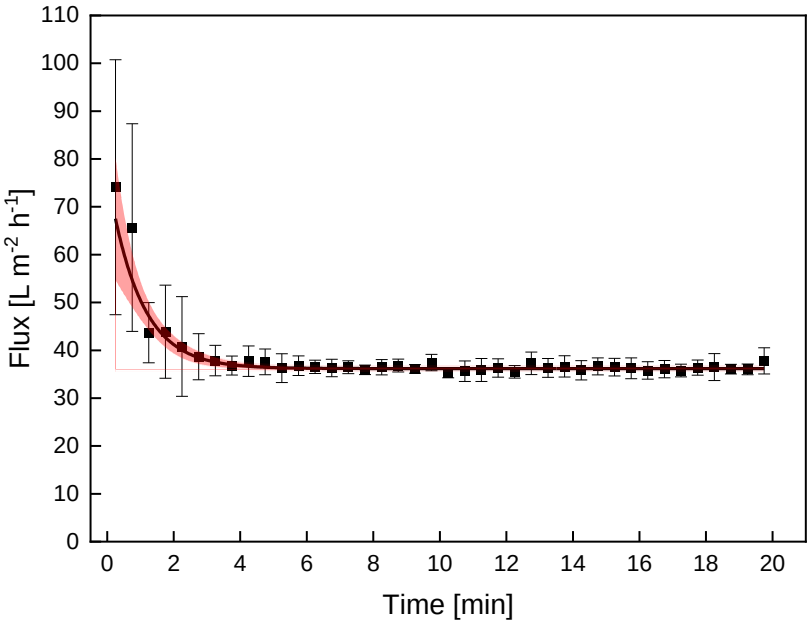

Figure 4-11. Flux progression during skim milk filtration at 50 °C, v = 1 m s^{-1} and Δp_{TM} = 1.8 bar for 20 min in an HFM averaged over the filtration runs of presented results.

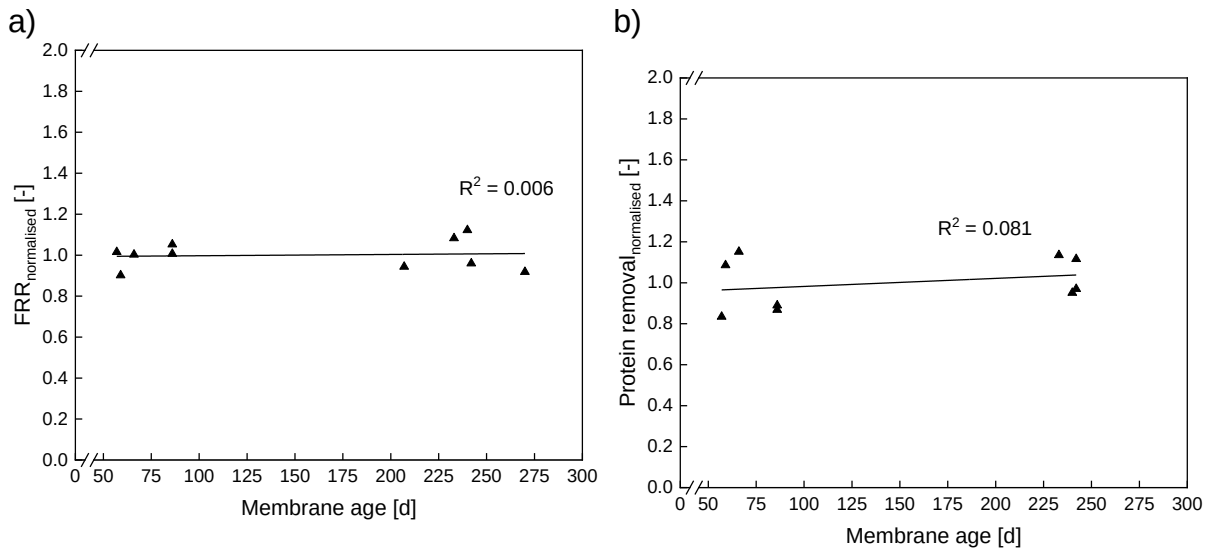

Figure 4-12. Influence of membrane age on $FRR_{normalised}$ (a) and protein $removal_{normalised}$ (b) for a steady cleaning with c_{NaOH} = 0.03%, v_{avg} = 2.2 m s^{-1} and $\Delta p_{TM,avg}$ = 0.35 bar. Normalisation was conducted by dividing each replicate's respective values of FRR and protein removal by the respective average FRR and protein removal for the above stated cleaning conditions. ANOVA observed no slope significantly different from zero at the 5% significance level.

5 Comparison of the efficiency of pulsed flow membrane cleaning in hollow fibre (HFM) and spiral-wound microfiltration membranes (SWM)[4]

Christian Kürzl[a]* and Ulrich Kulozik

Chair of Food and Bioprocess Engineering, TUM School of Life Sciences, Technical University of Munich, Weihenstephaner Berg 1, Freising, Germany

[a] New affiliation: Professorship Food Process Engineering, TUM School of Life Sciences, Technical University of Munich, Weihenstephaner Berg 1, 85354 Freising, Germany

* Corresponding author

Summary and contribution of the doctoral candidate

While fouling, e.g. by proteins during skim milk MF, and subsequent cleaning is a major issue and challenge across all membrane types, the extent of fouling and the cleanability of membranes varies mainly depending on the membrane's geometry. Besides the HFM examined in the previous chapter, SWM are widely used in the dairy industry. Here, FSM layers are separated by a spacer net wrapped around a permeate collection tube. Compared to the free flow geometry in HFM, the presence of spacers in FSM and SWM, on the one hand, acts as a turbulence promoter leading to more turbulent bulk flow and, on the other hand, causes flow shadows directly behind spacer filaments. These flow shadows lead to areas not contributing to filtration and pose cleanability issues that also facilitate biofouling and thus threaten product safety. As pulsed flow was presumed to enhance turbulence, it was hypothesised to be particularly beneficial in membrane systems containing flow shadows, e.g., induced by spacers, as it could help overcome the limited cleanability of e.g. FSM and SWM.

Accordingly, this study comparatively assessed cleaning efficiency in HFM and FSM by monitoring FRR, protein removal and conducting surface analyses via SEM. Additionally, the concentration of the cleaning agent NaOH was varied (0%, 0.03% and 0.3%) to assess the interplay between the mechanical enhancement caused by pulsed flow and the chemical cleaning effect caused by different NaOH concentrations.

---

[4] Original publication: Kürzl and Kulozik (2023b): Kürzl, C.; Kulozik, U. 2023. Comparison of the efficiency of pulsed flow membrane cleaning in hollow fibre (HFM) and spiral-wound microfiltration membranes (SWM). Food and Bioproducts Processing 139, 166–177. doi: 10.1016/j.fbp.2023.03.012. Adapted original manuscript. Adaptations of the manuscript refer to enumeration type, citation style, spelling, notation of units, format, and merging of all lists of references into one at the end of the dissertation. Permission for the reuse of the article is granted by by Elsevier Limited.

Regarding the concentration of cleaning agent, cleaning of FSM benefitted from pulsed flow without a cleaning agent (protein removal +36%), which implies positive effects also during rinsing steps. Without a cleaning agent, no positive effects could be observed in HFM, presumably due to the absence of flow shadows. In general, the results demonstrated that the interplay between the chemical cleaning part loosening the deposit and pulsed flow as the mechanical part removing the loosened deposit drastically changes with the cleaning agent concentration. As expected, the most pronounced improvements in protein removal were found in FSM (+48%), not in HFM (+32%), at c_{NaOH} = 0.03%. SEM images of FSM cleaned with steady and pulsed flow confirmed the positive impact of pulsed flow on areas subject to flow shadows under steady flow: It depicted distinct residues shaped like the former spacer grid for steady flow cleaned membranes and only some unspecific residues for pulsed flow cleaned membranes.

The doctoral candidate designed the experimental approach for this study based on a critical review of the literature. Data acquisition was mainly done by the doctoral candidate. The doctoral candidate also developed the experimental concept, analysed, interpreted and plotted the data. The manuscript was written and reviewed by the doctoral candidate. The co-author contributed to the project outline, the discussion of results, and the revision of the manuscript.

Abstract

Membrane cleaning is a particular issue for spiral-wound membranes (SWM), as their cleanability is limited due to spacer-induced flow shadows behind spacer filaments. One option to enhance membrane cleaning efficiency is applying pulsed flow, characterised by a cyclic transition between high and low flow rates. This study examined how the cleaning success in hollow fibre membranes (HFM) and spiral-wound membranes (SWM) can be enhanced by pulsed flow at varying concentrations of the cleaning agent NaOH. The cleaning success was determined by protein removal and flux recovery analyses as well as scanning electron microscopy (SEM) imaging of cleaned membrane surfaces. The highest increase in cleaning efficiency as a result of pulsed flow was found for SWM at c_{NaOH} = 0.03% (pH 11.3), where protein removal was increased by 48% over steady flow cleaning. SEM analyses confirmed that this was due to the pulsation-induced turbulence allowing improved access to spacer-induced flow shadows. Overall, cleaning success with pulsed flow at c_{NaOH} = 0.03% could be improved in both HFM and SWM over that of steady flow at c_{NaOH} = 0.30%, implying distinct reductions in chemicals consumption or shortened cleaning times when applying pulsed flow.

Highlights:

- Improved cleaning success during cleaning without NaOH in spiral-wound membranes
- Highest efficiency in spiral-wound membrane cleaning (at c_{NaOH} = 0.03%)
- Results imply distinct reductions in chemicals consumption with pulsed flow
- Results imply distinct reductions in energy consumption with pulsed flow

Keywords: alternative flow types; protein removal; flux recovery ratio; hollow fibre membrane; spiral wound membrane

5.1 Introduction

The separation of skim milk in whey proteins (d = 2–6 nm) (Brans et al. 2004) and casein micelles (d = 20–300 nm) (Brans et al. 2004) using microfiltration (MF) membranes is a major operation in the dairy industry yielding two main protein fractions with different applications and functionalities. However, the accumulation of retained components on and in the membrane material (Bartlett et al. 1995; Bird and Bartlett 2002; Cui et al. 2010) leads to a declining flux and protein permeation during the filtration process. Combined with the temperature dependant progression of biofouling (Schiffer and Kulozik 2020), this causes the necessity of frequent cleaning cycles to recover the initial filtration performance and ensure reproducible product quality. These cleaning cycles are chemicals- and energy-intensive and cause significant downtime of the filtration plant as they consist of several rinsing and chemical cleaning steps.

Single alkaline cleaning agents such as NaOH are usually insufficient to completely remove organic residues such as proteins (Bird and Bartlett 2002; Blanpain-Avet et al. 2009; Berg et al. 2014). Additionally, for concentrations of $c_{NaOH} \geq 0.1\%$, declining flux values have been reported to occur after an initial flux peak during cleaning (Bird and Bartlett 2002; Makardij et al. 1999). This phenomenon was discussed as being due to forcing swollen and detached proteins back into the pores (Bartlett et al. 1995; Bird and Bartlett 2002) or caustic-induced gelation of whey proteins with subsequent re-attachment to the membrane (Mercadé-Prieto and Chen 2005). Therefore, several chemical and mechanical methods (as specified further below) to enhance cleaning power have been investigated. Chemical enhancements often comprise the addition of enzymes, sequestrants, chlorines or surfactants (Ng et al. 2017; D'Souza and Mawson 2005). Nonetheless, besides increasing the environmental impact, wastewater pollution and costs, excessive chemical cleaning can also impair the membrane's life span (D'Souza and Mawson 2005; Rabiller-Baudry et al. 2021).

In contrast to chemical cleaning methods to enhance cleaning efficiency, adding mechanical methods often requires plant modifications or other investment costs. However, these methods can potentially improve not only the individual cleaning steps within a cleaning-in-place (CIP) cycle but also the entirety of the cleaning and filtration cycle. These mechanical enhancements include backflushing (Amar et al. 1990), backpulsing (Mores and Davis 2002; Parnham and Davis 1996; Redkar et al. 1996; Rodgers and Sparks 1992), turbulence promoters (Howell et al. 1993; Hartinger et al. 2020a; Krstić et al. 2002) and pulsed flow (Gillham et al. 2000; Blel et al. 2009a; Blel et al. 2009b; Yang et al. 2019; Augustin et al. 2010; Bode et al. 2007; Föste et al. 2013; Kürzl et al. 2022a). The latter is defined by pulsation frequency and amplitude, determined by the duration and difference between flow velocities' minimum and maximum phases and related pressure conditions. It was already investigated for both filtration and cleaning of various feed systems in different materials and geometries.

Besides several aspects influencing pulsation efficiency and related modes of action already identified, a lack of knowledge remains, particularly for the membrane cleaning of complex fouling matrices such as cross-linked, difficult-to-remove milk protein deposits. These aspects will be elaborated on in the following paragraphs.

Factors already identified to positively influence pulsation efficiency include the pulsation frequency (Gillham et al. 2000; Blel et al. 2009a; Blel et al. 2009b; Yang et al. 2019; Kürzl et al. 2022a), pulsation amplitude (Gillham et al. 2000; Blel et al. 2009a; Blel et al. 2009b; Augustin et al. 2010; Kürzl et al. 2022a), the annular effect (Richardson and Tyler 1929; Schlichting and Gersten 2006; Zhao and Cheng 1996; Camacho et al. 2012) and the flow regime (Gillham et al. 2000; Weidemann et al. 2014). For complex steel piping geometries, pulsed flow was also found to provide better access to areas considered flow shadows under steady flow conditions, such as elbows or extensions (Augustin et al. 2010; Föste et al. 2013). Therefore, it is conceivable that pulsed flow could also lead to a more efficient cleaning for membranes with complex geometry, like spiral-wound membranes (SWM). As mentioned above, these module types are affected by intense deposit formation and, therefore, more difficult cleaning, which has not been investigated so far.

Another critical aspect to consider is the feed system. While several studies on pulsed filtration of model systems, such as yeast (Weinberger and Kulozik 2021c; Howell et al. 1993) or silica (Hadzismajlovic and Bertram 1998, 1999; Bertram et al. 1993) suspensions, found significant improvements in the filtration flux, a study by Weinberger and Kulozik (2021a) on the pulsed MF for casein/whey protein fractionation using hollow fibre modules (HFM) observed an impaired filtration performance in terms of whey protein transmission into the permeate. This unexpected effect during pulsed flow filtration of skim milk was attributed to two aspects. Firstly, it was attributed to the small particle sizes of whey proteins and casein micelles, causing a lower influence of hydrodynamic forces than for larger particles used in previous studies (Altmann and Ripperger 1997); secondly, the extensive cross-linking of deposited caseins compared to other model systems was reported as a decisive factor. Casein micelles are highly hydrated, sponge-like and compressible structures with internal porosity that can form gel-like structures under higher transmembrane pressures (Δp_{TM}) and high concentrations (Horne 2020; Bouchoux et al. 2010; Bouchoux et al. 2009; Gebhardt et al. 2012; Qu et al. 2015). Hence, it was assumed that the temporarily high $\Delta p_{TM, max}$ within each pulse during pulsed flow filtration caused additional and irreversible compaction of the deposit instead of loosening effects (Weinberger and Kulozik 2021a). In contrast, our recent study on pulsed membrane cleaning after skim milk MF showed that pulsed flow can improve cleaning efficiency (Kürzl et al. 2022a), despite the unfavourable particle sizes and otherwise extensive cross-linkings. This was explained by the differences in the feed systems of both studies. While Weinberger and Kulozik (2021a) utilised pulsed flow during MF of skim milk with unhindered

protein cross-linking, our previous study utilised pulsed flow during membrane cleaning after skim milk MF with a low concentrated cleaning agent, namely 0.03% NaOH (pH 11.3), which loosens the deposit and cleaves parts of the cross-linking between milk proteins and the membrane, thus facilitating increased removal by mechanical forces (Gillham et al. 2000; Mercadé-Prieto et al. 2008). Hence, the intactness and intensity of remaining deposit cross-linking and, thus, c_{NaOH} play a decisive role in the effectiveness of pulsed flow.

Accordingly, this study reports on the influence of c_{NaOH} on the impact of pulsed flow on cleaning success; in particular, for the absence of NaOH and thus unhindered cross-linking, low concentrated NaOH (0.03%, pH 11.2), where positive effects of pulsed flow have already been reported, and high concentrated NaOH (0.30%, pH 12.0), where flux declines have been reported to limit cleaning success under steady flow cleaning (Bird and Bartlett 2002; Bartlett et al. 1995; Makardij et al. 1999).

The main types of membrane module geometries used in the dairy industry are ceramic tubular membranes, and spiral-wound membranes (SWM), which are flat sheet membranes separated between layers by a spacer net wrapped around a permeate collection tube. Also, HFM are a commonly used module type in pharmaceutical applications and also emerging in dairy applications. Due to different materials and geometries, each type has different pros and cons; a detailed performance comparison of the common membrane types was reported by Schopf et al. (2021b). While the shapes of tubular membranes and HFM are similar to pipes with open cross-sections, the spacers integrated into SWM act as turbulence promoters creating additional eddies (Geraldes 2002; Han et al. 2018b; Gu et al. 2017) in certain areas, disturbing the prevalent flow patterns and thereby reducing the critical Reynolds number (Re_{crit}) from 2300 in pipes (Rott 1990) to 35-400 depending on the spacer geometry (Koutsou et al. 2007; Schwinge et al. 2002; Geraldes 2002). However, computational fluid dynamics (CFD) simulations (Han et al. 2018b; Geraldes 2002; Schwinge et al. 2003; Gu et al. 2017; Kavianipour et al. 2017) and experimental works (Hartinger et al. 2020a) showed that this also leads to flow shadows with increased fouling accumulation in the close vicinity behind spacer filaments. Pulsed flow could be particularly advantageous for such membranes as it further increases turbulence (Blel et al. 2009a; Blel et al. 2009b; Augustin et al. 2010; Kürzl et al. 2022a) and provides better access of mechanical effects to these disadvantaged areas (Augustin et al. 2010; Föste et al. 2013). Accordingly, pulsed flow could help overcome one of the major drawbacks of membrane systems containing spacer-filled channels such as SWM, i.e. limited cleanability.

We hypothesise that the advantage of pulsed flow cleaning increases in membrane systems containing spacer-filled channels. The influence of membrane geometry was assessed in an HFM and an SWM, vicarious for membranes containing spacer-filled flow channels, which also exist in other flat sheet module types. The hypothesis is based on

previous studies observing flow shadows (Schwinge et al. 2003; Kavianipour et al. 2017; Fischer et al. 2020) with increased deposition (Hartinger et al. 2020a) in SWM, while other studies showed improved access to such flow shadows with pulsed flow (Augustin et al. 2010; Föste et al. 2013). Another study also suggested a synergistic effect between pulsed flow and baffles (Howell et al. 1993), such as spacers. To prove or disprove these hypothesises, we comparatively applied steady and pulsed flow cleaning after skim milk filtration in membrane systems mentioned above, characterised by the presence or absence of spacer nets. The cleaning success was determined by measuring flux recovery ratio (FRR) and protein removal upon the progress of membrane cleaning. To further assess the influence of pulsed cleaning on particle removal in the spacer-net vicinity in SWM, SEM-imaging was performed on membranes cleaned with steady or pulsed flow.

5.2 Material and methods

5.2.1 Skim milk

Filtration with deposit formation for subsequent cleaning experiments was conducted with pasteurised skim milk (74°C, 28 s) purchased from the dairy Molkerei Weihenstephan (Freising, Germany). The skim milk was stored at 4°C for a maximum of five days.

5.2.2 Filtration plant

A custom-designed lab-scale filtration plant was used for all experimental filtration and cleaning trials. A simplified piping and instrumentation diagram is given elsewhere, including a detailed description of its components (Kürzl et al. 2022a). In brief, the feed solution was pumped through the membrane modules by a centrifugal pump (Levitronix GmbH, Zurich, Switzerland), which can produce steady and pulsed flow by cycling between high and low pump capacity.

The setup was compatible with exchanging the membrane housings for different membrane systems. In this study, HFM and SWM were compared. To study how membranes containing spacers, such as industrial SWM, are affected by pulsed flow cleaning, an SWM was simulated on a lab scale by a test cell containing a flat sheet membrane piece and a diamond-shaped non-woven feed spacer (44 mil) (see Figure 5-1). This led to a channel height of d_i = 1.12 mm. The test cell was described in detail by Hartinger et al. (2019b). The size of the distance plates was designed to prevent membrane movement within the test cell while not leading to visible indentations of the spacer grid on the membrane surface.

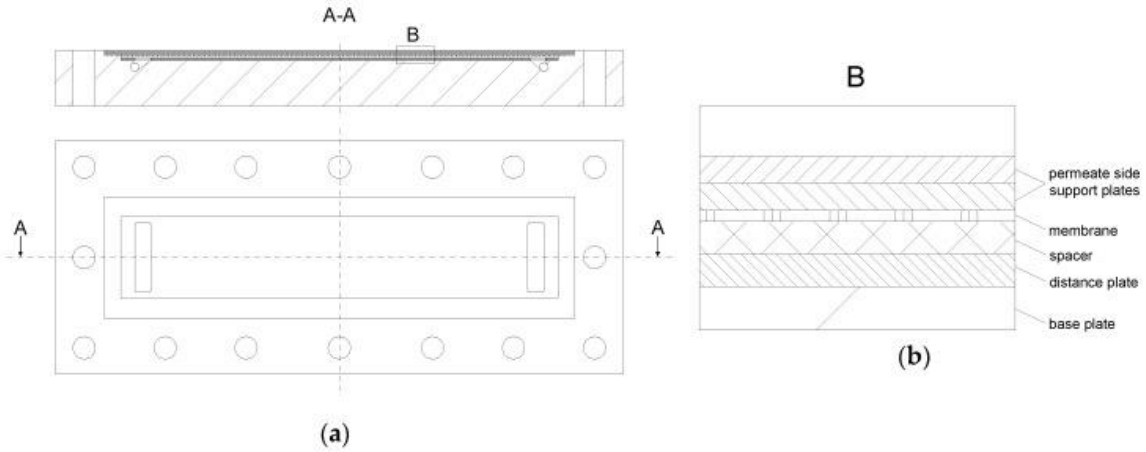

Figure 5-1. Architecture of a single test cell (a). Detail B shows the different inlays in the test cell during a filtration test (b) (Hartinger et al. 2019b).

For both membrane systems, the feed inlet pressure p_1, the retentate outlet pressure p_2 and the permeate pressure p_3 were measured directly at the respective outlet. These were required to control the Δp_{TM} (eq. (5-1)).

$$\Delta p_{TM} = \frac{p_1 + p_2}{2} - p_3 \tag{5-1}$$

Similarly, the permeate flow rate $\dot{V}_{per}$ was measured behind the permeate outlet of the respective housing to calculate the permeate flux J (eq. (5-2)) depending on the active membrane area $A_{membrane}$.

$$J = \frac{\dot{V}_{per}}{A_{membrane}} \tag{5-2}$$

The main pulsation variables are the frequency f, which is the number of pulsation cycles per second where one cycle duration is defined as the sum of high and low pump capacity phase t_{max} and t_{min} (eq. (5-3)), and the pulsation amplitude in terms of Δv as the difference between v_{max} and v_{min} and $\Delta\tau_w$ as the concomitant difference between $\tau_{w,\,max}$ and $\tau_{w,\,min}$ (eq. (5-4) and (5-5) respectively).

$$f = \frac{1}{t_{max} + t_{min}} \tag{5-3}$$

$$\Delta v = v_{max} - v_{min} \tag{5-4}$$

$$\Delta\tau_w = \tau_{w,max} - \tau_{w,min} \tag{5-5}$$

To calculate the wall shear stress τ_w, the pressure drop Δp_L between the feed inlet and the retentate outlet can be used according to equations (5-6) and (5-7).

$$\Delta p_L = p_1 - p_2 = \frac{1}{2} \cdot \lambda \cdot \frac{L}{d_i} \cdot \rho \cdot v^2 = \frac{4 \cdot L \cdot \tau_W}{d_i} \tag{5-6}$$

$$\tau_w = \frac{\Delta p_L \cdot d_i}{4 \cdot L} \quad (5\text{-}7)$$

where λ is the friction factor, L is the membrane length, d_i is the inner diameter of a hollow fibre capillary or the theoretical channel height in the flat-sheet membrane (FSM) cell without a spacer, ρ is the density, and v is the flow velocity.

It is to be noted that the calculation of average wall shear stress in spacer-filled channels only provides a rough estimation and that the local values of wall shear stress highly depend on the position relative to the spacer grid.

5.2.3 Membranes

To analyse the effect of membrane geometry on the efficiency of pulsed flow cleaning, experiments with HFM and SWM were comparatively assessed. Details on the utilised membranes are depicted in Table 5-1. The MF-HFM is made from polyethersulfone (PES) with an inner diameter d_i of 1.5 mm, and a maximum pore size (MPS) of 0.2 µm. The MF-HFM module (L = 0.5 m) had an active membrane area of 0.0233 m^2 using ten hollow fibres. As a lab-scale replacement for an MF-SWM, an MF-FSM (L = 0.2 m) made from polyvinylidenfluorid (PVDF) with a nominal pore size (NPS) of 0.3 µm and an active membrane area of 0.008 m^2 was used. The test cell will be referred to as SWM from here on.

Table 5-1. Characteristics of lab-scale membranes.

Membrane specification	Material	Pore size/ MWCO	L [mm]	d_i [mm]	$A_{membrane}$ [m^2]	Manufacturer
MF-HFM	PES	MPS = 0.20 µm	500	1.50	0.0233	Pentair X-Flow BV
MF-SWM Test cell	PVDF	NPS = 0.30 µm	200	1.12	0.008	SUEZ WTS Germany GmbH

5.2.4 Experimental procedure

Overall, all steps were performed at 50 °C. Deionised water was used in all steps except filtration and combined with cleaning agents, where applicable. Details were described in our earlier study (Kürzl et al. 2022a). In brief, the pure water flux was first measured to obtain the clean membrane's initial permeability before filtration. Filtration with skim milk for 20 min and $\Delta p_{TM,\ Filtration}$ = 1.8 bar was then conducted to generate a reproducible deposit. Afterwards, the milk was drained and the membrane plant was carefully rinsed with water to remove the remaining bulk milk and loosely bound material. The following cleaning experiments were

performed for 20 min in circulation under variable flow conditions and NaOH concentrations (c_{NaOH}) (Halag Chemie AG, Aadorf, Switzerland). Samples for protein analysis were collected from the feed tank after 1, 3, 5, 7, 10, 15 and 20 min of cleaning time.

An overview of conducted cleaning experiments is given in Table 5-2. As our previous study demonstrated the relevance of pulsation conditions such as amplitude, frequency and flow conditions such as v_{avg} and $\Delta p_{TM, avg}$, the setup was designed to enable comparable pulsed flow conditions $\Delta\tau_w$, $\Delta p_{TM, avg}$ and $\Delta p_{TM, cycle}$ between HFM and SWM at identical flow rates as well as comparable v_{avg} and $\Delta p_{TM, avg}$ between steady and pulsed flow cleaning experiments within a membrane. It should be noted that although experiments in SWM were conducted at lower Re than in HFM, the resulting turbulences are hardly comparable between HFM and SWM due to the reduced Re_{crit} in SWM (Koutsou et al. 2007; Schwinge et al. 2002; Geraldes 2002).

After the cleaning experiment, a second water flux measurement was conducted to provide the flux recovery ratio (FRR) (eq. (5-8)) as an indicator for hydraulic cleanliness. The respective water permeabilities were obtained by dividing the water flux J by Δp_{TM}. Finally, where cleaning evaluation indicated incomplete cleaning (FRR < 90%), an additional cleaning cycle with industrial cleaning agents was performed to restore membrane permeability.

$$FRR = \frac{water\ permeability_{after\ cleaning}}{water\ permeability_{before\ filtration}} \tag{5-8}$$

Table 5-2. Conducted cleaning experiments with associated levels of variables.

Membrane	Flow mode	c_{NaOH}	$\dot{V}_{avg}$	v		Re_{avg}	τ_w		Δp_{TM}		Frequency
		[%]	[L h^{-1}]	[m s^{-1}]		[-]	[Pa]		[bar]		[Hz]
				Δ	avg		Δ	avg	Δ	avg	f
MF-HFM	steady	0.0	140	n.a.	2.2	5250	n.a.	22.9	n.a.	0.35	n.a.
MF-HFM	pulsed	0.0	140	2.5	2.2	5250	47.5	30.0	0.5	0.35	0.5
MF-SWM	steady	0.0	140	n.a.	0.87	1547	n.a.	23.8	n.a.	0.35	n.a.
MF-SWM	pulsed	0.0	140	0.99	0.87	1547	52.4	32.7	0.5	0.35	0.5
MF-HFM[a]	steady	0.03	140	n.a.	2.2	5250	n.a.	22.9	n.a.	0.35	n.a.
MF-HFM[a]	pulsed	0.03	140	2.5	2.2	5250	47.5	30.0	0.5	0.35	0.5
MF-SWM	steady	0.03	140	n.a.	0.87	1547	n.a.	23.8	n.a.	0.35	n.a.
MF-SWM	pulsed	0.03	140	0.99	0.87	1547	52.4	32.7	0.5	0.35	0.5
MF-HFM	steady	0.03	45	n.a.	0.7	1670	n.a.	4.1	n.a.	0.35	n.a.
MF-HFM	pulsed	0.03	45	1.1	0.7	1670	9.5	4.8	0.24	0.35	0.5
MF-SWM	steady	0.03	45	n.a.	0.28	498	n.a.	4.4	n.a.	0.35	n.a.
MF-SWM	pulsed	0.03	45	0.44	0.28	498	9.3	5.1	0.5	0.35	0.5
MF-HFM	steady	0.30	140	n.a.	2.2	5250	n.a.	22.9	n.a.	0.35	n.a.
MF-HFM	pulsed	0.30	140	2.5	2.2	5250	47.5	30.0	0.5	0.35	0.5
MF-SWM	steady	0.30	140	n.a.	0.87	1547	n.a.	23.8	n.a.	0.35	n.a.
MF-SWM	pulsed	0.30	140	0.99	0.87	1547	52.4	32.7	0.5	0.35	0.5

[a]Data from Kürzl et al. (2022a).

5.2.5 Analyses and calculations

According to the method by Kürzl et al. (2022b), concentration, purification and quantification of proteins in the cleaning solution was performed using a combination of solid-phase extraction (SPE) and reversed-phase high-performance liquid chromatography (RP-HPLC). Agilent ChemStation software (Rev. B.04.03) was used to analyse RP-HPLC chromatograms. OriginPro 2021 (OriginLab Corporation, Northampton, MA, USA) was used to plot, fit and statistically evaluate the data. While error bars are given to indicate the variability between replicates, one-way analysis of variance (ANOVA) was used to evaluate and confirm statistical significance between data sets at the 5% level ($p < 0.05$). All experiments were done at least in triplicates.

Surface characterisation of SWM was conducted by scanning electron microscopy (SEM), where samples were collected after cleaning and cut from the centre of the membrane piece. After freeze-drying, the samples were sputtered with gold (20 s) and examined in a JSM-IT100 InTouchScope (JEOL Ltd., Tokyo, Japan) SEM at a voltage of 14 kV with the concomitant software (V1.050). It is to be noted that this method only allows a characterisation of the surface but not of any remaining internal fouling.

5.3 Results and discussion

5.3.1 Cleaning without a cleaning agent (c_{NaOH} = 0.00%)

Firstly, the effect of the flow mode on cleaning efficiency was assessed without adding a cleaning agent (c_{NaOH} = 0.00%). The resulting cleaning progressions for HFM and SWM are depicted in Figure 5-2.

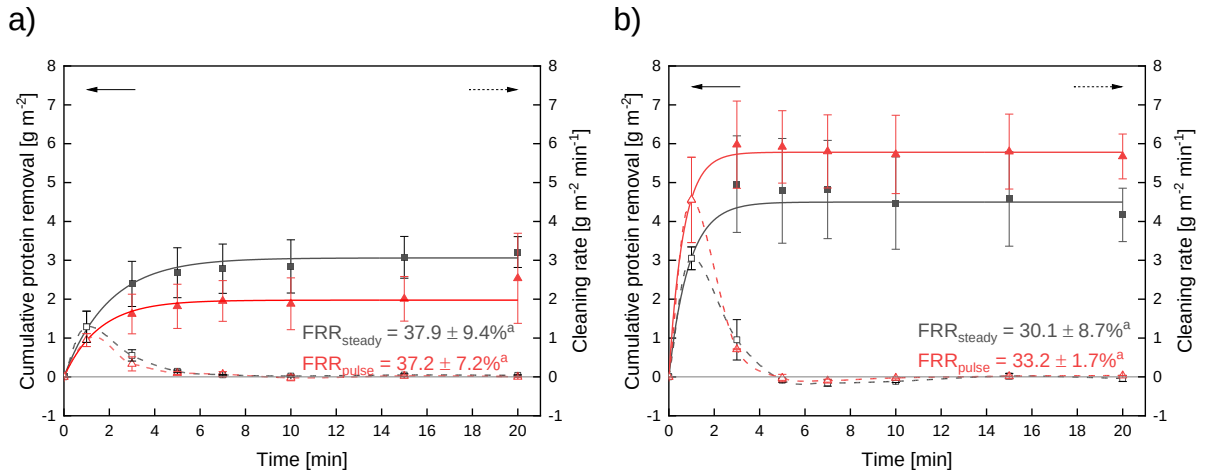

Figure 5-2. Cumulative protein removal (solid lines) and cleaning rate (dotted lines) of HFM (a) and SWM (b) cleaned without NaOH (c_{NaOH} = 0.0%) under steady (black) and pulsed flow (red). Cleaning conditions: f = 0.5 Hz, $\Delta\tau_{w,\,HFM}$ = 47.5 Pa, $\Delta\tau_{w,\,SWM}$ = 52.4 Pa, $\Delta p_{TM,\,avg}$ = 0.35 bar. $^{a\text{-}b}$ different letters indicate significant differences in FRR between flow modes ($p < 0.05$). Curves were asymptotically fitted with data points weighed by standard deviation resulting in $R^2 > 0.99$ for each curve.

For HFM (Figure 5-2a), steady and pulsed flow show similar cleaning rates and cumulative protein removal. In both flow modes, the cleaning rate approaches zero after 10 min, with pulsed flow reaching a slightly but not significantly lower cumulative protein removal after 20 min of 2.54 ± 1.16 g min^{-1} compared to 3.21 ± 0.40 g min^{-1} for steady flow. FRR also displays no differences between steady flow (FRR_{steady} = 37.9 ± 9.4%) and pulsed flow (FRR_{pulsed} = 37.2 ± 7.2%) cleaning. The missing positive effect of pulsed flow under these cleaning conditions compared to cleaning results reported earlier for c_{NaOH} = 0.03% in HFM (Kürzl et al. 2022a) can be explained by the missing chemical support of NaOH loosening the deposit by cleaving non-covalent bonds (Gillham et al. 2000; Fan et al. 2019), which made it more susceptible to removal by fluid forces. Feed characteristics have previously been determined as critical in studies on pulsed flow microfiltration with different feed systems (Weinberger and Kulozik 2021a, 2021c). In this case, the fluid behaviour in pulsed milk filtration studies should be somewhat comparable to that in the pulsed cleaning of milk residues without a cleaning agent (c_{NaOH} = 0.00%) despite differences in feed density and viscosity, as the deposit remains chemically undisturbed and its structure and stability being mainly governed by its internal cross-linking and that with the membrane. Also, previous studies discussed the effectiveness of pulsed flow filtration as dependent on the presence and intensity of deposit cross-linking (Weinberger and Kulozik 2021c). Hence, for cleaning HFM without NaOH, the

missing positive effects of pulsed flow can be attributed to the intactness of cross-linking within the milk protein deposit.

However, a different behaviour was observed for SWM (Figure 5-2b) due to its fundamentally different geometrical characteristics. While FRR_{pulsed} = 33.2 ± 1.7% was slightly but insignificantly increased over FRR_{steady} = 30.1 ± 8.7%, the cleaning rate of pulsed flow was significantly higher within the first minute. Also, its cumulative protein removal was constantly increased, reaching a final removal of 5.67 ± 0.58 g m^{-1}, which is 36.0% higher than that of steady flow with 4.17 ± 0.69 g m^{-1}. It is to be noted that the overall level of deposit amount found was distinctly higher in SWM than in HFM, which can be attributed to spacer-induced flow shadows behind spacer filaments allowing amplified protein deposition in SWM (Hartinger et al. 2020a).

The discrepancy in improvements in protein removal and FRR were discussed previously as being due to those cleanliness indicators not correlating linearly (Kürzl et al. 2022a; Blanpain-Avet et al. 2009) or the improved protein removal with pulsed flow mainly occurring on the membrane surface but not internally (Kürzl et al. 2022a). The latter seems unlikely here as the SWM used has a larger pore size (0.3 µm) than the HFM (0.2 µm), facilitating fluid flow access through the membrane pores. The larger discrepancy of no FRR increase and a simultaneous 36% protein removal increase in SWM suggests, compared to results from HFM, that this observation in SWM is geometry-related. It could be due to the steady flux measurement being prone to the same flow shadows as steady cleaning. Consequently, the steady flux measurement would be unable to detect additional protein removal near spacer filaments as these areas hardly contribute to flux during steady flux measurement regardless of fouling being present or absent. This would explain the observed indifference of FRR_{steady} and FRR_{pulsed} despite significant differences in protein removal and lead to an underestimation of hydraulic cleanliness in pulsed flow cleaning. It also highlights the importance of an additional chemical cleanliness evaluation, especially in membrane systems containing spacers.

An increased removal within flow shadows being achievable without adding a chemical cleaning agent also suggests that those deposits largely consist of reversible and loosely bound fouling. This seems reasonable, as deposits within flow shadows should, besides lower flow velocities, also be subjected to a considerably lower local Δp_{TM} and thus less compaction during steady flow filtration. The fact that the difference in cumulative protein removal between pulsed and steady flow does not change between 1 min (1.503 g m^{-2}) and 20 min (1.505 g m^{-2}) means that the main effect of pulsed flow is reached within the first minute of cleaning, which supports the explanation that most of the additionally removed fouling was only loosely bound with removal not depending on swelling or fatigue effects. However, no final conclusion

regarding the true kinetics of cleaning progression can be drawn due to the wide spread of values of replicates at the beginning of cleaning.

5.3.2 Cleaning with a low concentrated cleaning agent (c_{NaOH} = 0.03%; pH 11.3)

To examine whether pulsed flow can also improve the removal of irreversible fouling in combination with a cleaning agent, cleaning experiments with NaOH at pH 11.3 (c_{NaOH} = 0.03%) were conducted.

In HFM (Figure 5-3a), both flow modes reach significantly higher protein removal and FRR values than without NaOH (see 5.3.1), with the steady-state values being reached after 10 min. However, the improvements due to the addition of NaOH are more pronounced for pulsed flow (FRR +102%, Protein removal +100%) than steady flow (FRR +78%, Protein removal +19%), indicating synergistic effects between pulsed flow and NaOH. In contrast to cleaning without NaOH, here pulsed flow reaches significant improvements in both protein removal (+32.0%) and FRR (+11.0%), with cleaning rates of pulsed flow being constantly but insignificantly higher than those of steady flow. Hence, in HFM, adding a cleaning agent is required to gain positive effects with pulsed flow, which supposedly can solely improve the removal of irreversible deposits when loosened by NaOH. It is also to be noted that protein removal of steady and pulsed flow does not significantly change for an increased membrane length of 1.0 m (see Figure 5-8). Hence, it can be concluded that also the pulsation efficiency does not significantly change, despite a slight decrease from an improvement of +32% protein removal to +26% protein removal compared to respective values of steady flow cleaning.

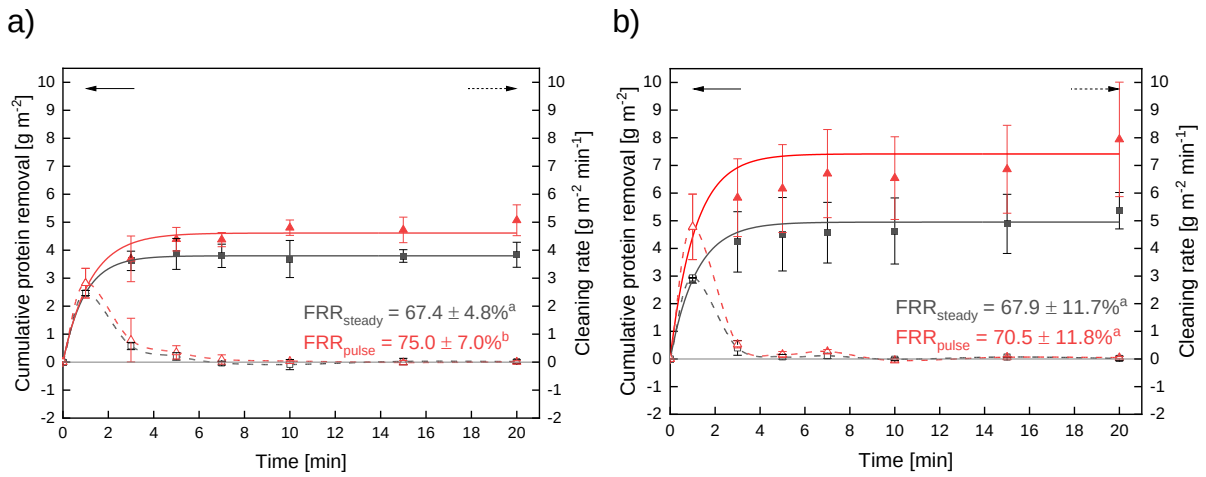

Figure 5-3. Cumulative protein removal (solid lines) and cleaning rate (dotted lines) of HFM (a) and SWM (b) cleaned with NaOH at pH 11.3 (c_{NaOH} = 0.03%) under steady (black) and pulsed flow (red). Cleaning conditions: f = 0.5 Hz, $\Delta\tau_{w,\,HFM}$ = 47.5 Pa, $\Delta\tau_{w,\,SWM}$ = 52.4 Pa, $\Delta p_{TM,\,avg}$ = 0.35 bar. $^{a-b}$ different letters indicate significant differences in FRR between flow modes ($p < 0.05$). Results for HFM from Kürzl et al. (2022a). Curves were asymptotically fitted with data points weighed by standard deviation resulting in $R^2 > 0.99$ for each curve.

While this confirms that pulsation efficiency is not significantly affected within common industrial membrane lengths of 1.0 m, this slight reduction in pulsation efficiency could be a

result of friction-related losses in shear stress along the membrane and thus be relevant for longer membranes or membranes aligned in series.

In SWM (Figure 5-3b), steady flow reaches an insignificantly increased protein removal (+28%) and a significantly increased FRR (+126%) compared to c_{NaOH} = 0.0%. In comparison, for pulsed flow at c_{NaOH} = 0.03%, protein removal (+91%) and FRR (+112%) significantly increase over the c_{NaOH} = 0.0% results. This indicates synergistic effects between pulsed flow and NaOH, similar as in HFM. Hence, adding NaOH leads to more pronounced improvements in cleaning success for pulsed flow, despite its already improved cleaning success at c_{NaOH} = 0.0%. Consequently, pulsed flow reaches a more pronounced improvement in protein removal over steady flow at c_{NaOH} = 0.03% (+48%) than at c_{NaOH} = 0.0% (+36%). Still, there are no differences in FRR, presumably due to the reasons discussed previously in chapter 5.3.1.

Overall, pulsed flow can significantly improve cleaning success in both HFM and SWM due to synergistic effects when combined with low-concentrated NaOH. Furthermore, SWM's improvements are more distinct due to the spacer-induced presence of flow shadows, to which pulsed flow can presumably provide improved access. This synergistic relation was also observed in a previous study by Howell et al. (1993) on the pulsed filtration of a 5% yeast, where they observed a 150% flux increase with pulsed flow in an unbaffled system and a 400% flux increase with pulsed flow in a baffled system.

Besides synergistic effects between pulsation and NaOH as well as pulsation and turbulence promoters, the results again confirm the increased protein deposition in the presence of spacers due to flow shadows. With a maximum removal of 7.94 ± 2.07 g m^{-2}, about 57% more protein was found on the SWM than on the HFM (maximum of 5.07 ± 0.55 g m^{-2}). Based on current and previous results (chapters 5.3.1 and 5.3.2), it is reasonable to assume that the increased efficiency of pulsed flow in SWM could also be due to the increased protein deposition after filtration. However, a study by Gillham et al. (2000) that investigated the influence of the deposit amount on the efficiency of pulsed and alternating flow reported an increase in the alternating flow efficiency but not in the pulsed flow efficiency with increasing protein coverage. As the transferability of those results to membrane systems is debatable, a visual inspection of the cleaned membranes (see chapter 5.3.4) will provide more insights into the mechanism of cleaning enhancement with pulsed flow.

Influence of the flow conditions

High amplitudes have previously been reported as a critical pulsation variable in HFM (Kürzl et al. 2022a; Weinberger and Kulozik 2021c). To investigate how the necessity of high amplitudes and average flow rates is influenced by the combination of pulsed flow with spacers, i.e. turbulence promoters, in SWM, supplementary trials in HFM and SWM with $\dot{V}_{avg}$ and Re reduced by 68% and thus $\Delta\tau_w$ reduced by 80% were conducted (Figure 5-4).

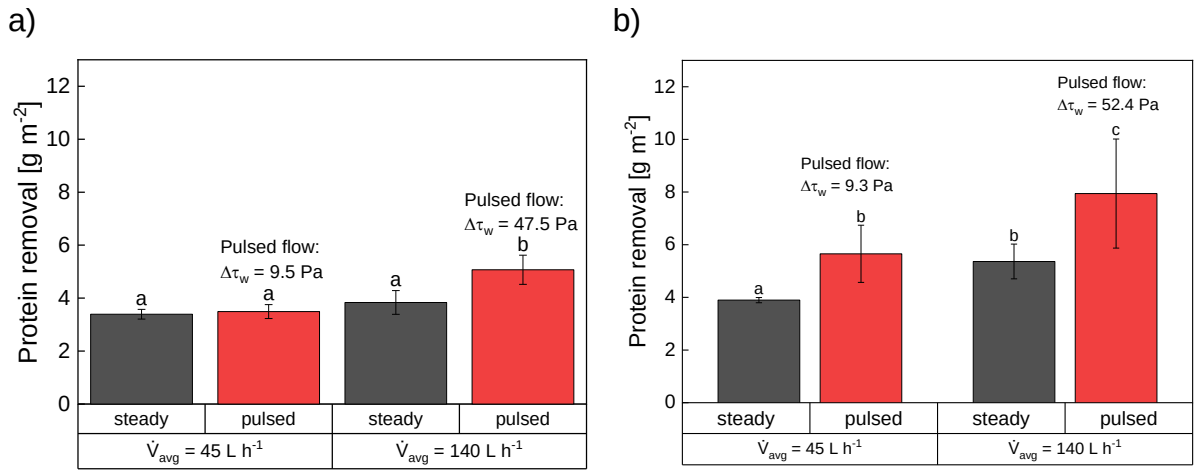

Figure 5-4. Influence of flow conditions and amplitude on cumulative protein removal in HFM (a) and SWM (b) cleaned with NaOH at pH 11.3 (c_{NaOH} = 0.03%) under steady (black) and pulsed flow (red). Overall cleaning conditions: f = 0.5 Hz, $\Delta p_{TM, avg}$ = 0.35 bar, $\Delta p_{TM, cycle}$ = 0.5 bar, c_{NaOH} = 0.03%. Specific flow conditions (HFM): $\Delta\tau_w$ = 9.5 Pa and Re_{steady} = 1670 at $\dot{V}_{avg}$ = 45 L h^{-1}, $\Delta\tau_w$ = 47.5 Pa and Re_{steady} = 5250 at $\dot{V}_{avg}$ = 140 L h^{-1}. Specific flow conditions (SWM): $\Delta\tau_w$ = 9.3 Pa and Re_{steady} = 498 at $\dot{V}_{avg}$ = 45 L h^{-1}, $\Delta\tau_w$ = 52.4 Pa and Re_{steady} = 1547 at $\dot{V}_{avg}$ = 140 L h^{-1}. $^{a\text{-}c}$ different letters indicate significant differences in protein removal between flow modes ($p < 0.05$). Results for HFM at $\dot{V}_{avg}$ = 140 L h^{-1} are from Kürzl et al. (2022a) and chapter 5.3.2. Results for SWM at $\dot{V}_{avg}$ = 140 L h^{-1} are also from chapter 5.3.2.

For steady flow in HFM (Figure 5-4a), the drastic change in flow rate, and thus Re, did not result in a significant change of the protein removal (3.39 ± 0.18 g m^{-2} at $\dot{V}_{avg}$ = 45 L h^{-1} versus 3.84 ± 0.45 g m^{-2} at $\dot{V}_{avg}$ = 140 L h^{-1}) but a slight change in FRR (62.77 ± 2.1% at $\dot{V}_{avg}$ = 45 L h^{-1} versus 67.4 ± 4.8% at $\dot{V}_{avg}$ = 140 L h^{-1}; see Figure 5-7a). Theses marginal differences in cleaning success, besides a fivefold shift in shear stress, are in accordance with the results from other studies, which attributed a minor relevance to the shear stress during steady flow cleaning of protein fouling (Blanpain-Avet et al. 2009; Bird and Bartlett 2002; Bartlett et al. 1995; Kürzl et al. 2022a). In contrast, for pulsed flow, there are significant differences between $\Delta\tau_w$ = 9.5 Pa (at $\dot{V}_{avg}$ = 45 L h^{-1}) and $\Delta\tau_w$ = 52.4 Pa (at $\dot{V}_{avg}$ = 140 L h^{-1}) for both protein removal (3.49 ± 0.26 g m^{-2} versus 4.39 ± 0.17 g m^{-2}) and FRR (62.6 ± 5.3% versus 72.0 ± 4.5%; see Figure 5-7a). While pulsed flow reportedly reached a significantly higher protein removal and FRR than steady flow at $\Delta\tau_w$ = 52.4 Pa, there is no significant difference between pulsed flow and steady flow at $\Delta\tau_w$ = 9.5 Pa neither in protein removal nor FRR. Compared to our previous study, where pulsed flow cleaning with a reduced amplitude still achieved significant improvements over steady cleaning (Kürzl et al. 2022a), the flow rate,

and thus Re, were simultaneously reduced in the present study. Hence, it can be assumed that pulsed flow imposes not only additional shear forces more efficiently but also has synergistic effects with the base turbulence depending on Re_{avg} and thus $\dot{V}_{avg}$.

In this regard, experiments in SWM (Figure 5-4b) provide more insights as they contain spacers acting as turbulence promotors. Here, for cleaning at $\dot{V}_{avg}$ = 45 L h $^{-1}$ with $\Delta\tau_w$ = 9.3 Pa, pulsed flow reached a 45% higher protein removal (5.65 ± 1.09 g m^{-2}) than steady flow (3 90 ± 0.10 g m^{-2}). In comparison, for a similar $\Delta\tau_w$ in HFM, cleaning with pulsed flow did not significantly improve protein removal over steady flow. Furthermore, pulsed flow reached a more pronounced improvement in protein removal over steady flow in SWM for $\Delta\tau_w$ = 9.3 Pa (+45%) than in HFM for $\Delta\tau_w$ = 47.5 Pa (+32%) despite an 80% lower amplitude and Re in SWM. This can be attributed to synergistic effects between pulsed flow and turbulence promoters such as spacer grids, which were discussed previously in chapter 5.3.2. Results at $\dot{V}_{avg}$ = 140 L h^{-1} further support this explanation where due to the increased amplitude of $\Delta\tau_w$ = 52.4 Pa, pulsed flow showed a more pronounced enhancement of protein removal by 48% over steady flow, as discussed previously. Regarding FRR (see Figure 5-7b), pulsed flow was slightly but insignificantly increased over steady flow at either flow rate, complying with the results of increased protein removal and the assumption of steady flux measurements being unable to detect improved removal within flow shadows.

5.3.3 Cleaning with a highly concentrated cleaning agent (c_{NaOH} = 0.30%; pH 12.0)

Compared to rinsing/cleaning without NaOH or cleaning at a moderate pH of 11.3 (c_{NaOH} = 0.03%), cleaning at pH 12.0 (c_{NaOH} = 0.30%) resembles harsh cleaning conditions near the chemical tolerance limit of many polymeric membranes with an expectable dominance of chemical cleaning aspects. This section examines whether pulsed flow can enhance cleaning efficiency under such conditions and reduce or avoid the previously re-attachment of detached foulants reported at such c_{NaOH} (Bird and Bartlett 2002; Bartlett et al. 1995; Bobe et al. 1998; Berg et al. 2014) by enhancing turbulence and shear stress.

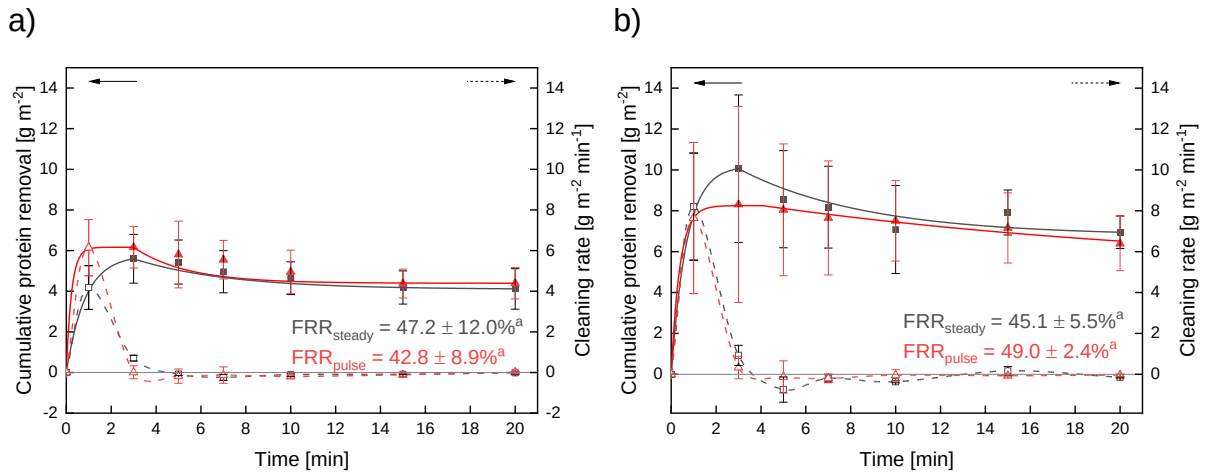

Figure 5-5. HFM (a) and SWM (b) cleaned with 0.30% NaOH (pH 12.0) under steady (black) and pulsed flow (red). Cleaning conditions: f = 0.5 Hz, $\Delta p_{TM,\,avg}$ = 0.35 bar, $\Delta p_{TM,\,cycle}$ = 0.50 bar. $^{a\text{-}b}$ different letters indicate significant differences in FRR between flow modes ($p < 0.05$).

For HFM (Figure 5-5a), cumulative protein removal reaches its maximum within 1-3 min. It proceeds to asymptotically decline until a final protein removal of 4.11 ± 1.00 g m^{-2} and 4.39 ± 0.77 g m^{-2} for steady and pulsed flow, respectively, with no significant differences between them at any point during cleaning. The cleaning rate reaching the highest values of all three concentrations at 1 min and the absence of differences between flow modes indicate the dominance of chemical effects over mechanical forces. Compliant with that, there are no significant differences in the extent of flux reduction (41 ± 12% for steady flow and 38 ± 7% for pulsed flow; see Figure 5-9a) and protein removal reduction (27 ± 3% for steady flow and 29 ± 3% for pulsed flow) after the initial peak at 3 min between pulsed and steady flow.

Nonetheless, compared to c_{NaOH} = 0.0%, both protein removal and FRR, which show no significant differences between flow modes, are increased (not significantly for steady flow) due to the additional chemical cleaning effects of NaOH for either flow mode. However, compared to c_{NaOH} = 0.03%, FRRs are significantly lower. Also, protein removal of steady flow reaches its maximum at c_{NaOH} = 0.3%, while protein removal of pulsed flow reaches its higher maximum at c_{NaOH} = 0.03%.

Protein removal and FRR for SWM, as depicted in Figure 5-5b, show similar results. Protein removal reaches its maximum after 3 min and then declines to final values of 6.95 ± 0.80 g m^{-2} and 6.39 ± 1.33 g m^{-2} with FRRs of 45.1 ± 5.5% and 49.0 ± 2.4% for steady and pulsed flow, respectively, without significant differences. Similarly to HFM, there are no significant differences in the extent of flux (50 ± 10% for steady flow and 51 ± 9% for pulsed flow; see Figure 5-9b) and protein removal decline (26 ± 14% for steady flow and 23 ± 8% for pulsed flow) after the initial peak. Comparing results of different c_{NaOH}, similar to HFM, protein removal and FRR at c_{NaOH} = 0.30% are increased compared to c_{NaOH} = 0.0% due to the additional chemical cleaning effects of NaOH. However, compared to c_{NaOH} = 0.03%, FRRs are significantly lower. Additionally, protein removal of steady flow is significantly increased over

that at c_{NaOH} = 0.03%, while protein removal of pulsed flow is significantly decreased over that at c_{NaOH} = 0.03%.

In both SWM and HFM, these results signify that for steady flow, the additional chemical cleaning power at c_{NaOH} = 0.30% is beneficial to cleaning success, despite the detrimental re-attachment of detached foulants. However, the higher NaOH concentration did not improve cleanliness for pulsed flow despite reports that the occurring flux decline can be reduced by increasing Re (Bird and Bartlett 2002), as also induced by pulsation. Another study investigating the alkaline cleaning of protein deposits reported alkali-induced swelling of polymeric membrane pores to facilitate in-pore fouling (Huang et al. 2021). Furthermore, Bird and Bartlett (2002) identified the cause of flux decline during MF membrane cleaning at $c_{NaOH} \geq 0.1\%$ for whey protein fouling not being concentration polarisation, i.e. reversible fouling, but rather irreversible fouling, as a pressure release and re-start of cleaning did not result in a flux change. They also found this to be pressure dependent, as increases in Δp_{TM} were found to significantly affect the extent of flux decrease and final flux recovery achieved (Bartlett et al. 1995; Bird and Bartlett 2002). Lastly, gel formation can be excluded as the underlying type of fouling as the deposited proteins are being diluted in cleaning solution. For a theoretical maximum removal of 10 g m^{-2} from a 0.08 m^2 membrane, this corresponds to an absolute deposit amount of 80 mg. To exceed the critical concentration of 200 g/L reported in literature to be required for gel formation (Qu et al. 2012) with this protein amount, it would have to be concentrated within < 0.4 mL of the 5 L cleaning solution. Additionally, with a considerable portion of caseins and whey proteins being a magnitude smaller than the nominal pore size of the membrane, the fouling phenomenon of gel formation is highly unlikely to occur in this filtration and related cleaning scenario. Hence, it can be assumed that the underlying fouling type was internal fouling. More specifically, this could either be swollen surface deposits being forced into the pores, as concluded by Bird and Bartlett (2002), or could be due to recirculation and redeposition of already removed deposits, i.e. forcing removed and swollen proteins back into the pores after the flux peak depending on the occurring maximum pressure conditions. Following from this, the lacking improvement with pulsed flow can be concluded to be due to the temporary higher $\Delta p_{TM, max}$ of pulsed flow compared to $\Delta p_{TM, avg}$ in steady flow causing increased in-pore fouling and thereby compensating the positive effects of increased turbulence. Hence, for pulsed flow, the optimum concentration of c_{NaOH} = 0.03% is located considerably lower than at steady flow with c_{NaOH} = 0.30% as the additional mechanical effects compensate for the low chemical cleaning power such that the removal of pulsed flow at c_{NaOH} = 0.03% is higher (+23% in HFM, +14% in SWM; both insignificant) than that of steady flow at c_{NaOH} = 0.30%. This is not only advantageous in terms of reduced cleaning consumption but also in terms of facilitated process control. Due to the decrease in cleaning success after an initial peak, cleaning at c_{NaOH} = 0.30% would require online monitoring of flux progression

and protein removal to adjust cleaning times to fit the peak in cleaning success. Furthermore, with industrial filtration plants usually consisting of several filtration units in series, each unit would reach the peak in cleaning success at different cleaning times due to local and temporal differences in foulant load, actual swelling time and thus differences in the temporal cleaning efficiency. As a consequence, separate cleaning, monitoring and process control would be required for each unit. This would not be an issue for cleaning with c_{NaOH} = 0.03%, as flux and protein removal remain constant after reaching the maximum cleaning success.

5.3.4 Surface analysis of cleaned membranes

To validate that pulsed flow causes improved access to flow shadows and thus improved protein removal, especially near spacer filaments, SWM cleaned with steady and pulsed flow were analysed by SEM, with virgin and fouled membrane surfaces in direct comparison (Figure 5-6). As a chemical concentration, c_{NaOH} = 0.03% (pH 11.3) was chosen, as the differences between steady and pulsed flow were most pronounced here.

The comparison of virgin membranes showed minor impurities or particles, with the pore structure of the membrane and a nominal particle size of 0.3 µm clearly visible at magnifications of x500 and x7500 (Figure 5-6a). The SEM image of a sample of the fouled membrane (Figure 5-6b) displayed no pore structure at a magnification of x500, as the membrane was entirely covered with milk protein deposits.

The membrane cleaned under steady flow conditions (Figure 5-6c) showed a mixture of a) and b) at a magnification of x500. Distinct protein residues and the underlying pore structure are visible, indicating a partially clean membrane surface. At a magnification of x30, protein residues following the shape of a contacting spacer filament can be seen with distinct residues perpendicularly crossed by a non-contacting spacer filament with less distinct residues, both filaments indicated by a white line as guide for the eye. These observations are supported by other studies observing flow shadows (Schwinge et al. 2003; Kavianipour et al. 2017; Fischer et al. 2020; Geraldes 2002) and, as a result, increased deposition (Hartinger et al. 2020a) near spacer filaments and the crossing points of filaments. Therefore, the remaining distinct fouling residues near and behind spacer filaments after steady flow cleaning seem well explainable.

The membrane cleaned by pulsed flow (Figure 5-6d), however, shows no such structured longitudinal clusters of protein residues that would indicate any areas affected by flow shadows at a magnification of x30. Overall, the membrane surface cleaned with pulsed flow appears similarly clean as the virgin membrane at magnifications of x500 and x7500. Nonetheless, some unspecific particles can be seen. According to the FRR_{pulsed} = 70.5 ± 11.8%, the membrane was not perfectly clean. This indicates that some residual

deposits, which pulsed flow could not completely remove from the membrane, were present as internal fouling as they cannot be observed with SEM.

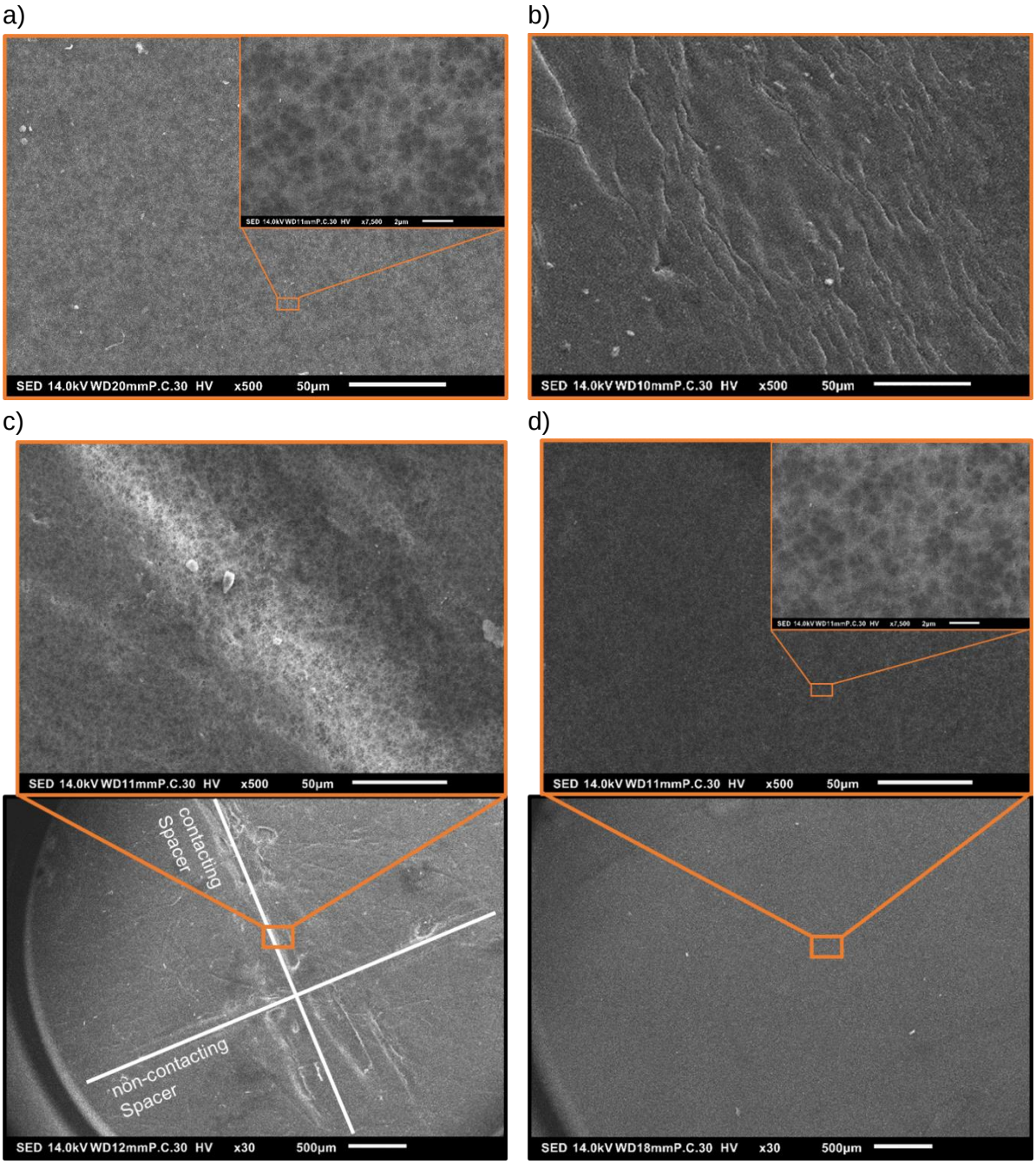

Figure 5-6. SEM images of a virgin membrane with a magnification of x500 and x7500 (a), a fouled membrane with a magnification of x500 (b), a membrane cleaned with steady flow with a magnification of x30 and x500 (c) and a membrane cleaned with pulsed flow with a magnification of x30, x500 and x7500 (d). Orange fields show the magnified membrane sections. White lines indicate spacer positions. Flow direction from top to bottom. Cleaning conditions in (c) and (d): f = 0.5 Hz, $\Delta\tau_W$ = 52.4 Pa, $\Delta p_{TM,\,avg}$ = 0.35 bar, c_{NaOH} = 0.03%.

Since the membrane length could not be varied in the flat sheet test cell, SEM pictures did not show any effect of a variation in the longitudinal sampling position on the extent or distribution of protein deposits for neither flow type. Hence, similar to HFM (see Figure 5-8),

no influence of the longitudinal membrane position or membrane length on the pulsation efficiency could be observed.

In summary, the visual analysis of membranes cleaned with steady and pulsed flow supports the hypothesis that flow shadows behind spacer net filaments in SWM impair the cleaning success under steady flow, while under pulsed flow, those flow shadows can be cleaned more effectively.

5.4 Conclusion

This study extends the knowledge on pulsed flow membrane cleaning after skim milk microfiltration by assessing the impact of combinations of factors contributing to membrane cleaning by varying NaOH concentrations, module types (HFM and SWM) and flow conditions (steady and pulsed flow) on cleaning efficiency.

While experiments in HFM underlined the importance of high $\Delta\tau_w$ and thus high v_{avg} for pulsation efficiency, lab-scale trials conducted with flat-sheet membranes covered by a spacer net, similar to SWM, showed higher pulsation efficiency already at lower v_{avg} and $\Delta\tau_w$. This is due to pulsed flow providing improved access to the exacerbated fouling in flow shadows near spacer filaments. This hypothesis could be affirmed by visual inspection of cleaned membranes. Hence, the largest effect of pulsed flow cleaning was detected for SWM-like membranes. This could be particularly important for industrial SWM, as they are limited in their maximum pressure drop in axial direction of flow, Δp_L, and accordingly limited in v_{avg} and $\Delta\tau_w$, to avoid membrane damage by the so-called membrane telescoping effect. While pulsed flow cannot extend the maximum working range of SWM, it can nevertheless substantially enhance its cleaning performance within the given specified operating axial pressure drop range. The improved access to flow shadows helps to reduce one of its main limitations and potential risk factors, i.e. limited cleanability. These results for SWM are also of industrial relevance, as pulsed cleaning with v_{avg} = 0.28 m s^{-1} achieving higher protein removal than steady cleaning at v_{avg} = 0.87 m s^{-1} could result in considerable reductions in energy consumption.

Without adding NaOH, positive effects of pulsed flow on cleaning efficiency were only observed in SWM (protein removal +36%). This is presumably due to additional, partly reversible, fouling in spacer net vicinity, to which pulsed flow provides improved access. This effect could also have positive implications for rinsing steps in cleaning-in-place (CIP) protocols as pulsed flow could be utilised to improve the deposit removal during rinsing steps between alkaline and acid cleaning steps and could thus possibly allow for reductions in concentrations of cleaning agents during the following chemical cleaning steps. However, the assessment of this interplay would require further investigation and should be validated using industrially sized SWM.

For low concentrated NaOH during alkaline cleaning (c_{NaOH} = 0.03%), pulsed flow achieved significantly better effects in protein removal than steady flow in both HFM (+32%) and SWM (+48%). For c_{NaOH} = 0.30%, pulsed flow could not enhance cleaning success in either membrane type, presumably due to the dominance of chemical effects. Nonetheless, cleaning with pulsed flow at c_{NaOH} = 0.03% achieved higher protein removal than the maximum removal achieved by steady flow at c_{NaOH} = 0.30% (+23% in HFM, +14% in SWM; both insignificant), which translates to an optional 90% reduction in cleaning agent concentration when utilising pulsed flow due to higher mechanical cleaning effects in synergistic interaction with chemical cleaning effects. In this regard, further studies are pending on the transfer of results to industrial cleaning agents and industrially sized SWM and the potential reduction of chemical concentrations due to the enhanced mechanical cleaning power of pulsed flow. Furthermore, the synergistic effects observed in SWM might be replicable in HFM when combined with new manufacturing concepts, that e.g. comprise a helical shape (Luelf et al. 2017; Tepper et al. 2022), thus also acting as a baffle and leading to increased turbulence.

Author Contributions

Conceptualisation, C.K.; methodology, C.K.; software, C.K.; validation, C.K.; formal analysis, C.K.; investigation, C.K.; resources, U.K.; data curation, C.K.; writing — original draft preparation, C.K.; writing — review and editing, C.K. and U.K.; visualisation, C.K.; supervision, U.K.; project administration, C.K.; funding acquisition, U.K. All authors have read and agreed to the published version of the manuscript.

Funding

This IGF Project of the FEI was supported via AiF to promote the Industrial Collective Research (IGF) of the German Ministry of Economic Affairs and Energy (BMWi), based on a resolution of the German Parliament. Project: AiF 57 EWN.

Acknowledgements

We gratefully thank Heidi Wohlschläger, Hermine Roßgoderer and Nora Biesenthal for their assistance with the RP-HPLC analysis of cleaning samples. Furthermore, we want to thank Siegfried Tuchborn from SIMA-tec GmbH and Christian Ederer, Erich Schneider, and Franz Fraunhofer in our workshop for technical support. We also want to thank Thomas Tran, Carina Malescha, Lina Dohm and Ramona Kammertöns for their experimental support. Finally, we thank Simon Schiffer, Roland Schopf and Martin Hartinger for fruitful discussions.

Conflicts of interests

The authors declare no conflict of interest. The authors declare no conflict of interest. The authors declare that they have no known competing financial interests or personal

relationships that could have influenced the work reported in this paper. The funders had no role in the design of the study; in the collection, analyses, or interpretation of data; in the writing of the manuscript, or in the decision to publish the results.

Supplementary

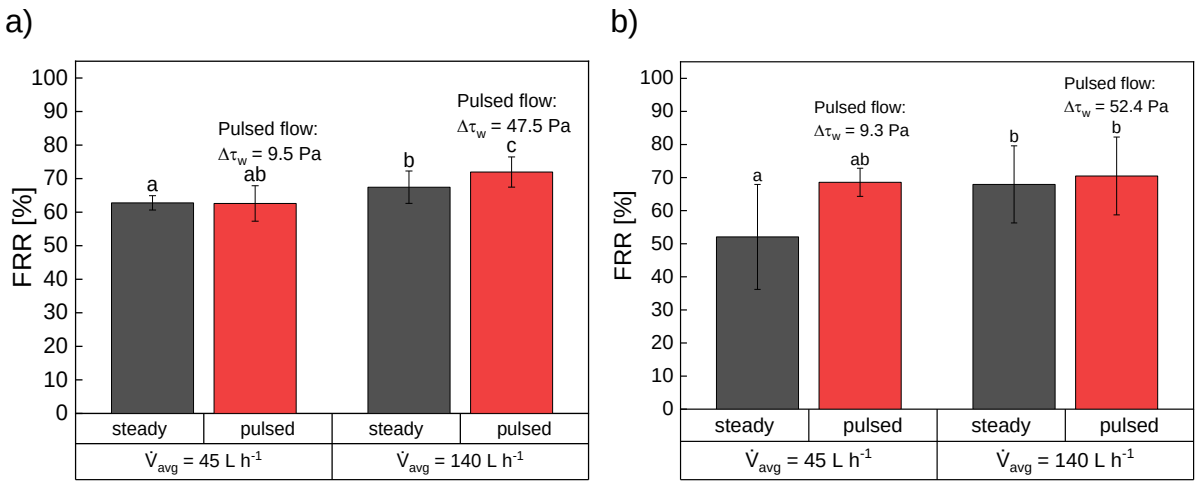

Figure 5-7. Influence of flow conditions and amplitude on FRR in HFM (a) and SWM (b) cleaned with NaOH at pH 11.3 (c_{NaOH} = 0.03%) under steady (black) and pulsed flow (red). Overall cleaning conditions: f = 0.5 Hz, $\Delta p_{TM,\,avg}$ = 0.35 bar, $\Delta p_{TM,\,cycle}$ = 0.35 bar, c_{NaOH} = 0.03%. Specific flow conditions (HFM): $\Delta\tau_w$ = 9.5 Pa and Re_{steady} = 1710 at $\dot{V}_{avg}$ = 45 L h^{-1}, $\Delta\tau_w$ = 47.5 Pa and Re_{steady} = 5319 at $\dot{V}_{avg}$ = 140 L h^{-1}. Specific flow conditions (SWM): $\Delta\tau_w$ = 9.3 Pa and Re_{steady} = 668 at $\dot{V}_{avg}$ = 45 L h^{-1}, $\Delta\tau_w$ = 52.4 Pa and Re_{steady} = 2076 at $\dot{V}_{avg}$ = 140 L h^{-1}. $^{a\text{-}c}$ different letters indicate significant differences in protein removal between flow modes ($p < 0.05$). Results for HFM at $\dot{V}_{avg}$ = 140 L h^{-1} are from Kürzl et al. (2022a) and chapter 5.3.2. Results for SWM at $\dot{V}_{avg}$ = 140 L h^{-1} are also from chapter 5.3.2.

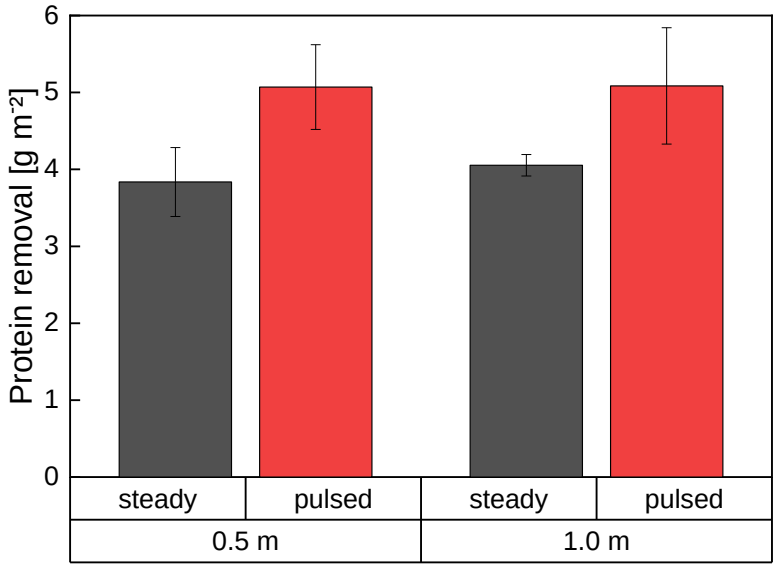

Figure 5-8. Influence of membrane length on protein removal in an HFM cleaned with NaOH at pH 11.3 (c_{NaOH} = 0.03%) under steady (black) and pulsed flow (red). Overall cleaning conditions: f = 0.5 Hz, $\Delta p_{TM,\,avg}$ = 0.35 bar, $\Delta p_{TM,\,cycle}$ = 0.35 bar, c_{NaOH} = 0.03%. Specific flow conditions (HFM): $\Delta\tau_w$ = 9.5 Pa and Re_{steady} = 1710 at $\dot{V}_{avg}$ = 45 L h^{-1}, $\Delta\tau_w$ = 47.5 Pa and Re_{steady} = 5319 at $\dot{V}_{avg}$ = 140 L h^{-1}.

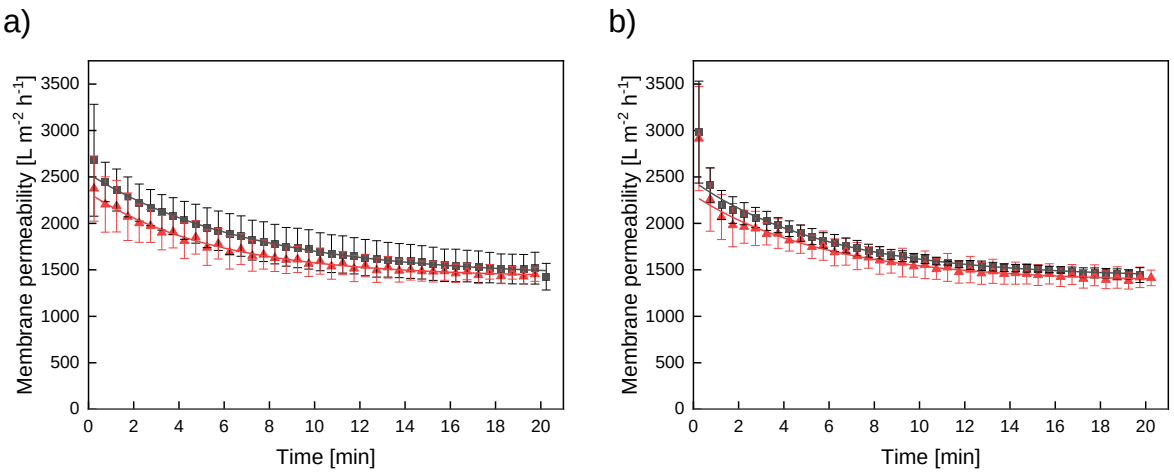

Figure 5-9. Influence of flow conditions and amplitude on Flux progression in HFM (a) and SWM (b) cleaned with NaOH at pH 11.3 (c_{NaOH} = 0.03%) under steady (black) and pulsed flow (red). Overall cleaning conditions: f = 0.5 Hz, $\Delta p_{TM,\,avg}$ = 0.35 bar, $\Delta p_{TM,\,cycle}$ = 0.35 bar, c_{NaOH} = 0.03%. Specific flow conditions (HFM): $\Delta\tau_w$ = 9.5 Pa and Re_{steady} = 1710 at $\dot{V}_{avg}$ = 45 L h^{-1}, $\Delta\tau_w$ = 47.5 Pa and Re_{steady} = 5319 at $\dot{V}_{avg}$ = 140 L h^{-1}. Specific flow conditions (SWM): $\Delta\tau_w$ = 9.3 Pa and Re_{steady} = 668 at $\dot{V}_{avg}$ = 45 L h^{-1}, $\Delta\tau_w$ = 52.4 Pa and Re_{steady} = 2076 at $\dot{V}_{avg}$ = 140 L h^{-1}. $^{a\text{-}c}$ different letters indicate significant differences in protein removal between flow modes ($p < 0.05$). Results for HFM at $\dot{V}_{avg}$ = 140 L h^{-1} are from Kürzl et al. (2022a) and chapter 5.3.2. Results for SWM at $\dot{V}_{avg}$ = 140 L h^{-1} are also from chapter 5.3.2.

6 Alternating Flow Direction improves Chemical Cleaning Efficiency in Hollow Fibre Membranes following Skim Milk Microfiltration[5]

Christian Kürzl[a]* and Ulrich Kulozik

Chair of Food and Bioprocess Engineering, TUM School of Life Sciences, Technical University of Munich, Weihenstephaner Berg 1, Freising, Germany

[a] New affiliation: Professorship Food Process Engineering, TUM School of Life Sciences, Technical University of Munich, Weihenstephaner Berg 1, 85354 Freising, Germany

* Corresponding author

Summary and contribution of the doctoral candidate

Besides pulsed flow, another approach to improving cleaning efficiency is alternating flow. It is characterised by an additional change in the feed-side flow direction after each pulsed flow cycle. While alternating flow already occurred during some studies on pulsed flow cleaning in steel geometries due to the type of pulsation-creation used, no systematic studies on alternating flow cleaning have been conducted yet. With the deposit formation being length-dependent, decreasing in intensity with Δp_{TM} from inlet to outlet, and low Δp_{TM} being beneficial for cleaning efficiency, a change in flow direction for cleaning after filtration should be of positive effect.

To assess the effects of alternating flow on cleaning efficiency, in the first step, the effects of frequency and amplitude were examined in HFM after skim milk MF. Also, experiments were conducted in membranes of different lengths (0.5 m and 1.0 m) to investigate the influence of membrane length on the efficiency of alternating flow cleaning. Lastly, experiments with steady backward flow were conducted with both membrane lengths to differentiate between the effects of permanent and cyclic flow reversal, i.e. alternating flow. Cleaning success was determined by monitoring FRR and protein removal.

It was found that both alternating and steady backward flow could significantly enhance hydraulic and chemical cleanliness at an increased membrane length of 1.0 m but not at 0.5 m. The central aspect identified as responsible for increased cleaning success is the increase in

[5] Original publication: Kürzl and Kulozik (2023a): Kürzl, C.; Kulozik, U. 2023. Alternating flow direction improves chemical cleaning efficiency in hollow fibre membranes following skim milk microfiltration. Journal of Food Engineering 356, 111587. doi: 10.1016/j.jfoodeng.2023.111587. Adapted original manuscript. Adaptations of the manuscript refer to enumeration type, citation style, spelling, notation of units, format, and merging of all lists of references into one at the end of the dissertation. Permission for the reuse of the article is granted by by Elsevier Limited.

the local ratio of flow velocity and, thus, shear stress to Δp_{TM} at the module inlet caused by steady or cyclic flow reversal. This phenomenon is due to the length dependant pressure drop combined with flow reversal leading to high flow velocities and simultaneous low Δp_{TM} at the membrane inlet where the deposition was most pronounced during filtration. Interestingly, no additional benefit of the cyclic flow reversal, i.e. alternating flow, over the permanent flow reversal, i.e. steady backward flow, could be observed. This was assumed to be due to alternating flow impairing pore clogging caused by the temporarily increased Δp_{TM} at the inlet during forward phases of high flow rate, which did not occur for steady backward flow.

The doctoral candidate designed the experimental approach for this study based on a critical review of the literature. Data acquisition was mainly done by the doctoral candidate. The doctoral candidate also developed the experimental concept, analysed, interpreted and plotted the data. The manuscript was written and reviewed by the doctoral candidate. The co-author contributed to the project outline, the discussion of results, and the revision of the manuscript.

Abstract

With efficient membrane cleaning remaining a challenge, novel approaches have promising potential to enhance cleaning efficiency. This study examined the concept of feed side cyclical and permanent flow reversal during membrane cleaning, to which so far it has not been applied to. Experiments were conducted in a hollow fibre microfiltration membrane with lengths of 0.5 m and 1.0 m using skim milk for deposit formation, NaOH as a cleaning agent, and flux recovery ratio and protein removal for cleaning evaluation. Overall, flow reversal was found to significantly increase cleaning success. Due to the length-dependent pressure drop and flow reversal, the local transmembrane pressure at the initial feed inlet $\Delta p_{TM,\,inlet}$ and thus the ratio of flow velocity to $\Delta p_{TM,\,inlet}$ was increased compared to steady forward flow cleaning. This proved beneficial as it combines high shear stress with low $\Delta p_{TM,\,inlet}$ where fouling was most pronounced after filtration.

Highlights:

- Cleaning success improved with alternating flow and steady backward flow
- Improvement due to increased ratio of $v/\Delta p_{TM}$ at the inlet with most severe fouling
- No benefit of alternating over steady backward flow due to temporarily higher Δp_{TM}

Keywords: alternating flow; pulsed flow; length dependency; flux recovery; protein removal

6.1 Introduction

Membrane-based separation is a major operation within food and pharmaceutical industries to fractionate, concentrate or purify complex solutes. Depending on the fractionation task and solute attributes, different particle retention, accumulation, and fouling intensities occur at the membrane surface and within the membrane during this process. The deposit formation-related decline in process efficiency and progression of biofouling (Schiffer and Kulozik 2020) cause the necessity of frequent cleaning cycles, which are chemicals and energy intensive processes, also causing significant production downtimes. The fractionation of complex biogenic solutions containing proteins, such as skim milk as a complex model fluid by microfiltration (MF) (Kulozik and Kersten 2002a), is particularly challenging in terms of deposit formation and cleaning due to extensive cross-linking between proteins and the formation of gel-like structures under high transmembrane pressures (Δp_{TM}) (Bouchoux et al. 2010; Gebhardt et al. 2012; Qu et al. 2015).

To improve fouling control and cleaning efficiency in membranes, several hydrodynamic methods such as backflushing (Amar et al. 1990), backpulsing (Mores and Davis 2002; Parnham and Davis 1996; Redkar et al. 1996; Rodgers and Sparks 1992), turbulence promoters (Howell et al. 1993; Hartinger et al. 2020a; Krstić et al. 2002), and pulsed/alternating flow (Gillham et al. 2000; Blel et al. 2009a; Blel et al. 2009b; Yang et al. 2019; Augustin et al. 2010; Bode et al. 2007; Föste et al. 2013; Kürzl et al. 2022a) have been proposed. Here, pulsed flow refers to constant fluctuations between a minimum and a maximum flow velocity with related pressure conditions, and alternating flow refers to a pulsed flow with additional cyclic feed-side flow reversal, i.e. a change of feed- and retentate-side. For pulsed flow, critical variables such as frequency (Blel et al. 2009a; Blel et al. 2009b; Gillham et al. 2000; Yang et al. 2019; Weidemann et al. 2014; Kürzl et al. 2022a), amplitude (Augustin et al. 2010; Blel et al. 2009a; Blel et al. 2009b; Gillham et al. 2000; Kürzl et al. 2022a), and the occurrence of flow reversal (Augustin et al. 2010; Blel et al. 2009a; Bode et al. 2007; Föste et al. 2013; Weidemann et al. 2014), i.e. alternating flow, could be identified, and modes of action, including increased turbulence (Augustin et al. 2010; Blel et al. 2009a; Blel et al. 2009b; Bode et al. 2007) and enhanced mass transfer (Blel et al. 2009a; Blel et al. 2009b; Gillham et al. 2000) were proposed. Alternating flow has already been proven beneficial for the separation efficiency during, e.g. the MF of model systems such as an aqueous solution of yeast and BSA by causing additional hydrodynamic instabilities (Weinberger and Kulozik 2021b, 2022). However, so far, the effects of periodically alternating flow on the filtration behaviour of complex biogenic solutions such as skim milk or the cleaning efficiency remain unknown.

Regarding cleaning processes, the hydrodynamic effects of alternating flow observed during fractionation should be transferable. In addition, the presence of a cleaning agent like NaOH changes the deposit structure by weakening non-covalent bonds (Mercadé-Prieto et al.

2008; Gillham et al. 2000), which could reinforce the hydrodynamic effects of alternating flow on cleaning efficiency. Besides the presence of a cleaning agent, the following two main aspects differentiate this scenario from the results of previous studies: Firstly, during alternating flow filtration, deposit formation can be controlled and reduced from the start (Weinberger and Kulozik 2021b), while a fully developed deposit has to be removed during cleaning. Secondly, previous studies have solely examined the separation of simple binary model systems of e.g. yeast and BSA (Weinberger and Kulozik 2022, 2021b; Howell et al. 1993). Contrary to those systems, fractionation of complex biogenic solutions, such as skim milk, causes a complex deposit formation and requires a thorough cleaning process. Hence, varying flow types during membrane cleaning after skim milk MF poses a fundamentally different scenario than varying flow types during the separation of model solutions.

Pulsed flow has already been successfully utilised in hollow fibre membranes (HFM) (Kürzl et al. 2022a; Kürzl and Kulozik 2023b) and spiral-wound membrane (SWM) (Kürzl and Kulozik 2023b) for membrane cleaning. Despite that no studies dedicated to alternating flow membrane cleaning, in some studies on pulsed flow cleaning of steel geometries, for specific amplitude settings and due to pistons and bellows being used to generate pulsation, temporary flow reversal, i.e. alternating flow, occurred (Gillham et al. 2000; Bode et al. 2007). Gillham et al. (2000) and Bode et al. (2007) claimed alternating flow as beneficial over pulsed and steady flow, presumably due to further intensified turbulences. Significant differences in surface roughness and porosity between steel piping used in previous works and membranes, changes in the complex fields of flow with components towards the porous wall, the mass transfer rates, and the shear stress distributions arise (Jha and Ajibade 2009; Ishak et al. 2008), do not allow to transfer results from impermeable to permeable walls.

Another critical aspect of alternating flow, found during alternating flow filtration studies to affect separation efficiency (Weinberger and Kulozik 2021b), is the intensity of length dependency. The length dependency of deposit formation is a cause of friction-related pressure loss over the membrane length (Δp_L) between the fluid and the membrane surface. It leads to a declining Δp_{TM} along the membrane module, causing more pronounced fouling at the module inlet than at the module outlet (Schopf et al. 2021a; Hartinger et al. 2020c; Hartinger et al. 2019b; Piry et al. 2008). Accordingly, these effects intensify with increasing flow velocity and membrane length. They have been extensively studied for skim milk MF in various module types, such as SWM (Hartinger et al. 2019b; Hartinger et al. 2020c), ceramic tubular membranes (CTM) (Piry et al. 2008), and HFM (Schopf et al. 2021a).

To our knowledge, the length dependency during membrane cleaning has so far not extensively been investigated beside our previous study not observing differences in protein removal with steady or pulsed flow when increasing the membrane length from 0.5 m to 1.0 m in an HFM (Kürzl and Kulozik 2023b). Nonetheless, it can be stated that the length-dependent

decline of Δp_{TM} along the membrane is also present during cleaning, presumably leading to axial differences in the cleaning efficiency. As a low Δp_{TM} has been reported beneficial for cleaning success (Bartlett et al. 1995; Bird and Bartlett 2002), a change in feed flow direction for cleaning after filtration should be of positive effect. It enables high crossflow velocities while ensuring a low Δp_{TM} at the initial or previous module inlet where deposit formation was most pronounced (Piry et al. 2008), and cleaning success was presumably limited due to the maximum Δp_{TM} occurring at the membrane inlet. This effect should increase with membrane length as for a longer module with the same average Δp_{TM}, the pressure drop along the module increases and thus, the local Δp_{TM}, at the previous inlet decreases.

Compared to steady backward or pulsed flow, alternating flow induces additional turbulences due to the periodic flow reversal. However, it remained unclear whether this positive characteristic prevails against the related occurrence of temporarily higher maximum Δp_{TM}, which has been reported decisive for the compaction of deposit structure (Qu et al. 2012; Hartinger et al. 2019a; Schiffer et al. 2020) and cleaning success (Bartlett et al. 1995; Bird and Bartlett 2002; Kürzl et al. 2022a) and would occur on both module sides due to cyclic flow reversal.

The objective was to assess whether membrane cleaning with flow modes including flow-reversal could improve cleaning success over that of steady flow and how this is affected by membrane length. To close the knowledge gaps, this study reports on the effects of permanent, i.e. steady backward flow, and cyclic changes, i.e. periodically alternating flow, in feed flow direction on cleaning efficiency in HFM after skim milk MF for a lab-scale membrane length of 0.5 m and, for validation, for an industrial-scale membrane length of 1.0 m. We hypothesise flow reversal to significantly improve the cleaning success due to flow reversal-related local effects of changes in Δp_{TM} and increased turbulence. Furthermore, the effects of alternating flow frequency and amplitude thereon were investigated. The cleaning success was determined by measuring the flux recovery ratio (FRR) as a hydraulic cleanliness criterion and the progression of protein removal as a chemical cleanliness criterion using a highly sensitive analytical method utilising solid-phase extraction (SPE) and reversed-phase high-performance liquid chromatography (RP-HPLC) (Kürzl et al. 2022b).

6.2 Material and methods

6.2.1 Skim milk

MF of pasteurised skim milk (74 °C, 28 s) purchased from the dairy Molkerei Weihenstephan (Freising, Germany) was used for deposit formation in all experiments. Before usage, the skim milk was stored at 4 °C for up to five days.

6.2.2 Filtration plant

A custom-designed lab-scale filtration plant (SIMA-tec GmbH, Schwalmtal, Germany) was used for all trials. The piping and instrumentation (P&I) diagram (Figure 6-1) shows the setup of the feed tank equipped with a double jacket, temperature sensor WIKA TR30 (WIKA Alexander Wiegand SE & Co. KG, Klingenberg, Germany), pressure sensors WIKA A-10 (WIKA Alexander Wiegand SE & Co. KG, Klingenberg, Germany), and flow sensors ABB FEH511 (ABB Automation Products GmbH, Göttingen, Germany) which provide ten data points per second.

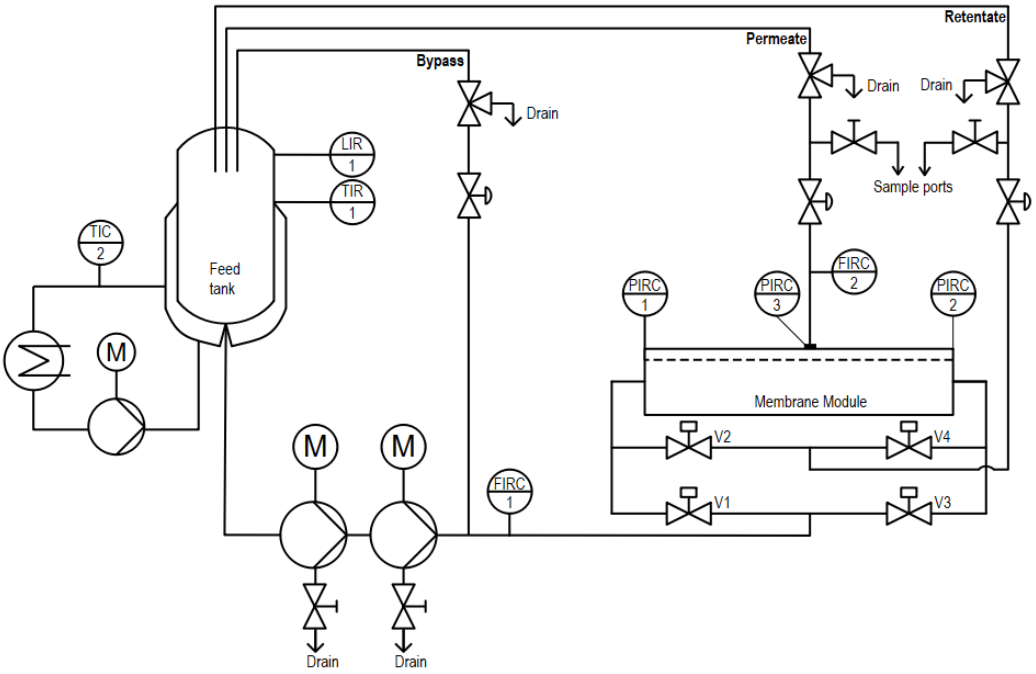

Figure 6-1. Piping and instrumentation (P&I) diagram of the membrane filtration plant.

Δp_{TM} and specific flux J were calculated by equations (6-1) and (6-3). The local Δp_{TM} at the membrane inlet (p_1) $\Delta p_{TM,\,inlet}$ was calculated by equation (6-2). For simplicity, the pressure or Δp_{TM} at the inlet, even under reversed flow, is always referred to as the pressure/Δp_{TM} at p_1.

$$\Delta p_{TM} = \frac{p_1 + p_2}{2} - p_3 \tag{6-1}$$

$$\Delta p_{TM,\,inlet} = p_1 - p_3 \tag{6-2}$$

$$J = \frac{\dot{V}_{per}}{A} \tag{6-3}$$

where p_1 is the feed inlet pressure, p_2 is the retentate outlet pressure, p_3 is the permeate pressure, J is the flux, $\dot{V}_{per}$ is the permeate flow rate, and A is the active membrane area. The

pressure drop Δp_L over the membrane length between inlet p_1 and outlet p_2 can be used to calculate the wall shear stress τ_W according to equation (6-4):

$$\Delta p_L = p_1 - p_2 = \frac{1}{2} \cdot \lambda \cdot \frac{L}{d_i} \cdot \rho \cdot v^2 = \frac{4 \cdot L \cdot \tau_W}{d_i} \quad (6\text{-}4)$$

where λ is the friction factor, L is the membrane length, d_i is the inner diameter of a hollow fibre, ρ is the density, and v is the crossflow velocity at the membrane inlet.

The two serially connected centrifugal pumps PuraLev-200MU (Levitronix GmbH, Zurich, Switzerland) with a contact-free impeller bearing allow for a rapid start-up and shut down, thus enabling versatile pulsed flow patterns, as described in previous works (Weinberger and Kulozik 2021a; Kürzl et al. 2022a).

Additionally, the four pneumatic valves allow changing the feed flow direction and hence enable alternating flow conditions. Closing valves V2 and V3 (with open valves V1 and V4) leads to a conventional forward crossflow from the membrane inlet at pressures sensor p_1 to the outlet at p_2. Backward crossflow from p_2 to p_1 was achieved by closing valves V1 and V4 (with open valves V2 and V3). A full alternating flow cycle consists of a forward pulsed flow cycle with defined phase durations of high and low flow rates and Δp_{TM}, a change in flow direction by opening and subsequently closing the respective valves with a delay of 0.1 s to minimise pressure peaks, and a backward pulsed flow cycle.

An exemplary alternating flow profile, which shows the time-resolved progression of the target pump capacity, the crossflow velocity and Δp_{TM}, is depicted in Figure 6-2. Here, the frequency f (eq. (6-5)) of alternating flow is defined as the duration of one forward/backward cycle consisting of a phase Δt_{max} with high (v_{max}) and a phase Δt_{min} with low (v_{min}) pump capacity.

$$f = \frac{1}{\Delta t_{max} + \Delta t_{min}} \quad (6\text{-}5)$$

$$\Delta v = v_{max} - v_{min} \quad (6\text{-}6)$$

$$\Delta p_{TM,\,cycle} = \Delta p_{TM,\,max} - \Delta p_{TM,\,min} \quad (6\text{-}7)$$

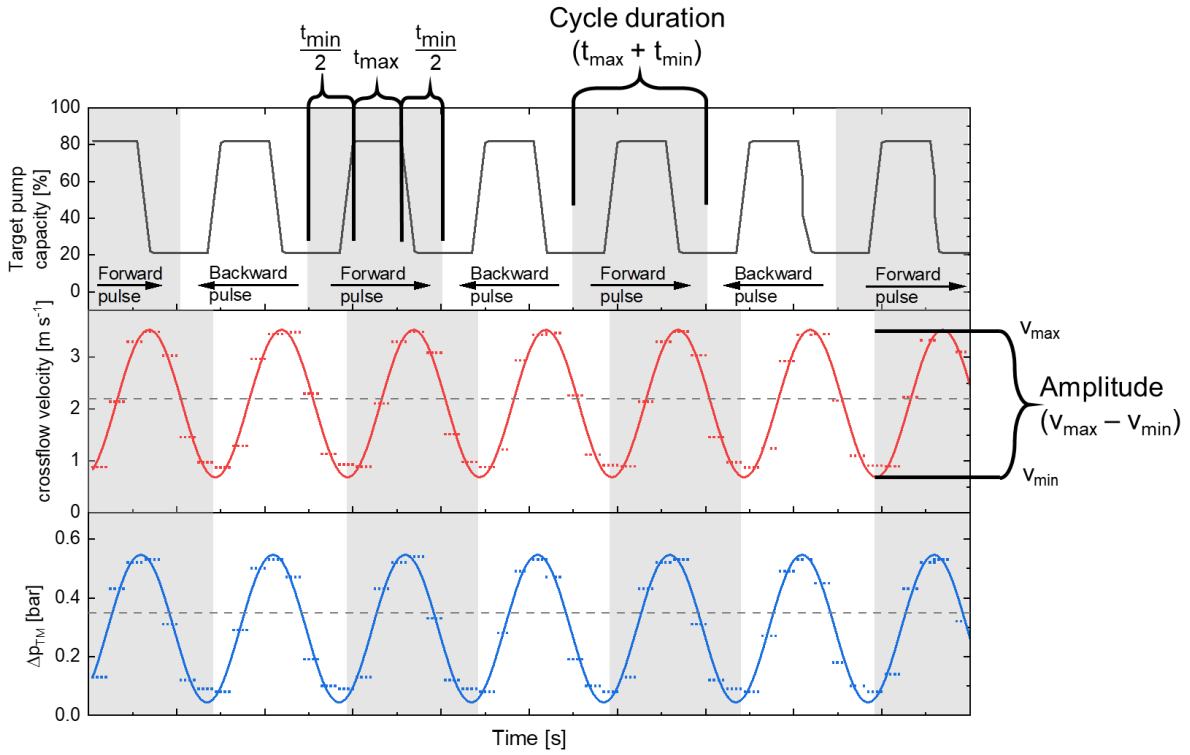

Figure 6-2. Profile of target pump capacity (black), crossflow velocity (red) and Δp_{TM} (blue) over several alternating cycles during cleaning. The dotted lines (grey) indicate each variable's average steady flow values.

The amplitudes Δv and $\Delta p_{TM,\,cycle}$ of alternating flow were defined as the difference between the respective minimum and maximum values with one forward/backward cycle (eq. (6-6) and (6-7)). Higher values than f = 0.5 Hz and Δv = 2.5 m s^{-1} were not feasible as the transition speed for pump capacity changes was technically limited. Due to the feed flow sensor F1 being located ahead of valves V1-V4, flow rates are always indicated as absolute values, regardless of the feed flow direction. Nonetheless, the combination of forward pulses and backward pulses causes a flow reversal, similar to experiments done by other authors reaching negative feed flow rates due to the specifications of the pump system (Gillham et al. 2000; Bode et al. 2007). The average values $\Delta p_{TM,\,avg}$ and v_{avg} resulting from the combination of alternating flow frequency and amplitude were calculated by equations (6-8) and (6-9). Complimentary steady crossflow cleaning experiments were always conducted at identical values of $\Delta p_{TM,\,avg}$ and v_{avg}.

$$\Delta p_{TM,\,avg} = \frac{\Delta t_{max} \cdot \Delta p_{TM,\,max} + \Delta t_{min} \cdot \Delta p_{TM,\,min}}{\Delta t_{max} + \Delta t_{min}} \tag{6-8}$$

$$v_{avg} = \frac{\Delta t_{max} \cdot v_{max} + \Delta t_{min} \cdot v_{min}}{\Delta t_{max} + \Delta t_{min}} \tag{6-9}$$

6.2.3 Membranes

MF-HFM with different fibre lengths of 0.5 m and 1.0 m were assessed to analyse the length dependency of alternating flow efficiency. MF-HFM made from polyethersulfone (PES) with an inner diameter d_i of 1.5 mm, and maximum pore size (MPS) of 0.2 µm and a nominal water flux of 700 L m^{-2} h^{1} at Δp_{TM} = 0.10 bar (Pentair X-Flow BV, Enschede, Netherlands) were used. With ten fibres per module, the HFM had an active membrane area of 0.0233 m^2 (L = 0.5 m) and 0.0459 m^2 (L = 1.0 m).

6.2.4 Experimental procedure

The details of the experimental procedure were described in a previous work (Kürzl et al. 2022a). Overall, all steps were performed at 50 °C. Deionised water was used in all steps except filtration and during cleaning in combination with NaOH. Before each experiment, the plant was rinsed to remove preservatives, and the pure water flux was measured as a baseline for the clean membrane permeability. Filtration with skim milk was then conducted at $\Delta p_{TM, Filtration}$ = 1.8 bar and v = 1 m s^{-1} to generate a reproducible deposit. Schopf et al. (2020) found no structural changes in the deposit and, related to that, a quasi-stationary flux after 20 min MF of skim milk. Hence, after 20 min of filtration, the milk was drained and the plant was rinsed to remove loosely bound material.

Subsequently, cleaning experiments were performed for 20 min with c_{NaOH} = 0.03% at pH 11.3 in circulation mode under variable flow conditions (see Table 6-1) and membrane specifications. These include alternating flow experiments at maximum fluctuation frequency and amplitude at two different membrane lengths to assess the influence of length dependency on alternating flow cleaning efficiency. Further runs were conducted at reduced frequencies and amplitudes to assess their influence on cleaning success. For each alternating flow cleaning experiment, a corresponding run with steady flow cleaning was conducted at identical v_{avg} and $\Delta p_{TM, avg}$. To further differentiate between the effects of a temporary flow reversal (as in alternating flow) and a permanent flow reversal (as in steady backward (bw) flow), additional experiments with steady forward (fw) and bw flow cleaning were conducted in these membranes.

Table 6-1. Conducted cleaning experiments with associated levels of variables.

Membrane	Flow mode [-]	Frequency [Hz]	v [m s^{-1}]			Δp_{TM} [bar]		
		f	Δ	avg	$\Delta p_{TM, cycle}$	avg	max	min
HFM (0.5 m)[a]	steady fw	0.00	0.0	2.2	0.00	0.35	0.35	0.35
HFM (0.5 m)	steady bw	0.00	0.0	2.2	0.00	0.35	0.35	0.35
HFM (0.5 m)	alternating	0.10	2.5	2.2	0.50	0.35	0.60	0.10
HFM (0.5 m)	alternating	0.25	2.5	2.2	0.50	0.35	0.60	0.10
HFM (0.5 m)	alternating	0.50	2.5	2.2	0.50	0.35	0.60	0.10
HFM (0.5 m)	alternating	0.50	0.5	2.2	0.10	0.35	0.40	0.30
HFM (0.5 m)	alternating	0.50	1.1	2.2	0.24	0.35	0.47	0.23
HFM (1.0 m)	steady fw	0.00	0.0	2.2	0.00	0.35	0.35	0.35
HFM (1.0 m)	steady bw	0.00	0.0	2.2	0.00	0.35	0.35	0.35
HFM (1.0 m)	alternating	0.50	2.5	2.2	0.50	0.35	0.60	0.10

[a]Data from Kürzl et al. (2022a).
fw = forward; bw = backward.

During cleaning, samples for protein analysis as an indicator of chemical cleanliness were collected from the feed tank after 1, 3, 5, 7, 10, 15, and 20 min. Cleaning rates were calculated according to eq. (6-10).

$$Cleaning\ rate = \frac{protein\ removal_{t_x} - protein\ removal_{t_{x-1}}}{t_x - t_{x-1}} \quad (6\text{-}10)$$

where t_x is the time of the current sampling and t_{x-1} is the time of the previous sampling.

After cleaning, the plant was rinsed to remove NaOH and loose deposit material. A second water flux measurement was conducted to calculate the percentage of recovered water flux, i.e. the FRR (eq. (6-11)), as an indicator for hydraulic cleanliness. An additional cleaning cycle with industrial cleaning agents was performed where FRR indicated incomplete cleaning (FRR < 90%).

$$FRR = \frac{water\ permeability_{after\ cleaning}}{water\ permeability_{initial}} = \frac{J_{after\ cleaning}}{\Delta p_{TM.\,after\ cleaning}} \Big/ \frac{J_{initial}}{\Delta p_{TM,\,initial}} \quad (6\text{-}11)$$

where $J_{initial}$ and $\Delta p_{TM,\,initial}$ are the values for J and Δp_{TM} of the clean membrane and $J_{after\ cleaning}$ and $\Delta p_{TM.\,after\ cleaning}$ are the respective values after cleaning.

6.2.5 Analyses and calculations

All experiments were done at least in triplicates. Analysis of protein samples from the cleaning solution was performed using a combination of SPE and RP-HPLC according to the method described by Kürzl et al. (2022b). Agilent ChemStation software (Rev. B.04.03) was used to analyse RP-HPLC chromatograms. OriginPro 2021 (OriginLab Corporation, Northampton, MA, USA) was used to plot, fit and statistically evaluate the data. One-way analysis of variance (ANOVA) was used to evaluate statistical significance between data sets at the 5% level ($p < 0.05$).

6.3 Results and discussion

6.3.1 Influence of alternating flow on cleaning success

The impact of alternating flow, generated by the custom-designed lab-scale filtration plant via controlled valves and additional piping, on cleaning success was assessed for maximum frequency (f = 0.5 Hz) and amplitude (Δv = 2.5 m s^{-1}, $\Delta p_{TM,\,cycle}$ = 0.50 bar), as the strongest removal forces were expected at these conditions. Comparative steady crossflow cleaning experiments were conducted at identical v_{avg} = 2.2 m s^{-1} and Δp_{TM} = 0.35 bar. The time-resolved cleaning progression (Figure 6-3) shows a significantly increased cleaning rate for alternating flow (+36%) over steady flow after 1 min of cleaning. After that, cleaning rates approached zero after 7 min of cleaning with insignificant differences between steady and alternating flow.

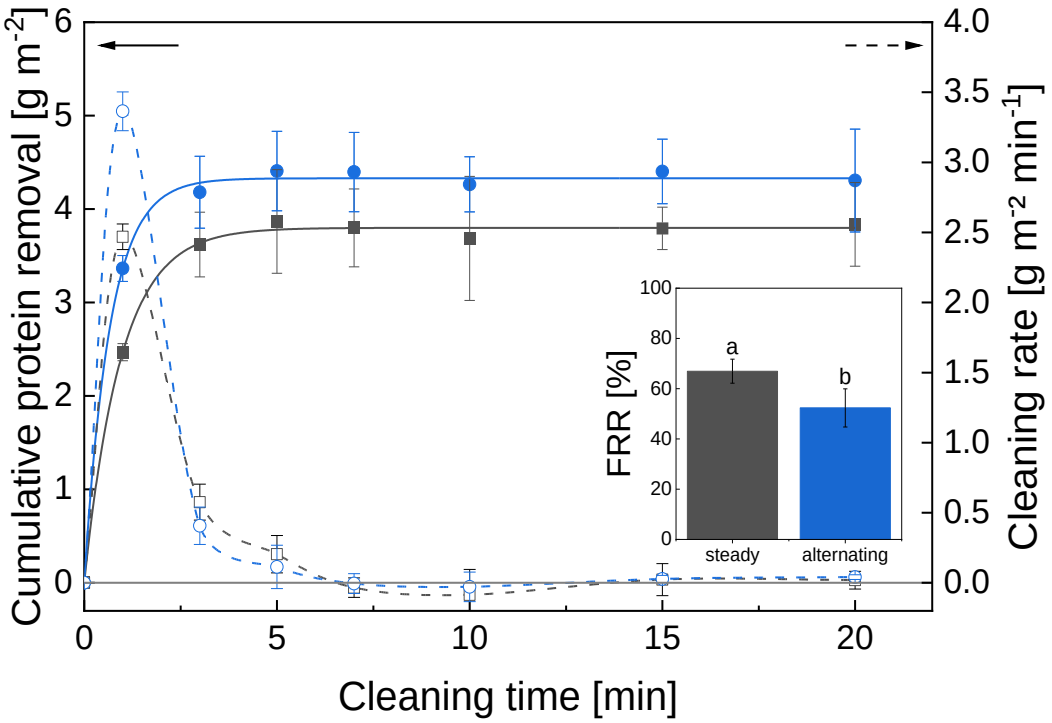

Figure 6-3. Cleaning progression in terms of cleaning rate (dashed lines) and cumulative protein removal (solid lines) for steady flow cleaning (black squares) and alternating flow cleaning (blue circles). Cleaning conditions: f = 0.5 Hz, v_{avg} = 2.2 m s^{-1}, Δv =2.5 m s^{-1}, $\Delta p_{TM,\,avg}$ = 0.35 bar, $\Delta p_{TM,\,cycle}$ = 0.50 bar. Steady flow cleaning was conducted at identical v_{avg} and $\Delta p_{TM,\,avg}$. Data of steady cleaning results from Kürzl et al. (2022a). $^{a\text{-}b}$ different letters indicate significant differences between FRR results ($p < 0.05$). Alternating flow leads to an initially increased cleaning rate after 1 min and an insignificantly increased cumulative protein removal after 20 min cleaning time while its FRR is significantly reduced compared to that of steady flow.

Accordingly, the cumulative protein removal of alternating flow reached a significantly higher value after 1 min than steady flow cleaning. This immediate positive influence of alternating flow on protein removal could be attributed to flow reversal causing increased turbulence, a reduced thickness of the laminar boundary layer and thus accelerated removal of loosely bound deposits compared to steady or pulsed flow (Kürzl et al. 2022a). Afterwards,

the curves of cumulative protein removal for steady and alternating flow cleaning converged while asymptotically approaching values of 4.31 ± 0.55 g m^{-2} and 3.84 ± 0.45 g m^{-2} for alternating and steady flow, respectively, with no significant differences between them.

Besides alternating flow nonetheless reaching a slightly higher protein removal, the FRR of alternating flow ($52.03 \pm 7.6\%$) was significantly lower than that of steady flow ($67.0 \pm 4.8\%$). The converged protein removal and overall decreased FRR of alternating flow cleaning appear to be in accordance with results from Weinberger and Kulozik (2022) for the alternating MF of an aqueous yeast and BSA mixture, which mainly presented improved protein permeation due to improved deposit control while simultaneously observing increased pore clogging and thus irreversible fouling, out of reach for the flow mechanics on the feed side above the membrane. Equivalently for cleaning, the overall deposit removal was slightly improved while FRR was decreased, which could also be due to pore clogging. This has already been hypothesised to be an adverse effect of pulsed flow for high $\Delta p_{TM,\,cycle}$ (Kürzl et al. 2022a) and could be more pronounced for alternating flow due to the additional flow reversal allocating length dependant Δp_{TM}-effects to both the membrane inlet and outlet.

Despite the additional cyclic flow reversal, alternating flow could not significantly enhance cleaning success over steady or pulsed flow cleaning (Kürzl et al. 2022a) at the chosen conditions. Accordingly, the following sections report on the influence of varying frequencies, amplitudes and length dependency effects on the efficiency of alternating flow cleaning in HFM.

6.3.2 Influence of alternating flow frequency and amplitude on cleaning efficiency

To investigate the behaviour of alternating flow at varying cycle times of forward and backward flow, its effect on cleaning success was compared at varying alternating flow frequencies. While previous results (chapter 6.3.1) with a frequency of 0.5 Hz correspond to cycle times of each 1 s forward and backwards, lower frequencies of 0.25 Hz and 0.1 Hz correspond to cycle times of 2 s and 5 s each, respectively.

The results (Figure 6-4) show a significant linear increase in protein removal (Figure 6-4b) with increasing frequencies. For decreasing frequencies, the phase durations increase. Thus, the holding times for high Δp_{TM} (during high flow phases) and for backward/forward phases increase during one alternating flow cycle. Consequentially, with fewer and less rapid fluctuations occurring, the temporal intensity of shear stress and flow direction fluctuations decreases. Hence, with decreasing frequencies, the positive effects of alternating flow, i.e. additional turbulence, decline while the adverse effects, i.e. pore clogging (as discussed in chapter 6.3.1), increase in intensity.

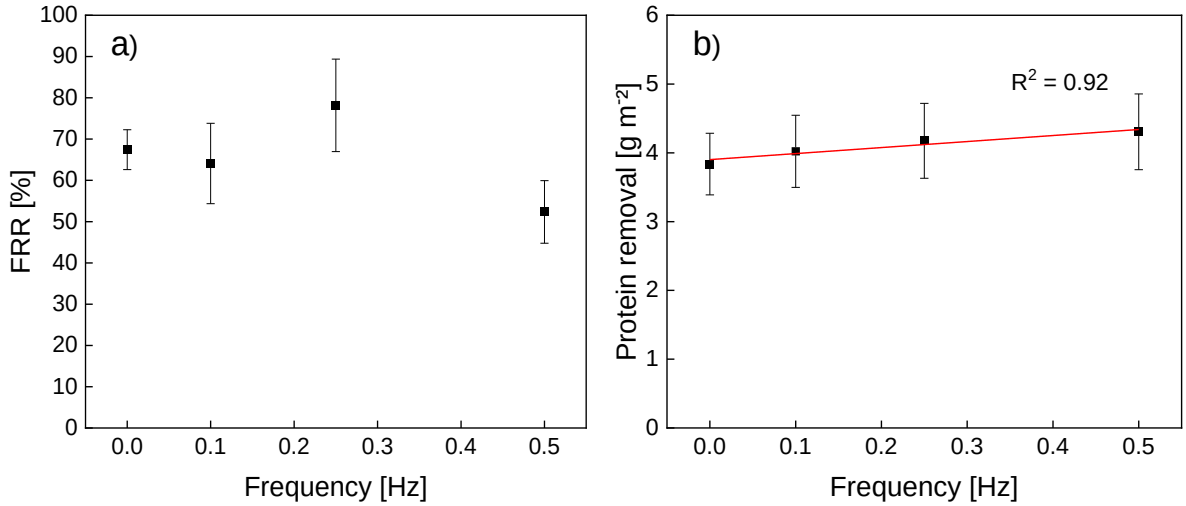

Figure 6-4. Influence of alternating flow frequency on FRR (a) and protein removal (b) in an MF-HFM for cleaning with NaOH at pH 11.3 (c_{NaOH} = 0.03%). Steady flow cleaning (f = 0.0 Hz) was conducted at identical $\Delta p_{TM, avg}$ and v_{avg}. Cleaning conditions: v_{avg} = 2.2 m s^{-1}, Δv = 2.5 m s^{-1}, $\Delta p_{TM, avg}$ = 0.35 bar, $\Delta p_{TM, cycle}$ = 0.5 bar. Protein removal significantly increases linearly with alternating flow frequency while FRR shows no such trend.

However, the results for FRR (Figure 4a) seem to be contradicting those of the protein removal (Figure 6-4b) as they depict no clear trend of decreasing cleaning success for decreasing frequencies of alternating flow. Compared to steady flow, the FRR of alternating flow was insignificantly decreased at 0.1 Hz (64.1 ± 9.7%; -4.3%) and insignificantly increased at 0.25 Hz (78.2 ± 11.2%; +16.7%). The only significant deviation from the steady flow FRR was observed at 0.50 Hz, as discussed in chapter 6.3.1. Hence, these progressions do not depict a clear trend and cannot solely be attributed to pore clogging. Instead, it seems to be due to a combination of enhanced protein removal and impaired pore-clogging. In other words, alternating flow achieved the most distinct but insignificant improvements in protein removal at 0.5 Hz and FRR at 0.25 Hz. It is to be noted that the feasibility of higher frequencies in changing pump capacity and flow direction, especially in industrial membrane systems, remains in question.

In addition to the temporal fluctuation component of alternating flow, the effect of fluctuation intensity, i.e. the amplitudes Δv and Δp_{TM}, were assessed by conducting comparative cleaning experiments with reduced amplitudes Δv = 0.5 m s^{-1} and Δv = 1.1 m s^{-1}. Compared to an amplitude of Δv = 2.5 m s^{-1}, this corresponds to reductions in ΔTW and $\Delta p_{TM\ cycle}$ of 58% and 52% for Δv = 1.1 m s^{-1} and 82% and 80% for Δv = 0.5 m s^{-1}.

The associated results for FRR, depicted in Figure 6-5a, still show a significant decrease for the reduced amplitude at Δv = 1.1 m s^{-1} (61.5 ± 9.0%) compared to steady flow (-8.8%) but a slight increase over alternating flow with Δv = 2.5 m s^{-1} (+17.6%). For Δv = 0.5 m s^{-1}, no difference can be observed towards steady flow or Δv = 1.1 m s^{-1}. Overall, a significant linear decrease of FRR with increasing amplitude could be observed. In terms of protein removal (Figure 6-5b), reduced amplitudes still led to increases in protein removal over steady

flow of +8.3% for Δv = 0.5 m s^{-1} (4.16 ± 0.33 g m^{-2}) and +16.4% for Δv = 1.1 m s^{-1} (4.47 ± 0.47 g m^{-2}). Furthermore, Δv = 1.1 m s^{-1} led to a slight increase in protein removal over alternating flow with Δv = 2.5 m s^{-1} (+3.7%).

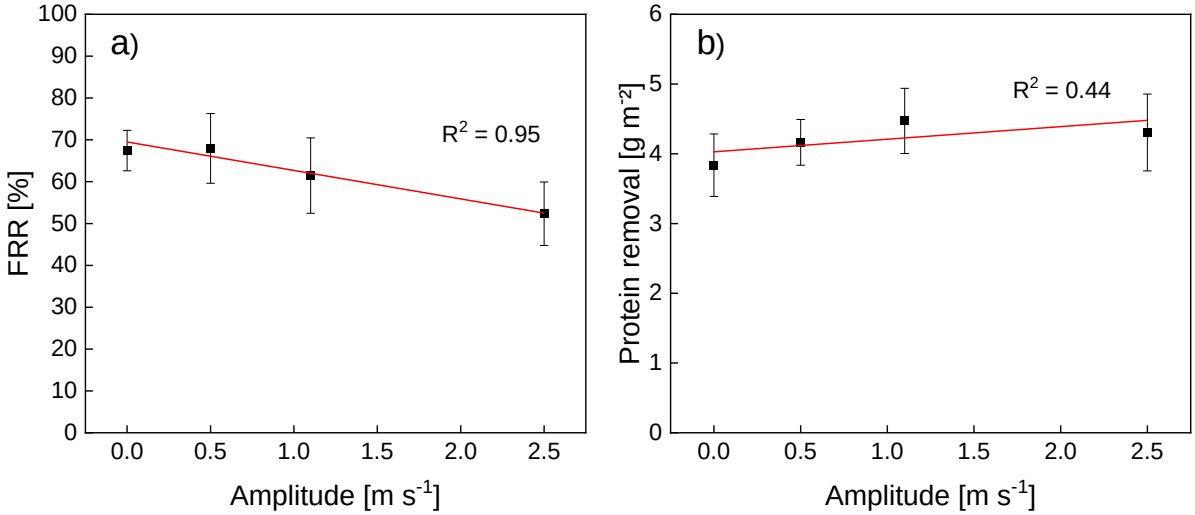

Figure 6-5. Influence of alternating flow amplitude on FRR (a) and protein removal (b) in an MF-HFM for cleaning with NaOH at pH 11.3 (c_{NaOH} = 0.03%). Steady flow cleaning (Δv = 0.0 m s^{-1}) was conducted at identical $\Delta p_{TM, avg}$ and v_{avg}. Cleaning conditions: f = 0.5 Hz; v_{avg} = 2.2 m s^{-1}; $\Delta p_{TM, avg}$ = 0.35 bar; Δv = 2.5 m s^{-1}: $\Delta p_{TM, cycle}$ = 0.50 bar; Δv = 1.1 m s^{-1}: $\Delta p_{TM, cycle}$ = 0.24 bar. FRR decreases linearly with alternating flow amplitude while protein removal remains increased over that of steady flow despite reduced alternating flow amplitudes.

The cleaning success of alternating flow benefitting from a 52% reduced $\Delta p_{TM, cycle}$ (at Δv = 1.1 m s^{-1} versus Δv = 2.5 m s^{-1}) on the one hand confirms the hypothesis stated in chapter 6.3.1 that the temporal and locally high Δp_{TM} on both module sides due to flow reversal is detrimental to cleaning success. Hence, for a lower $\Delta p_{TM, cycle}$ and thus also $\Delta p_{TM, max}$ (see Table 6-1), the adverse effects of alternating flow, presumably causing increased pore clogging on both module entry and end, are less pronounced. On the other hand, cleaning success not being impaired by the simultaneous 56% reduction in Δv seems to contradict previous studies determining higher amplitudes as crucial for cleaning efficiency (Kürzl et al. 2022a; Augustin et al. 2010; Gillham et al. 2000). This could be due to the amplitude, when considering both flow directions, being technically a lot higher than for pulsed flow, such that the amplitude within one flow direction does not play as significant a role as flow reversal itself.

6.3.3 Influence of membrane length and flow direction on cleaning efficiency

With length dependency effects expected to affect the local cleaning performance, cleaning experiments should comparatively be assessed in a module with an industry-standard length of 1.0 m. Besides conventional steady fw and alternating flow, steady bw flow was also utilised to differentiate between the effects of temporary and permanent flow reversal. The results for FRR and cumulative protein removal are depicted in Figure 6-6a and Figure 6-6b, respectively.

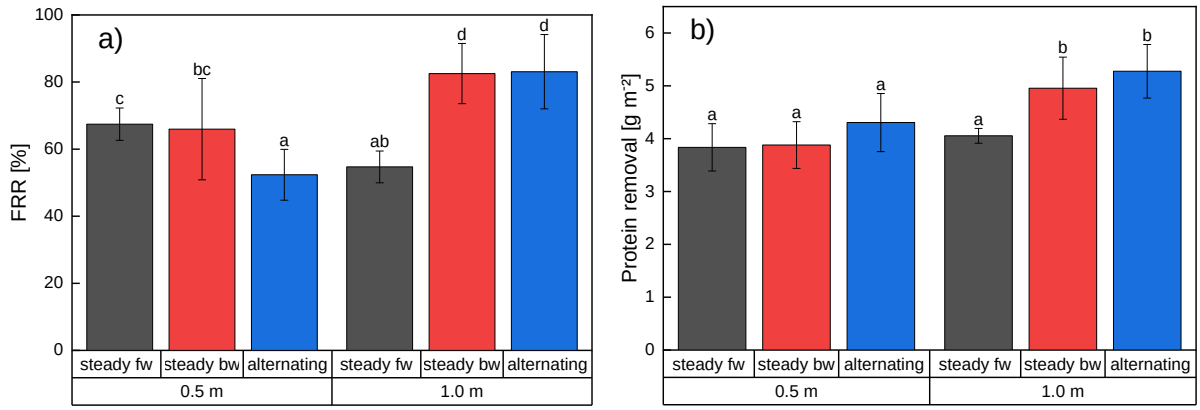

Figure 6-6. Influence of membrane length and flow type on FRR (a) and protein removal (b) for steady forward (fw) flow (black), steady backward (bw) flow (red) and alternating flow (blue). Cleaning conditions: c_{NaOH} = 0.03% (pH 11.3), f = 0.5 Hz, $\Delta p_{TM, avg}$ = 0.35 bar, $\Delta p_{TM, cycle}$ = 0.50 bar, v_{avg} = 2.2m s^{-1}, Δv = 2.5 m s^{-1}. Results for steady fw (0.5 m) and alternating flow (0.5 m) are from chapter 6.3.1. $^{a-c}$ different letters indicate significant differences between flow types ($p > 0.05$). Both permanent and cyclic flow reversal benefit from increased membrane lengths, both in terms of FRR and protein removal, presumably due to a combination of length dependency effects and an increased $v/\Delta p_{TM, inlet}$ where fouling was most pronounced after filtration.

For conventional steady fw crossflow, a change in the membrane length from 0.5 m to 1.0 m led to a significant decrease in FRR (-19%) and no significant change in the protein removal. Despite an identical $\Delta p_{TM, avg}$ for both membrane lengths, the local $\Delta p_{TM, inlet}$ was higher for the 1.0 m membrane (0.60 bar) than for the 0.5 m membrane (0.49 bar), as summarised in Table 6-2, due to the length dependant pressure drop along the membrane. Consequently, the local ratio of flow velocity to Δp_{TM} at the inlet ($v/\Delta p_{TM, inlet}$) was decreased for the 1.0 m membrane (4.5 m s^{-1} bar^{-1} at 0.5 m versus 3.7 m s^{-1} bar^{-1} at 1.0 m). Hence, with fouling being most pronounced at the membrane inlet, an increased $\Delta p_{TM, inlet}$ and a reduced $v/\Delta p_{TM, inlet}$ could account for a decreased FRR. It could impair the removal of in-pore fouling, which, compared to deposits on the membrane, would affect the FRR stronger than protein removal.

Table 6-2. Comparison of pressure and flow velocity conditions during different flow types and membrane lengths at the module inlet p_1. The data depicts $\Delta p_{TM,\ inlet}$ being decreased and $v/\Delta p_{TM,\ inlet}$ being increased over conventional steady fw flow, particularly for increased membrane lenghts and temporarily during certain cycle phases of alternating flow.

Membrane length	Variable	steady fw	steady bw		alternating					
							fw phase		bw phase	
		avg	avg	Δ[1]	avg	Δ[1]	high v	low v	high v	low v
0.5 m	$\Delta p_{TM,\ inlet}$ [bar]	0.49	0.19	-0.30	0.31	-0.18	0.90	0.12	0.22	0.08
	$v/\Delta p_{TM,\ inlet}$ [m s^{-1} bar^{-1}]	4.5	11.2	+6.8	10.4	+6.0	3.10	8.30	8.50	21.30
1.0 m	$\Delta p_{TM,\ inlet}$ [bar]	0.60	0.09	-0.51	0.33	-0.27	1.15	0.10	0.06	0.05
	$v/\Delta p_{TM,\ inlet}$ [m s^{-1} bar^{-1}]	3.7	25.5	+21.9	29.30	+25.6	2.89	8.10	17.50	88.00

[1] compared to steady fw.

For steady bw flow, i.e. a permanent flow reversal contrary to the flow direction during deposit formation, a change in membrane length affects both FRR and protein removal. At 0.5 m, steady bw flow reached no improvements over steady fw flow, neither in FRR nor in protein removal despite a decreased $\Delta p_{TM,\ inlet}$ (Δ = -0.30 bar) and an increased $v/\Delta p_{TM,\ inlet}$ (Δ = +6.77 m s^{-1} bar^{-1}). These value changes compared to steady fw are only due to the change in the flow direction, causing the maximum pressures to switch from the inlet p_1 to the outlet p_2 and minimum pressures switching vice versa. With these values suggesting but not showing an improved cleaning success, the absent improvement could be due to changes in $\Delta p_{TM,\ inlet}$ and $v/\Delta p_{TM,\ inlet}$ not sufficiently pronounced to achieve significant improvements. At 1.0 m, both FRR and protein removal of steady bw flow were significantly increased by +25% over values at 0.5 m. This could be due to $\Delta p_{TM,\ inlet}$ being further reduced to 0.09 bar due to the intensified pressure drop in the longer module and thus $v/\Delta p_{TM,\ inlet}$ being further increased. Additionally, FRR and protein removal values are significantly increased by +51% and +22% over those of steady fw flow at 1.0 m. These improvements can also be connected to enhanced flow conditions, i.e. a decreased $\Delta p_{TM,\ inlet}$ (Δ = -0.51 bar) and an increased ratio $v/\Delta p_{TM,\ inlet}$ (Δ = +21.9 m s^{-1} bar^{-1}). It is to be noted that this pressure change could not be replicated in steady fw flow as too low Δp_{TM} at the inlet would cause negative pressures at the outlet and could potentially damage the membrane, depending on its material and module geometry.

For alternating flow in a 0.5 m membrane, as discussed in chapter 6.3.1, no significant improvements could be observed. However, alternating flow in a 1.0 m membrane achieved significant improvements in both FRR (+52%) and protein removal (+30%) over steady fw flow.

Despite the cyclic flow reversal and fluctuating shear stress with a further increased $v/\Delta p_{TM,\,inlet}$ (Δ = +25.6 m s^{-1} bar^{-1}) of alternating flow, no significant differences to steady bw flow could be observed. As the results of alternating flow seem to contradict other studies observing benefits of alternating flow over pulsed flow during filtration (Weinberger and Kulozik 2021b, 2022) and cleaning (Gillham et al. 2000; Blel et al. 2009a), the underlying cause must be based on effects not occurring in feed system or plant setups of previous studies. In particular, the hypothesis of impaired pore clogging as an adverse effect is based on the combination of open-pored MF membranes with the widespread particle size distribution of milk proteins (Brans et al. 2004), leading to a stronger pore-clogging effects compared to other studies on the filtration of model particles (Weinberger and Kulozik 2021b) or the cleaning of smooth steel surfaces (Gillham et al. 2000).

Separating values from the phases of high and low v within the respective flow direction of alternating flow indicates why alternating flow is not superior to steady bw flow. While $v/\Delta p_{TM,\,inlet}$ was temporarily increased over that of steady fw and bw flow, mostly during bw and fw phases of low flow rate, it was also temporarily decreased during fw phases of high v. This was due to the fluctuating component of alternating flow causing 84% and 92% higher maximum values of $\Delta p_{TM,\,inlet}$ for 0.5 m and 1.0 m membranes, respectively, compared to steady fw flow. Previous studies investigating the influence of Δp_{TM} on the filtration performance (Qu et al. 2012; Hartinger et al. 2019a; Schiffer et al. 2020) and removal of resulting protein residues during cleaning (Bartlett et al. 1995; Bird and Bartlett 2002; Kürzl et al. 2022a) found the maximum occurring Δp_{TM} being decisive for filtration and cleaning performance due to irreversible deposit compaction. Hence, alternating flow's fluctuating component provides additional turbulence but also increased deposit compaction. This combination of a compacted deposit and increased turbulence could result in the observed slight increase in protein removal and hypothesised reason of impaired pore-clogging for the decreased FRR. The temporarily increased turbulence and thus wall shear stress causes improved removal of the bulk deposit, which is well accessible by shear forces. Simultaneously, the temporarily increased $\Delta p_{TM,\,inlet}$ leads to impaired pore-clogging within the membrane pores, which are less accessible by shear forces.

An overall comparison of results for both membrane lengths and all flow types (see Figure 6-7) confirms the positive impact of an increased $v/\Delta p_{TM,\,inlet}$ on protein removal and depicts a significant linear correlation. A similar trend of a linear increase can be observed for FRR (see Figure 6-8). This also underlines the assumption that positive results of steady bw and alternating flow are due to the increased $\Delta(v/\Delta p_{TM,\,inlet})$ caused by cyclic/permanent flow reversal at different membrane lengths but without apparent benefits of cyclic changes in the flow direction as in alternating flow. $\Delta(v/\Delta p_{TM,\,inlet})$ being the underlying reason for changes in cleaning efficiency is also in line with a previous study not observing differences in pulsed flow

efficiency for increased membrane length, as no flow reversal occurred for pulsed flow and thus, $v/\Delta p_{TM,\ inlet}$ did not differ for either membrane length (Kürzl and Kulozik 2023b).

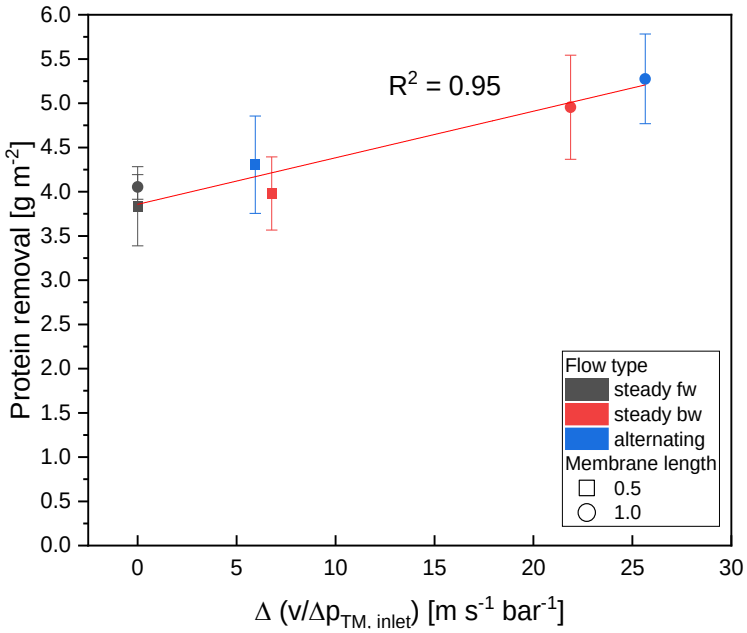

Figure 6-7. Cumulative protein removal as a function of the increase in the ratio of flow velocity to local Δp_{TM} ($v/\Delta p_{TM,\ inlet}$) over steady fw flow cleaning (black) for steady bw (red) and alternating flow (blue). Membrane lengths: 0.5 m (squares), 1.0 m (circles). Cleaning conditions: f = 0.5 Hz, v_{avg} = 2.2 m s^{-1}, Δv =2.5 m s^{-1}, $\Delta p_{TM,\ avg}$ = 0.35 bar, $\Delta p_{TM,\ cycle}$ = 0.50 bar. Steady fw and bw flow cleaning was conducted at identical v_{avg} and $\Delta p_{TM,\ avg}$. Data of steady fw cleaning results from Kürzl et al. (2022a). The data confirms that increased $\Delta(v/\Delta p_{TM,\ inlet})$, as caused by cyclic or permanent flow reversal, lead to a significant linear increase in protein removal.

Hence, the positive effects of cyclic/permanent flow reversal are enhanced for increasing membrane length due to an improved $\Delta(v/\Delta p_{TM,\ inlet})$ over steady fw flow. Nevertheless, the additional component of alternating flow, i.e. cyclic flow reversal, cannot provide an added value, presumably due to contrary effects simultaneously benefitting and impairing cleaning success, such as increased turbulence and impaired pore clogging.

6.4 Conclusion

This study demonstrated the usefulness and limitations of cyclic (alternating) and permanent (steady bw) flow reversal during membrane cleaning with 0.03% NaOH after milk MF for protein fractionation. Compared to conventional steady fw flow conditions, both hydraulic and chemical cleanliness could significantly be enhanced by alternating and steady bw flow. Nonetheless, with all FRRs < 90 % and the initial total protein deposition unknown, a complete cleaning cannot be assumed. Future studies should extend the knowledge of alternating flow behaviour by its interaction with different chemical cleaning scenarios including industrially established compounded cleaning agents.

The central aspect identified responsible for increased cleaning success is the increase in the local ratio of flow velocity and thus shear stress to Δp_{TM} at the membrane inlet caused by the length-dependent pressure drop along the membrane module combined with a change in the flow direction. This led to the minimum Δp_{TM} temporarily occurring at the membrane inlet, where the deposition was most pronounced, and caused the observed increase in $v/\Delta p_{TM, inlet}$ and thus cleaning success. Contrary to the previously stated hypothesis and observation from other studies (Gillham et al. 2000; Blel et al. 2009a; Weinberger and Kulozik 2021b), the additional cyclic component of alternating flow provided no substantial benefit over steady bw flow or pulsed flow cleaning, presumably due to impaired pore clogging as a result of temporarily increased $\Delta p_{TM, inlet}$ during phases of high flow rate. To validate this hypothesis, further studies should be conducted towards a lower susceptibility to in-pore fouling, e.g. using membranes with smaller pore sizes and feed solutions with larger particles and a narrower particle size distribution.

Additionally, alternating flow filtration and cleaning should be assessed in membrane types suffering from flow shadows, such as flat-sheet and spiral-wound membrane modules (Hartinger et al. 2020a; Schwinge et al. 2002; Han et al. 2018b), as the additional turbulence caused by alternative flow types may be of particular advantage here.

Finally, it should be noted that implementing alternating or steady bw flow during cleaning, such as realised in this study with controlled valves and additional piping, would be complex and costly on an industrial scale. Accordingly, these flow types' benefits must be carefully weighed against the effort necessary for implementation, which would also depend on the plant scale.

Author Contributions:

Conceptualisation, C.K.; methodology, C.K.; software, C.K.; validation, C.K.; formal analysis, C.K.; investigation, C.K.; resources, U.K.; data curation, C.K.; writing—original draft preparation, C.K.; writing—review and editing, C.K. and U.K.; visualisation, C.K.; supervision, U.K.; project administration, C.K.; funding acquisition, U.K. All authors have read and agreed to the published version of the manuscript.

Funding

This IGF Project of the FEI was supported via AiF to promote the Industrial Collective Research (IGF) of the German Ministry of Economic Affairs and Energy (BMWi), based on a resolution of the German Parliament. Project: AiF 57 EWN.

Acknowledgements

We gratefully thank Heidi Wohlschläger, Hermine Roßgoderer and Nora Biesenthal for their assistance with the RP-HPLC analysis of cleaning samples, as well as Dirk Weber from Pentair X-Flow BV for providing hollow fibre membranes. Furthermore, we want to thank Siegfried Tuchborn from SIMA-tec GmbH and Christian Ederer, Erich Schneider, and Franz Fraunhofer in our workshop for technical support. We also want to thank Lina Dohm and Thomas Tran for their experimental support. Finally, we want to thank Simon Schiffer, Roland Schopf, Maria Weinberger, and Martin Hartinger for fruitful discussions.

Conflicts of interests

The authors declare no conflict of interest. The authors declare no conflict of interest. The authors declare that they have no known competing financial interests or personal relationships that could have influenced the work reported in this paper. The funders had no role in the design of the study; in the collection, analyses, or interpretation of data; in the writing of the manuscript, or in the decision to publish the results.

Supplementary

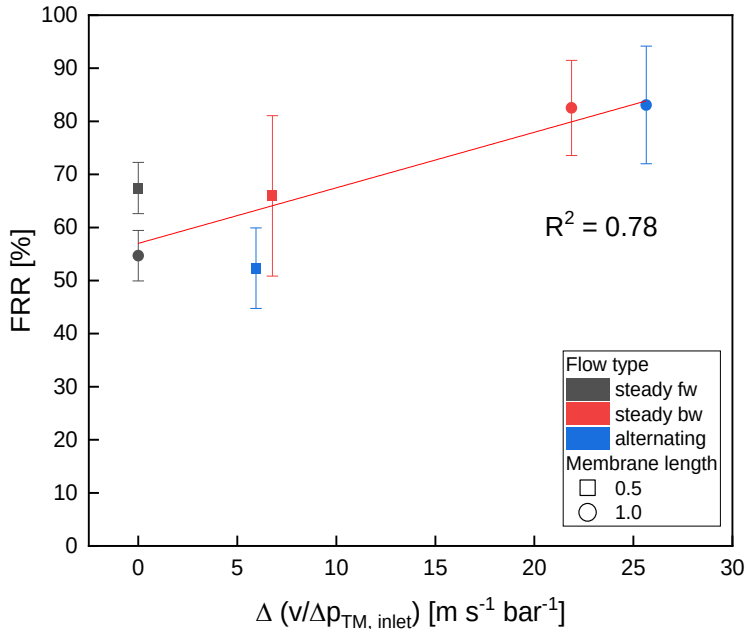

Figure 6-8. FRR as a function of the increase in the ratio of flow velocity to local Δp_{TM} ($v/\Delta p_{TM, inlet}$) over steady fw flow cleaning (black) for steady bw (red) and alternating flow (blue). Membrane lengths: 0.5 m (squares), 1.0 m (circles). Cleaning conditions: f = 0.5 Hz, v_{avg} = 2.2 m s^{-1}, Δv =2.5 m s^{-1}, $\Delta p_{TM, avg}$ = 0.35 bar, $\Delta p_{TM, cycle}$ = 0.50 bar. Steady fw and bw flow cleaning was conducted at identical v_{avg} and $\Delta p_{TM, avg}$. Data of steady fw cleaning results from Kürzl et al. (2022a). The data confirms that increased $\Delta(v/\Delta p_{TM, inlet})$, as caused by cyclic or permanent flow reversal, lead to a linear increase in FRR.

7 Influence of Pulsed and Alternating Flow on the Filtration Performance during Skim Milk Microfiltration with Flat-Sheet Membranes[6]

Christian Kürzl[a]* and Ulrich Kulozik

Chair of Food and Bioprocess Engineering, TUM School of Life Sciences, Technical University of Munich, Weihenstephaner Berg 1, Freising, Germany

[a] New affiliation: Professorship Food Process Engineering, TUM School of Life Sciences, Technical University of Munich, Weihenstephaner Berg 1, 85354 Freising, Germany

* Corresponding author

Summary and contribution of the doctoral candidate

Previous studies have already reported positive effects of alternative flow types on the fractionation and cleaning efficiency in membrane processes. However, an impaired filtration performance was reported for the fractionation of skim milk with MF due to the protein cross-linking in combination with pressure peaks causing increased deposit compaction in HFM at 10°C (Weinberger and Kulozik 2021a). Nevertheless, our previous results (chapter 5) indicated alternative flow types being most beneficial for membrane types suffering from flow shadows. Hence, the hypothesis was that the synergistic effects between alternative flow types and a filtration system containing spacers and, thus, flow shadows could overcome the adverse effects of pressure peaks by distinctly improving access to former flow shadows, increasing the active membrane area, more evenly distributing shear forces across the flow channel and, thus, improving filtration efficiency.

Steady, pulsed and alternating flow filtration was conducted with skim milk at 50°C in an FSM to investigate this hypothesis. Additionally, steady flow conditions were varied for an extensive performance evaluation. During filtration, the flux, permeation and mass flow were monitored. After filtration, membranes were extracted, and the deposited proteins were marked with Coomassie-colouring. Correlating the colour intensity with protein concentrations allowed a quantitative surface analysis of the local protein concentrations on the membrane sample.

---

[6] Original publication: Kürzl and Kulozik (2023c): Kürzl, C.; Kulozik, U. 2023. Influence of Pulsed and Alternating Flow on the Filtration Performance during Skim Milk Microfiltration with Flat-Sheet Membranes. Separation and Purification Technology 321, 124234. doi: 10.1016/j.seppur.2023.124234. Adapted original manuscript. Adaptations of the manuscript refer to enumeration type, citation style, spelling, notation of units, format, and merging of all lists of references into one at the end of the dissertation. Permission for the reuse of the article is granted by by Elsevier Limited.

The results of surface analyses showed significantly reduced deposit amounts for pulsed and alternating flow compared to steady flow. Additionally, the spread of local protein concentrations was distinctly reduced, translating to a more homogenous deposition caused by the pulsed and alternating flow-induced improved access to flow shadows. Regarding filtration performance, pulsed flow was superior to alternating flow and all steady flow conditions. The increased flux and strongly increased WP permeation significantly improved the time-resolved and cumulative WP mass transfer. With starting values being higher and diminishing slower and less pronounced, this emphasises the improved deposit control. While the energy consumption of pulsed and alternating flow is increased over average steady flow conditions due to the additional changes in pump capacity and flow direction, the advantages of alternative flow types outweigh the increased energy demand. Accordingly, in terms of sustainability, pulsed and alternating flow achieved substantial reductions in the specific pump energy consumptions by 69% and 60%, respectively, compared to the optimum steady flow conditions with maximum flow rate and 29% and 8%, compared to the average steady flow conditions.

The doctoral candidate designed the experimental approach for this study based on a critical review of the literature. Data acquisition was mainly done by the doctoral candidate. The doctoral candidate also developed the experimental concept, analysed, interpreted and plotted the data. The manuscript was written and reviewed by the doctoral candidate. The co-author contributed to the project outline, the discussion of results, and the revision of the manuscript.

Abstract

Control of deposit formation during skim milk microfiltration (MF) remains challenging, particularly in membranes with spacer nets between membrane layers like flat-sheet and spiral-wound membranes, due to the extensive occurrence of flow shadows behind spacer filaments. One approach to improve process control and efficiency is applying pulsed or alternating flow, which creates regular fluctuations in shear stress, pressure and, for alternating flow, in flow direction. This study assessed the effects of these alternative flow types and compared them to conventional steady crossflow on deposit formation and filtration performance. Flux and protein permeation were monitored during filtration. After filtration, the membranes were removed and deposited proteins stained by Coomassie-blue. The visual analysis of the stained membranes confirmed that the alternative flow types improved access to flow shadows behind spacer filaments by causing a significantly reduced deposition or enhanced removal. Consequently, the reduced deposit formation with pulsed and alternating flow led to enhancements in the steady-state whey protein mass flow by > 8% and > 37% over

any steady flow conditions. Considering the flow-specific pump energy demands, pulsed and alternating flow not only improved filtration performance, but also reduced specific energy consumption relative to whey protein mass transfer by > 60%.

Highlights:

- Improved access to flow shadows behind spacer filaments with alternative flow types
- Median deposition reduced by 53% for pulsed flow and 79% for alternating flow
- Steady-state whey protein mass flow increased by >8% (alternating) and >37% (pulsed)
- Significant reductions in the specific pump energy consumption by >60%
- Increased process efficiency and sustainability with alternative flow types

Keywords: alternative flow types; flux; protein permeation; Coomassie-colouring; sustainability

7.1 Introduction

Membrane-based separation of skim milk by microfiltration (MF) into its two main protein fractions, whey proteins (d = 2 – 6 nm) (Brans et al. 2004) and caseins (d = 20 – 300 nm) (Brans et al. 2004), is processed to utilise different applications and functionalities of the protein fractions. The main process limitation is deposit formation due to the retention of particles on and in the membrane (Bartlett et al. 1995; Bird and Bartlett 2002), causing a decline in flux and permeation (Ripperger and Altmann 2002; Ng et al. 2018). Additionally, biofouling can limit production times depending on the filtration temperature (Schiffer and Kulozik 2020).

The characteristics and intensity of deposit formation can vary widely for different feed systems and process conditions (Hartinger et al. 2019b; Schiffer et al. 2020; Doudiès et al. 2021; Gésan-Guiziou et al. 1999; Weinberger and Kulozik 2021a, 2021c; Wemsy Diagne et al. 2013). In the MF of skim milk, casein micelles, which are sponge-like, compressible and porous structures, are the main foulant that can form gel-like structures under high concentrations and transmembrane pressures (Δp_{TM}) (Horne 2020; Bouchoux et al. 2010; Bouchoux et al. 2009; Qu et al. 2015). While increases in the flow velocity v have been shown to mainly affect flux due to increased shear forces limiting deposit formation (Schiffer et al. 2020), increases in Δp_{TM} above the limiting flux at 1.0 bar mainly reduced the protein permeation by irreversibly compacting the deposit structure (Schiffer et al. 2020; Hartinger et al. 2019b; Gésan-Guiziou et al. 1999). Due to friction-related axial pressure losses within the membrane, Δp_{TM} and thus the intensity of deposit formation decreases along the membrane length (Piry et al. 2008). Regarding filtration temperature, elevated temperatures of 50 – 55 °C have shown the highest performance in terms of flux despite filtration time being limited to 7 h due to biofouling (Schiffer and Kulozik 2020). This poses an ecological and economic issue to process sustainability, as membrane fouling generates a need for regular cleaning cycles, which are chemical and energy-intensive processes, leading to downtimes of several hours per filtration cycle.

As biofouling at elevated temperatures could only be reduced by more intense heat treatment of the milk before filtration, which would include significant losses in product quality (Kessler 1996), other approaches to enhance filtration performance and thus sustainability were investigated. One of these approaches contains the transition from a steady to an unsteady flow, i.e. pulsed flow with a cyclic transition between phases of high and low flow rate with related pressure conditions, and alternating flow with an additional cyclic feed-side flow reversal. These fluctuations were argued to increase turbulence (Kürzl et al. 2022a; Augustin et al. 2010; Bode et al. 2007), wall shear stress and mass transfer (Gillham et al. 2000; Blel et al. 2009a; Blel et al. 2009b) and thus to loosen up deposits and improve filtration (Weinberger and Kulozik 2021c; Howell et al. 1993) and cleaning efficiency (Kürzl et al. 2022a; Gillham et al. 2000). Besides modes of action, high frequencies and amplitudes (Howell et al. 1993;

Weinberger and Kulozik 2021c; Gillham et al. 2000) were identified as critical aspects of pulsed and alternating flow for distinct improvements in process efficiency. However, the advantage of pulsed and alternating flow differed widely in previous studies, depending on the chosen feed and membrane system: For aqueous model systems, such as yeast and BSA suspensions, significant improvements in filtration performance were reported for both pulsed (Weinberger and Kulozik 2021c; Howell et al. 1993) and alternating flow (Weinberger and Kulozik 2021b) in hollow fibre membranes (HFM), whereas improvements with alternating flow were more pronounced due to the additional cyclic flow reversal further enhancing hydrodynamic instabilities. Contrary to these results, pulsed flow filtration with skim milk in HFM led to impaired filtration performance (Weinberger and Kulozik 2021a). It was concluded that for skim milk, due to the extensive cross-linking of its proteins in deposited layers, the temporary pressure peaks in the high flow velocity phases of pulsed flow led to stronger irreversible compression, thus impairing membrane permeability and filtration performance (Weinberger and Kulozik 2021a). Notably, alternating flow filtration of skim milk has not yet been investigated in this context.

In terms of membrane geometry, a study by Howell et al. (1993) examining the combined effects of pulsed flow and the presence or absence of baffles on the filtration performance of yeast solutions in tubular membranes suggested synergistic effects between pulsed flow and baffles resulting in distinctly improved flux values. These effects could be attributed to the combination of pulsed flow and membranes containing baffles enhancing turbulence, generating unsteady eddies (Augustin et al. 2010; Gillham et al. 2000) and causing the annular effect (Richardson and Tyler 1929; Schlichting and Gersten 2006), i.e. a shift in the maximum velocity from the channel centre towards the channel wall. Nonetheless, for membranes containing spacers, such as flat-sheet membranes (FSM) or spiral-wound membranes (SWM), spacer filaments not only act as baffles causing turbulence but also lead to flow shadows behind spacer filaments (Hartinger et al. 2020a; Han et al. 2018b; Geraldes 2002; Kavianipour et al. 2017; Fischer et al. 2020). Here, the combined effects remain unknown, but the enhanced turbulence could provide improved access to such flow shadows. Hence, the impact of spacer-containing membranes on the pulsed and alternating flow efficiency during skim milk MF needs to be investigated.

We hypothesise that the synergistic effects between unsteady, i.e. pulsed and alternating, flow and a filtration system both containing baffles and being subject to flow shadows, e.g. caused by spacers in FSM, can prevent or compensate the adverse effects of pressure peaks, observed for pulsed skim milk MF in HFM, by distinctly improving access to former flow shadows and increasing wall shear stress.

This hypothesis should be validated by conducting skim milk MF in an FSM with steady, pulsed and alternating flow at the optimum maximum frequency and amplitude conditions.

Besides comparing pulsed and alternating flow with steady flow under average flow and pressure conditions, comparison with maximum conditions should also be consulted to account for industrial processes commonly utilising steady flow under maximum pump capacity conditions. The filtration performance was assessed by monitoring flux and protein permeation and calculating the protein mass flow and cumulative mass transfer. Furthermore, to fathom the effects of different flow conditions on deposit formation, the membrane surfaces should be extracted after filtration and visually analysed by Coomassie-blue staining and computational image analysis. Lastly, the inclusion of specific pump energy consumptions per unit mass of whey protein transferred related to different flow types and conditions allowed to evaluate their impact on the process efficiency and sustainability.

7.2 Material and methods

7.2.1 Flat-sheet filtration plant & realisation of alternative flow types

The experiments were conducted on a filtration test cell in a custom-designed lab-scale filtration plant (SIMAtec GmbH, Schwalmtal, Germany). Details on the plant components (Kürzl and Kulozik 2023a) and the filtration test cell (Hartinger et al. 2019b) are given elsewhere. In brief, the filtration plant (Figure 7-1) consisted of a feed tank (5 L), two centrifugal pumps connected in series (PuraLev-200MU, Levitronix GmbH, Zurich, Switzerland), manual throttles for pressure adjustments, a flat sheet membrane test cell, sample ports for permeate and retentate sampling, and sensors measuring flow rate (ABB FEH511, ABB Automation Products GmbH, Göttingen, Germany), pressure (WIKA A-10, WIKA Alexander Wiegand SE & Co. KG, Klingenberg, Germany) and temperature (WIKA TR30, WIKA Alexander Wiegand SE & Co. KG, Klingenberg, Germany) for process control. The product-contacting surfaces were all stainless steel (EN 1.4571) or polymers (EPDM, PFA, PVC).

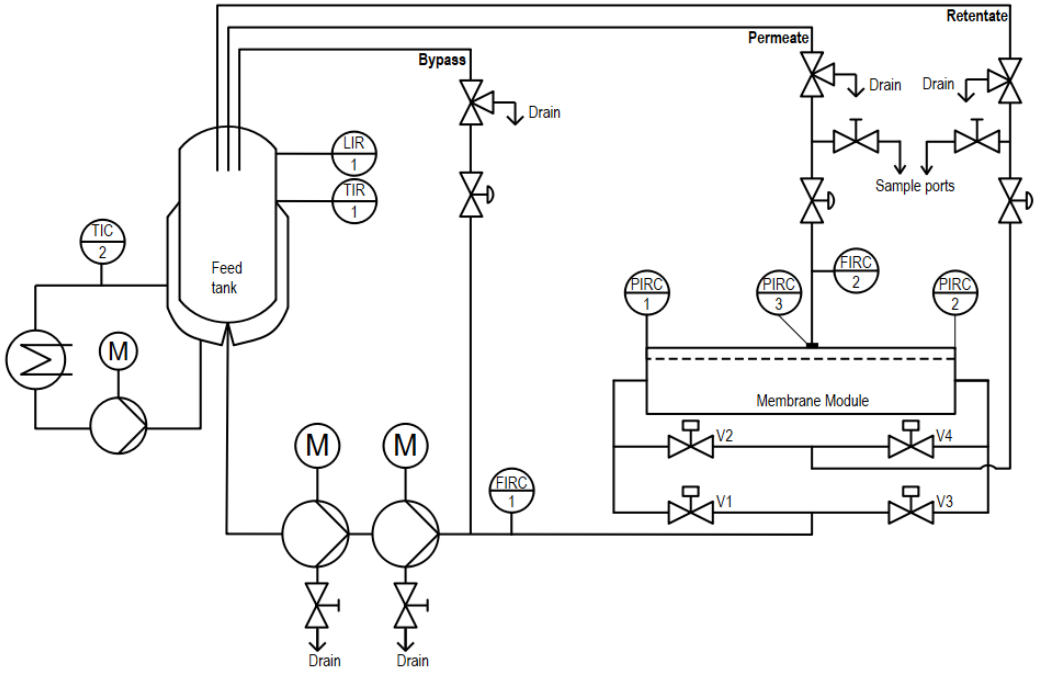

Figure 7-1. Piping and instrumentation (P&I) diagram of the membrane filtration plant (Kürzl and Kulozik 2023a).

Next to conventional steady flow, pulsed flow was realised by rapid up- and downwards ramps in pump capacity, enabled by the inductive control and contact-free impeller bearing of the centrifugal pumps. Pulsed flow consists of forward crossflow with defined phase durations of high and low flow rates and related Δp_{TM} (eq. (7-1)).

$$\Delta p_{TM} = \frac{p_1 + p_2}{2} - p_3 \tag{7-1}$$

where p_1 is the feed-side pressure, p_2 is the retentate-side pressure, and p_3 is the permeate-side pressure.

Alternating flow was implemented by additional piping combined with the controlled opening of pneumatic valves V1 and V4 (with V2 and V3 closed) for conventional forward crossflow and consecutive opening of valves V2 and V3 (with V1 and V4 closed) for temporary backward crossflow. A delay of 0.1 s between opening and closing of respective valves minimised pressure peaks. As the feed flow sensor F1 is located ahead of the alternating flow valves V1-V4, the respective flow rates of both forward and backward cycles are indicated as absolute values. An alternating flow cycle in total consists of one forward and one backward pulsed flow cycle. The frequency f (eq. (7-2)) of pulsed and alternating flow is defined by the duration of one forward/backward cycle which contains one phase Δt_{max} of high (v_{max}) and one phase Δt_{min} of low crossflow velocities (v_{min}).

$$f = \frac{1}{\Delta t_{max} + \Delta t_{min}} \tag{7-2}$$

The second main characteristic, the amplitudes of pulsed and alternating flow, in terms of Δv (eq. (7-3)) and $\Delta p_{TM,\,cycle}$ (eq. (7-4)), are defined as the difference between the respective maximum and minimum values. Due to limitations imposed by the pump, the maximum values of frequency and Δv were f = 0.5 Hz and Δv = 0.6 m s^{-1}, respectively.

$$\Delta v = v_{max} - v_{min} \tag{7-3}$$

$$\Delta p_{TM,\,cycle} = \Delta p_{TM,\,max} - \Delta p_{TM,\,min} \tag{7-4}$$

7.2.2 Filtration fluid and membrane characteristics

Pasteurised skim milk (74°C, 28 s) was purchased from a local dairy (Molkerei Weihenstephan, Freising, Germany). Its protein content of 34.70 ± 1.18 mg/mL, as determined by reversed-phase high-performance liquid chromatography (RP-HPLC), was in accordance with literature values (Walstra and Jenness 1984; Swaisgood 2003; Bijl et al. 2013; Bobe et al. 1998).

The filtration test cell (L = 0.2 m) contained an MF membrane (SUEZ WTS Germany GmbH, Ratingen, Germany) made from polyvinylidenfluorid (PVDF) with a nominal pore size (NPS) of 0.3 µm and an active membrane area $A_{Membrane}$ of 0.008 m^2. In this study, a non-woven diamond spacer (Intermas, Barcelona, Spain) was used to secure a consistent flow channel. Its spherical filaments had an inter-filament distance of 3.6 mm and a thickness of 0.65 mm. The resulting channel height d_i of 1.12 mm (44 mil) without the spacer, the channel width d_c (4 cm) and the feed flow rate $\dot{V}_{Feed}$ were used to calculate v according to equation (7-5). Complementing this, the permeate flow rate $\dot{V}_{permeate}$ was used to calculate the permeate flux J (eq. (7-6)).

$$v = \frac{\dot{V}_{Feed}}{d_i \cdot d_c} \tag{7-5}$$

$$J = \frac{\dot{V}_{permeate}}{A_{membrane}} \tag{7-6}$$

7.2.3 Experimental design

Prior to filtration trials, 4 L of skim milk were heated to the process temperature of 50 °C and an unused flat sheet membrane together with the diamond spacer were inserted into the test cell. To remove the mixed phase of rinsing water in the test cell being drained by milk, the plant was then rinsed by draining 0.5 L of retentate and 0.1 L of permeate. Afterwards, the retentate was recirculated to ensure a consistent feed composition throughout one experiment, regardless of filtration performance. Samples of permeate and retentate were taken after 5,

10, 15, 20, 30, 45, 55, and 60 min of filtration. After RP-HPLC analysis according to Dumpler et al. (2017), the concentration of certain milk proteins *i* in the permeate $c_{i,p}$ and retentate $c_{i,r}$, e.g. whey proteins (WP) or caseins (CN), were used to compare filtration performances according to their permeation P_i (eq. (7-7)) and mass flow $\dot{m}_i$ (eq. (7-8)).

$$P_i = \frac{c_{i,p}}{c_{i,r}} \tag{7-7}$$

$$\dot{m}_i = J \cdot c_{i,p} \tag{7-8}$$

The examined filtration conditions and flow types are summarised in Table 7-1 and a schematic visualisation of the flow velocity and Δp_{TM} progression over time is depicted in Figure 7-2.

Table 7-1. Conducted filtration experiments with associated levels of variables.

Flow mode [-]	Frequency [Hz]	v [m s^{-1}]				Re [-]	Δp_{TM} [bar]			
	f	max	min	Δv	avg	avg	max	min	$\Delta p_{TM,\,cycle}$	avg
$steady_{avg}$	0	0.6	0.6	0	0.6	1104	1.0	1.0	0	1.0
$steady_{max}$	0	0.9	0.9	0	0.9	1657	1.7	1.7	0	1.7
$steady_{v\text{-}max}$	0	0.9	0.9	0	0.9	1657	1.0	1.0	0	1.0
pulsed	0.50	0.9	0.3	0.6	0.6	1104	1.7	0.3	1.4	1.0
alternating	0.50	0.9	0.3	0.6	0.6	1104	1.7	0.3	1.4	1.0

Pulsed and alternating flow were conducted at the plant-specific maximum of f = 0.5 Hz and Δv = 0.6 m s^{-1} (with $\Delta p_{TM,\,cycle}$ = 1.4 bar) as these were shown to be the most potent pulsed/alternating flow filtration conditions in previous studies (Weinberger and Kulozik 2021c, 2021b). The comparison with steady flow was conducted at three different steady flow conditions.

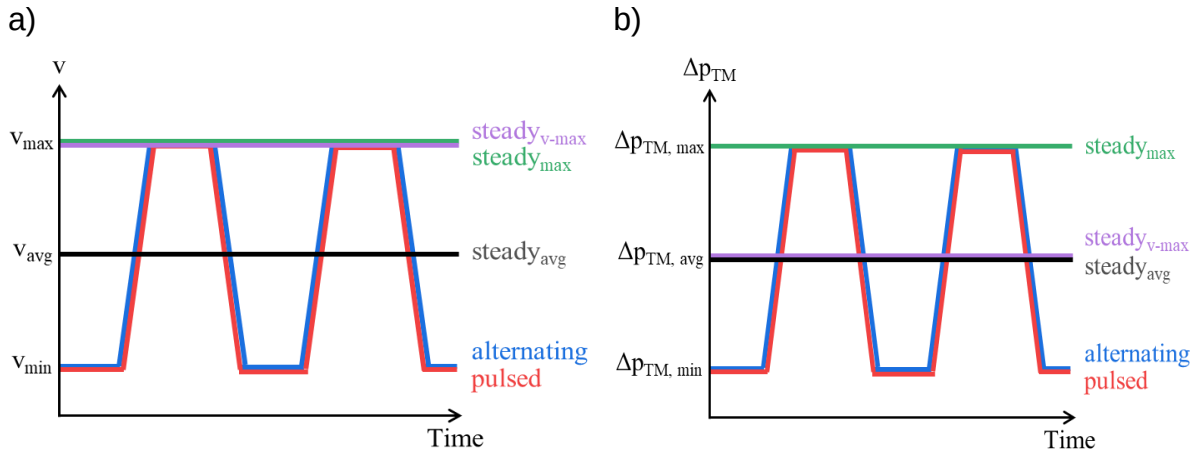

Figure 7-2. Schematic progression of v (a) and Δp_{TM} (b) over time for $steady_{avg}$ (black), $steady_{v\text{-}max}$ (purple), $steady_{max}$ (green), pulsed (red) and alternating (blue) flow filtration. For alternating flow, despite a feed-side change in flow direction, backward flow is also depicted with positive flow velocities due to the feed flow sensor F1 being located ahead of the alternating flow valves V1-V4.

At first, pulsed and alternating flow were compared to average settings ($steady_{avg}$) of flow rate (v_{avg}) and Δp_{TM} ($\Delta p_{TM,\,avg}$) (eqs. (7-9) and (7-10)). For pulsed/alternating flow, this corresponds to temporary increases and decreases in pump capacity compared to $steady_{avg}$.

$$\Delta p_{TM,\,avg} = \frac{\Delta t_{max} \cdot \Delta p_{TM,\,max} + \Delta t_{min} \cdot \Delta p_{TM,\,min}}{\Delta t_{max} + \Delta t_{min}} \tag{7-9}$$

$$v_{avg} = \frac{\Delta t_{max} \cdot v_{max} + \Delta t_{min} \cdot v_{min}}{\Delta t_{max} + \Delta t_{min}} \tag{7-10}$$

Secondly, pulsed and alternating flow were compared to the maximum settings ($steady_{max}$) of both v (v_{max}) and Δp_{TM} ($\Delta p_{TM,\,max}$) which occurred during pulsed/alternating flow. Pulsed/alternating flow then corresponds to temporary decreases in flow and pressure conditions with overall lower average values.

Thirdly, pulsed and alternating flow were compared to the supposed optimum steady flow filtration conditions ($steady_{v\text{-}max}$) with v_{max} and a medium $\Delta p_{TM,\,avg}$ (Schopf et al. 2021a) achieved by throttling. Here, pulsed/alternating flow corresponds to a temporary decrease in flow conditions with temporary increases and decreases in pressure conditions. This allows a comparison of the effects of a flow velocity increase in steady flow and the utilization of pulsed/alternating flow on filtration performance. Accordingly, pulsed/alternating flow showing improved filtration performance compared to $steady_{max}$ and $steady_{v\text{-}max}$ would imply distinct reductions in the required energy consumption. Details will be discussed in chapter 7.3.3.

After 60 min, filtration was terminated as this was shown to be sufficient to reach a steady-state (Hartinger et al. 2019b; Schiffer et al. 2020). Then, the membrane was removed from the test cell, shortly soaked in deionised water (T = 20 °C, t = 30 s) to remove loosely bound milk residues and then further analysed as described in the following chapter 7.2.4. Finally, the test cell was reassembled without a membrane sheet and the filtration plant underwent a cleaning cycle comprising a combined caustic and enzymatic cleaning step (0.4% v/v Ultrasil 67 & 0.5% v/v Ultrasil 69new, Ecolab Deutschland GmbH) followed by a rinsing step, an acidic cleaning step (0.4% v/v Ultrasil 75, Ecolab Deutschland GmbH) and another rinsing step.

7.2.4 Membrane staining and image analysis

The staining and image analysis used in this study was conducted according to the method described by Hartinger et al. (2020b) at room temperature (20 °C). In short, after filtration, the membrane was first extracted from the test cell, shortly rinsed with deionised water (30 s) to remove residual feed and dried in a desiccator (30 min). It was then stained by Coomassie Brilliant Blue (CBB, GE Healthcare Bio-Sciences, Chalfont St Giles, Great Britain) for 10 min and consecutively destained in ethanol for 3 min, both under gentle shaking (8 rpm,

angle of 10°). This led to a blue colouring whose intensity was proportional to the local protein amount. After air-drying (30 min), the membrane was analysed in a gel imaging and documentation system (Gel Doc XR+, Bio-Rad Laboratories, Inc., Hercules, CA, USA) via black-and-white imaging. Deposit amounts could thus be correlated with the local grey value. After protein quantification with RP-HPLC (Dumpler et al. 2017), the concurring calibration was conducted. Measurement of a virgin membrane served as a blank. Simultaneous measurements of a reference plate with a defined grey value validated consistent illumination during each measurement as the luminance depends on the brightness of the light source and affects the measurement of grey values. For calibration, homogeneous deposit layers with varying protein concentrations were produced in a small dead-end test cell. The membrane sheets were then cut in half, where one half was stained as described above and one half was immersed in guanidine buffer (6 M, 60 min) and analysed with RP-HPLC according to Dumpler et al. (2017). Hence, grey values obtained from staining, after subtracting blank values of the stained membrane without protein deposition, could be correlated with the corresponding protein amounts detected on the membrane surface. The resulting fit could then be used to determine local protein amounts based on the respective staining intensity. Agilent ChemStation software (Rev. B.04.03) was used to analyse RP-HPLC chromatograms. Using ImageJ (Version 1.51f, National Institutes of Health, Bethesda, MD, USA), the grey values were evaluated, correlated to a colour spectrum defined by a look-up table and illustrated by 2D and 3D surface plots.

7.2.5 Data analysis

OriginPro 2021 (OriginLab Corporation, Northampton, MA, USA) was used to plot, fit and statistically evaluate the data. One-way analysis of variance (ANOVA) was used to evaluate statistical significance between data sets at the 5% level ($p < 0.05$). All experiments were done at least in triplicates and error bars depict the standard deviation of replicates. Graphs of visual analysis depict single runs.

7.3 Results and discussion

7.3.1 Surface analysis of fouled membranes

With deposit formation highly affecting filtration performance, the influence of different flow types, on the spatial distribution of proteinaceous foulants was investigated by false colour (Figure 7-3; left) and topographic images (Figure 7-3; right). It is to be noted, that for topographic images, the depicted height resembles the deposit amount, but provides no indication of the actual deposit height as the areas of increased deposition could also be

subject to increased compaction. Also, the red colour marks areas of ≥ 10 g m^{-2} protein beyond which no quantitative differentiation between protein amounts can be made. Additionally, numerical data of false colour images were evaluated as the relative and cumulative distribution of protein amounts observed on the membrane surface (Figure 7-4). For comparison with pulsed and alternating flow, conventional $steady_{avg}$ crossflow experiments were conducted at average v and Δp_{TM} conditions as for the alternative flow types.

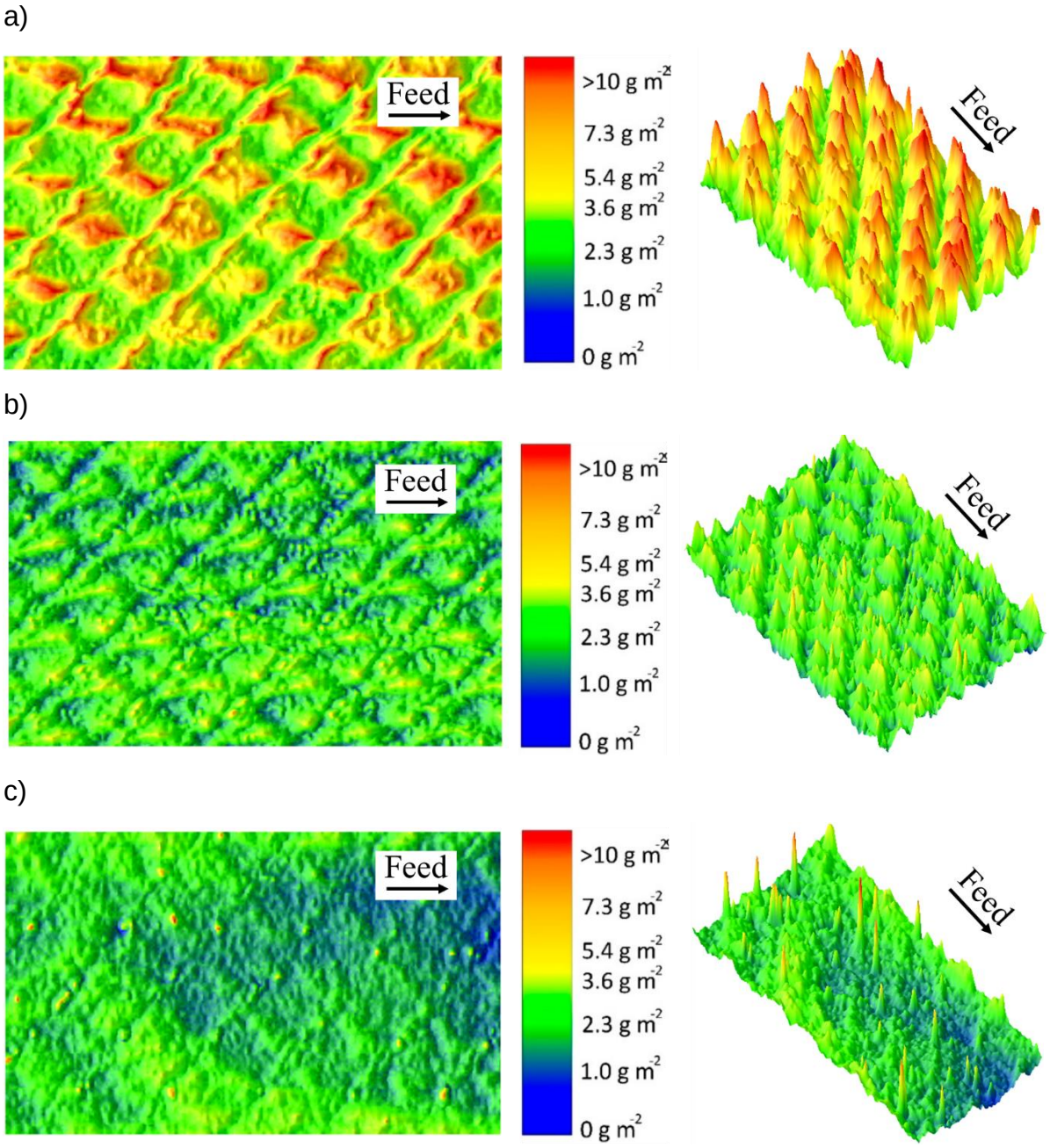

Figure 7-3. False colour (left) and topographic image of the deposit formed during MF of skim milk with $steady_{avg}$ flow (a), pulsed flow (b) and alternating flow (c). Filtration conditions: T = 50 °C, t = 60 min, v_{avg} = 0.6 m s^{-1} (pulsed/alternating flow: v_{max} = 0.9 m s^{-1}, v_{min} = 0.3 m s^{-1}, Δv = 0.6 m s^{-1}), $\Delta p_{TM, avg}$ = 1.0 bar (pulsed/alternating flow: $\Delta p_{TM, max}$ = 1.7 bar, $\Delta p_{TM, min}$ = 0.3 bar, $\Delta p_{TM, cycle}$ = 1.4 bar).

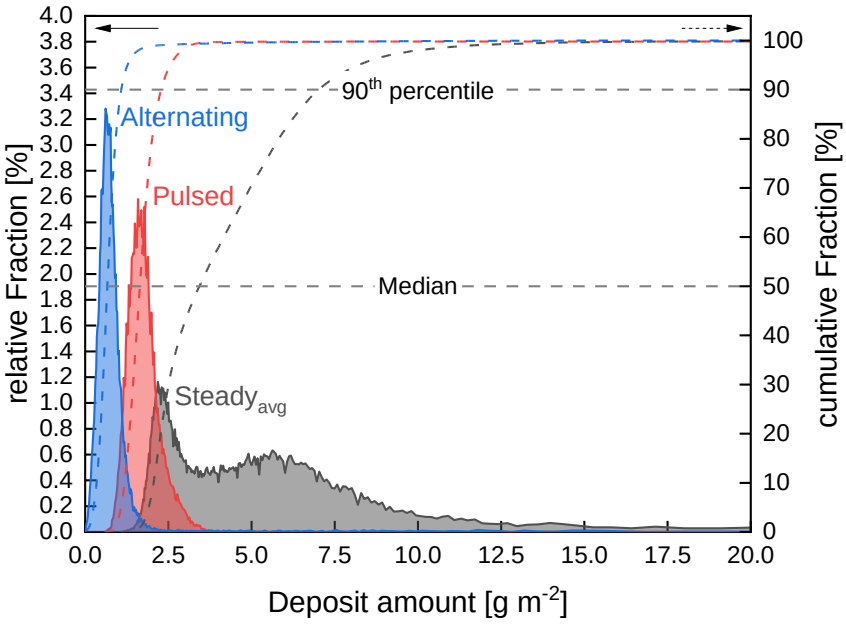

Figure 7-4. Comparison of the relative fractions (solid line) and cumulative fractions (dotted line) of deposit amounts for steady flow (grey), pulsed flow (red) and alternating flow (blue). Values >10 g m^{-2} can only be evaluated qualitatively. Filtration conditions: T = 50 °C, t = 60 min, v_{avg} = 0.6 m s^{-1} (pulsed/alternating flow: v_{max} = 0.9 m s^{-1}, v_{min} = 0.3 m s^{-1}, Δv = 0.6 m s^{-1}), $\Delta p_{TM,\,avg}$ = 1.0 bar (pulsed/alternating flow: $\Delta p_{TM,\,max}$ = 1.7 bar, $\Delta p_{TM,\,min}$ = 0.3 bar, $\Delta p_{TM,\,cycle}$ = 1.4 bar).

Steady flow

For $steady_{avg}$ flow (Figure 7-3a), the distribution pattern of deposited proteins fits the rectangular grid shape of the diamond spacer. Areas directly behind the membrane-contacting spacer filaments (flow direction from left to right) running from the bottom left to the top right show the highest deposit amounts due to flow shadows being present, causing reduced wall shear stress, as observed in computational fluid dynamics (CFD) simulations (Schwinge et al. 2003; Geraldes 2002; Han et al. 2018b) and a previous study on the spatial distribution of deposits for filtration of milk concentrate (Hartinger et al. 2020a).

Simultaneously, membrane areas directly below the contacting spacer filaments show the lowest deposit amounts due to being hardly accessible to flow or particles. Membrane areas below the non-contacting spacer also show the lowest deposit amounts of > 1.0 g m^{-2} due to the bulk flow being directed around the non-contacting spacer towards the membrane surface (Schwinge et al. 2003; Geraldes 2002; Han et al. 2018b). Additionally, the crossflow velocity increases due to the narrowing of the flow channel (Koutsou et al. 2009). The inhomogeneity in the remaining areas between spacer filaments can be explained by the spacer filaments, i.e. baffles, inducing turbulence, which causes an overall reduced (compared to areas directly behind the spacer) but inhomogeneous deposition. The relative distribution of protein amounts observed on the membrane surface (Figure 7-4) for $steady_{avg}$ shows two peaks at 2.2 g m^{-2} and 5.6 g m^{-2}. Combined with the cumulative distribution reaching its median

at 3.4 g m^{-2} and the 90th percentile at 7.0 g m^{-2}, this confirms the presence of significant and inhomogeneous fouling, particularly behind contacting spacer strands. Results from the study conducted by Hartinger et al. (2020a) for a diamond spacer showed a significantly higher median of 5.5 g m^{-2}. However, this difference seems reasonable as milk concentrates with a concentration factor (CF) CF3 were used in the previous study compared to the unconcentrated milk (CF1) used in the current study.

Pulsed flow

Compared to steady flow, deposition after filtration with a pulsed crossflow (Figure 7-3b & Figure 7-4) still partially depicts the shape of the previous spacer positions. Nonetheless, both the deposit amount and the gap between maximum and minimum protein deposition are reduced. Pulsed flow led to significant reductions in all membrane areas: For areas below the non-contacting spacer filaments, where the lowest deposition occurs, the deposit amount was reduced by >40% (>0.6 g m^{-2}). For areas behind spacer filaments, where deposition is most pronounced, the 90th percentile was reached at 2.3 g m^{-2}, which is 67% lower than for steady flow. The median deposition was also reduced by 53% to 1.6 g m^{-2}, which is identical to the peak of the distribution of relative fractions. Hence, it can be concluded that pulsed flow significantly improves deposition control by firstly reducing the overall deposition rate and secondly by increasing deposit homogeneity. Thirdly, the 90th percentile being most distinctly reduced translates to pulsed flow achieving a particularly improved deposit control in areas of most severe fouling, which are behind spacer filaments. This visually confirms the hypothesis that pulsed flow leads to improved deposit control in skim milk filtration due to pulsed flow causing a more efficient distribution of local fluid forces in the vicinity of the membrane (Kürzl et al. 2022a) and improved access to flow shadows (Kürzl and Kulozik 2023b) as a cause of increased turbulence. Whether the improved deposit control results in an improved filtration performance will be investigated in chapter 7.3.2. Nonetheless, the current results seem to contradict those obtained by Weinberger and Kulozik (2021a) who also investigated the pulsed filtration of skim milk, but found an impaired deposit formation with pulsed flow. The underlying cause was discussed to be the irreversible compression of the milk protein deposit caused by pressure peaks in the high flow velocity phases compensating the positive effects of pulsed flow found for other feed solutions (Howell et al. 1993; Weinberger and Kulozik 2021c). The main differences between the current and previous study are the filtration temperature (50 °C versus 15 °C) and the membrane geometry (FSM versus HFM), which could both be responsible for the improved advantage of pulsed flow in the current study. The reduced temperature translates to a 150% increase in viscosity (Whitaker et al. 1927), causing increased resistance to flow and increased boundary layer height (Chen et al. 2021; Wu et al. 2017), which presumably impeded the turbulence-inducing effect of pulsed flow. The presence of flow shadows and the improved access to those areas in FSM due to pulsed flow could be

a critical aspect of the membrane geometry improving the advantageousness of pulsed flow in FSM over that in HFM. Such synergistic effects were also assumed responsible in a previous study on the pulsed cleaning of MF membranes after skim milk filtration, where the improvement in cleaning efficiency with pulsed flow was more pronounced in FSM than in HFM (Kürzl and Kulozik 2023b). The results of another study, which examined the pulsed filtration of yeast solutions in tubular membranes, also suggested synergistic effects between pulsed flow and baffles (Howell et al. 1993).

Alternating flow

Lastly, alternating flow filtration with its additional cyclic flow reversal shows the lowest deposit amounts of all three flow types, with the minimum deposit amounts observed being < 0.1 g m^{-2}. The median is reached at 0.7 g m^{-2}, which translates to 79% and 56% reductions compared to steady and pulsed flow. According to the 90^{th} percentile reached at 1.1 g m^{-2}, protein amounts in areas of maximum deposition are also reduced by 84% and 52% compared to steady and pulsed flow. Hence, alternating flow leads to the least pronounced and most homogeneous deposit formation caused by the additional cyclic flow reversal, presumably inducing additional turbulence and providing improved access to flow shadows compared to both steady and pulsed flow. While this is in accordance with previous results on the filtration of a model system containing yeast as retained fraction and BSA as permeable component (Weinberger and Kulozik 2021b), the effects of alternating flow on the resulting filtration performance of milk in FSM will, for the first time, be discussed in chapter 7.3.2.

Overall, the visual surface analysis results show that the disruption of steady flow patterns by pulsed flow or with additional flow reversal, as in alternating flow, causes a reduction in the amount of deposit and an increase in deposit homogeneity with increased access to flow shadows. Whether the remaining deposit amounts created during pulsed and alternating flow filtration of skim milk are more loosely bound or more compacted than that of steady flow, as stated by Weinberger and Kulozik (2021a), cannot simply be assessed by the established visual analysis. Hence, the following chapter will assess the effect of deposits formed with different flow types on filtration performance.

7.3.2 Influence of pulsed and alternating flow on filtration performance

As the deposit formation is known to determine filtration behaviour, the effects of different flow types on the time-resolved filtration performance were assessed by monitoring flux, as well as permeation and mass flow of WP and CN during a filtration duration of 60 min.

During filtration, the flux of steady$_{avg}$ flow (Figure 7-5a) remained relatively constant at 59 L m^{-2} h^{-1}. However, its WP permeation (Figure 7-5b) declined by 24.0% from 26.2% to 19.9% due to progressive deposit formation hindering the passage of proteins.

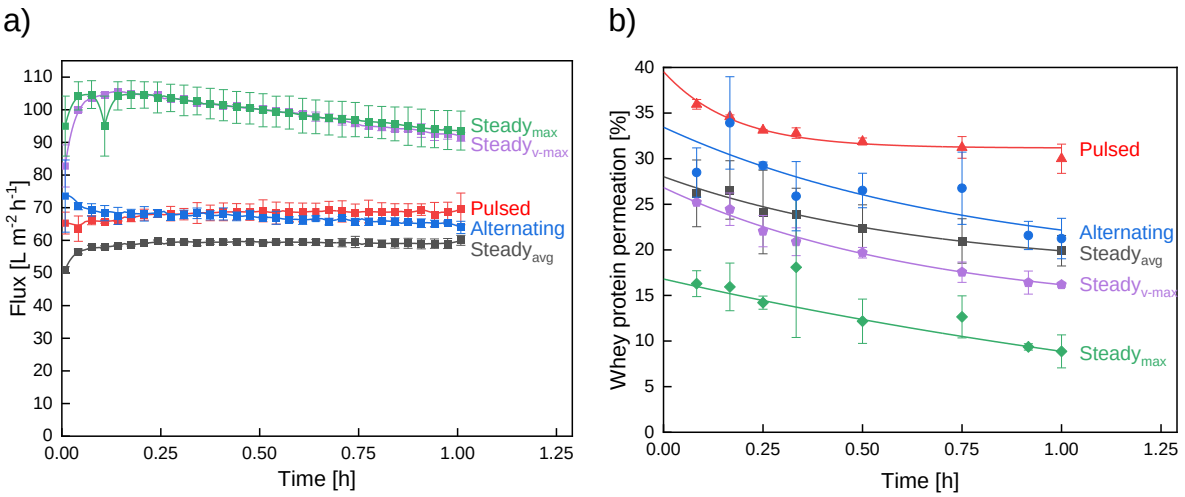

Figure 7-5. Progression of flux (a) and WP permeation (b) of steady$_{avg}$ (black), steady$_{v\text{-}max}$ (purple), steady$_{max}$ (green), pulsed (red) and alternating (blue) flow filtration. Filtration conditions: T = 50 °C; t = 60 min; steady$_{avg}$: v_{avg} = 0.6 m s^{-1}, $\Delta p_{TM,\,avg}$ = 1.0 bar; steady$_{v\text{-}max}$: v_{max} = 0.9 m s^{-1}, $\Delta p_{TM,\,avg}$ = 1.0 bar; steady$_{max}$: v_{max} = 0.9 m s^{-1}, $\Delta p_{TM,\,max}$ = 1.7 bar; pulsed/alternating flow: v_{max} = 0.9 m s^{-1}, v_{min} = 0.3 m s^{-1}, Δv = 0.6 m s^{-1}, $\Delta p_{TM,\,avg}$ = 1.0 bar, $\Delta p_{TM,\,max}$ = 1.7 bar, $\Delta p_{TM,\,min}$ = 0.3 bar, $\Delta p_{TM,\,cycle}$ = 1.4 bar.

In comparison, the flux of pulsed flow also remained stable, but at an 18% higher value of 69.6 L m^{-2} h^{-1}. Its WP permeation declined less distinctly during filtration by 16.7% from 36.0% to 30.0% at a 50.8% higher value, while its CN permeation reached the highest level of all flow types. Details thereon can be found in the appendix (Figure 7-8). The combination of increased starting flux and permeation, a less distinct decline in permeation and thus increased steady-state permeation validates that the reduced and more homogeneous deposition achieved with pulsed flow, as discussed in chapter 7.3.1, causes significant improvements in both flux and protein permeability.

Despite alternating flow further reducing deposition and improving its homogenous distribution compared to pulsed and steady flow (see chapter 7.3.1), no flux or protein permeation improvements could be observed over pulsed flow. Its flux started at a higher value (73.6 L m^{-2} h^{-1}) but decreased to a slightly lower value of 64.0 L m^{-2} h^{-1}. Additionally, its WP permeation decreased more sharply by 26.7% from 30% to 22% without visibly reaching a steady-state. With the surface analysis implying improved deposit control, the underlying cause for a reduced filtration performance compared to pulsed flow must be based on internal fouling or compaction of remaining fouling. Also, with the additional cyclic flow reversal as the main difference between pulsed and alternating flow, the cause must be related to flow reversal. Firstly, it is known that the maximum occurring Δp_{TM} determines both filtration performance (Qu et al. 2012; Hartinger et al. 2019a; Schiffer et al. 2020) and cleaning success (Bartlett et al. 1995; Bird and Bartlett 2002; Kürzl et al. 2022a) for milk protein deposits. Hence,

the $\Delta p_{TM,\,max}$ occurring during pulsed and alternating flow is 70% higher than $\Delta p_{TM,\,avg}$ occurring during $steady_{avg}$ flow. This will presumably negatively influence and thus limit the filtration performance of those flow types, despite the fluctuating stress and induced turbulence. The consequence could be increased compaction or intensified inner pore blockage within the remaining deposits that cannot be controlled by fluctuating stress and turbulence. This effect will be most pronounced at the membrane inlet because Δp_{TM} and thus the intensity of deposit formation decreases along the membrane length. Hence, for alternating flow, where the inlet and outlet cyclically change places, the negative effect of impaired pore clogging or deposit compaction would be intensified and could therefore explain the reduced filtration performance compared to pulsed flow.

Nonetheless, the filtration performance was significantly improved when utilising pulsed or alternating flow, despite using the same v_{avg} and $\Delta p_{TM,\,avg}$ as in $steady_{avg}$ flow. To compare the superior pulsed flow with the maximum conditions applicable under steady flow, as commonly applied in industrial practice, additional steady flow experiments for both a throttled ($steady_{v\text{-}max}$ with v_{max} and $\Delta p_{TM,\,avg}$) and unthrottled ($steady_{max}$ with v_{max} and $\Delta p_{TM,\,max}$) system were conducted. Since the flow velocity was 50% higher compared to pulsed, alternating and $steady_{avg}$ flow, $steady_{v\text{-}max}$ and $steady_{max}$ flow filtration led to higher flux levels. For both $steady_{v\text{-}max}$ and $steady_{max}$, flux started at a higher maximum value of 105.0 L m^{-2} h^{-1} and then declined by 12.4% to 92.0 L m^{-2} h^{-1}, which is 56.0% and 32.2% higher than that of $steady_{avg}$ and pulsed flow. In contrast to flux, there are significant differences in the WP permeation between $steady_{v\text{-}max}$ and $steady_{max}$ caused by the differences in Δp_{TM}. Although a previous study suggested local increases in permeation with increasing v (Hartinger et al. 2020c), for $steady_{v\text{-}max}$ the steady-state WP permeation of 16.2% is slightly decreased compared to that of $steady_{avg}$. The WP permeation of $steady_{max}$ showed the most substantial WP permeation decline during filtration (45.4%) from 16.3% to 8.9%, corresponding to the lowest values of the examined filtration conditions. The permeation of CN showed similar results (Figure 7-8). These results were expected due to the permanently 50% increased Δp_{TM} causing further deposit compaction and thus impairing the permeation of both WP and CN.

In summary, pulsed flow reached its steady-state in combined terms of flux as well as CN and WP permeation earliest, where WP permeation underwent the smallest decline, and steady-state permeation was >50.8% increased over any steady flow combination, confirming the best deposit control. The flux was 18% greater than with $steady_{avg}$ flow, but 24% lower than with $steady_{max}$ and $steady_{v\text{-}max}$ flow. To assess which combination of flux and WP permeation resulting from different flow conditions causes the highest overall filtration performance, the progression of WP mass flow (Figure 7-6a) and cumulative WP mass transport (Figure 7-6b) were compared between different flow conditions.

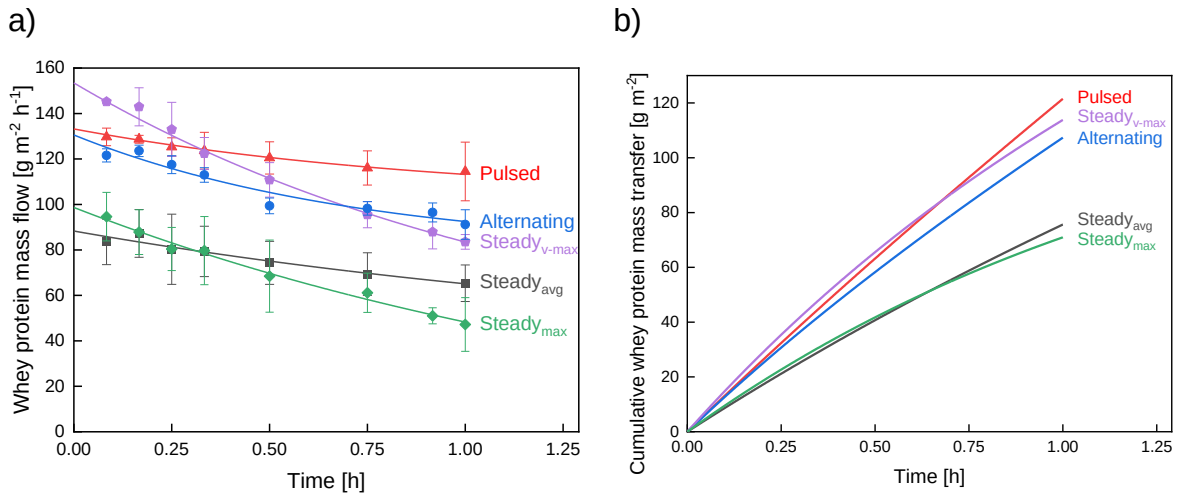

Figure 7-6. Progression of current WP mass flow (a) and cumulative WP mass transfer (b) during $steady_{avg}$ (black), $steady_{v\text{-}max}$ (purple), $steady_{max}$ (green), pulsed (red) and alternating (blue) flow filtration. Filtration conditions: T = 50 °C; t = 60 min; $steady_{avg}$: v_{avg} = 0.6 m s^{-1}, $\Delta p_{TM,\,avg}$ = 1.0 bar; $steady_{v\text{-}max}$: v_{max} = 0.9 m s^{-1}, $\Delta p_{TM,\,avg}$ = 1.0 bar; $steady_{max}$: v_{max} = 0.9 m s^{-1}, $\Delta p_{TM,\,max}$ = 1.7 bar; pulsed/alternating flow: v_{max} = 0.9 m s^{-1}, v_{min} = 0.3 m s^{-1}, Δv = 0.6 m s^{-1}, $\Delta p_{TM,\,avg}$ = 1.0 bar, $\Delta p_{TM,\,max}$ = 1.7 bar, $\Delta p_{TM,\,min}$ = 0.3 bar, $\Delta p_{TM,\,cycle}$ = 1.4 bar.

Due to the low flux and medium permeation during $steady_{avg}$ flow and the low permeation during $steady_{max}$ flow filtration, their WP mass flow reached the lowest levels after 60 min with 65 g m^{-2} h^{-1} and 47 g m^{-2} h^{-1}. Hence, their cumulative WP mass transport also depicts the lowest filtration performance. Between $steady_{v\text{-}max}$, pulsed and alternating flow, their order in terms of WP mass flow changed over time. $Steady_{v\text{-}max}$ started at the highest WP mass flow due to its high flux but fell below that of pulsed flow after 30 min and below that of alternating flow after 45 min due to decreasing flux and permeation reaching 84 g m^{-2} h^{-1} after 60 min. Alternating and pulsed flow exceeded this value by 8% with 91 g m^{-2} h^{-1} and 37% with 115 g m^{-2} h^{-1}, respectively. Accordingly, the cumulative WP mass transport with pulsed flow surpassed $steady_{v\text{-}max}$ after 42 min. It is to be noted that the CN mass flow (Figure 7-9a) and CN mass transfer (Figure 7-9b) also reached the highest values for pulsed flow.

Changing perspective from a time-resolved to a volume-resolved view, the benefits of alternative flow types appear more distinctly pronounced (Figure 7-7). The cumulated WP mass transfer of $steady_{avg}$ and $steady_{v\text{-}max}$ increased similarly with the accumulation of permeate flow due to their similar permeation. Due to the higher flow rate and thus flux, $steady_{v\text{-}max}$ reached both more cumulative WP mass transfer and flux in 60 min filtration. Their final values of cumulative WP mass transfer achieved per accumulated permeate volume are 1.27 g L^{-1} for $steady_{avg}$ and 1.15 g L^{-1} for $steady_{v\text{-}max}$. Again, $steady_{max}$ reached the lowest value of 0.71 g L^{-1} due to the combination of a large amount of accumulated permeate with the lowest amount of WP mass transfer. Additionally to reaching the highest WP mass flow after 60 min filtration, pulsed flow also showed the highest volume-based separation efficiency with 1.77 g L^{-1} of WP mass transfer per accumulated permeate, followed by alternating flow with 1.58 g L^{-1}. Hence, due to a lower flux and higher mass transfer, the volume-based separation

efficiency was >39% improved for pulsed flow compared to any set of steady flow conditions. Despite these experiments being conducted in circulation mode, the described results imply benefits for filtration in concentration mode or diafiltration mode. For the removal of e.g. 70 g m^{-2} of WP via the permeate, pulsed and alternating flow required a permeation of 37.5 L m^{-2} and 41.1 L m^{-2}, respectively, while $steady_{avg}$, $steady_{v\text{-}max}$ and $steady_{max}$ required a permeation of 53.7 L m^{-2}, 54.5 L m^{-2} and 97.5 L m^{-2}, respectively. Hence, for the mentioned process modes of concentration and diafiltration, using alternative flow types could translate to both a higher WP concentration in the permeate and a lower amount of permeate/washing volume required to achieve the same WP mass transfer. Despite these implied advantages for concentrating/separating proteins and diafiltration, it is to be noted, that possible effects of associated characteristics that change during the process, e.g. the feed viscosity or protein concentration, on the efficiency of operating in pulsed or alternating flow mode need to be investigated separately.

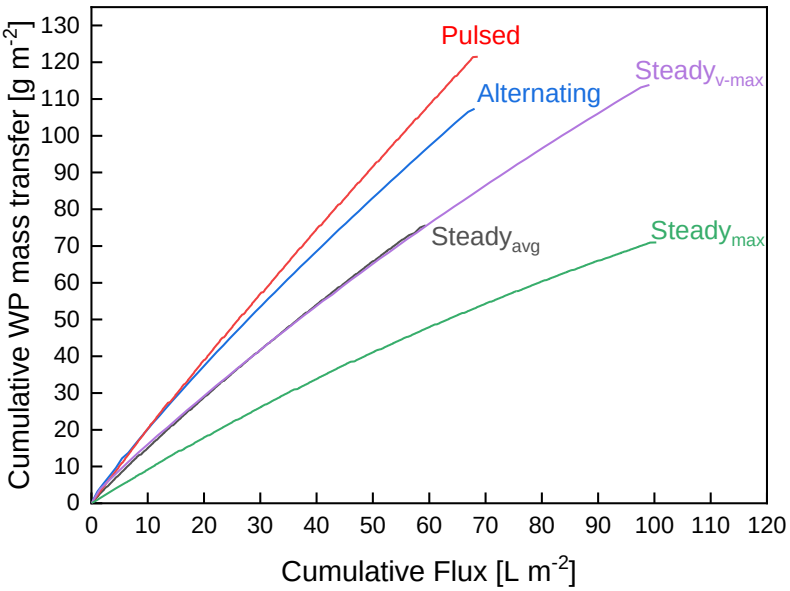

Figure 7-7. Comparison of the cumulative WP mass transfer per cumulative flux for $steady_{avg}$ (black), $steady_{v\text{-}max}$ (purple), $steady_{max}$ (green), pulsed (red) and alternating (blue) flow filtration. Filtration conditions: T = 50 °C, t = 60 min, v_{avg} = 0.6 m s^{-1} (pulsed/alternating flow: v_{max} = 0.9 m s^{-1}, v_{min} = 0.3 m s^{-1}, Δv = 0.6 m s^{-1}), $\Delta p_{TM,\,avg}$ = 1.0 bar (pulsed/alternating flow: $\Delta p_{TM,\,max}$ = 1.7 bar, $\Delta p_{TM,\,min}$ = 0.3 bar, $\Delta p_{TM,\,cycle}$ = 1.4 bar).

7.3.3 Influence of flow types on process sustainability

To assess the effects of different flow types on the process sustainability, the respective changes in pump energy consumptions were included in the filtration performance evaluation in Table 7-2. It depicts the flow velocity, WP mass flow, pump energy consumption and specific pump energy consumption of each examined set of flow conditions, normalised for $steady_{avg}$ flow. The specific energy consumption was calculated by dividing the energy consumption by

the WP mass flow of a respective flow type. The normalisation was obtained by dividing all values of the respective variable by that of $steady_{avg}$ (see appendix B). $Steady_{max}$ and $steady_{v\text{-}max}$ cause a 196% increase in pump energy consumption due to the increased flow rate. For $steady_{max}$, the simultaneously decreased WP mass flow causes a 309% increase in the specific pump energy consumption, translating to a significantly reduced energy efficiency and process sustainability. For $steady_{v\text{-}max}$, the increase in WP mass flow cannot compensate the additionally required pump energy, thus also resulting in a 129% increase in specific energy consumption and thus decreased sustainability. Despite the identical flow velocity, both pulsed and alternating flow cause increased energy consumptions over $steady_{avg}$ flow. For pulsed flow, the energy consumption is increased by 25% due to constant changes in pump capacity. For alternating flow, it is increased by 29% due to the additional changes in the flow direction. However, the resulting benefits in WP mass flow outweigh the increased energy demand. Accordingly, pulsed and alternating flow reduce the specific energy consumption by 29% and 8% compared to $steady_{avg}$ flow. Compared to $steady_{v\text{-}max}$, which achieved the highest filtration performance of the three steady flow combinations, the reductions in the specific energy consumption with pulsed and alternating flow are 69% and 60%.

Table 7-2. Influence of different flow types on filtration performance and pump energy consumption.

Flow mode [-]	v[d] [-]	WP mass flow[ad] [-]	Energy consumption[bd] [-]	Specific energy consumption[cd] [-]
$steady_{avg}$	1.0	1.00	1.00	1.00
$steady_{max}$	1.5	0.72	2.96	4.09
$steady_{v\text{-}max}$	1.5	1.29	2.96	2.29
pulsed	1.0	1.77	1.25	0.71
alternating	1.0	1.40	1.29	0.92

[a] Considered as steady-state after 60 min filtration.
[b] Data for steady, pulsed and $steady_{max}$ from Kürzl et al. (2022a).
[c] The specific energy consumption of the pump was calculated by dividing the energy consumption by the WP mass flow.
[d] Results of flow velocity, WP mass flow, energy consumption and specific energy consumption were normalised for $steady_{avg}$ flow. Normalisation was done by dividing all values of the respective variable by that of $steady_{avg}$.

Hence, besides an increased filtration performance, both pulsed and alternating flow led to more efficient utilisation of invested pump energy and fluid forces compared to all steady flow combinations. This is particularly important as membrane processes can make up >50% of the environmental impact of the production phase in milk protein fractionation (Gésan-Guiziou et al. 2019).

7.4 Conclusion

This study showed that pulsed and alternating flow effectively control deposit formation during skim milk MF. Compared to conventional steady crossflow, they provided improved access to flow shadows behind spacer filaments due to increased turbulences caused by cyclic fluctuations in shear stress, pressure and, for alternating flow, in flow direction. This led to reductions in protein deposition by 53% for pulsed flow and 79% for alternating flow, including a more homogenous distribution of deposits on the membrane surface. The reduced deposition in areas of prevailing flow shadows could help improve the cleanability of spacer-containing membranes such as FSM and spiral-wound modules, where this poses a main limitation of an otherwise efficient membrane system in terms of packing density or permeation (Schopf et al. 2021b).

While the visual examination of membranes after alternating flow filtration suggested the best deposit control, analysis of filtration performance was inferior to that of pulsed flow. This was attributed to the adverse effects of Δp_{TM} peaks, usually occurring at the inlet due to its length dependency, being present at both module sides due to the cyclic changes in the flow direction. Nonetheless, both pulsed and alternating flow led to enhancements of >8% and >37% in steady-state WP mass flow over any set of steady flow conditions. Hence, the application of pulsed and alternating flow is superior to an increase in crossflow velocity in steady flow. Due to additional differences in required pump energy, this leads to reductions in the specific energy consumption of 69% and 60% for pulsed and alternating flow, thus significantly enhancing economic and ecological process efficiency and sustainability, particularly for pulsed flow. Furthermore, the results also provided positive indications for alternative flow types improving the efficiency of other process modes, e.g. the WP removal during protein concentration or the washing efficiency during diafiltration. However, the application of alternative flow types in other process modes with changing feed characteristics, such as viscosity, requires a separate assessment.

While the implementation of pulsed and alternating flow in industrial membrane systems might be associated with financial and labour costs, it will barely affect its environmental impact as the equipment part has been shown only to make up <15% of the total environmental impact of the milk protein fractionation task (Gésan-Guiziou et al. 2019). Contrary to that, membrane processes during filtration and cleaning cycles, for which pulsed and alternating flow also proved beneficial (Kürzl et al. 2022a; Kürzl and Kulozik 2023b, 2023a), are the main contributors to the environmental impact (Gésan-Guiziou et al. 2019). While current and previous results demonstrated the advantageousness of pulsed and alternating flow in significantly improving process efficiency and sustainability, the combined effects of pulsed or alternating flow on filtration and subsequent cleaning are yet to be investigated.

Author Contributions:

Conceptualisation, C.K.; methodology, C.K.; software, C.K.; validation, C.K.; formal analysis, C.K.; investigation, C.K.; resources, U.K.; data curation, C.K.; writing—original draft preparation, C.K.; writing—review and editing, C.K. and U.K.; visualisation, C.K.; supervision, U.K.; project administration, C.K.; funding acquisition, U.K. All authors have read and agreed to the published version of the manuscript.

Funding

This IGF Project of the FEI was supported via AiF to promote the Industrial Collective Research (IGF) of the German Ministry of Economic Affairs and Energy (BMWi), based on a resolution of the German Parliament. Project: AiF 57 EWN.

Acknowledgements

We gratefully thank Heidi Wohlschläger for her assistance with the RP-HPLC analysis. Furthermore, we want to thank Siegfried Tuchborn from SIMA-tec GmbH and Christian Ederer, Erich Schneider, and Franz Fraunhofer in our workshop for technical support. We also want to thank Carolin Modesto for her experimental support. Finally, we want to thank Simon Schiffer, Roland Schopf and Martin Hartinger for fruitful discussions.

Conflicts of interests

The authors declare no conflict of interest. The authors declare that they have no known competing financial interests or personal relationships that could have influenced the work reported in this paper. The funders had no role in the design of the study; in the collection, analyses, or interpretation of data; in the writing of the manuscript, or in the decision to publish the results.

Supplementary A

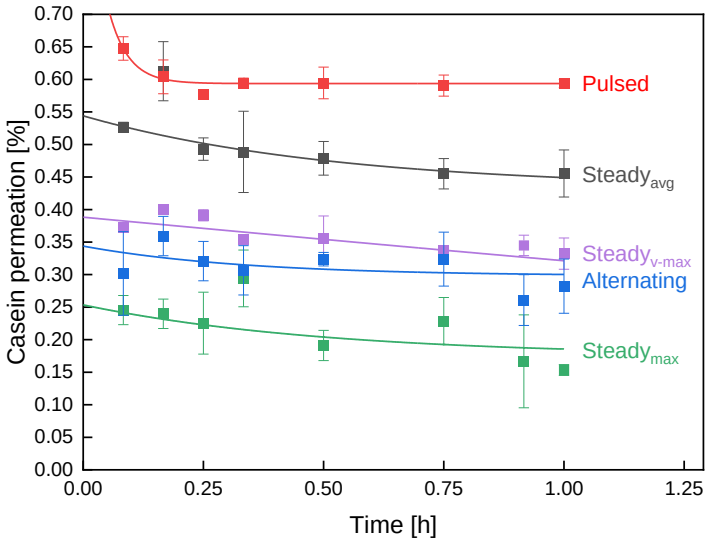

Figure 7-8. Progression of CN permeation during steady$_{avg}$ (black), steady$_{v\text{-}max}$ (purple), steady$_{max}$ (green), pulsed (red) and alternating (blue) flow filtration. Filtration conditions: T = 50 °C; t = 60 min; steady$_{avg}$: v_{avg} = 0.6 m s^{-1}, $\Delta p_{TM,\,avg}$ = 1.0 bar; steady$_{v\text{-}max}$: v_{max} = 0.9 m s^{-1}, $\Delta p_{TM,\,avg}$ = 1.0 bar; steady$_{max}$: v_{max} = 0.9 m s^{-1}, $\Delta p_{TM,\,max}$ = 1.7 bar; pulsed/alternating flow: v_{max} = 0.9 m s^{-1}, v_{min} = 0.3 m s^{-1}, Δv = 0.6 m s^{-1}, $\Delta p_{TM,\,avg}$ = 1.0 bar, $\Delta p_{TM,\,max}$ = 1.7 bar, $\Delta p_{TM,\,min}$ = 0.3 bar, $\Delta p_{TM,\,cycle}$ = 1.4 bar.

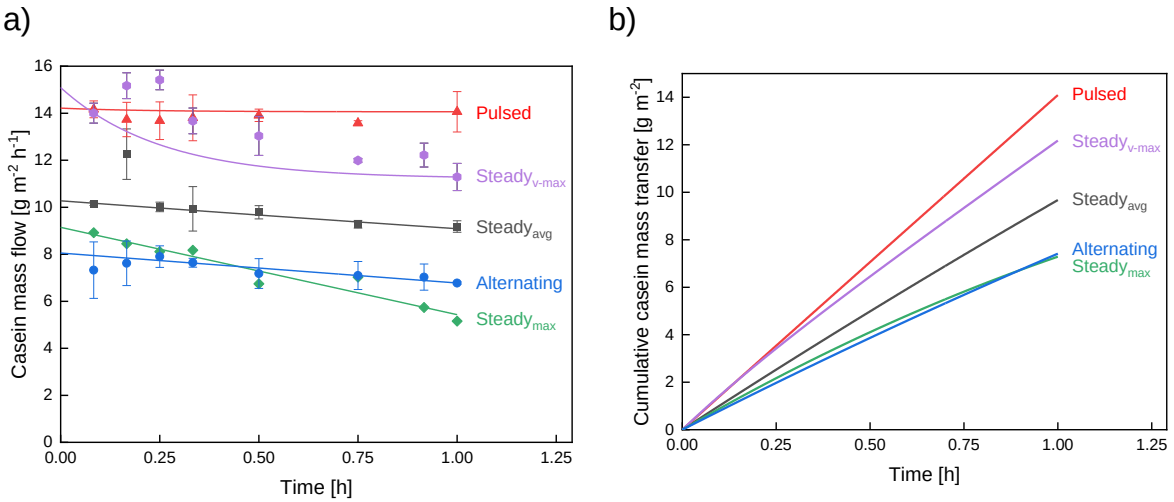

Figure 7-9. Progression of current CN mass flow (a) and cumulative CN mass transfer (b) during steady$_{avg}$ (black), steady$_{v\text{-}max}$ (purple), steady$_{max}$ (green), pulsed (red) and alternating (blue) flow filtration. Filtration conditions: T = 50 °C; t = 60 min; steady$_{avg}$: v_{avg} = 0.6 m s^{-1}, $\Delta p_{TM,\,avg}$ = 1.0 bar; steady$_{v\text{-}max}$: v_{max} = 0.9 m s^{-1}, $\Delta p_{TM,\,avg}$ = 1.0 bar; steady$_{max}$: v_{max} = 0.9 m s^{-1}, $\Delta p_{TM,\,max}$ = 1.7 bar; pulsed/alternating flow: v_{max} = 0.9 m s^{-1}, v_{min} = 0.3 m s^{-1}, Δv = 0.6 m s^{-1}, $\Delta p_{TM,\,avg}$ = 1.0 bar, $\Delta p_{TM,\,max}$ = 1.7 bar, $\Delta p_{TM,\,min}$ = 0.3 bar, $\Delta p_{TM,\,cycle}$ = 1.4 bar.

Supplementary B. Calculation of normalised values

Exemplary, the specific energy consumption of pulsed flow $E_{spec,\,pulsed}$ is calculated by dividing the energy consumption of pulsed flow filtration E_{pulsed} by its steady-state WP mass flow $\dot{m}_{WP,\,pulsed}$ (eq. (7-11)). The normalised specific energy consumption of pulsed flow $E_{norm,\,spec,\,pulsed}$ (eq. (7-12)) is then obtained by dividing the specific energy consumption of pulsed flow filtration $E_{spec,\,pulsed}$ by that of steady$_{avg}$ flow filtration $E_{spec,\,steady-avg}$.

$$E_{spec,\,pulsed} = \frac{E_{pulsed}}{\dot{m}_{WP,\,pulsed}} \tag{7-11}$$

$$E_{norm,\,spec,\,pulsed} = \frac{E_{spec,\,pulsed}}{E_{spec,\,steady-avg}} \tag{7-12}$$

8 Increasing Performance of Spiral-Wound Modules (SWMs) by Improving Stability against Axial Pressure Drop and Utilising Pulsed Flow[7]

Christian Kürzl[a*], Martin Hartinger, Patrick Ong, Roland Schopf, Simon Schiffer and Ulrich Kulozik

Chair of Food and Bioprocess Engineering, TUM School of Life Sciences, Technical University of Munich, Weihenstephaner Berg 1, Freising, Germany

[a] New affiliation: Professorship Food Process Engineering, TUM School of Life Sciences, Technical University of Munich, Weihenstephaner Berg 1, 85354 Freising, Germany

* Corresponding author

Summary and contribution of the doctoral candidate

While the previous studies found positive effects of alternative flow types, particularly pulsed flow, on filtration performance and cleaning success, particularly in FSM vicarious for SWM, there are some hurdles for transferring these results from lab-scale with FSM to pilot-scale with SWM. Firstly, the previous approach of using rapid pump capacity ramps for pulsation creation is currently not feasible at an industrial scale with higher flow rates. Hence, a novel approach to creating pulsed flow without requiring rapid pump capacity ramps had to be developed. Secondly, the previous positive results in FSM were conducted at pressure drops above the current limitations of SWM. Thus, more mechanically stable SWM modules would enable utilising the full potential of pulsed flow at high flow velocities with large amplitudes in SWM suffering from flow shadows. Thirdly, the transfer of results from FSM to SWM was previously reported to be difficult for e.g. certain spacer geometries (Hartinger et al. 2020a), which induces the necessity of validating lab-scale FSM results in industrial-scale SWM. Overall, this combined approach of enabling the utilisation of pulsed flow on industrial-scale membrane modules and stabilising SWM by adding feed-side glue connections aimed to overcome the limitations of SWM by increasing the range of applicable shear stress and improving access to flow shadows.

---

[7] Original publication: Kürzl et al. (2023): Kürzl, C.; Hartinger, M.; Ong, P.; Schopf, R.; Schiffer, S.; Kulozik, U. 2023. Increasing Performance of Spiral-Wound Modules (SWMs) by Improving Stability against Axial Pressure Drop and Utilising Pulsed Flow. *Membranes* 9 *13*, 791. doi: 10.3390/membranes13090791. Adapted original manuscript. Adaptations of the manuscript refer to enumeration type, citation style, spelling, notation of units, format, and merging of all lists of references into one at the end of the dissertation. No special permission is required to reuse all or part of the article published by MDPI.

The novel approach to pulsation creation comprises a bypass controlled by a pneumatic valve and manual throttle, enabling pulsed flow with a defined frequency, amplitude, and similar flow profile as in lab-scale trials but at a constant pump capacity. While the positive effects of pulsed flow on filtration performance (WP mass flow increased by 26%) and cleaning success (protein removal increased by 28%) could be confirmed in SWM, the improvements were less distinct than in FSM. Despite the underlying cause not entirely being confirmed, it was presumed to be due to geometrical differences causing local differences in fouling intensity at the module inlet and outlet. Besides this novel approach enabling pulsed flow in industrial-scale modules, the developed bypass system poses an energetic drawback for singular modules, as parts of the pump energy dissipate by being returned unused to the feed tank. Nonetheless, in most industrial applications, many modules are installed in series and parallel. Hence, this bypass could also feed a second module alternatingly with pulsed flow phases, leaving no energy unused.

The stabilisation of SWM was done by adding feed-side glue connections between membrane sheets in the radial direction across the membrane length of a used SWM. Despite these glue stripes slightly increasing the axial pressure drop and being added under non-ideal glueing conditions, i.e. in a used module, the glue stripes improved the module's short-term stability against axial displacement by > 100% along the whole membrane diameter. Hence, higher flow rates and increased amplitudes under pulsed flow could be applied to the glue-connected SWM.

The doctoral candidate designed the experimental approach for this study based on a critical review of the literature. Data acquisition was mainly done by the doctoral candidate. Also, the doctoral candidate developed the experimental concept, analysed, interpreted and plotted data. The manuscript was written and reviewed by the doctoral candidate. The co-authors contributed to the project outline, the discussion of results, the execution of experiments, and the revision of the manuscript.

Abstract

Spacer-induced flow shadows and limited mechanical stability due to module construction and geometry are the main obstacles to improving the filtration performance and cleanability of microfiltration spiral-wound membranes (SWM), applied to milk protein fractionation in this study. The goal of this study was first to improve filtration performance and cleanability by utilising pulsed flow in a modified pilot-scale filtration plant. The second goal was to enhance membrane stability against module deformation by flow-induced friction in the axial direction (“membrane telescoping”). This was accomplished by stabilising membrane layers, including spacers, at the membrane inlet by glue connections. Pulsed flow

characteristics similar to those reported in previous lab-scale studies could be achieved by establishing an on/off bypass around the membrane module, thus enabling a high-frequency flow variation. Pulsed flow significantly increased filtration performance (target protein mass flow into the permeate increased by 26%) and cleaning success (protein removal increased by 28%). Furthermore, adding feed-side glue connections increased the mechanical membrane stability in terms of allowed volume throughput by ≥100% compared to unmodified modules, thus allowing operation with higher axial pressure drops, flow velocities and pulsation amplitudes.

Keywords: pulsed flow; module stability; axial pressure loss; telescoping; membrane performance

Graphical abstract:

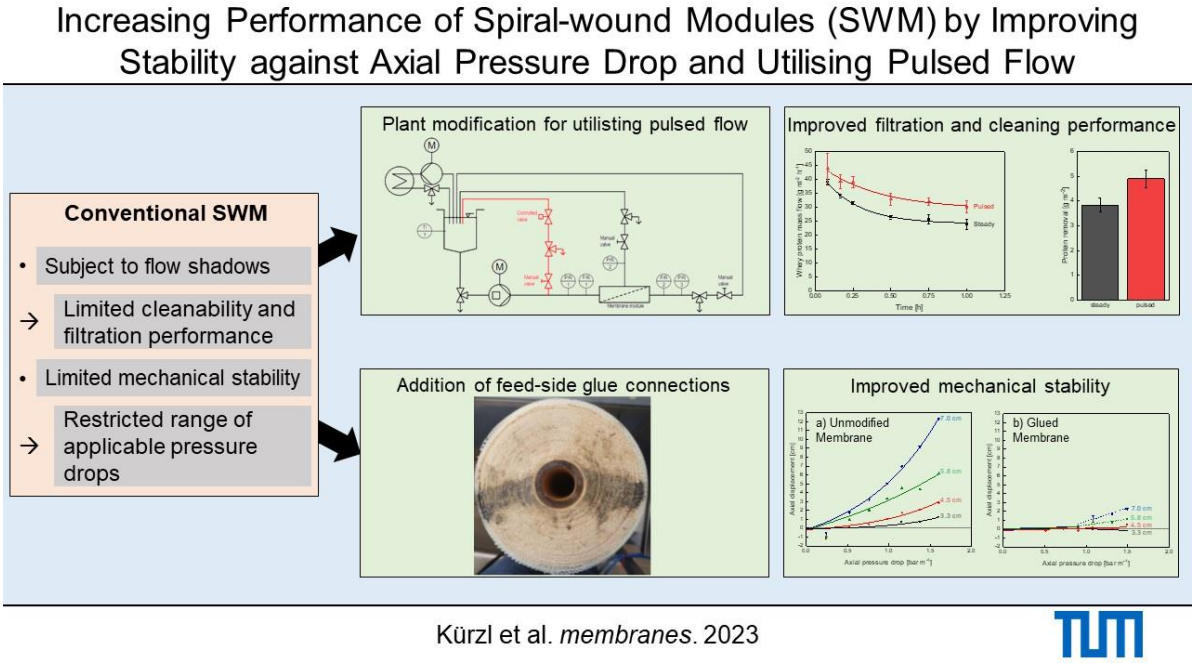

8.1 Introduction

The membrane-based separation of a feed solution into the permeable components (permeate) and the retained components (retentate) is widely applied across various industries. Within this process, the main challenge is controlling deposit formation, i.e., fouling, which results from the accumulation of retained feed components on and in the membrane structure (Bartlett et al. 1995; Bird and Bartlett 2002; Cui et al. 2010; Saxena et al. 2009; Baker 2012). With deposits acting as a secondary selective layer, this causes separation efficiency in terms of flux and protein permeation decreasing gradually during filtration (Ng et al. 2017; Ripperger and Altmann 2002; Ripperger and Grein 2007). Additionally, frequent cleaning cycles are required to maintain membrane performance and product quality due to the feed- and temperature-dependent occurrence and progression of biofouling (Schiffer and Kulozik 2020; Chamberland et al. 2019; Burgess et al. 2010; Carrascosa et al. 2021; Ng et al. 2018). For dairy applications, one important example is the fractionation of skim milk protein into its major protein components: whey proteins (particle diameter d_P = 3–6 nm (Brans et al. 2004)) and casein micelles (d_P = 20–300 nm (Brans et al. 2004)) via microfiltration (MF; nominal pore size = 0.1–0.3 µm). This poses a particular challenge for the application of fouling and cleaning as casein micelles can form highly compressible and cross-linked gel layers at high concentrations and high-pressure conditions (Qu et al. 2012; Qu et al. 2015; Bouchoux et al. 2009; Bouchoux et al. 2010; Horne 2020). Deposit formation cannot be reverted by pressure release (Hartinger et al. 2019b), and accumulated protein can only be incompletely removed by rinsing steps (Bartlett et al. 1995; Bird and Bartlett 2002; Blanpain-Avet et al. 2009).

Besides feed composition, the membrane performance largely depends on processing conditions. Up to limiting conditions, transmembrane pressure (Δp_{TM}) increases can be used to achieve gains in flux. However, beyond limiting conditions, further increases in Δp_{TM} do not cause further flux increases but solely result in additional, partly irreversible (Hartinger et al. 2019b) deposit compaction and fouling (Ripperger and Altmann 2002). Another option to enhance membrane performance is by increasing the flow velocity v, and thus the wall shear stress τ_w, as this reduces fouling (Samuelsson et al. 1997; Defrance and Jaffrin 1999; Qiu and Davies 2015; Farhat et al. 2016; Altmann and Ripperger 1997). Nonetheless, the maximum applicable crossflow velocities in SWMs are limited by geometry-related or constructional aspects, thus also limiting fouling control and cleanability.

Regarding membrane geometry, fouling depends on the membrane length and varies along the membrane (Hartinger et al. 2020c). Due to friction, an axial pressure loss (Δp_L) over the membrane length is induced. This causes a decrease in Δp_{TM} and thus in the fouling intensity from the module inlet towards the module outlet (Hartinger et al. 2020c). The main industrially used module configurations are ceramic tubular membranes (CTMs), hollow-fibre membranes (HFMs) and SWMs, which all have their typical pros and cons. Compared to CTMs

and HFMs, SWMs offer the highest packing density, i.e., active membrane area per module, and thus the highest whey protein mass flow per module (Schopf et al. 2021b). On the contrary, SWMs suffer from flow shadows behind spacer filaments (Kürzl and Kulozik 2023b, 2023c; Fischer et al. 2020; Geraldes 2002; Han et al. 2018b; Kavianipour et al. 2017; Schwinge et al. 2002; Koutsou et al. 2007; Hartinger et al. 2020a) and, therefore, limited cleanability (Kürzl and Kulozik 2023b) and mechanical stability. In SWMs, the membrane permeate pockets are formed by glueing together individual membrane sheets, which are then wrapped around a central permeate collection tube and fixed by an outer hull. Thus, the SWMs' stability mainly depends on the stability of glued bond joints and the friction between the membrane sheets, which results from the strength of the wrapping.

The stability of bond joints depends on several construction-related aspects, such as the glue composition (Habenicht 2008), the design (Dilger 2010) and overlapping length of connections (Grote et al. 2018) and the glue layer thickness (Habenicht 2008). Apart from that, process-related aspects, such as the speed of stress application, the intensity and kind of stress (Habenicht 2008), the process temperature (Habenicht 2008) and the duration of stress application, have significant effects (Habenicht 2008; Althof 1984). Due to membrane pockets formed by glueing together membrane sheets, the permeate side is susceptible to failure, especially by negative Δp_{TM}, which stresses bond joints via peeling and can cause tearing of the membrane pockets. To avoid this, manufacturers usually limit the maximum negative Δp_{TM} to around 0.3 bar.

A more common failure mechanism in SWMs is telescoping, which describes an axial displacement of the membrane pockets caused by frictional losses along the module (Δp_L) acting on the membrane envelope. Hence, the strength of the wrapping determines the amount of friction between membrane sheets and thus its stability against axial displacement. However, besides a lower risk of telescoping, stronger wrapping can also press spacers into the membrane surface, thus reducing the active membrane area and even disrupting the selective layer (Karabelas et al. 2018). The trade-off between stability against axial deformation and membrane performance led to manufacturers limiting the friction-related axial pressure drop Δp_L to 1.3 bar m^{-1} despite the commonly added stability support against axial displacement via anti-telescoping devices (ATD). With Δp_L and thus v being limited, this significantly restricts options to control deposit formation, e.g., by conventionally established higher crossflow velocities in SWMs compared to the other module types described above.

Several process-oriented approaches trying to increase membrane performance have been investigated to cope with this limitation. One example is applying pulsed flow, i.e., a non-steady flow defined by its amplitude, in other words the difference between maximum and minimum flow and pressure conditions, and its frequency. Several studies demonstrated the positive influence of pulsed flow on filtration (Kürzl and Kulozik 2023c; Weinberger and Kulozik

2021c) and cleaning performance (Kürzl and Kulozik 2023b; Kürzl et al. 2022a) for various feed solutions, including milk. For membranes containing spacers, such as SWMs, particularly strong effects of pulsed flow on filtration and cleaning performance were reported due to pulsed flow reducing flow shadows due to enhanced turbulence (Kürzl and Kulozik 2023b, 2023c) at high frequencies (Kürzl et al. 2022a; Gillham et al. 2000; Blel et al. 2009a; Blel et al. 2009b; Weidemann et al. 2014; Yang et al. 2019) and amplitudes (Kürzl et al. 2022a; Gillham et al. 2000; Blel et al. 2009a; Blel et al. 2009b; Weidemann et al. 2014; Augustin et al. 2010).

However, some aspects exacerbate the transferability of lab-scale results to industrial-scale SWM modules. Firstly, the approaches to pulsation creation used in previous lab-scale studies either included piston or bellows units (Gillham et al. 2000; Bode et al. 2007) or specialised inductively controlled pumps that could create pulsed flow by rapidly increasing and decreasing pump capacity (Kürzl and Kulozik 2023b, 2023c; Kürzl et al. 2022a). The former approach temporarily induced distinct back-pressure and is thus incompatible with SWMs. To the authors' knowledge, the latter one is unavailable on a larger scale. Secondly, the transferability of results from studies with FSMs to SWMs has been considered to be problematic for certain spacer geometries due to the curvature of the feed channel and its influence on the radial distribution of v (Hartinger et al. 2020a). Thirdly, due to the limited applicable pressure drops in SWMs, the highest applicable flow velocity and pulsation amplitude are also limited. In particular, positive results for pulsed filtration in a previous study using an SWM-like flat sheet membrane system (FSM) were found for pressure losses up to 2.55 bar m^{-1} (Kürzl and Kulozik 2023c), which is beyond the allowed limit of SWM modules. Thus, the advantage of pulsed flow might be reduced or absent for current SWM modules.

Hence, the potential beneficial effect of pulsed flow in filtration and cleaning remains to be evaluated for industrial-scale SWMs. Therefore, a novel approach was developed to create pulsed flow without back-pressure from the permeate side or relying on rapid pump capacity ramps. Then, pulsed flow can be utilised to assess the efficacy of pulsed flow MF of skim milk and subsequent membrane cleaning in SWMs. With previous studies observing improved pulsed flow efficiency for increased amplitudes and at pressure drops above the current limits of industrial SWMs, stability-enhanced modules could support the efficiency of pulsed flow manifold by enabling higher crossflow velocities, axial pressure drops and pulsed flow amplitudes. Hence, this study also investigates an approach to improve module stability against telescoping by adding glue connections on the feed side between membrane pockets, as this should provide additional resistance against the displacement of individual sheets in the axial direction.

Accordingly, this study aims to overcome the limitations of SWMs by two means. The first one is process-oriented and functions by modifying an existing plant for utilising pulsed flow and then assessing its efficacy in filtration and cleaning. The second approach is

membrane-oriented and functions by creating a more robust SWM by adding glue connections on the feed side between membrane pockets, including spacers, to enhance its mechanical stability. For comparing steady and pulsed flow, filtration performance was evaluated in terms of permeate flux, protein permeation and protein mass flow. Cleaning success was evaluated hydrodynamically by measuring the flux recovery ratio (FRR) and chemically by analysing the protein removal achieved during cleaning. To investigate the effect of additional glue connections on module stability, the axial displacement of membrane layers in an unmodified and a glued membrane system was measured at different flow rates and radial distances to the module centre.

8.2 Material and methods

8.2.1 Filtration plant and experimental design

An established pilot-scale filtration plant (Figure 8-1) was designed to resemble a typical industrial setup. It mainly consisted of a double-screw-type displacement pump (FDS 2-3, Fristam Pumpen KG, Hamburg-Bergedorf, Germany), which is insensitive to moderate pressure surges and commonly used in several dairy applications in which, e.g., highly viscous fluids such as milk concentrates need to be processed, and a membrane housing with the established module configuration 6338 (length L = 0.96 m; diameter d = 0.16 m). Additionally, pressure sensors and flow meters allow the monitoring and controlling of the transmembrane pressure Δp_{TM} (see eq. (8-1)), feed flow rate and permeate flux J (see eq. (8-2)).

$$\Delta p_{TM} = \frac{p_1 + p_2}{2} - p_3 \tag{8-1}$$

where p_1 is the feed-side pressure, p_2 is the retentate-side pressure and p_3 is the permeate-side pressure.

$$J = \frac{\dot{V}_{per}}{A_{membrane}} \tag{8-2}$$

where $\dot{V}_{per}$ is the permeate flow rate and $A_{membrane}$ is the membrane area.

A separate heat exchanger loop combined with a temperature sensor enables precise temperature control of the filtration fluids before entering the membrane loop. Thus, the system can process various filtration feeds at defined temperatures, withstanding pressure surges and varying the installed membrane module’s geometry and pore size.

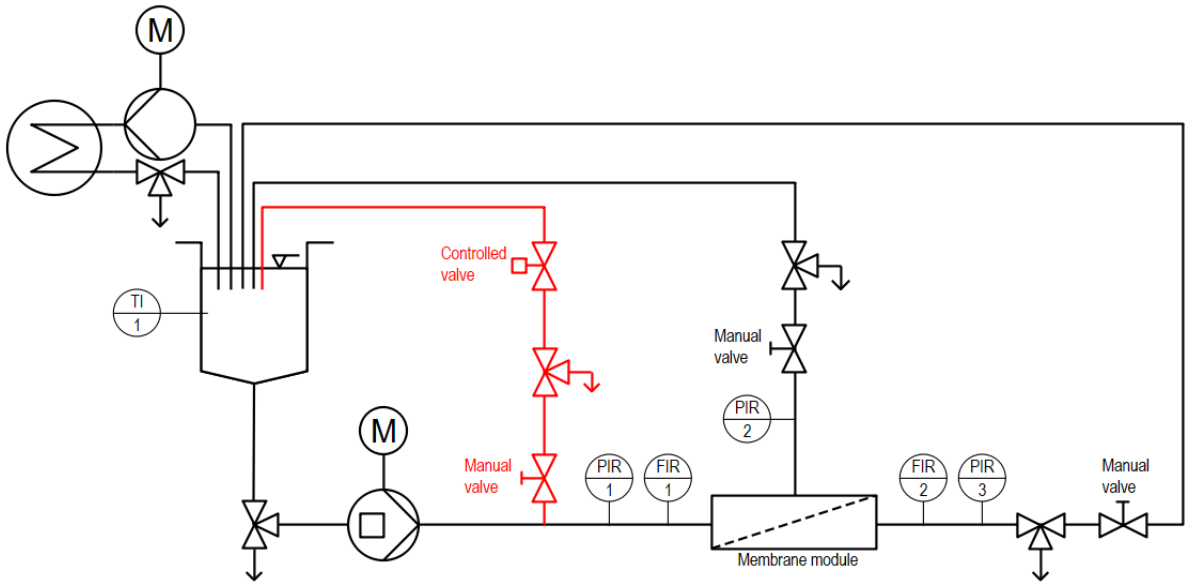

Figure 8-1. Piping and instrumentation (P and I) diagram of an established membrane filtration plant setup (black parts) consisting of feed pump, feed tank, sampling valves, manual throttling valves, a heating cycle consisting of another feed pump and heat exchanger, as well as various flow, pressure and temperature sensors. The red parts show the complimentary addition of a controlled bypass for utilising pulsed flow, including a manual throttling valve to control the pulsation amplitude and a controlled valve to control the pulsation frequency.

8.2.2 Plant modification and experimental design to utilise pulsed flow

To enable applying a pulsed flow to a standard membrane filtration plant setup without a pump capable of rapidly transitioning between high and low flow rates, a controlled bypass was added upstream of the membrane inlet flow meter and pressure sensor (see Figure 8-1). Accordingly, the bypass-related flow rate or pressure reductions could be monitored with installed sensors. The bypass comprised a relay-controlled pneumatic valve capable of fully closing or opening the bypass within 0.5 s at defined intervals. Hence, by determining the phase durations where the bypass was open (Δt_{min}) or closed (Δt_{max}), flow rate and pressure reach their minimum ($\dot{V}_{min}$, v_{min} and $\Delta p_{TM,\,min}$) or maximum ($\dot{V}_{max}$, v_{max} and $\Delta p_{TM,\,max}$), respectively, and thus control the pulsation frequency f (eq. (8-3)).

$$f = \frac{1}{\Delta t_{max} + \Delta t_{min}} \tag{8-3}$$

The additional manual valve allows control over the extent of flow rate reduction when the bypass is opened and thus the amplitude of pulsed flow in terms of flow rate (eq. (8-4)), flow velocity (eq. (8-5)) and Δp_{TM} (eq. (8-6)).

$$\Delta\dot{V} = \dot{V}_{max} - \dot{V}_{min} \tag{8-4}$$

$$\Delta v = v_{max} - v_{min} \tag{8-5}$$

$$\Delta p_{TM,\,cycle} = \Delta p_{TM,\,max} - \Delta p_{TM,\,min} \quad (8\text{-}6)$$

where $\Delta\dot{V}$ is the amplitude of flow rate, Δv is the amplitude of flow velocity and $\Delta p_{TM,\,cycle}$ is the amplitude of Δp_{TM}. It is to be noted that the flow velocity was calculated for a theoretical channel height without a spacer and a channel width of the SWM's spiral length. Hence, calculating *v* for spacer-filled channels can only provide a rough estimation, with local values highly depending on the position relative to the spacer grid.

All pulsed flow experiments were conducted at 50 °C, resembling a typical industrial filtration temperature (Schiffer and Kulozik 2020). The membrane was an MF SWM (GE JX6338C50) with a nominal pore size of 0.3 µm, the material polysulfone, a spacer height of 1.27 mm (50 mils), an active membrane area of 15.6 m^2, a diameter of 6.3 inches (16 cm) and a length of 38 inches (96 cm). Pasteurised skim milk (74 °C, 28 s) from a local dairy (Molkerei Weihenstephan, Freising, Germany) was used for deposit formation in all steady and pulsed flow filtration and cleaning experiments. Apart from filtration, deionised (DI) water was used in all other steps, either pure for rinsing or combined with chemicals for cleaning. As high frequencies (Kürzl et al. 2022a; Gillham et al. 2000; Blel et al. 2009a; Blel et al. 2009b; Weidemann et al. 2014; Yang et al. 2019) and amplitudes (Kürzl et al. 2022a; Gillham et al. 2000; Blel et al. 2009a; Blel et al. 2009b; Weidemann et al. 2014; Augustin et al. 2010) were found to be beneficial for pulsed flow efficiency, the respective maximum values that were possible with the current setup were used in the pulsed flow filtration and cleaning experiments. Regarding Δp_{TM}, the average values were chosen to resemble typical process conditions. $\Delta p_{TM,\,avg}$ during cleaning resembles the lowest possible value without reaching negative values for $\Delta p_{TM\,min}$ and still enabling the identical flow velocity amplitude as during filtration (details see below).

Filtration experiments

Before filtration, the membrane was conditioned with Ultrasil 69 (0.4% *v*/*v*, Ecolab Deutschland, Monheim am Rhein, Germany) at 50 °C for 20 min. After an intermediate rinsing step to avoid chemical residues, milk was heated to the process temperature by the heat exchanger loop, and filtration was initiated. Pulsed flow filtration was conducted with f = 0.5 Hz, the highest technically possible $\Delta\dot{V}$ = 10 $m^3\ h^{-1}$, due to pump capacity limitations ($\dot{V}_{max}$ = 14 $m^3\,h^{-1}$ with $\Delta p_{L,\,max}$ = 0.83 bar m^{-1} and v_{max} = 0.37 m s^{-1}, $\dot{V}_{min}$ = 4 $m^3\ h^{-1}$ with $\Delta p_{L,\,min}$ = 0.14 bar m^{-1} and v_{min} = 0.11 m s^{-1}, $\dot{V}_{avg}$ = 9 $m^3\ h^{-1}$ with $\Delta p_{L,\,avg}$ = 0.35 bar m^{-1} and v_{avg} = 0.24 m s^{-1}) and $\Delta p_{TM,\,cycle}$ = 1.50 bar ($\Delta p_{TM\,max}$ = 1.75 bar, $\Delta p_{TM,\,min}$ = 0.25 bar, $\Delta p_{TM,\,avg}$ = 1.00 bar). The average $\Delta p_{TM,\,avg}$ and $\dot{V}_{avg}$ were used for conducting comparative steady flow filtration runs. During the filtration duration of 60 min, samples were taken from permeate and retentate sample ports after 5, 10, 15, 30, 45 and 60 min. Protein permeation for a specific milk

protein P_i was calculated by equation (8-7) by its respective concentrations in the permeate $c_{i,\,p}$ and retentate $c_{i,\,r}$. Similarly, $c_{i,\,p}$ and Flux *J* were used to calculate an individual protein's permeating mass flow $\dot{m}_i$ into the filtrate (eq. (8-8)).

$$P_i = \frac{c_{i,\,p}}{c_{i,\,r}} \tag{8-7}$$

$$\dot{m}_i = J \cdot c_{i,\,p} \tag{8-8}$$

After each filtration experiment, the membrane was rinsed and then cleaned with combined caustic (0.8% *v*/*v*, Ecolab Germany) and enzymatic (0.3% *v*/*v* Ultrasil 67, Ecolab GmbH, Monheim am Rhein, Germany) cleaning agents for 40 min, followed by another rinsing step and an acidic cleaning step (0.4% *v*/*v* Ultrasil 75, Ecolab GmbH, Monheim am Rhein, Germany) for 20 min at 50 °C. To verify sufficient cleaning success and thus ensure long-term membrane functionality, the membrane's pure water flux was measured before each filtration run.

Cleaning experiments

Before filtration, the membrane was conditioned, and the initial water flux J_0 was measured. Filtration was then conducted for 40 min at 50 °C, $\dot{V}$ = 5 m³ h⁻¹ and Δp_{TM} = 1.7 bar with skim milk. Afterwards, the milk was drained, and the membrane system was carefully rinsed to remove bulk milk and loosely bound material. The following cleaning experiments were conducted with NaOH at pH 11.3 (c_{NaOH} = 0.03%) for 20 min at 50 °C in circulation under either steady or pulsed flow mode. Due to the NaOH solution volume being high compared to the membrane area to be cleaned (yielding a specific cleaning volume of 6.4 L per square meter of active membrane area), an excess of cleaning agent compared to the amount of protein to be removed was present. Thus, the experiments should not be affected by the excessive consumption of cleaning agents causing distorted protein removal or changes in the pH. Pulsed flow cleaning was conducted with f = 0.5 Hz, the maximum technically viable $\Delta\dot{V}$ = 10 m³ h⁻¹ ($\dot{V}_{max}$ = 14 m³ h⁻¹ with $\Delta p_{L,\,max}$ = 0.83 bar m⁻¹ and v_{max} = 0.37 m s⁻¹, $\dot{V}_{min}$ = 4 m³ h⁻¹ with $\Delta p_{L,\,min}$ = 0.14 bar m⁻¹ and v_{min} = 0.11 m s⁻¹, $\dot{V}_{avg}$ = 9 m³ h⁻¹ with $\Delta p_{L,\,avg}$ = 0.35 bar m⁻¹ and v_{avg} = 0.24 m s⁻¹) and $\Delta p_{TM,\,cycle}$ = 1.00 bar ($\Delta p_{TM,\,max}$ = 1.15 bar, $\Delta p_{TM,\,min}$ = 0.15 bar, $\Delta p_{TM,\,avg}$ = 0.60 bar). The average $\Delta p_{TM,\,avg}$ and $\dot{V}_{avg}$ were used for comparative steady flow cleaning runs. For evaluating chemical cleaning success in terms of protein removal, samples were taken from the feed vessel after 20 min cleaning. Subsequently, the cleaning solution was drained, the system rinsed, and the water flux after cleaning J_1 was measured to evaluate the hydraulic cleanliness in terms of flux recovery ratio (FRR) (see eq. ((8-9)) reached by the applied cleaning protocol. If the cleaning evaluation indicated incomplete cleaning (FRR <

90%), an additional cleaning procedure with industrial cleaning agents, analogous to filtration experiments, was conducted to evaluate long-term membrane functionality.

$$FRR = \frac{J_1}{J_0} \quad (8\text{-}9)$$

It is to be noted that while identical pulsation frequencies as in previous FSM studies could be achieved with this approach and setup, the maximum applicable amplitudes and flow velocities were significantly lower in the current study due to limitations in pump capacity.

8.2.3 Membrane modification and experimental design to investigate increased axial pressure drops

To investigate increased axial pressure drops, the plant's double-screw-type displacement pump (see Figure 8-1) was replaced by a larger centrifugal pump capable of creating a feed pressure of 4.8 bar and a maximum feed flow rate of 45 $m^3\ h^{-1}$. In this scenario, experiments were conducted with used membranes put out of operation at an industrial plant to be free for establishing potentially destructive conditions. The membranes were provided by a local dairy, where they had been used for the filtration of dairy fluids for several months. The membranes (Koch Industries, Wichita, KS, USA) had a separation range of 10 kDa, a 31 mil (0.79 mm) diamond-shaped spacer and an active membrane area of 19.1 m^2, a diameter of 6.3 inch (16 cm) and a length of 38 inch (96 cm). It is to be noted that the used membranes showed no apparent membrane failures despite a few areas with dislocated spacers between non-displaced membrane sheets.

To assess the effect of feed-side glue connections on membrane stability, modified membranes were obtained by inserting a two-component adhesive (Araldite 2014-1, Huntsman Corporation, Salt Lake City, UT, USA) into the dry spacer channels with a syringe and thus glueing together the membrane sheets. This procedure resulted in semi-circular glue connections (d = 2 cm) placed in a radial direction along the membrane diameter (Figure 8-2). After hardening for several days, the modified membranes were comparatively assessed with unmodified membranes for their axial pressure drop stability.

Figure 8-2. The membrane module was modified by adding glue dots (see black areas) radially along the membrane diameter.

For axial stability experiments, the membranes were initially rinsed with deionised (DI) water with open permeate valves to allow the permeate pockets to be filled. To simulate the filtration of fouling-intensive feeds such as skim milk, where permeate production is substantially low and thus the influence of flux on the length dependency of crossflow velocity is negligibly small, axial stability experiments with water were conducted with the permeate valve closed (Δp_{TM} = 0.0 bar). The membrane was then subjected to an initial axial pressure drop of 0.3 bar m^{-1} for 5 min. After assessing the axial displacement relative to the permeate collection tube at four equidistant points (radial distances 3.3 cm, 4.5 cm, 5.8 cm, 7.0 cm) in the radial direction of the SWM with a Vernier calliper, this procedure was repeated, increasing the axial pressure drop by 0.2 bar m^{-1} up to 1.5 bar m^{-1}. This approach allowed the evaluation of the displacement depending both on the applied axial pressure drop and the radial distance of displaced membrane sheets to the permeate collection tube.

Preliminary experiments with unmodified membranes and an ATD showed no significant displacement at either radial position for pressure drops < 4.0 bar m^{-1} (see Figure 8-3), contrary to industrial reports and restrictions stated by membrane manufacturers. This contradicting observation is presumably due to displacements with ATD only caused by long-term stress, as bond joints and polymers are known to migrate under constant stress (Althof 1984). As these long-term scenarios are hard to reproduce at lab scale, the following

experiments were conducted without an ATD to exclusively assess the axial stability of the membrane module without the support of an ATD.

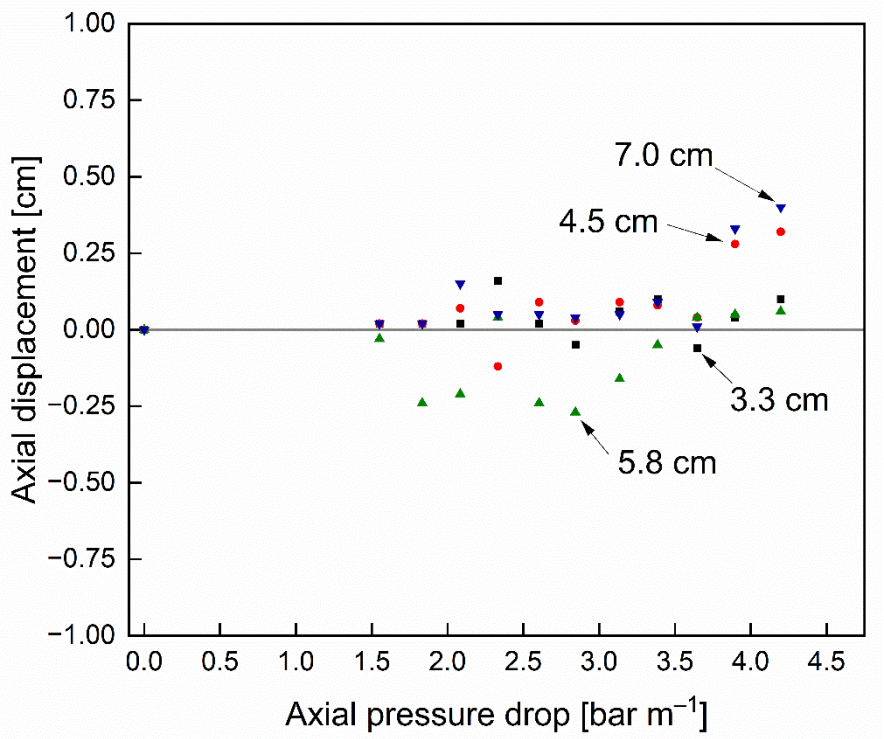

Figure 8-3. Influence of the axial pressure drop and radial position on the axial displacement of membrane sheets with an ATD. The grey reference line indicates no axial displacement.

8.2.4 Chemical and statistical analyses

The contents of caseins and whey proteins in filtration and cleaning samples were analysed by reversed-phase high-performance liquid chromatography (RP-HPLC) as described by Dumpler et al. (2017). Agilent ChemStation software (Rev. B.04.03) was used to analyse RP-HPLC chromatograms.

Data were plotted, fitted and statistically evaluated using OriginPro 2021 (OriginLab Corporation, Northampton, MA, USA). Statistical significance between data sets was assessed using a one-way analysis of variance (ANOVA) at the 5% level ($p < 0.05$). Depicted error bars represent the standard deviation of replicates, whereas all cleaning and filtration experiments were conducted at least in triplicates. Due to membrane failure/rupture accompanying axial displacements, stability experiments could only be conducted as single runs.

8.3 Results and discussion

8.3.1 Optimisation of SWM's process efficiency via the utilisation of pulsed flow

8.3.1.1 Validation of plant modifications

As larger pumps are normally incapable of rapidly producing quickly transitioning conditions between high and low flow rates, pulsed flow was created by installing a bypass, temporarily reducing the pressure and flow rates reaching the membrane module. An overview of the resulting pulsed flow characteristics is given in Figure 8-4.

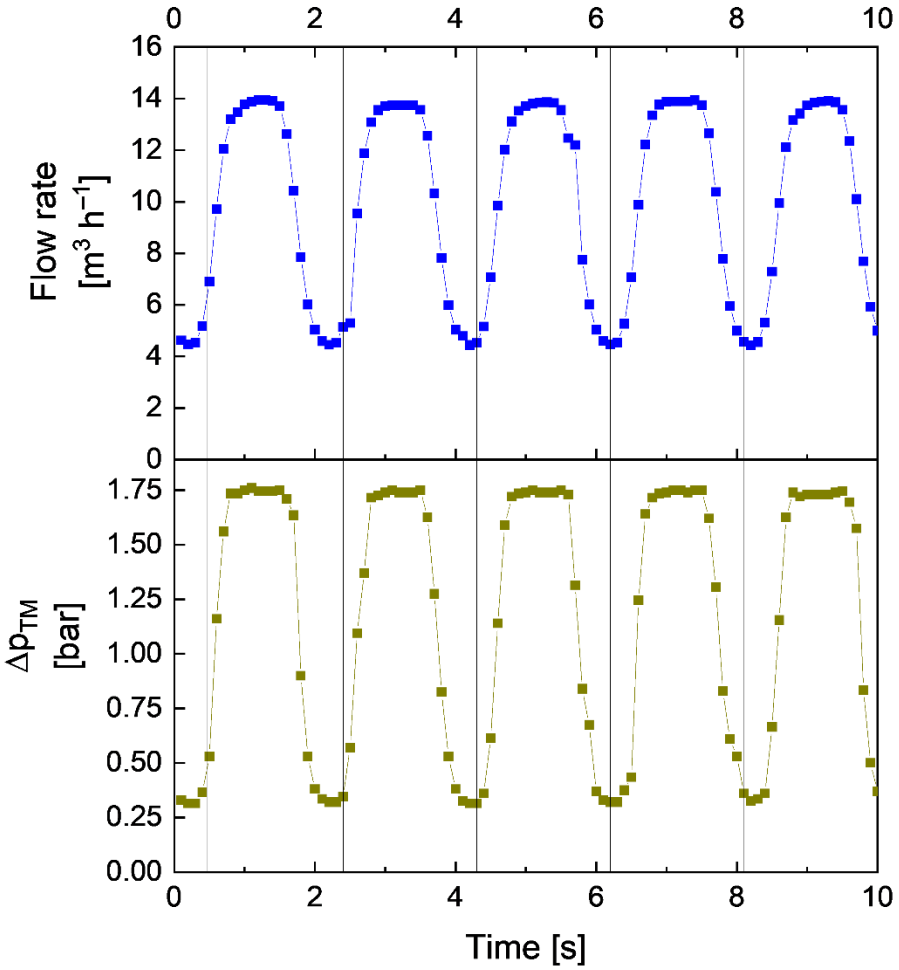

Figure 8-4. Time-resolved progression of feed flow rate and Δp_{TM} over several flow cycles during pulsed filtration. Pulsed flow conditions: $\Delta\dot{V}$ = 10 $m^3\,h^{-1}$ ($\dot{V}_{max}$ = 14 $m^3\,h^{-1}$, $\dot{V}_{min}$ = 4 $m^3\,h^{-1}$, $\dot{V}_{avg}$ = 9 $m^3\,h^{-1}$) and $\Delta p_{TM,\,cycle}$ = 1.50 bar ($\Delta p_{TM,\,max}$ = 1.75 bar, $\Delta p_{TM,\,min}$ = 0.25 bar, $\Delta p_{TM,\,avg}$ = 1.00 bar).

Figure 8-4 depicts the time-resolved progression of flow rate $\dot{V}$ and Δp_{TM}. With this approach to pulsation creation and the specific setup used in this study, a maximum frequency of 0.5 Hz with an amplitude >10 $m^3\,h^{-1}$ could be realised. Hence, compared to previous lab-scale studies using steep transitioning ramps of inductively controlled pumps to generate pulsed flow (Kürzl and Kulozik 2023b, 2023c; Kürzl et al. 2022a; Kürzl and Kulozik 2023a), the same maximum frequencies can be achieved at tenfold higher flow rates. Also, the profiles of flow rate and Δp_{TM} progression correspond to those of lab-scale experiments with rapid ramps

creating pulsed flow (Kürzl et al. 2022a). It is to be noted that while other valves with shorter opening and closing times might enable higher pulsation frequencies, they might also induce intensified pressure surges on the plant equipment, which could cause enhanced wear. However, the current setup with f = 0.5 Hz did not cause any damage or wear on sensitive plant components, such as sensors or valves, within a pulsed flow operation of four months. Contrary to other approaches of creating pulsed flow, such as via bellows or piston units (Gillham et al. 2000; Bode et al. 2007), it is also of advantage that the occurrence of negative Δp_{TM} values can be avoided. This is particularly important for SWMs, where negative Δp_{TM} must not exceed 0.3 bar, according to membrane manufacturers´ specifications, as this would stress the bond joints of membrane pockets and could result in membrane failure. Overall, the bypass as a technical option to produce pulsed flow conditions resembles a low-effort and cost-efficient approach to creating similar pulsed flow profiles on a pilot scale with industrially sized membranes as in lab-scale studies. Nonetheless, it is to be noted that with this novel approach to pulsation creation, the energy efficiency is decreased compared to that of the previous system using rapid pump capacity ramps (Kürzl and Kulozik 2023c; Kürzl et al. 2022a). In this case, pumps will not alternately increase and decrease in pump capacity, but are instead continuously run at maximum capacity, despite a large share of flow temporarily not reaching the membrane during the low-flow pulsation phases.

8.3.1.2 Influence of pulsed flow on filtration performance in industrial-scale SWM

The mass flow resulting from flux and permeation was analysed to assess the effect of pulsed flow on the time-resolved filtration performance in industrial SWMs during 60 min filtration. The strongest impacts of pulsed flow were reported for high frequencies (Kürzl et al. 2022a; Gillham et al. 2000; Blel et al. 2009a; Blel et al. 2009b; Weidemann et al. 2014; Yang et al. 2019) and amplitudes (Kürzl et al. 2022a; Gillham et al. 2000; Blel et al. 2009a; Blel et al. 2009b; Weidemann et al. 2014; Augustin et al. 2010). Accordingly, pulsed flow experiments were run with the best combination of frequency and amplitude applicable to the current setup. The mass flow of whey protein, i.e., the targeted permeating component (Figure 8-5), for pulsed flow was permanently increased over that of steady flow throughout filtration. While the whey protein mass flow with steady flow decreased from 38.9 g m^{-2} h^{-1} by 39% to 23.8 g m^{-2} h^{-1}, pulsed flow decreased from 43.7 g m^{-2} h^{-1} by 31% to 30.0 g m^{-2} h^{-1}. Hence, the initial mass flow (+12%), steady-state mass flow (+26%) and its decrease during filtration (−21%) were all improved with pulsed flow. These results demonstrate an improved initial and continuous deposit control with pulsed flow resulting in a 26% increased whey protein mass flow compared to steady flow at steady-state.

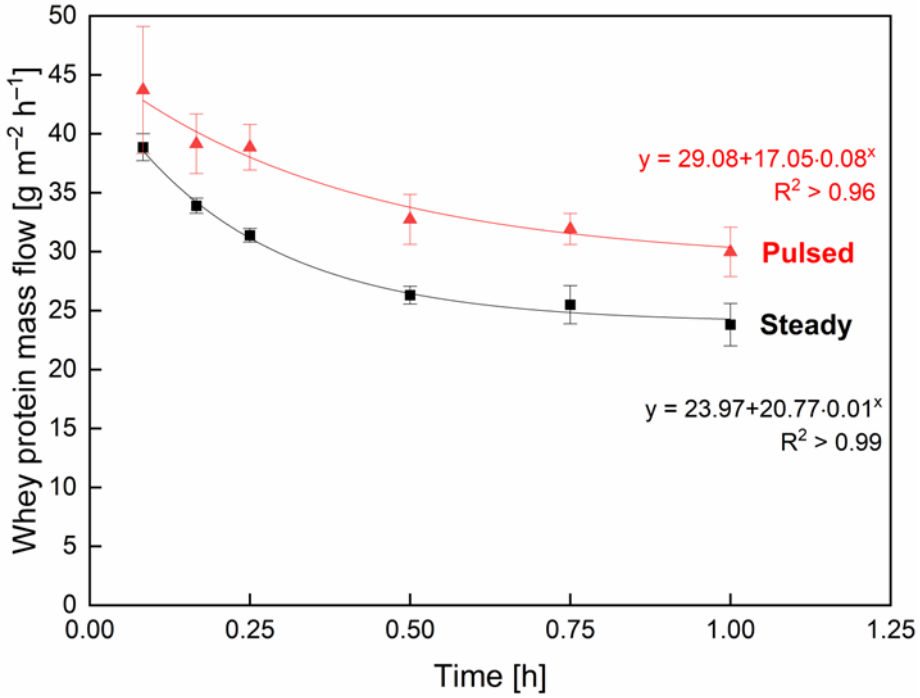

Figure 8-5. Influence of steady (black squares) and pulsed (red triangles) flow on whey protein mass flow during skim milk MF. Filtration conditions $\Delta\dot{\mathbf{V}}$ = 10 m^3 h^{-1} ($\dot{\mathbf{V}}_{max}$ = 14 m^3 h^{-1}, $\dot{\mathbf{V}}_{min}$ = 4 m^3 h^{-1}, $\dot{\mathbf{V}}_{avg}$ = 9 m^3 h^{-1}) and $\Delta p_{TM,\,cycle}$ = 1.50 bar ($\Delta p_{TM,\,max}$ = 1.75 bar, $\Delta p_{TM,\,min}$ = 0.25 bar, $\Delta p_{TM,\,avg}$ = 1.00 bar).

The observed improvements in filtration performance with pulsed flow are generally in accordance with our previous lab-scale study (Kürzl and Kulozik 2023c). The increased mass flow, induced by enhanced flux and permeation, is the result of improved access to flow shadows causing improved deposit control with less fouling (Kürzl and Kulozik 2023c). The small differences in performance improvement with pulsed flow between lab-scale and industrial-scale membranes, particularly regarding whey protein permeation, could arise from the fact that the highest applied axial pressure drop, and thus the flow velocity, was much lower ($\Delta p_{L,\,max}$ = 0.83 bar m^{-1}) compared to that in the previous study ($\Delta p_{L,\,max}$ = 2.55 bar m^{-1}) with FSM. The same applies to the amplitude (Δv = 0.26 m s^{-1} versus Δv = 0.60 m s^{-1}) (Kürzl and Kulozik 2023c), as explained above. Frequency and amplitude have both been previously identified to be critical aspects for pulsed flow efficiency (Kürzl et al. 2022a; Gillham et al. 2000; Blel et al. 2009a; Blel et al. 2009b; Augustin et al. 2010).

8.3.1.3 Influence of pulsed flow on cleaning efficiency in industrial-scale SWM

To also examine the effect of pulsed flow on cleaning efficiency with the modified filtration plant for industrial-scale SWMs, cleaning experiments with NaOH at pH 11.3 (c_{NaOH} = 0.03%) were conducted after steady flow filtration. Again, pulsed flow experiments were conducted at the maximum frequency and amplitude settings possible with the current setup. The results of comparing steady and pulsed flow cleaning experiments were evaluated using FRR (Figure 8-6, left) and total protein removal (Figure 8-6, right) as assessment criteria.

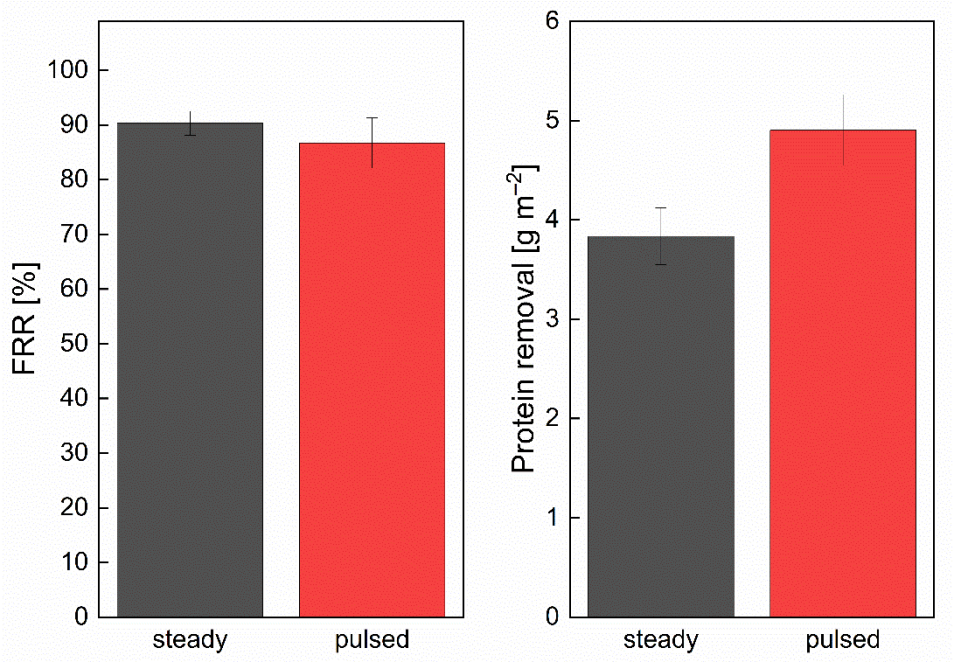

Figure 8-6. Influence of steady (black) and pulsed (red) flow on FRR (left) and protein removal (right) during membrane cleaning after skim milk MF. Cleaning conditions: $\Delta\dot{\mathbf{V}}$ = 10 m^3 h^{-1} ($\dot{\mathbf{V}}_{max}$ = 14 m^3 h^{-1}, $\dot{\mathbf{V}}_{min}$ = 4 m^3 h^{-1}, $\dot{\mathbf{V}}_{avg}$ = 9 m^3 h^{-1}) and $\Delta p_{TM,\,cycle}$ = 1.00 bar ($\Delta p_{TM,\,max}$ = 1.15 bar, $\Delta p_{TM\,min}$ = 0.15 bar, $\Delta p_{TM,\,avg}$ = 0.60 bar).

Regarding FRR, there were no significant differences between flow modes, with 90 ± 2% for steady and 87 ± 5% for pulsed flow. Nonetheless, the protein removal achieved with pulsed flow (4.90 ± 0.36 g m^{-2}) was significantly increased by 28% over that achieved with steady flow cleaning (3.83 ± 0.29 g m^{-2}). With pulsed flow improving access to flow shadows (Kürzl and Kulozik 2023b, 2023c; Kürzl et al. 2022a; Augustin et al. 2010; Föste et al. 2013; Gu et al. 2017; Schwinge et al. 2003; Schwinge et al. 2004; Koutsou et al. 2009) and thus improving removal particularly in these areas, the reason for the absence of improvements in FRR could be due to the steady water flux measurements being prone to the same flow shadows behind spacer filaments as steady flow cleaning. As shown in a previous study for FSMs, fouling residues in areas subject to flow shadows could only partially be removed by steady flow cleaning, whereas no distinct residues in those areas could be observed for pulsed flow cleaning (Kürzl and Kulozik 2023b). As these observations were only reflected by an increased protein removal but not an increase in FRR, it can be assumed that the additional protein removal near spacer filaments could not be detected by steady flux measurements. This is presumably due to these areas hardly contributing to flux under steady flow, regardless of fouling being present or absent, and translates to an overestimation of hydraulic cleanliness for steady flow and an underestimation thereof for pulsed flow cleaning. This explanation also highlights FRR being insufficient as a singular tool for cleaning evaluation, particularly for membranes subject to flow shadows, such as FSMs or SWMs. Overall, similar to the filtration experiments (chapter 8.3.1.2), the positive results from lab-scale trials could be confirmed, but the benefits were less pronounced, due to reasons explained above.

Another factor when comparing FSM and SWM results is the membrane length, which could also affect the results of pulsation efficiency. Due to the length dependency of Δp_L, Δp_{TM} and fouling, the membrane length was previously identified in HFM to affect the cleaning efficiency for flow modes inducing flow reversal (Kürzl and Kulozik 2023a) but not for conventional steady or pulsed flow (Kürzl and Kulozik 2023b). Nonetheless, due to significant geometrical differences between HFMs and SWMs, a declining efficiency of pulsation effects with increasing membrane length in SWMs, e.g., due to propagating flow and pressure waves being partially absorbed by the friction with spacer filaments, cannot be excluded. Nonetheless, the lower flow velocity and amplitude, limited by the maximum pressure drop applicable and thus the stability of SWMs, remain the most probable causes for the observed differences between FSMs and SWMs. Hence, the following sections will investigate an approach to improve module stability in SWMs under operating conditions currently out of reach.

8.3.2 Optimisation of SWM's mechanical stability by feed-side glue connections

First, the effect of glue connections on the filtration behaviour was to be assessed since the glued areas reduce the inlet cross-section of the module. Therefore, the relationship between axial pressure drop and volume flow rates was compared for a glued and an unmodified membrane (Figure 8-7).

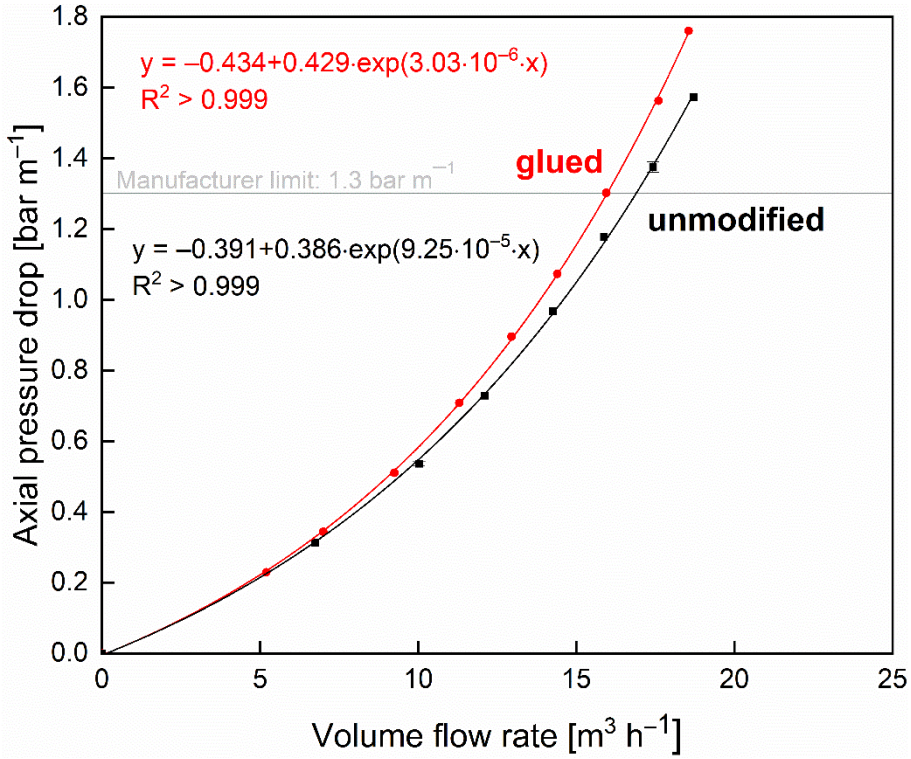

Figure 8-7. Axial pressure drop at different feed flow rates of the glued (red) and unmodified (black) membrane without an ATD.

The unmodified membrane reaches the maximum axial pressure drop of 1.3 bar m^{-1} at 16.9 m^3 h^{-1}, and the glued membrane already at 15.9 m^3 h^{-1}. This means that for an identical

maximum pressure drop of 1.30 bar m^{-1}, the modified membrane could only be operated at a six percent lower volume flow rate than the unmodified membrane. Hence, potential improvements in module stability need to be more pronounced than the enhanced axial pressure drop induced by the glued sections. Otherwise, if glued connections could not provide sufficient stability improvements, the enhanced axial pressure drop would further limit the highest applicable flow velocities. Also, it is to be noted that the glued connections were added to the SWM after its manufacture. Therefore, the areas covered with glue were larger and less well-shaped than they could be when created during the SWM manufacturing process.

Furthermore, the effect of additional glue connections on the short-term stability of the membranes without an ATD was assessed in terms of the axial displacement at different radial positions caused by different axial pressure drops (Figure 8-8).

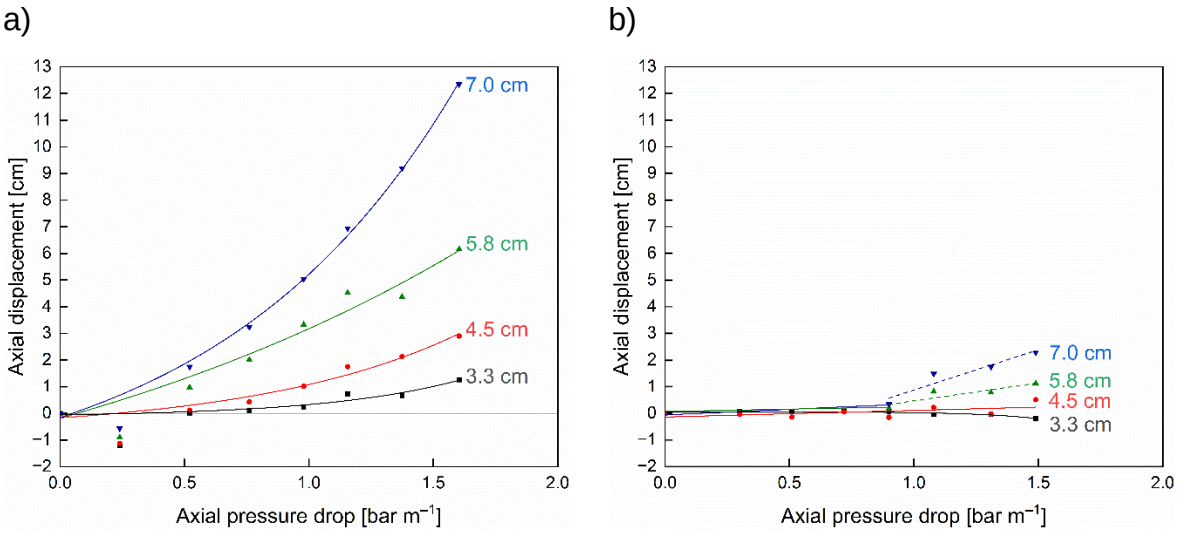

Figure 8-8. Axial displacement of the unmodified (a) and glued (b) membrane caused by axial pressure drops at different radial distances to the module centre without an ATD. The grey reference lines indicate no axial displacement. Lines are a guide for the eye.

Due to the absence of an ATD, the critical axial pressure drop, where axial displacement starts to occur, was reached at 0.5 bar m^{-1} for the unmodified membrane (Figure 8-8a). Beyond this point, the axial displacement increased exponentially as a function of axial pressure drop. Also, the displacement was most pronounced for the membrane parts in the radially outer positions, i.e., farthest away from the central collection tube (7.0 cm), as the pockets are only fixed to the central collection tube and the outer part is only held in place by the friction induced by the module wrapping. Hence, the outer part cannot take up high forces in the axial direction and thus is pushed towards the rear part of the module 879% further than the inner part (12.34 cm displacement at 7.0 cm radial distance versus 1.26 cm displacement at 3.3 cm radial distance) where most of the axial forces can be taken up by the connection to the central collection tube. Even at pressure drops of 1.5 bar m^{-1}, above the manufacturer limit of 1.3 bar m^{-1}, only a slight axial displacement <1.0 cm of the inner membrane envelope could be observed. Overall, these results emphasise both the instability,

particularly of the outer SWM parts, against telescoping as well as the necessity and potential advantages of additional stabilisers, such as glued connections, for module stability.

The glued membrane (Figure 8-8b) showed vastly different results with no displacement up to an axial pressure drop of 1.0 bar m^{-1}. This translates to an overall 100% stability increase compared to the unmodified membrane with significant displacements already observed at 0.5 bar m^{-1}. Considering the displacements at different radial positions, they are all significantly reduced. For the inner part, i.e., 3.3 cm and 4.5 cm, no significant displacement can be observed for axial pressure drops up to 1.5 bar m^{-1}. At 4.5 cm radial distance and 1.5 bar m^{-1}, the displacement in the glued membrane was 82% reduced compared to that of the unmodified membrane (0.5 cm versus 2.9 cm). In the outer part (7.0 cm radial distance) at 1.5 bar m^{-1}, where displacement was most pronounced for both membranes, the displacement could be reduced by 81% (2.3 cm versus 12.3 cm). An overview of the achieved reductions in axial displacements with the modified membrane compared to the unmodified membrane shows an exponential increase for increasing pressure drops (see Figure 8-9a) and radial distances to the module centre (see Figure 8-9b). Hence, improvements of the modified membrane are most pronounced for outer membrane parts and at increased axial pressure drops or flow velocities.

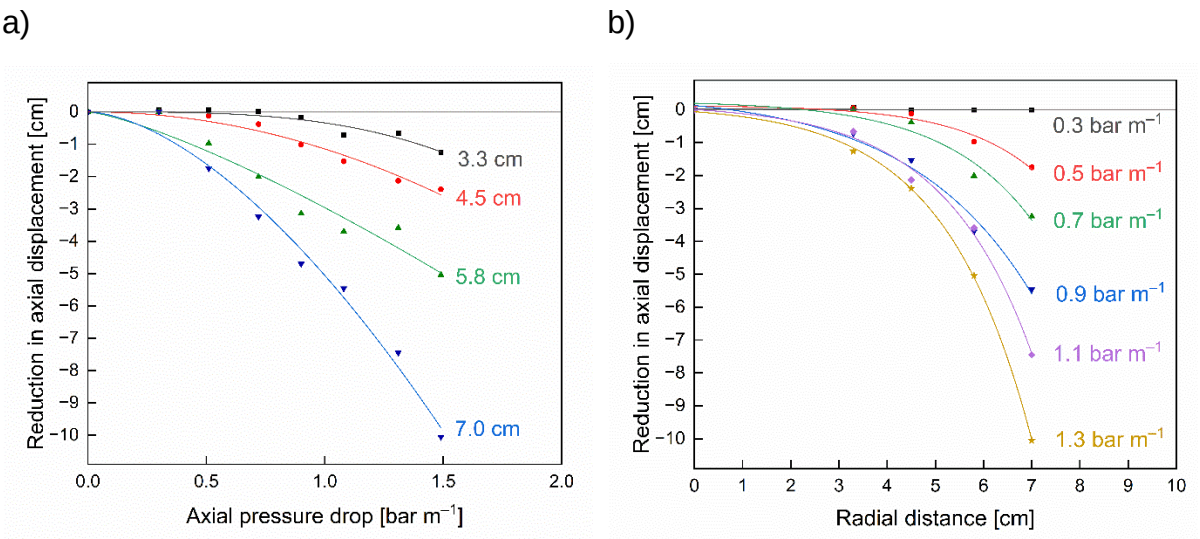

Figure 8-9. Reductions in axial displacement achieved by the glued membrane compared to the unmodified membrane at different feed flow rates (a), i.e., axial pressure drops and different radial distances to the module centre (b) without an ATD. The values were obtained by subtracting the displacement of the unmodified membrane from the glued membrane (see Figure 8). Lines are a guide for the eye.

Besides the observed stability increases, axial displacement still occurred due to the increasingly stressed bond joints eventually rupturing at their weakest point. As a consequence, the supportive effect of this bond joint vanished, and axial displacement occurred. Nevertheless, due to the supportive effect of the remaining membrane sheet connections, the resulting axial displacement could be significantly reduced compared to an

envelope without glued bond joints. The related failure mechanism was a rupture of the glue connections. An additional failure mechanism, e.g., the axial displacement of the feed spacer, as observed in the used membranes, could not be observed for the glued membranes, which also underlines their enhanced stability.

It is to be noted that due to glue connections being added after SWM manufacturing and for used membranes, the adhesion between the selective and support layer, as well as the glue connections and their geometry, might not be ideal. Hence, it can be assumed that if prepared under ideal conditions, the stability improvements gained by glue connections would be more pronounced.

8.4 Conclusion

This study presented two approaches to successfully reduce the limitations of SWMs regarding cleanability and mechanical stability. The first approach, focusing on processing, transferred and utilised the concept of pulsed flow to industrial-scale membranes by adding a controlled bypass. This led to similar flow characteristics but less distinct process improvements during filtration and cleaning compared to previous lab-scale studies using FSMs (Kürzl and Kulozik 2023b, 2023c). While the underlying causes for the observed differences between lab-scale FSMs and industrial-scale SWMs could not entirely be determined, they are presumably due to the reduced flow velocity and pulsation amplitude applicable in SWMs. Nonetheless, significant improvements for both filtration (mass flow +26%) and cleaning performance (protein removal +28%) could be confirmed for pulsed flow. It is to be noted that while this approach was associated with low effort and investment cost on the pilot scale, a transfer to industrial-scale systems, often encompassing several membrane housings, i.e., filtration units, would require an efficient implementation of the additional controlled bypass into each filtration unit. This could be performed by, e.g., combining two filtration units into one pulsation unit where the flow control is managed by a controlled three-way diverting valve instead of a controlled bypass. This way, one filtration unit would be in the high flow rate phase while the other filtration unit would be in the low flow rate phase. One advantage of this approach would be that no pump energy would be left unused as bypass flow but instead split between two filtration units pulsing inversely. Despite the advantages of pulsed flow, the necessity of adding the respective type of pulsation creation to every filtration unit is given for each type of pulsation creation and should thus be considered upon implementation.

The second approach, focusing on membrane construction, applied glue connections between membrane sheets in the radial direction across the membrane width of a used SWM. As a result, the axial pressure drop at a given flow rate was slightly increased. However, the

stability against axial displacement without an ATD was increased by ≥100% across the whole membrane diameter. Consequently, the enhanced axial pressure drop at the inlet partly compensated the glued connections' positive effect. Nevertheless, the positive effect of enhanced stability predominates over the disadvantage of enhanced axial pressure drop. Thus, higher flow rates and increased amplitudes under pulsed flow are expected to be applicable to the glue-connected SWM. Due to glue connections being added under non-ideal conditions, i.e., after manufacturing and for used membranes, it can be assumed that stability improvements would be more pronounced under ideal glueing conditions. In the case of manufacturing the interconnections between the membrane pockets simultaneously with the SWM itself, the bonds could be formed slimmer but longer to leave more free inlet cross-sections. Additionally, the effect of those glue connections might be enhanced by optimising their location, orientation and extent within the membrane module. However, since the effects on module stability could only be assessed with short-term experiments under extreme conditions, i.e., without an ATD, long-term stability tests should be conducted to confirm the enhanced stability for conventional setups with an ATD.

Finally, the combined maximum achievable advantages of using a stabilised SWM with pulsed flow allowing for increased pulsation amplitudes at increased flow rates should be assessed to facilitate weighing the required implementation effort versus the gained advantage, particularly from an economic and ecological point of view.

Author Contributions: Conceptualization, C.K., M.H., R.S. and S.S.; data curation, C.K., M.H. and P.O.; formal analysis, C.K. and M.H.; funding acquisition, U.K.; investigation, C.K., M.H. and P.O.; methodology, C.K. and M.H.; project administration, C.K.; resources, U.K.; software, C.K. and M.H.; supervision, U.K.; validation, C.K. and M.H.; visualization, C.K. and M.H.; writing—original draft, C.K. and M.H.; writing—review and editing, C.K., M.H. and U.K. All authors have read and agreed to the published version of the manuscript.

Funding: This IGF Project of the FEI was supported via AiF to promote the Industrial Collective Research (IGF) of the German Ministry of Economic Affairs and Energy (BMWi), based on a resolution of the German Parliament. Project: AiF 57 EWN.

Institutional Review Board Statement: Not applicable

Data Availability Statement: The datasets generated during and/or analysed during the current study are available from the corresponding author on reasonable request.

Acknowledgments: We gratefully thank Heidi Wohlschläger for her assistance with the RP-HPLC analysis of samples. Furthermore, we want to thank Christian Ederer, Erich Schneider and Franz Fraunhofer in our workshop for technical support. We also want to thank

Diana Kellhammer and Franz Kuhnert for their experimental support. Finally, we want to thank Nikolaus Adams and Steffen Schmidt from the Chair of Aerodnamics and Fluid Mechanics for organisationally supporting parts of this work.

Conflicts of Interest: The authors declare no conflict of interest. The authors declare that they have no known competing financial interests or personal relationships that could have influenced the work reported in this paper. The funders had no role in the design of the study; in the collection, analyses, or interpretation of data; in the writing of the manuscript, or in the decision to publish the results.

9 Overall discussion and main findings

Despite pressure-driven filtration processes being a major operation unit in several applications across various industries, its central issues of fouling and the removal thereof have not been satisfactorily solved yet. Fouling leads to continuous reductions in filtration performance, and biofouling at typical industrial filtration temperatures of 50-55 °C can limit filtration time to 7 h (Schiffer and Kulozik 2020). The subsequent cleaning of fouled membranes consisting of several chemical cleaning and rinsing steps is a chemical, energy and time-intensive process requiring up to 4 h. With membrane cleaning consuming a large portion of the filtration process' operating costs (Regula et al. 2014), total environmental impact (Gésan-Guiziou et al. 2019) and potential production time, novel approaches are required to improve filtration and cleaning efficiency. One of the most promising approaches is creating an unsteady flow, i.e. pulsed or alternating flow. While some studies reported positive results on the pulsed/alternating flow filtration of model feed solutions and the cleaning of steel geometries with varying mechanisms assumed and different types of pulsation-creation used, no general relations to membrane cleaning with complex feed solutions such as skim milk can be deduced. This is due to fundamental differences in the feed characteristics, the resulting fouling characteristics, and the flow characteristics due to the additional flow perpendicular towards and through the wall/membrane in membranes. As a result of the increased complexity of membrane systems, additional factors, such as Δp_{TM} (Schopf and Kulozik 2021) and length-dependency of fouling (Gésan et al. 1993; Piry et al. 2008; Hartinger et al. 2020c), that play crucial roles in conventional steady flow filtration and cleaning need to be investigated.

Hence, this thesis aimed to systematically investigate the effects of pulsed and alternating flow on membrane cleaning success following skim milk microfiltration and shed light on the underlying modes of action. This was done by first developing a novel method capable of separately quantifying traces of milk protein residues in cleaning solutions. Secondly, protein removal as a chemical and FRR as a hydraulic cleanliness criterion were used to assess the cleaning success of the different flow types. Thirdly, where applicable, SEM or Coomassie-colouring were used to investigate local deposit patterns during filtration and deposit residues after cleaning. Hereby, several factors potentially affecting process performance were varied. These included but were not limited to frequency, amplitude, membrane length, module geometry or cleaning agent concentration. The following chapters aim to summarise and discuss the main findings of the six presented peer-reviewed scientific publications (see chapters 3 – 8) and provide an overarching and meaningful context.

9.1 Modes of action for pulsed and alternating flow cleaning

9.1.1 Pulsed flow

Pulsed flow, fluctuating between maximum and minimum flow and pressure conditions with a defined frequency and amplitude, was attributed different modes of action by different studies. These included induced turbulence (Blel et al. 2009a; Blel et al. 2009b; Bode et al. 2007; Augustin et al. 2010), near-wall flow reversal (Blel et al. 2009a; Blel et al. 2009b; Bode et al. 2007; Augustin et al. 2010; Weidemann et al. 2014; Föste et al. 2013), enhanced mass transfer (Blel et al. 2009a; Blel et al. 2009b; Gillham et al. 2000), deposit fatigue due to pressure fluctuations (Gillham et al. 2000), and the annular effect (Richardson and Tyler 1929; Schlichting and Gersten 2006). Nonetheless, it is to be noted that some of these interpretations might be related to differences in the approach to pulsation-creation sometimes leading to negative pressures, backflush and flow reversal (Gillham et al. 2000; Bode et al. 2007). The novel results obtained in this thesis, with a pulsation-creation approach avoiding negative pressures and uncontrolled flow reversal, confirmed the mode of action involving a combination of pulsation-induced turbulence (see chapters 5, 7 and 8) and fluctuating relaxation and compaction of the deposit (see chapter 4), which altogether weaken forces stabilising the deposit layer material.

Regarding the latter, results shown in chapter 4 first indicated the relative changes in v and Δp_{TM} affecting pulsation efficiency in removing irreversible fouling during different cleaning phases phases in the presence of the cleaning agent NaOH. In detail, a fluid inertia-related delay of v compared to Δp_{TM} by 0.2 s was observed, translating to v_{max} being reached when Δp_{TM} already starts its decrease into the relaxation phase (see Figure 9-1). With a stronger delay of 0.6 s, flux reaches its peak in the relaxation phase near $\Delta p_{TM, min}$, which indicates deposit relaxation outweighing the decreasing v and τ_w, and appears to be due to the relaxing deposit becoming more accessible and thus increasingly removable by shear forces. Accordingly, this underlines the importance of high frequencies and amplitudes as frequency correlates with the fluctuation speed and, thus, relative phase delay, while amplitude correlates with the intensity of fluctuations. Inversely similar, flux reaches its minimum during the compaction phase as Δp_{TM} increases stronger than the delayed v, with deposit compaction outweighing the increasing v and τ_w. Besides frequency and amplitude Δv, this also indicates the importance of $\Delta p_{TM, cycle}$. With results reporting improved protein removal for the given flow characteristics after 20 min cleaning with numerous cycle changes between relaxation/compaction phases with low/high flow rates and reported influences of *f*, Δv and $\Delta p_{TM, cycle}$ (see chapter 9.2), the results indicate a complex interplay between flow and pressure conditions.

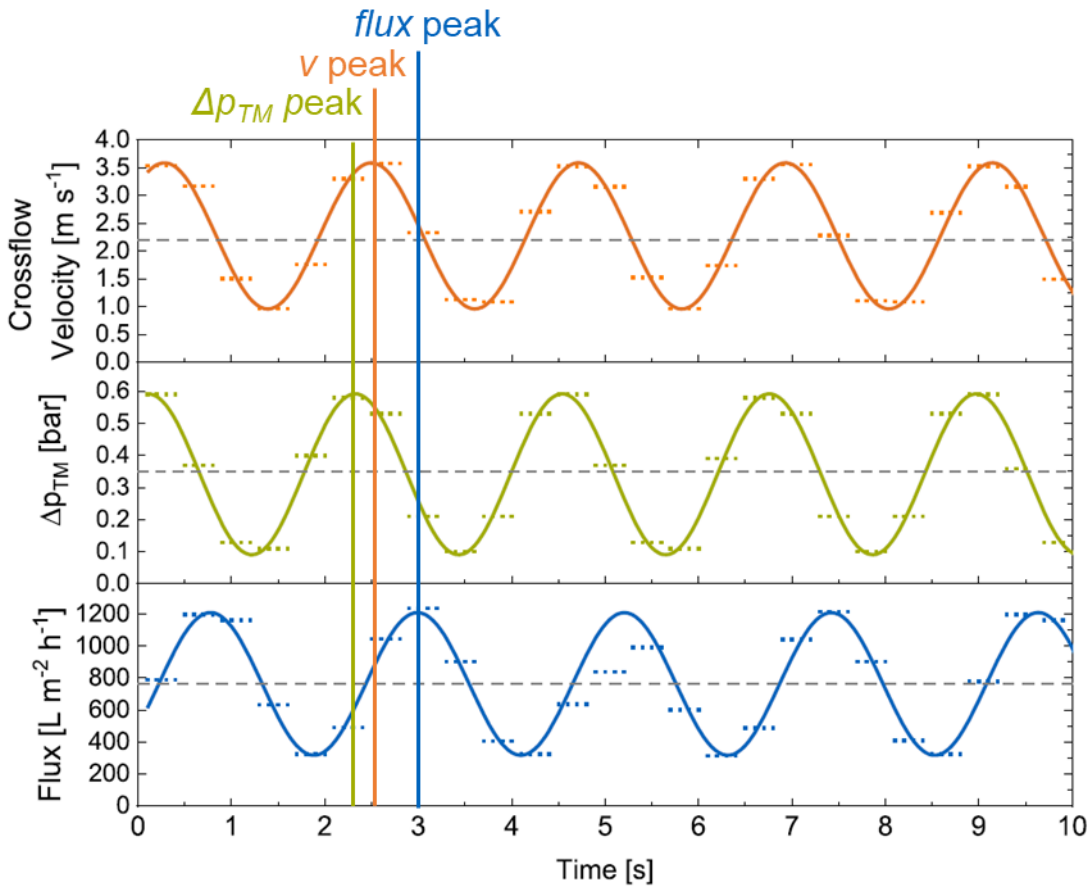

Figure 9-1. Time-resolved progression of crossflow velocity (orange), Δp_{TM} (green) and flux (blue) over several cycles during cleaning with f = 0.5 Hz and Δv = 2.5 m s^{-1}. The dotted lines (grey) indicate averaged values of each variable. Vertical lines mark the respective peak times of v, Δp_{TM} and flux. The graph was modified from Figure 4-7.

Notably, the positive effect of pulsed flow might only be related to removing external deposit layers but not internal fouling (see Figure 9-2). This can firstly be expected due to deposit layers being most exposed to hydrodynamic forces as a consequence of their location in the feed/retentate channel and secondly underlined by results from chapters 3 – 8. The data analogously shows, for different setups and parameters analysed, that pulsed flow cleaning results in significant improvements in protein removal, i.e. chemical cleanliness, but only little to no significant improvements in FRR, i.e. hydraulic cleanliness. Assuming that internal fouling consists of little amounts of protein blocking entire pores while external deposits consist of large amounts of protein with a relatively low impact on flux, the results of improved protein removal with little impact on flux would translate to pulsed flow mainly improving external deposit removal. Hence, as shown by several previous studies (Blanpain-Avet et al. 2009; Berg et al. 2014; Wemsy Diagne et al. 2013; Bartlett et al. 1995), some residues would remain on and in the membrane for steady flow cleaning due to NaOH being an imperfect cleaning agent (see detailed discussion in chapter 1.5.2). In contrast, pulsed flow cleaning would significantly improve deposit layer removal and slightly improve internal fouling removal with some unspecific residues remaining on the membrane surface (see Figure 5-9) and presumably within the membrane's pore structure.

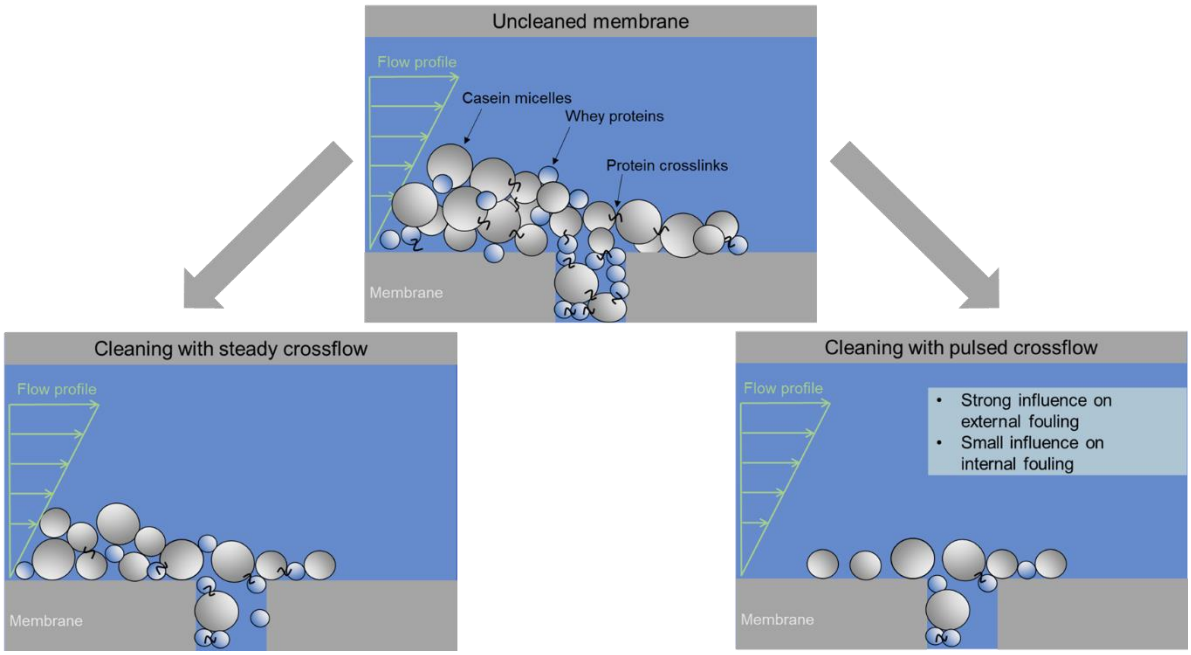

Figure 9-2. Schematic overview of the presumed effect of steady and pulsed flow on NaOH cleaning efficiency in membranes with a free flow channel such as HFM or CTM.

As the fouling type mostly affected by pulsed flow, external deposit layer formation mainly consists of irreversible fouling. Unsurprisingly, in membranes with free flow channels, such as HFM or CTM, pulsed flow requires support from a chemical cleaning agent such as NaOH to improve cleaning success effectively. In this regard, an optimum cleaning pH of 11.5 was also found to best support the mechanical enhancements of pulsed flow. At the same time, high concentrations of NaOH or the absence thereof led to no improvements for pulsed flow cleaning (see chapter 4 for details).

The second portion of the presumed mode of action of pulsed flow, i.e. induced turbulence, is of particular importance for membrane types suffering from flow shadows and the resulting fields of application. Additionally to the deposit layer formation exposed to feed/retentate flow, as it dominates fouling in HFM and CTM, membranes suffering from flow shadows, such as FSM or SWM, carry extensive fouling in these areas. Results showed that these residues are mainly reversible deposits, as pulsed flow could improve the cleaning success in FSM (see chapter 5) without the addition of a cleaning agent, i.e. c_{NaOH} = 0.0%. Furthermore, improvements in combination with a cleaning agent (NaOH, pH 11.5) were more pronounced for FSM (see chapter 5) and SWM (see chapter 8) than HFM (see chapters 4 and 5). This additional turbulence is particularly beneficial as depending on the effective Re, an increased formation and shedding of vortices occurs (Geraldes 2002; Han et al. 2018b; Schwinge et al. 2003; Fischer et al. 2020) which helps improve access to former flow shadows and remove present deposits (see Figure 9-3). Hence, it is hypothesized that beyond the effects of pulsed flow on cleaning success in HFM, where most irreversible fouling could be removed in combination with a cleaning agent, the additional positive effects of pulsed flow on

cleaning success in FSM and SWM are due to improved access to flow shadows helping remove mostly reversible deposits present in these areas.

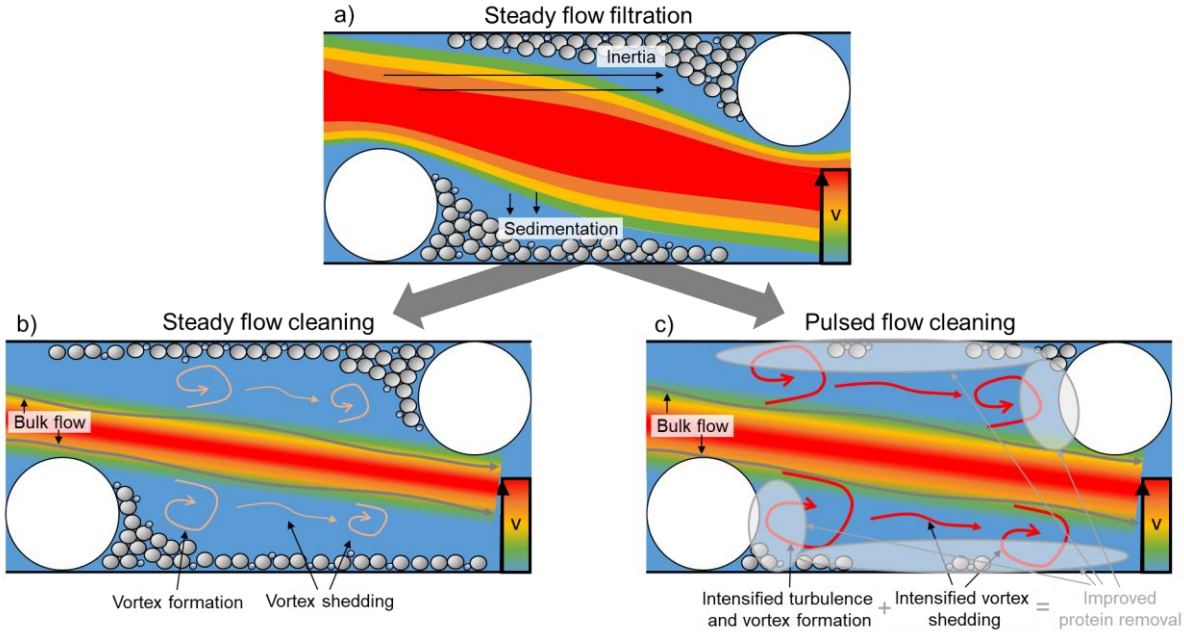

Figure 9-3. Schematic overview of the presumed effect of pulsed flow on cleaning efficiency in membranes suffering from flow shadows such as FSM or SWM.

Interestingly, a study by Howell et al. (1993) suggested synergistic effects between baffles and pulsed flow for the filtration of a yeast suspension despite those baffles not creating flow shadows near the membrane. Hence, it appears that the effects of pulsed flow and baffles inducing turbulence amplify each other when combined, irrespective of additional positive effects such as providing improved access to flow shadows. Accordingly, future studies should also investigate the effects of pulsed flow in combination with novel HFM geometries, such as sinusoidal/helical shapes (Luelf et al. 2017; Tepper et al. 2022; Roth et al. 2019; Wiese et al. 2019) that supposedly also act as baffles and lead to increased turbulences. Consequently, combining these innovative approaches could help further improve process efficiency during filtration and cleaning in HFM.

The practical implications of the current results are that in open channel membranes, i.e. HFM and CTM, pulsed flow can exclusively improve chemical cleaning (see chapter 4) but not rinsing steps (see chapter 5) nor filtration (Weinberger and Kulozik 2021a), at least for a complex medium with intensive fouling such as skim milk. However, for membranes suffering from flow shadows, i.e. FSM and SWM, pulsed flow can improve the entire process chain of filtration (see chapter 7), rinsing (see chapter 5) and chemical cleaning (see chapter 5 and 8).

9.1.2 Alternating flow

For alternating flow, it was initially hypothesized that its effect would surpass that of pulsed flow due to the additional feed-side flow reversal posing further stress on the deposits and technically translating to vastly higher amplitudes. This seemed particularly probable as previous studies on pulsed flow cleaning of steel geometries found substantial increases in cleaning success when a system-related flow reversal, i.e. alternating flow, occurred (Gillham et al. 2000; Bode et al. 2007). However, due to the increased complexity of membrane systems with an additional flow through the wall/membrane and the importance of Δp_{TM}, different results were observed. Hence, it was found that some factors relevant to pulsed flow, such as frequency and amplitude, had more negligible effects on alternating flow membrane cleaning. Instead, a factor irrelevant to studies investigating steel geometries but highly relevant in membrane filtration, i.e. length-dependent pressure and fouling effects (Piry et al. 2008; Schopf et al. 2021a; Hartinger et al. 2020c), played a crucial role in alternating flow efficiency (see chapter 6).

The main influencing factors identified in this regard are the improvement in the local ratio of $v/\Delta p_{TM}$ as well as reductions in the local $\Delta p_{TM, inlet}$ causing improvements with alternating flow for membranes with distinct length dependency. Unsurprisingly, cleaning success of steady flow decreased for increasing membrane length due to the increased Δp_L causing an increased $\Delta p_{TM, inlet}$ despite an identical $\Delta p_{TM, avg}$. Results of complementary experiments to differentiate between the effects of a temporary and cyclic flow reversal, as in alternating flow, and a permanent flow reversal, as in steady backwards flow, demonstrated a permanent flow reversal during cleaning (compared to filtration) being a beneficial alternative to conventional forward flow cleaning. The advantage is that this approach enables very low Δp_{TM} at the feed-side membrane end (see Figure 9-4), where most severe deposition formed during filtration. Complimentarily, the local ratio of $v/\Delta p_{TM}$ also increases, presumably causing the observed chemical and hydraulic improvements in fouling removal.

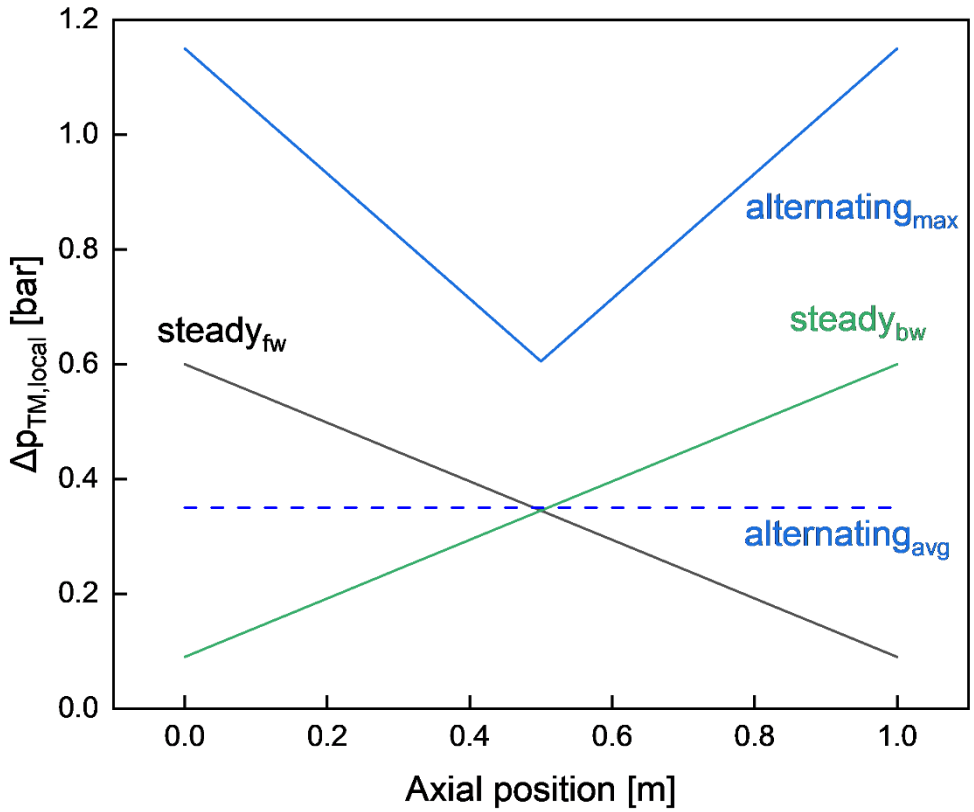

Figure 9-4. Local $\Delta p_{TM,max}$ values as a function of the axial membrane position/length for steady forward (fw) flow (grey), steady backwards (bw) flow (green), as well as the respective average (avg) (dotted blue line) and maximum (max) values (solid blue line) occurring during an alternating flow cycle. The axial position refers to the conventional feed inlet side as the membrane's front (0.00 m) and the respective retentate outlet as its end (1.0 m). The average Δp_{TM} for all three flow types was identical (0.35 bar)

For alternating flow with cyclic flow reversals, no further improvements could be seen beyond a permanent flow reversal despite the additional stress of pulsed flow and fluctuating flow directions. This is due to the pulsation causing temporarily higher $\Delta p_{TM,\,max}$ during each cycle and the cyclic flow reversal applying those values to both membrane sides equally. The local maximum values occurring during a complete alternating flow cycle are also depicted in Figure 9-4. With $\Delta p_{TM,\,max}$ being generally referred to as the determining factor for filtration and cleaning efficiency and this value being significantly increased along the whole membrane length for alternating flow, the otherwise additionally positive aspects of pulsation are presumably compensated by the increased local Δp_{TM} values. It is to be noted that the mentioned benefits of permanent and cyclic flow reversal only occurred for membranes with distinct length dependencies, i.e. for industrial membrane lengths of 1.0 m but not lab-scale membranes of 0.5 m. Another important aspect is that these experiments were exclusively conducted in HFM. Hence, no statements can be made regarding the efficiency of alternating flow in improving access to flow shadows in FSM beyond the effects of pulsed flow. Future studies should include these aspects to compare pulsed and alternating flow efficiency in FSM/SWM.

9.2 Overview of factors influencing the efficiency of pulsed/alternating flow

A summary of the factors identified in the studies included in this thesis to affect the efficiency of pulsed/alternating flow is provided in Figure 9-5. The following section will summarise the most important details of each category.

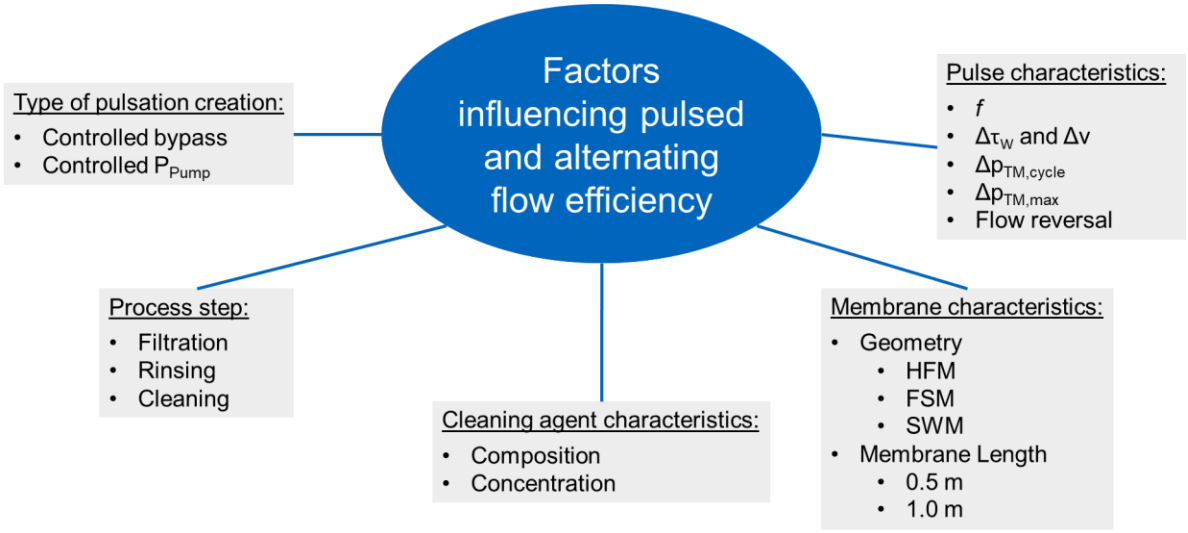

Figure 9-5. Summary of factors identified in this thesis to influence pulsed or alternating flow efficiency.

Pulse characteristics

For both pulsed and alternating flow, using the maximum frequency possible with the present setup resulted in the most pronounced improvements in protein removal over steady flow cleaning (see chapters 4 and 6). This is presumably due to the frequency of velocity fluctuations determining the intensity of induced turbulence and is in accordance with results from previous studies (Gillham et al. 2000; Yang et al. 2019; Weidemann et al. 2014; Blel et al. 2009a; Blel et al. 2009b).

Regarding amplitude, a distinction between flow velocity amplitude Δv and transmembrane pressure amplitude $\Delta p_{TM,\,cycle}$ and the related $\Delta p_{TM,\,max}$ is required. For Δv, similarly to frequency and in accordance with previous studies (Augustin et al. 2010; Blel et al. 2009a; Blel et al. 2009b; Gillham et al. 2000), using the maximum value during pulsed and alternating flow cleaning resulted in the most pronounced increase in protein removal over steady flow cleaning.

However, in terms of pressure conditions, that were irrelevant in previous studies examining the cleaning of steel geometries (Gillham et al. 2000; Bode et al. 2007; Blel et al. 2009a), medium values were found to be most beneficial to pulsed flow cleaning success. On the one hand, low/ absent pressure fluctuation (i.e. $\Delta p_{TM,\,cycle}$ = 0.0 bar) is detrimental to pulsation efficiency and cleaning success despite a high frequency and Δv. This was argued

to result from the missing cyclic deposit relaxation and compaction that would otherwise, combined with the inertia-related slightly delayed shear stress peaks and the induced turbulence, cause improved protein removal. On the other hand, higher values of $\Delta p_{TM,\,cycle}$ (e.g. 0.74 bar) are also detrimental as they are accompanied by high values of $\Delta p_{TM,\,avg}$ and $\Delta p_{TM,\,max}$. For alternating flow, the detrimental effects of $\Delta p_{TM,\,max}$ are more pronounced due to the additional cyclic flow reversal causing the local $\Delta p_{TM,\,max}$ to occur on both membrane ends (compare Figure 9-4).

The effects of flow reversal were found to be primarily related to the inversion of the length-dependant decrease in Δp_{TM}, as this shifted the length-dependant lowest local Δp_{TM} from the membrane outlet to the membrane inlet, where deposition was most pronounced during filtration. This also translated to a permanent flow reversal, i.e. steady backwards flow from the retentate side, to being similarly advantageous as alternating flow. However, the effect of pressure conditions during alternating flow on cleaning success needs further investigation.

Membrane characteristics

Different membrane lengths were only found to affect alternating flow but not pulsed flow efficiency (see chapter 6). Hence, for membrane lengths in HFM of at least 1.0 m, no decrease in pulsed flow efficiency by e.g. friction could be observed. However, for alternating flow, membrane length plays a crucial role as with increasing membrane length, the respective minimum Δp_{TM} at the inlet induced by flow reversal further decreases. Hence, the local ratio of shear stress to Δp_{TM} also increases at the inlet, where the deposition was most pronounced during filtration, with increasing membrane length, and cleaning success increasing accordingly.

Regarding the membrane geometry, the most pronounced improvements were found for FSM (see chapter 5) and SWM (see chapter 8). While in HFM, only the removal of irreversible fouling could be enhanced in combination with NaOH, the additional flow shadows in FSM and SWM allowed the pulsed flow to also improve the removal of primarily reversible deposits in those areas by improving access to it due to enhanced turbulence. The differences in pulsed flow efficiency between FSM and SWM were attributed to geometrical differences regarding the angle of feed inflow and retentate outflow towards and from the membrane. The effects of alternating flow on cleaning efficiency in FSM or SWM are yet to be investigated.

Cleaning agent characteristics

This thesis used NaOH as a cleaning agent because it is one of the most used and studied (D'Souza and Mawson 2005; Ng et al. 2017). With the cleaning action of NaOH requiring a threshold pH > 11.2 to cleave non-covalent bonds in proteinaceous deposits (Mercadé-Prieto et al. 2008; Gillham et al. 2000) and being hindered at larger pH values above pH 12.0 (Bird and Bartlett 2002; Makardij et al. 1999), effects of the chemical cleaning action on the interplay with a mechanical enhancement by pulsed flow were expected. Accordingly, due to the extensive cross-linking and gelation occurring during skim milk MF at high pressures (Bouchoux et al. 2010; Bouchoux et al. 2009; Qu et al. 2015; Gebhardt et al. 2012), pulsed flow could only improve the removal of irreversible deposits when supported by NaOH at a suitable pH range of 11.3 – 11.6 (c_{NaOH} = 0.03 – 0.05 %) (see chapter 5 and Figure 9-6). For higher pH values > 12.0 (c_{NaOH} = 0.30 %), pulsed flow had a detrimental effect on cleaning success. This could be attributed to the adverse effects reported for NaOH at these pH values to force swollen and detached proteins back into the pores (Mercadé-Prieto et al. 2008; Mercadé-Prieto and Chen 2005), further intensified by the high Δp_{TM} occurring temporarily during pulsed flow phases. Without NaOH (c_{NaOH} = 0.0%), only improvements regarding reversible fouling could be observed, as the remaining irreversible fouling is too tightly bound without chemical support. The relevance of these results in improving the individual process steps of filtration, rinsing and cleaning will be discussed in the following paragraph. It is worth noting that the effects of cleaning pH were only examined for pulsed flow. Nonetheless, the underlying principles of the interplay between mechanical and chemical action are comparable for pulsed and alternating flow. Compliant with that, the results of chapter 7 prove that both pulsed and alternating flow can support process efficiency in FSM during the MF of skim milk, i.e. for an intact deposit without the chemical support by NaOH. Also, no statements can be made on the transfer of those results to more complex cleaning agents containing e.g. enzymes and surfactants, as their different modes of action support the cleaning success in different ways. Accordingly, their interactions with pulsed/alternating flow cannot be predicted and need separate investigation.

Process step

With pulsed flow without chemical support presumably only affecting reversible deposit removal and with chemical support also affecting irreversible removal, different efficacies of pulsed/alternating flow arose for the different process steps involved in a filtration process unit, i.e. filtration, rinsing and chemical cleaning. Accordingly, for membrane types such as HFM with a free flow channel and mainly irreversible deposits dominating fouling, pulsed flow can only support steps where chemical support loosens the deposit. Hence, positive effects of

pulsed flow where only observed for chemical cleaning, but not during rinsing, i.e. in the absence of NaOH (see chapter 5) or during the MF of skim milk (Weinberger and Kulozik 2021a). However, for other membrane types such as FSM and SWM, that are e.g. subject to flow shadows due to spacers, pulsed and alternating flow can improve access to those flow shadows and thus also improve the efficiency of rinsing steps (c_{NaOH} = 0.0%) (see chapter 5) and the MF of skim milk (see chapters 7 & 8).

Type of pulsation creation

As previously discussed, the approach to pulsation-creation can significantly affect different aspects of pulsed/alternating flow. The use of bellows, diaphragms or piston units (Gupta et al. 1992; Olayiwola and Walzel 2009; Gillham et al. 2000; Bode et al. 2007) limits process control of individual variables, such as flow and pressure. Additionally, negative pressures occur that could damage SWM and result in permeate-side backwash and alternating flow depending on the intensity of bellows/piston strokes (Bode et al. 2007; Gillham et al. 2000). The approach chosen by Weidemann et al. (2014) and Yang et al. (2019) using spray nozzles is challenging to scale up as the effect of the spray nozzle is very punctual and largely depends on the spraying distance and angle. Also, this approach is only compatible with small dead-end filtration cells. Larger membranes would require a comprehensive network of countless spray nozzles and not be energy-efficient. Hence, this thesis and previous studies (Weinberger and Kulozik 2021a, 2021c, 2021b, 2022) chose a different approach utilising modern pump technology to create pulsed flow via rapid pump capacity ramps. With additional throttles, pressure conditions could widely be adjusted independently of flow conditions while maintaining a sinusoidal pattern of flow and pressure condition progression (compare Figure 4-1). Additional piping allowed the controlled utilisation of alternating flow without any negative pressures (see Figure 6-1). Admittedly, implementing alternating flow this way would be complex and expensive. Besides the additional piping, several precisely controlled valves are required for each membrane to run in alternating flow mode. Another limitation of this approach is that such pumps enabling rapid pump capacity ramps are currently unavailable at industrial scale. Hence, another novel approach applicable at an industrial scale had to be developed. The details of these findings will be discussed in chapter 9.4.

9.3 Comparison of pulsed and alternating flow efficiency

To compare the efficiency of pulsed and alternating flow for membrane cleaning after skim milk MF, an overview of improvements in hydraulic cleanliness (ΔFRR) and chemical cleanliness (ΔProtein removal) compared to steady flow cleaning is given in Figure 9-6.

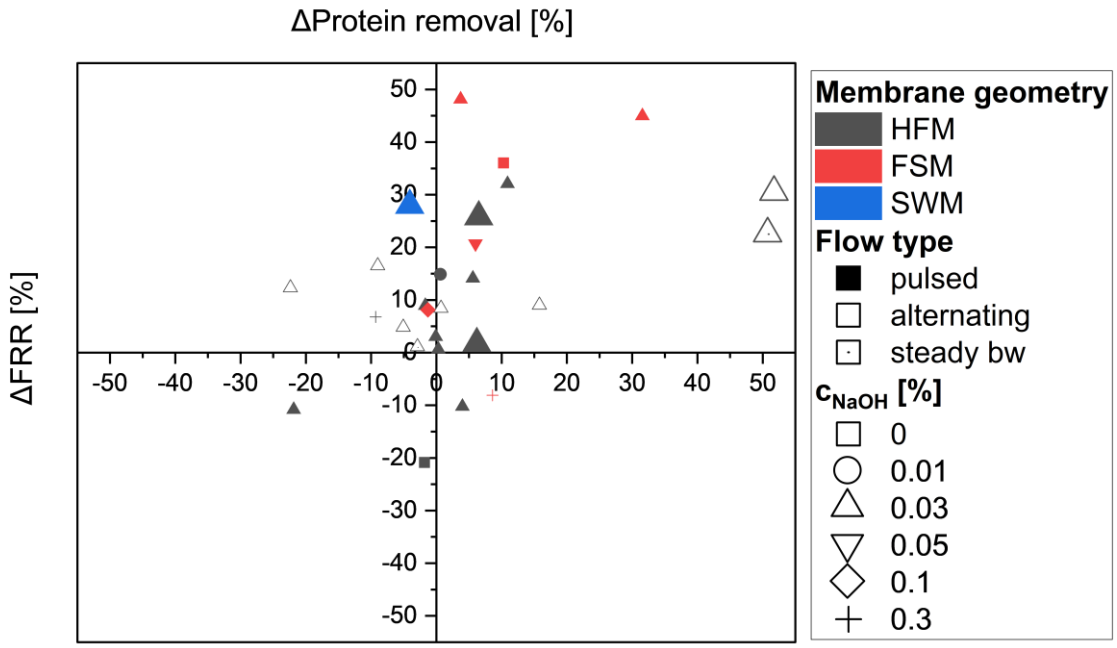

Figure 9-6. Overview of improvements obtained for pulsed and alternating flow membrane cleaning after skim milk MF compared to steady flow cleaning.

As previously discussed, the exact correlation between hydraulic and chemical cleanliness remains unknown (Blanpain-Avet et al. 2009). FRR proved particularly unreliable for evaluating cleanliness after pulsed/alternating flow for membranes containing flow shadows (see chapter 5). Hence, the focus lied on achieving improvements in chemical cleanliness. Nonetheless, many sets of cleaning variables resulted in both hydraulic and chemical improvements. The most pronounced increases in FRR were observed for alternating and steady bw flow in a 1.0 m HFM (ΔFRR >50 %) with a significant chemical improvement of ~30 %. The most significant chemical improvements were all achieved in FSM membranes and reached ΔProtein removal >45 %. Notably, all of these results were obtained for maximum *f* = 0.5 Hz, the respective maximum Δv and a pH 11.3 (c_{NaOH} = 0.03 %). The only exception is that substantial chemical improvements >35% could also be achieved in FSM without a cleaning agent due to extensive flow shadows and related reversible fouling. More minor improvements in chemical cleaning success (ΔProtein removal >30%) at otherwise identical conditions were observed for SWM and HFM, or FSM with slight deviations in pH (c_{NaOH} = 0.01% and 0.05%). Further reductions in improvements were observed for decreased *f*, Δv, differing pH values or changes in pressure conditions. Notably, the overall results depicted as a boxplot (see Figure 9-7) show that alternative flow types only slightly influence hydraulic

cleanliness, with the median being close to zero improvement and the lower and upper quartiles being spread between -5 and +10 % improvement. In contrast, the median improvement for protein removal is at +10 %, and the lower and upper quartiles are spread between +5 and +25 % improvement. Hence, while many different sets of pulsed/alternating flow cleaning variables improved hydraulic and chemical cleanliness, it can be concluded that alternative flow types primarily affect chemical cleanliness. This macroscopic view of results supports one of the initial hypotheses which is that pulsed/alternating flow mainly improves deposit layer removal and, to a lesser extent, internal fouling, as the proteins in the deposit make up a large portion of the total fouling, but their removal has a low impact on flux.

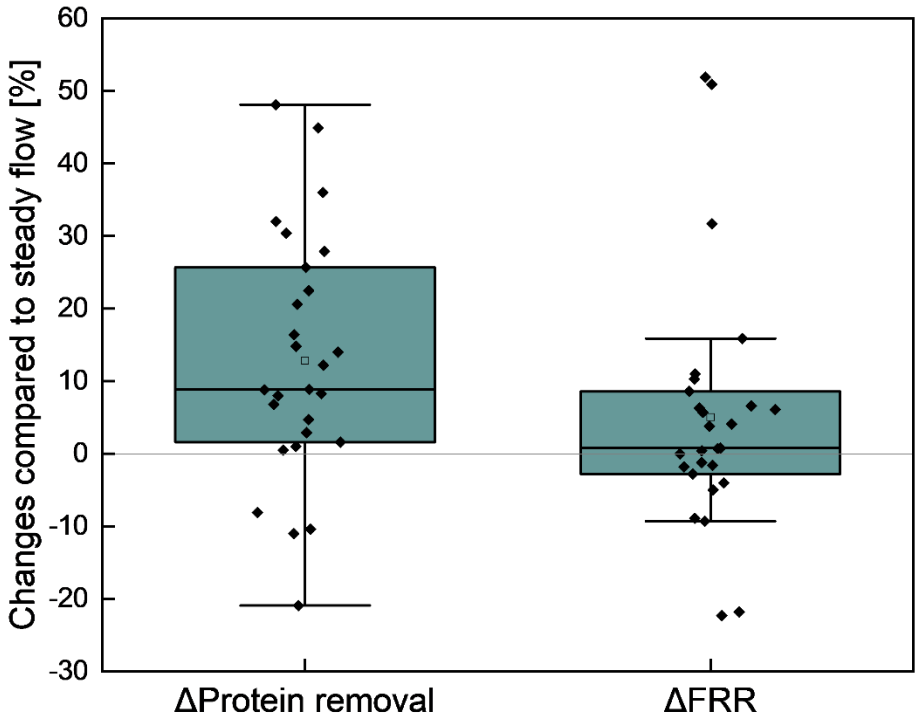

Figure 9-7. Changes obtained in FRR and protein removal for different sets of pulsed/alternating flow cleaning variables compared to the respective steady flow cleaning conditions.

Besides the improvements in process efficiency, the associated amounts of required pump energy must also be considered. Overall, both pulsed and alternating flow require 25 % and 29 % more energy than running the pump at identical average flow velocity in steady flow ($steady_{avg}$) due to the constant changes in pump capacity and the cyclic flow reversal (see Figure 9-8a). The conventional alternative for enhancing process efficiency in a steady flow without pulsed/alternating flow and precise pressure control would be running the plant at maximum pump capacity ($steady_{max}$), which in this scenario translates to a 196 % increase in energy consumption. However, as previously stated, pulsed and alternating flow utilise energy input much more efficiently than increases in flow velocity for steady flow. Taking the improvements for pulsed/alternating flow and the absent improvements for $steady_{max}$ into

account (see Figure 9-8b) results in the specific energy consumption, i.e. the energy consumption per unit of the process-related target value (whey protein mass flow for filtration and protein removal for cleaning) (see Figure 9-8c).

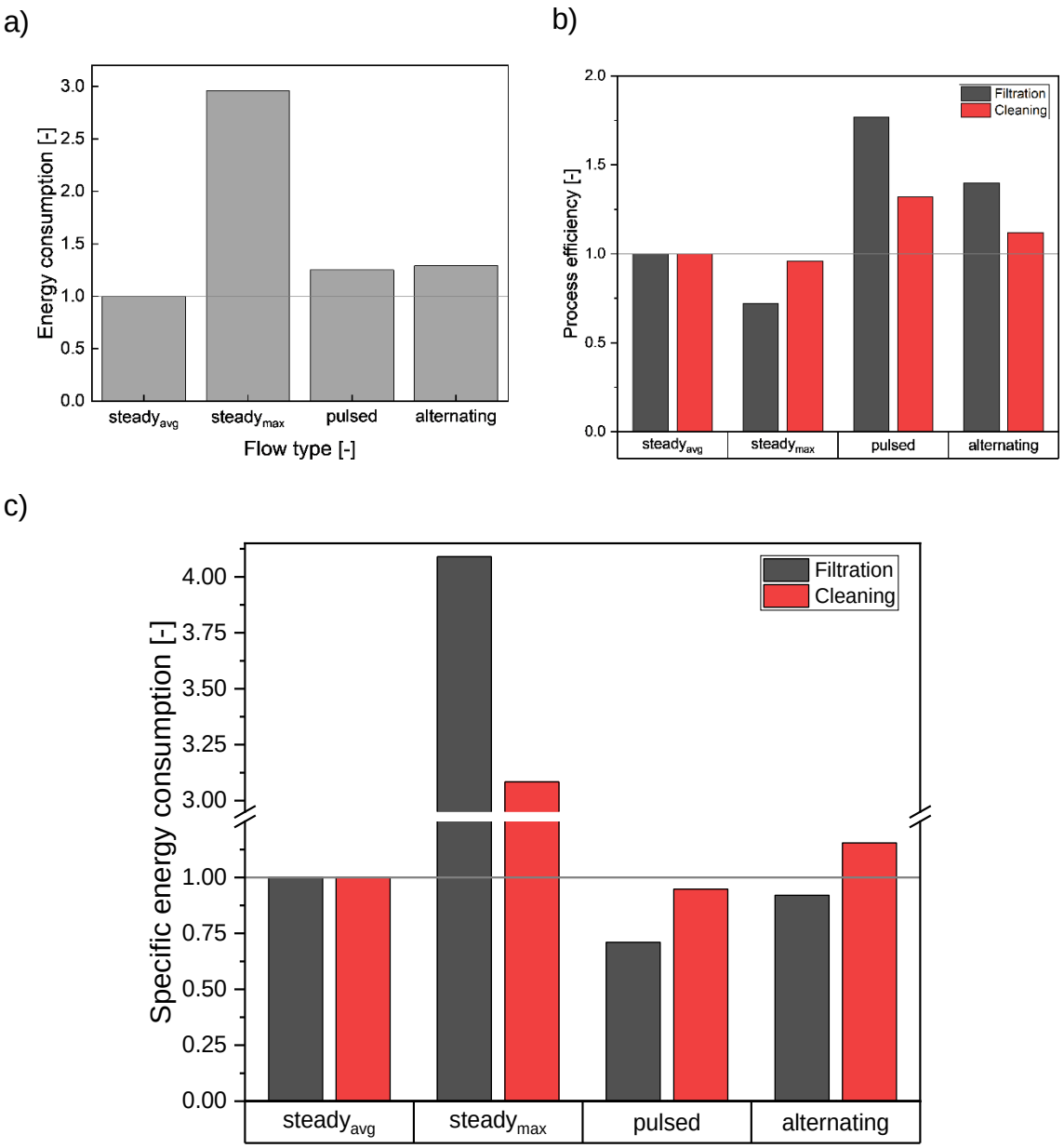

Figure 9-8. Energy consumptions normalised for steady$_{avg}$ flow conditions (a), process efficiency in terms of whey protein mass flow for filtration and protein removal for cleaning normalised for steady$_{avg}$ flow conditions (b), and the resulting specific energy consumptions, calculated by dividing the energy consumption by the respective whey protein mass flow (in FSM) or protein removal (in HFM) and normalised for steady$_{avg}$ flow conditions (c). The data was partially taken from Table 4-3 and Table 7-2.

The data confirms the inefficiency of pump capacity increases under steady flow, as for both filtration and cleaning, the specific energy consumption increases by 208 % and 309 %, meaning that substantially more energy is required to achieve 1 g m^{-2} h^{-1} of whey protein mass flow or 1 g m^{-2} of protein removal. For alternating flow filtration in FSM, energy efficiency increases as the specific energy consumption decreases by 8 %. However, the increased

cleaning success for alternating flow cleaning in HFM cannot compensate the additional energy consumption, leading to a 15 % increase in the specific energy consumption. In contrast, pulsed flow reduced the specific energy consumption by 29 % for filtration in FSM and 5 % for cleaning in HFM. It is worth noting that the improvements for cleaning are even more pronounced in FSM. Hence, it can be concluded that pulsed poses the most efficient way to utilise pump energy input and, thus, improve the process efficiency and sustainability of the filtration and cleaning process.

9.4 Industrial filtration plant design enabling pulsed/alternating flow

The plant modifications necessary to enable pulsed (Figure 9-9a) and alternating flow (Figure 9-9b) on lab-scale differ widely. For pulsed flow, only a special pump-type is required to enable rapid pump capacity ramps and, thus, utilisation of pulsed flow. In contrast, additional piping and four controlled valves are necessary for alternating flow to enable the feed-side flow reversal.

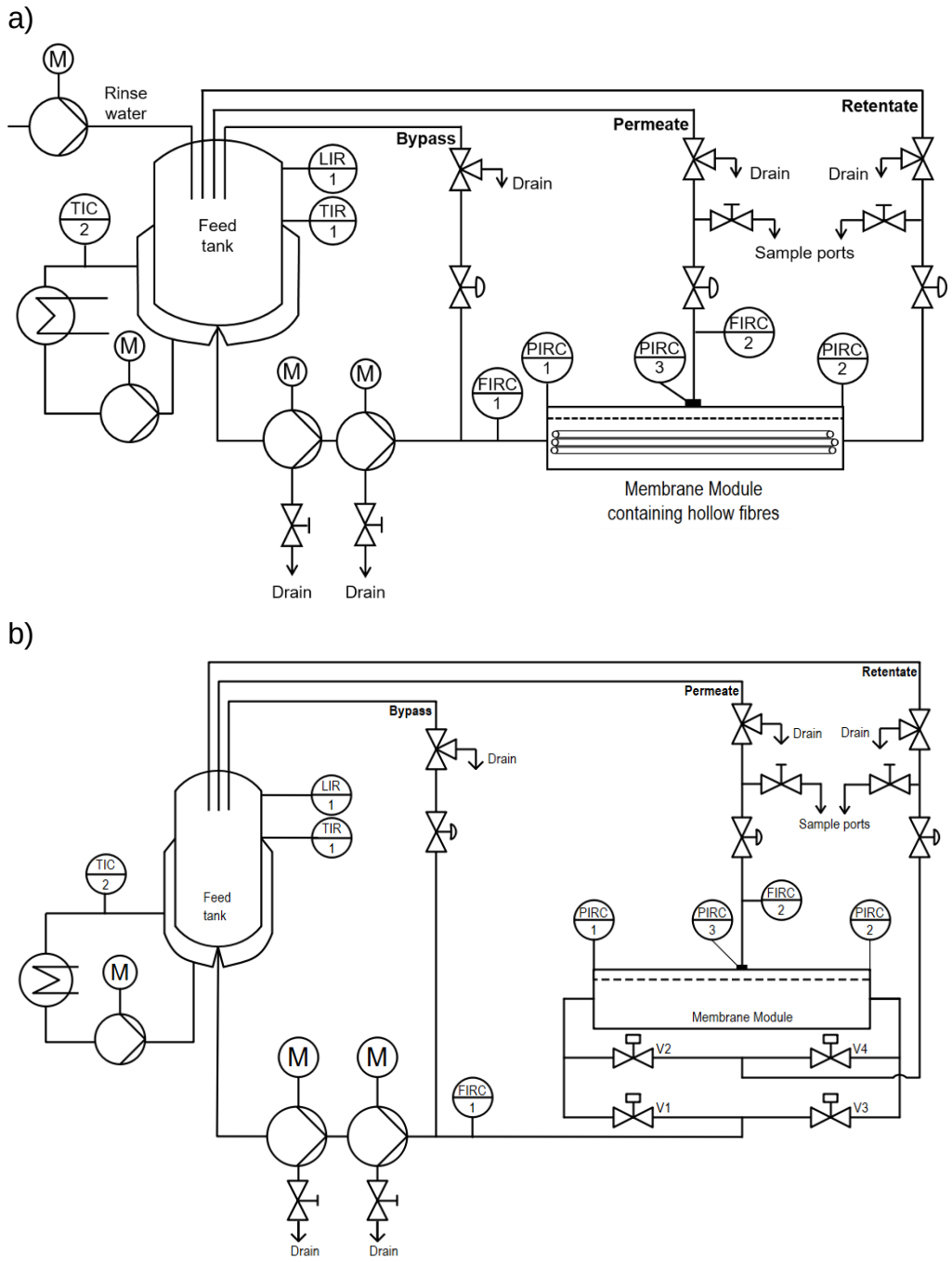

Figure 9-9. Comparison of the plant equipment required to realise pulsed flow (a) (graph taken from Figure 4-1) and alternating flow (b) (graph taken from Figure 6-1).

Another approach had to be developed for the scale-up to industrial membrane modules, as currently no pumps are available that could enable such rapid pump capacity ramps at an industrial scale.

The novel process design (see chapter 8) included an additional bypass (Figure 9-10a) containing a relay-controlled pneumatic valve to define the frequency of pulsed flow, i.e. when the bypass opens and closes, and a manual valve to define the amplitude of the pulsed flow, i.e. the flow rate taken away from the membrane by the cyclically opened bypass.

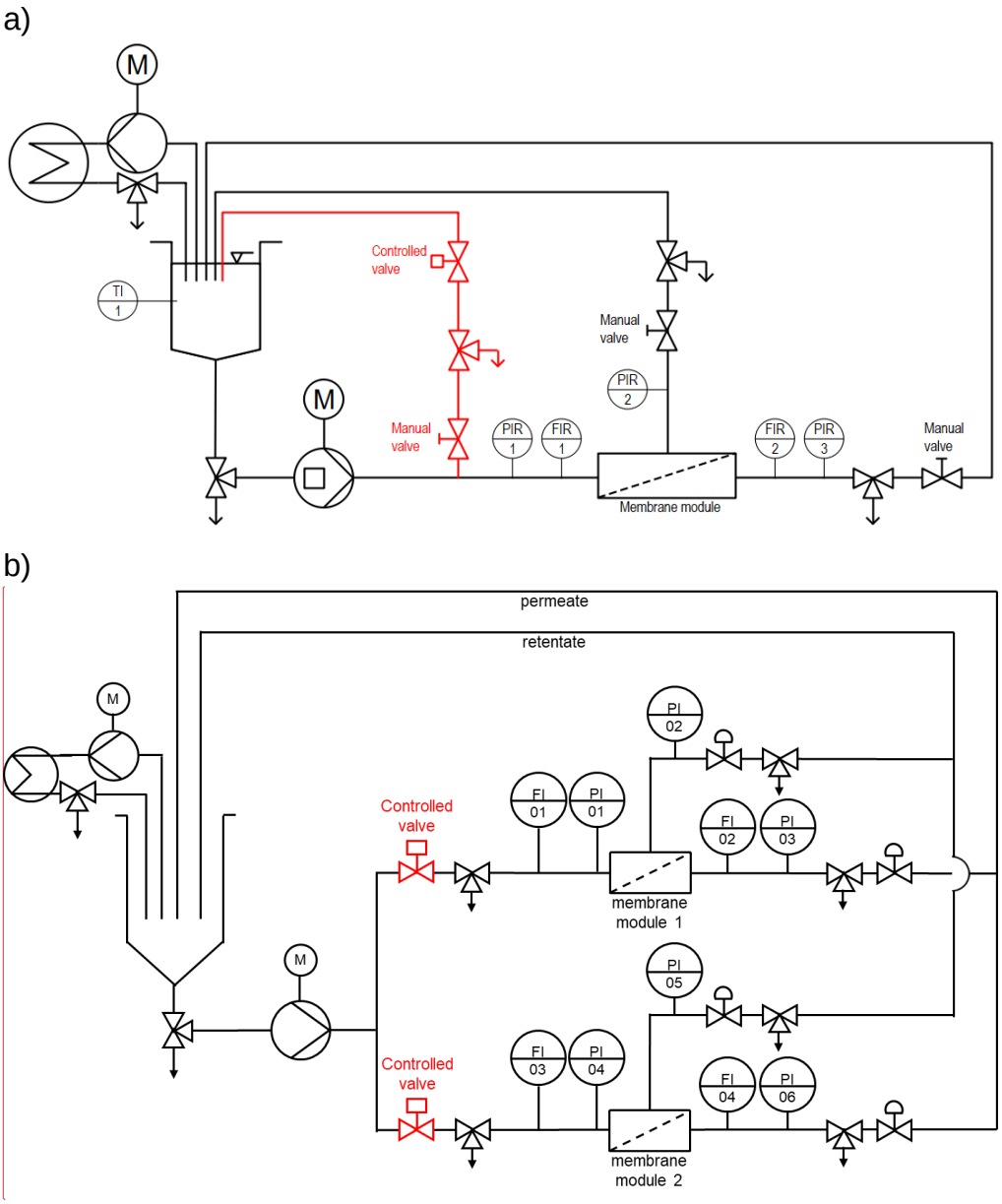

Figure 9-10. Piping and instrumentation diagram of an established membrane filtration plant (black parts) and the addition of a complimentary bypass (red parts) to enable pulsed flow for a singular membrane (a) (graph taken from Figure 8-1) or multiple membranes, here shown exemplarily for one pair of membranes (b) coupled to utilise both energy streams created by pulsed flow efficiently. Membrane modules 1 and 2 could also each be replaced by several parallel modules being fed by one controlled valve.

The main limitation/ drawback of this bypass-approach is that, despite pulsed flow utilised that way still being more efficient than steady flow, a large portion of the pump energy input will be returned to the feed tank unused. However, this would not be an issue for larger filtration plants with at least two parallel membranes. The reason is that this bypass could then instead feed a second membrane filtration stage simultaneously. Hence, a pair of two membrane filtration stages, each possibly consisting of several parallel membranes, would then inversely be fed by high and low flow rate phases without any energy remaining unused. Also, adding a dedicated bypass or a special pump capable of rapid pump capacity ramps would not be necessary. Instead, one pump running with maximum capacity combined with two controlled valves could feed two membrane filtration stages, possibly consisting of several membranes (see Figure 9-10b). One additional prerequisite for simultaneously feeding two membranes with pulsed flow would be that the controlled valve can rapidly close not only fully but also partially. This is crucial to enable a flow rate and pressure above zero for the low flow rate phase of the membranes behind the respective valve. Overall, this approach to pulsation-creation of having pulsation units consisting of two membrane stages fed by one pump poses a cost- and energy-efficient way to enable pulsed flow even in large-scale industrial filtration plants.

In contrast, implementing alternating flow for industrial-scale filtration plants would still require all the mentioned additional piping and controlled valves, as shown in Figure 9-9b, plus the novel approach to pulsation-creation via pulsation units of two membrane filtration stages (see Figure 9-10b). Implementing steady backwards flow, as discussed in chapter 4 as a viable alternative to alternating flow, would still require the exhaustive changes necessary to enable alternating flow except for the pulsation-creation parts. As neither steady backwards nor alternating flow provide substantial benefits over pulsed flow despite the significantly higher costs and effort necessary to implement those flow types, pulsed flow can be considered superior for lab-scale and industrial-scale applications.

9.5 Conclusions for an optimised filtration and cleaning process using pulsed/alternating flow

As reported, several factors influence the efficiency of pulsed and alternating flow. Overall, high frequencies and high amplitudes (with medium pressure conditions) positively affected process performance. Depending on the module type, different process steps could be improved.

Regarding chemical cleaning, a pH of 11.3-11.6 best supported the mechanical enhancements of pulsed flow by loosening irreversible deposits. For HFM, which are mostly free of flow shadows and dominated by the irreversible deposit layers, only chemical cleaning

could be improved with pulsed flow when supported by NaOH. For SWM or FSM that are subject to distinct flow shadows and, thus, contain additional mostly reversible fouling in the spacer vicinity, process performance could also be improved without an additional cleaning agent, i.e. during filtration and rinsing (c_{NaOH} = 0.0%), due to the improved access to flow shadows. Accordingly, with synergistic effects between baffles/ flow shadows and pulsed flow presumed, more pronounced improvements in HFM might be achievable by combining pulsed flow with e.g. helically twisted HFM. Regarding the industrial application of pulsed flow for the MF of skim milk, additional aspects, such as the concentration of skim milk or the influence of filtration temperature, should be addressed due to the increased viscosities possibly affecting the efficiency of mechanical enhancements. However, these aspects should be the subject of future studies.

Overall, the present results not only translated to improved filtration performance or cleaning success but also proved to utilise present flow forces more efficiently, as a substantial increase in steady flow velocity did not result in similar improvements. Accordingly, a significant reduction in the specific pump energy consumption during those processes was observed, translating to a more economically and ecologically sustainable filtration and cleaning process.

Nonetheless, it is worth noting that so far, most results regarding FRR as an imperfect cleanliness criterion indicated incomplete cleaning for every flow type when combined with NaOH alone. Hence, future studies could also consider examining more complex cleaning agents containing e.g. enzymes or surfactants to further investigate the interactions between mechanical enhancements and individual cleaning additives.

Based on current knowledge, pulsed flow can be considered superior to alternating flow for the MF of skim milk and subsequent cleaning due to the lower cost and effort necessary for implementation despite similarly strong improvements over steady flow. At both lab- and industrial-scale, pulsed flow could efficiently be utilised with little plant modifications and, depending on the membrane geometry, provide significant improvements in the filtration performance, the mechanical and chemical cleaning success during rinsing and chemical cleaning, and thus, the sustainability of the process unit membrane filtration.

10 References

Abdul Rahman, A. F. H. B., & Abu Seman, M. N. B. (2018). Polyacrylic-polyethersulfone membrane modified via UV photografting for forward osmosis application. *Journal of Environmental Chemical Engineering, 6*(4), 4368–4379, doi: 10.1016/j.jece.2018.06.038.

Adams, M. C., Hurt, E. E., & Barbano, D. M. (2015). Effect of soluble calcium and lactose on limiting flux and serum protein removal during skim milk microfiltration. *Journal of Dairy Science, 98*(11), 7483–7497, doi: 10.3168/jds.2015-9474.

Al-Akoum, O., Ding, L., Chotard-Ghodsnia, R., Jaffrin, M. Y., & Gésan-Guiziou, G. (2002). Casein micelles separation from skimmed milk using a VSEP dynamic filtration module. *Desalination, 144*(1-3), 325–330, doi: 10.1016/S0011-9164(02)00337-5.

Allie, Z., Jacobs, E. P., Maartens, A., & Swart, P. (2003). Enzymatic cleaning of ultrafiltration membranes fouled by abattoir effluent. *Journal of Membrane Science, 218*(1-2), 107–116, doi: 10.1016/S0376-7388(03)00145-5.

Althof, W. (1984). *Verformungs-und Festigkeitseigenschaften von Klebstoffen bei Kurz-und Langzeitbeanspruchung* (1st edn).

Altmann, J., & Ripperger, S. (1997). Particle deposition and layer formation at the crossflow microfiltration. *Journal of Membrane Science, 124*(1), 119–128, doi: 10.1016/S0376-7388(96)00235-9.

Amar, R., Gupta, B. B., & Jaffrin, M. Y. (1990). Apple juice clarification using mineral membranes: fouling control by backwashing and pulsating flow. *Journal of Food Science, 55*(6), 1620–1625, doi: 10.1111/j.1365-2621.1990.tb03585.x.

Ang, W. S., Lee, S., & Elimelech, M. (2006). Chemical and physical aspects of cleaning of organic-fouled reverse osmosis membranes. *Journal of Membrane Science, 272*(1-2), 198–210, doi: 10.1016/j.memsci.2005.07.035.

Anvari, A., Yancheshme, A. A., Tavakolmoghadam, M., Rekabdar, F., & Safekordi, A. (2019). Effect of TiO2 nanoparticles on antifouling and separation properties of PVDF/PAN blend membrane. *Desalination and Water Treatment, 154*, 92–100, doi: 10.5004/dwt.2019.24072.

Argüello, M. A., Álvarez, S., Riera, F. A., & Álvarez, R. (2005). Utilization of enzymatic detergents to clean inorganic membranes fouled by whey proteins. *Separation and Purification Technology, 41*(2), 147–154, doi: 10.1016/j.seppur.2004.05.005.

Armbruster, S., Cheong, O., Lölsberg, J., Popovic, S., Yüce, S., & Wessling, M. (2018). Fouling mitigation in tubular membranes by 3D-printed turbulence promoters. *Journal of Membrane Science, 554*, 156–163, doi: 10.1016/j.memsci.2018.02.015.

Augustin, W., & Bohnet, M. (1999). Influence of pulsating flow on fouling behaviour. In *International Conference on Mitigation of Heat Exchanger Fouling and Its Economic and Environmental Implications, Banff, Canada, July* : begell.

Augustin, W., Fuchs, T., Föste, H., Schöler, M., Majschak, J.-P., & Scholl, S. (2010). Pulsed flow for enhanced cleaning in food processing. *Food and Bioproducts Processing, 88*(4), 384–391, doi: 10.1016/j.fbp.2010.08.007.

Avlonitis, S. A., Avlonitis, D. A., Kralis, K., & Metaxa, A. (2010). Water hammer simulation in spiral wound reverse osmosis membranes. *Desalination and Water Treatment, 13*(1-3), 74–81, doi: 10.5004/dwt.2010.1052.

Bacchin, P., Aimar, P., & Field, R. W. (2006). Critical and sustainable fluxes: Theory, experiments and applications. *Journal of Membrane Science, 281*(1-2), 42–69, doi: 10.1016/j.memsci.2006.04.014.

Baker, R. W. (2012). *Membrane technology and applications*. Chichester, UK: John Wiley & Sons, Ltd.

Bansal, B., Al-Ali, R., Mercadé-Prieto, R., & Chen, X. D. (2006). Rinsing and cleaning of α-lactalbumin fouled MF membranes. *Separation and Purification Technology, 48*(2), 202–207, doi: 10.1016/j.seppur.2005.07.012.

Bartlett, M., Bird, M. R., & Howell, J. A. (1995). An experimental study for the development of a qualitative membrane cleaning model. *Journal of Membrane Science, 105*(1-2), 147–157, doi: 10.1016/0376-7388(95)00052-E.

Bégoin, L., Rabiller-Baudry, M., Chaufer, B., Hautbois, M.-C., & Doneva, T. (2006). Ageing of PES industrial spiral-wound membranes in acid whey ultrafiltration. *Desalination, 192*(1-3), 25–39, doi: 10.1016/j.desal.2005.10.009.

Belitz, H.-D., Grosch, W., & Schieberle, P. (2008). *Lehrbuch der Lebensmittelchemie*. Berlin, Heidelberg: Springer Berlin Heidelberg.

Berg, T. H. A., Knudsen, J. C., Ipsen, R., van den Berg, F., Holst, H. H., & Tolkach, A. (2014). Investigation of consecutive fouling and cleaning cycles of ultrafiltration membranes used for whey processing. *International Journal of Food Engineering, 10*(3), 367–381, doi: 10.1515/ijfe-2014-0028.

Bertram, C. D., Hoogland, M. R., Li, H., Odell, R. A., & Fane, A. G. (1993). Flux enhancement in crossflow microfiltration using a collapsible-tube pulsation generator. *Journal of Membrane Science, 84*(3), 279–292, doi: 10.1016/0376-7388(93)80023-Q.

Bijl, E., van Valenberg, H. J. F., Huppertz, T., & van Hooijdonk, A. C. M. (2013). Protein, casein, and micellar salts in milk: current content and historical perspectives. *Journal of Dairy Science, 96*(9), 5455–5464, doi: 10.3168/jds.2012-6497.

Bird, M. R., & Bartlett, M. (2002). Measuring and modelling flux recovery during the chemical cleaning of MF membranes for the processing of whey protein concentrate. *Journal of Food Engineering, 53*(2), 143–152, doi: 10.1016/S0260-8774(01)00151-0.

Blanpain-Avet, P., Doubrovine, N., Lafforgue, C., & Lalande, M. (1999). The effect of oscillatory flow on crossflow microfiltration of beer in a tubular mineral membrane system

– Membrane fouling resistance decrease and energetic considerations. *Journal of Membrane Science, 152*(2), 151–174, doi: 10.1016/S0376-7388(98)00214-2.

Blanpain-Avet, P., Migdal, J. F., & Bénézech, T. (2009). Chemical cleaning of a tubular ceramic microfiltration membrane fouled with a whey protein concentrate suspension—Characterization of hydraulic and chemical cleanliness. *Journal of Membrane Science, 337*(1-2), 153–174, doi: 10.1016/j.memsci.2009.03.033.

Blel, W., Le Gentil-Lelièvre, C., Bénézech, T., Legrand, J., & Legentilhomme, P. (2009a). Application of turbulent pulsating flows to the bacterial removal during a cleaning in place procedure. Part 1: Experimental analysis of wall shear stress in a cylindrical pipe. *Journal of Food Engineering, 90*(4), 422–432, doi: 10.1016/j.jfoodeng.2008.07.008.

Blel, W., Legentilhomme, P., Bénézech, T., Legrand, J., & Le Gentil-Lelièvre, C. (2009b). Application of turbulent pulsating flows to the bacterial removal during a cleaning in place procedure. Part 2: Effects on cleaning efficiency. *Journal of Food Engineering, 90*(4), 433–440, doi: 10.1016/j.jfoodeng.2008.07.019.

Bobe, G., Beitz, D. C., Freeman, A. E., & Lindberg, G. L. (1998). Separation and Quantification of Bovine Milk Proteins by Reversed-Phase High-Performance Liquid Chromatography. *Journal of Agricultural and Food Chemistry, 46*(2), 458–463, doi: 10.1021/jf970499p.

Bode, K., Hooper, R. J., Paterson, W. R., Wilson, D. I., Augustin, W., & Scholl, S. (2007). Pulsed flow cleaning of whey protein fouling layers. *Heat Transfer Engineering, 28*(3), 202–209, doi: 10.1080/01457630601064611.

Bohner, H. F., & Bradley, R. L. (1992). Effective cleaning and sanitizing of polysulfone ultrafiltration membrane systems. *Journal of Dairy Science, 75*(3), 718–724, doi: 10.3168/jds.s0022-0302(92)77808-4.

Bonfatti, V., Grigoletto, L., Cecchinato, A., Gallo, L., & Carnier, P. (2008). Validation of a new reversed-phase high-performance liquid chromatography method for separation and quantification of bovine milk protein genetic variants. *Journal of Chromatography. A, 1195*(1-2), 101–106, doi: 10.1016/j.chroma.2008.04.075.

Bonizzi, I., Buffoni, J. N., & Feligini, M. (2009). Quantification of bovine casein fractions by direct chromatographic analysis of milk. Approaching the application to a real production context. *Journal of Chromatography. A, 1216*(1), 165–168, doi: 10.1016/j.chroma.2008.11.045.

Boonthanon, S., Hwan, L., Vigneswaran, S., Aim, R., & More, J. C. (1991). Application of pulsating cleaning technique in crossflow microfiltration. *Filtration & Separation, 28*(3), 199–201, doi: 10.1016/0015-1882(91)80076-H.

Bouchoux, A., Cayemitte, P.-E., Jardin, J., Gésan-Guiziou, G., & Cabane, B. (2009). Casein micelle dispersions under osmotic stress. *Biophysical Journal, 96*(2), 693–706, doi: 10.1016/j.bpj.2008.10.006.

Bouchoux, A., Gésan-Guiziou, G., Pérez, J., & Cabane, B. (2010). How to squeeze a sponge: casein micelles under osmotic stress, a SAXS study. *Biophysical Journal, 99*(11), 3754–3762, doi: 10.1016/j.bpj.2010.10.019.

Bradford, M. M. (1976). A rapid and sensitive method for the quantitation of microgram quantities of protein utilizing the principle of protein-dye binding. *Analytical Biochemistry, 72*(1-2), 248–254, doi: 10.1016/0003-2697(76)90527-3.

Brans, G., Schroën, C. G., van der Sman, R. G., & Boom, R. M. (2004). Membrane fractionation of milk: state of the art and challenges. *Journal of Membrane Science, 243*(1-2), 263–272, doi: 10.1016/j.memsci.2004.06.029.

Burgess, S. A., Lindsay, D., & Flint, S. H. (2010). Thermophilic bacilli and their importance in dairy processing. *International Journal of Food Microbiology, 144*(2), 215–225, doi: 10.1016/j.ijfoodmicro.2010.09.027.

Byhlin, H., & Jönsson, A.-S. (2003). Influence of adsorption and concentration polarisation on membrane performance during ultrafiltration of a non-ionic surfactant. *Desalination, 151*(1), 21–31, doi: 10.1016/S0011-9164(02)00969-4.

Cabero, M. L., Riera, F. A., & Álvarez, R. (1999). Rinsing of ultrafiltration ceramic membranes fouled with whey proteins: effects on cleaning procedures. *Journal of Membrane Science, 154*(2), 239–250, doi: 10.1016/S0376-7388(98)00294-4.

Calderone, V., Giuffrida, M. G., Viterbo, D., Napolitano, L., Fortunato, D., Conti, A., et al. (1996). Amino acid sequence and crystal structure of buffalo alpha-lactalbumin. *FEBS letters, 394*(1), 91–95, doi: 10.1016/0014-5793(96)00933-7.

Camacho, F. J., Martinez, R., & Rendon, L. (2012). *The Richardson's Annular effect and a transient solution of oscillating pressure-driven flow in circular pipes* .

Carrascosa, C., Raheem, D., Ramos, F., Saraiva, A., & Raposo, A. (2021). Microbial Biofilms in the Food Industry-A Comprehensive Review. *International journal of environmental research and public health, 18*(4), doi: 10.3390/ijerph18042014.

Causserand, C., Rouaix, S., Lafaille, J.-P., & Aimar, P. (2006). Degradation of polysulfone membranes due to contact with bleaching solution. *Desalination, 199*(1-3), 70–72, doi: 10.1016/j.desal.2006.03.144.

Chamberland, J., Messier, T., Dugat-Bony, E., Lessard, M.-H., Labrie, S., Doyen, A., et al. (2019). Influence of feed temperature to biofouling of ultrafiltration membrane during skim milk processing. *International Dairy Journal, 93*, 99–105, doi: 10.1016/j.idairyj.2019.02.005.

Chang, H., Liang, H., Qu, F., Liu, B., Yu, H., Du, X., et al. (2017). Hydraulic backwashing for low-pressure membranes in drinking water treatment: A review. *Journal of Membrane Science, 540*, 362–380, doi: 10.1016/j.memsci.2017.06.077.

Chang, S., & Fane, A. (2001). The effect of fibre diameter on filtration and flux distribution — relevance to submerged hollow fibre modules. *Journal of Membrane Science, 184*(2), 221–231, doi: 10.1016/S0376-7388(00)00626-8.

Cheison, S. C., Lai, M.-Y., Leeb, E., & Kulozik, U. (2011). Hydrolysis of β-lactoglobulin by trypsin under acidic pH and analysis of the hydrolysates with MALDI–TOF–MS/MS. *Food Chemistry, 125*(4), 1241–1248, doi: 10.1016/j.foodchem.2010.10.042.

Chen, M., Li, Q., Cheng, L., Wang, X., Lyu, C., & Fan, Q. (2021). A Study to Investigate the Viscosity Effect on Micro-Confined Fluids Flow in Tight Formations Considering Fluid–Solid Interaction. *Frontiers in Earth Science, 9*, doi: 10.3389/feart.2021.795842.

Compton, S. J., & Jones, C. G. (1985). Mechanism of dye response and interference in the Bradford protein assay. *Analytical Biochemistry, 151*(2), 369–374, doi: 10.1016/0003-2697(85)90190-3.

Congdon, R. W., Muth, G. W., & Splittgerber, A. G. (1993). The binding interaction of Coomassie blue with proteins. *Analytical Biochemistry, 213*(2), 407–413, doi: 10.1006/abio.1993.1439.

Cui, Z. F., Jiang, Y., & Field, R. W. (2010). Fundamentals of pressure-driven membrane separation processes. In *Membrane technology* (pp. 1–18). Oxford: Elsevier.

Cui, Z. F., & Taha, T. (2003). Enhancement of ultrafiltration using gas sparging: a comparison of different membrane modules. *Journal of Chemical Technology & Biotechnology, 78*(2-3), 249–253, doi: 10.1002/jctb.763.

Cui, Z. F., & Wright, K. (1996). Flux enhancements with gas sparging in downwards crossflow ultrafiltration: performance and mechanism. *Journal of Membrane Science, 117*(1-2), 109–116, doi: 10.1016/0376-7388(96)00040-3.

Dalgleish, D. G. (2011). On the structural models of bovine casein micelles—review and possible improvements. *Soft Matter, 7*(6), 2265–2272, doi: 10.1039/C0SM00806K.

Dalgleish, D. G., & Corredig, M. (2012). The structure of the casein micelle of milk and its changes during processing. *Annual review of food science and technology, 3*, 449–467, doi: 10.1146/annurev-food-022811-101214.

Daufin, G., Merin, U., Labbé, J.-P., Quémerais, A., & Kerhervé, F. L. (1991). Cleaning of inorganic membranes after whey and milk ultrafiltration. *Biotechnology and Bioengineering, 38*(1), 82–89, doi: 10.1002/bit.260380111.

Deeth, H. C., Khusniati, T., Datta, N., & Wallace, R. B. (2002). Spoilage patterns of skim and whole milks. *The Journal of Dairy Research, 69*(2), 227–241, doi: 10.1017/s0022029901005301.

Defrance, L., & Jaffrin, M. Y. (1999). Comparison between filtrations at fixed transmembrane pressure and fixed permeate flux: application to a membrane bioreactor used for wastewater treatment. *Journal of Membrane Science, 152*(2), 203–210, doi: 10.1016/S0376-7388(98)00220-8.

Derjaguin, B., & Landau, L. (1993). Theory of the stability of strongly charged lyophobic sols and of the adhesion of strongly charged particles in solutions of electrolytes. *Progress in Surface Science, 43*(1-4), 30–59, doi: 10.1016/0079-6816(93)90013-L.

Díez, B., & Rosal, R. (2020). A critical review of membrane modification techniques for fouling and biofouling control in pressure-driven membrane processes. *Nanotechnology for Environmental Engineering, 5*(2), doi: 10.1007/s41204-020-00077-x.

Dilger, K. (2010). Selecting the right joint design and fabrication techniques. In *Advances in Structural Adhesive Bonding* (pp. 295–315). Sawston: Elsevier.

Dincau, B., Tang, C., Dressaire, E., & Sauret, A. (2022). Clog mitigation in a microfluidic array via pulsatile flows. *Soft Matter, 18*(9), 1767–1778, doi: 10.1039/d2sm00013j.

Ding, L., Al-Akoum, O., Abraham, A., & Jaffrin, M. Y. (2002). Milk protein concentration by ultrafiltration with rotating disk modules. *Desalination, 144*(1-3), 307–311, doi: 10.1016/S0011-9164(02)00334-X.

Doudiès, F., Loginov, M., Hengl, N., Karrouch, M., Leconte, N., Garnier-Lambrouin, F., et al. (2021). Build-up and relaxation of membrane fouling deposits produced during crossflow ultrafiltration of casein micelle dispersions at 12 °C and 42 °C probed by in situ SAXS. *Journal of Membrane Science, 618*, 118700, doi: 10.1016/j.memsci.2020.118700.

D'Souza, N. M., & Mawson, A. J. (2005). Membrane cleaning in the dairy industry: a review. *Critical Reviews in Food Science and Nutrition, 45*(2), 125–134, doi: 10.1080/10408690490911783.

Dumpler, J., Wohlschläger, H., & Kulozik, U. (2017). Dissociation and coagulation of caseins and whey proteins in concentrated skim milk heated by direct steam injection. *Dairy Science & Technology, 96*(6), 807–826, doi: 10.1007/s13594-016-0304-3.

Duriyabunleng, H., Petmunee, J., & Muangnapoh, C. (2001). Effects of the Ultrasonic Waves on Microfiltration in Plate and Frame Module. *Journal of Chemical Engineering of Japan, 34*(8), 985–989, doi: 10.1252/jcej.34.985.

Ebrahimi, M., Kerker, S., Schmitz, O., Schmidt, A. A., & Czermak, P. (2018). Evaluation of the fouling potential of ceramic membrane configurations designed for the treatment of oilfield produced water. *Separation Science and Technology, 53*(2), 349–363, doi: 10.1080/01496395.2017.1386217.

Efome, J. E., Rana, D., Matsuura, T., & Lan, C. Q. (2016). Enhanced performance of PVDF nanocomposite membrane by nanofiber coating: A membrane for sustainable desalination through MD. *Water research, 89*, 39–49, doi: 10.1016/j.watres.2015.11.040.

EHEDG (2018). DOC 8: Hygienic Design Principles (3rd edn). Frankfurt: EHEDG Guidelines.

Engler, J. (2000). Particle fouling of a rotating membrane disk. *Water research, 34*(2), 557–565, doi: 10.1016/S0043-1354(99)00148-7.

Faibish, R. S., Elimelech, M., & Cohen, Y. (1998). Effect of Interparticle Electrostatic Double Layer Interactions on Permeate Flux Decline in Crossflow Membrane Filtration of Colloidal Suspensions: An Experimental Investigation. *Journal of colloid and interface science, 204*(1), 77–86, doi: 10.1006/jcis.1998.5563.

Falade, J. A., Ukaegbu, J. C., Egere, A. C., & Adesanya, S. O. (2017). MHD oscillatory flow through a porous channel saturated with porous medium. *Alexandria Engineering Journal, 56*(1), 147–152, doi: 10.1016/j.aej.2016.09.016.

Fan, L., Chen, X. D., & Mercadé-Prieto, R. (2019). On the nature of the optimum cleaning concentration for dairy fouling: High NaOH concentrations inhibit the cleavage of non-covalent interactions in whey protein aggregates. *LWT - Food Science and Technology, 101*, 519–525, doi: 10.1016/j.lwt.2018.11.050.

Farhat, N. M., Staal, M., Bucs, S., van Loosdrecht, M., & Vrouwenvelder, J. S. (2016). Spatial heterogeneity of biofouling under different cross-flow velocities in reverse osmosis membrane systems. *Journal of Membrane Science, 520*, 964–971, doi: 10.1016/j.memsci.2016.08.065.

Farrell, H. M., Jimenez-Flores, R., Bleck, G. T., Brown, E. M., Butler, J. E., Creamer, L. K., et al. (2004). Nomenclature of the proteins of cows' milk--sixth revision. *Journal of Dairy Science, 87*(6), 1641–1674, doi: 10.3168/jds.S0022-0302(04)73319-6.

Field, R. W., Hughes, D., Cui, Z. F., & Tirlapur, U. (2008). Some observations on the chemical cleaning of fouled membranes. *Desalination, 227*(1-3), 132–138, doi: 10.1016/j.desal.2007.08.004.

Field, R. W., Wu, D., Howell, J. A., & Gupta, B. B. (1995). Critical flux concept for microfiltration fouling. *Journal of Membrane Science, 100*(3), 259–272, doi: 10.1016/0376-7388(94)00265-Z.

Fischer, N., Masoudian, M., & Germann, N. (2020). Impact of non-Newtonian fluid behavior on hydrodynamics and mass transfer in spacer-filled channels. *Fluid Dynamics Research, 52*(6), 65502, doi: 10.1088/1873-7005/abb91e.

Flint, S. H., Brooks, J., Bremer, P., Walker, K., & Hausman, E. (2002). The resistance to heat of thermo-resistant streptococci attached to stainless steel in the presence of milk. *Journal of industrial microbiology & biotechnology, 28*(3), 134–136, doi: 10.1038/sj.jim.7000229.

Föste, H., Schöler, M., Majschak, J.-P., Augustin, W., & Scholl, S. (2013). Modeling and validation of the mechanism of pulsed flow cleaning. *Heat Transfer Engineering, 34*(8-9), 753–760, doi: 10.1080/01457632.2012.741499.

Fox, P. F., & Brodkorb, A. (2008). The casein micelle: Historical aspects, current concepts and significance. *International Dairy Journal, 18*(7), 677–684, doi: 10.1016/j.idairyj.2008.03.002.

Fox, P. F., Uniacke-Lowe, T., McSweeney, P. L. H., & O'Mahony, J. A. (2015). *Dairy chemistry and biochemistry*. Cham, Heidelberg, New York, Dordrecht, London: Springer.

France, T. C., Bot, F., Kelly, A. L., Crowley, S. V., & O'Mahony, J. A. (2021a). The influence of temperature on filtration performance and fouling during cold microfiltration of skim milk. *Separation and Purification Technology, 262*, 118256, doi: 10.1016/j.seppur.2020.118256.

France, T. C., Kelly, A. L., Crowley, S. V., & O'Mahony, J. A. (2021b). Cold Microfiltration as an Enabler of Sustainable Dairy Protein Ingredient Innovation. *Foods, 10*(9), doi: 10.3390/foods10092091.

Frank, J. F., & Koffi, R. A. (1990). Surface-adherent Growth of Listeria monocytogenes is Associated with Increased Resistance to Surfactant Sanitizers and Heat. *Journal of Food Protection, 53*(7), 550–554, doi: 10.4315/0362-028x-53.7.550.

Gallot-Lavallee, T., LALANDE, M., & Corrieu, G. (1984). Cleaning Kinetics Modeling of Holding Tubes Fouled during Milk Pasteurization. *Journal of Food Process Engineering, 7*(2), 123–142, doi: 10.1111/J.1745-4530.1984.TB00642.X.

Gbadebo, S. A., Said, S. A. M., & Habib, M. A. (1999). Average Nusselt number correlation in the thermal entrance region of steady and pulsating turbulent pipe flows. *Heat and Mass Transfer, 35*(5), 377–381, doi: 10.1007/s002310050339.

Gebhardt, R. (2014). Effect of filtration forces on the structure of casein micelles. *Journal of Applied Crystallography, 47*(1), 29–34, doi: 10.1107/S1600576713029841.

Gebhardt, R., Steinhauer, T., Meyer, P., Sterr, J., Perlich, J., & Kulozik, U. (2012). Structural changes of deposited casein micelles induced by membrane filtration. *Faraday Discussions, 158*, 77-88; discussion 105-24, doi: 10.1039/C2FD20022H.

Geraldes, V. (2002). Flow management in nanofiltration spiral wound modules with ladder-type spacers. *Journal of Membrane Science, 203*(1-2), 87–102, doi: 10.1016/S0376-7388(01)00753-0.

Gésan, G., Daufin, G., Merin, U., Labbé, J.-P., & Quémerais, A. (1993). Fouling during constant flux crossflow microfiltration of pretreated whey. Influence of transmembrane pressure gradient. *Journal of Membrane Science, 80*(1), 131–145, doi: 10.1016/0376-7388(93)85138-M.

Gésan-Guiziou, G., Boyaval, E., & Daufin, G. (1999). Critical stability conditions in crossflow microfiltration of skimmed milk: transition to irreversible deposition. *Journal of Membrane Science, 158*(1-2), 211–222, doi: 10.1016/S0376-7388(99)00017-4.

Gésan-Guiziou, G., Sobańtka, A. P., Omont, S., Froelich, D., Rabiller-Baudry, M., Thueux, F., et al. (2019). Life Cycle Assessment of a milk protein fractionation process: Contribution of the production and the cleaning stages at unit process level. *Separation and Purification Technology, 224*, 591–610, doi: 10.1016/j.seppur.2019.05.008.

Gillham, C. R., Fryer, P. J., Hasting, A. P., & Wilson, D. I. (1999). Cleaning-in-Place of Whey Protein Fouling Deposits. *Food and Bioproducts Processing, 77*(2), 127–136, doi: 10.1205/096030899532420.

Gillham, C. R., Fryer, P. J., Hasting, A. P., & Wilson, D. I. (2000). Enhanced cleaning of whey protein soils using pulsed flows. *Journal of Food Engineering, 46*(3), 199–209, doi: 10.1016/S0260-8774(00)00083-2.

Gitis, V., Haught, R., Clark, R., Gun, J., & Lev, O. (2006). Application of nanoscale probes for the evaluation of the integrity of ultrafiltration membranes. *Journal of Membrane Science, 276*(1-2), 185–192, doi: 10.1016/j.memsci.2005.09.055.

Greene, R. F., & Pace, C. N. (1974). Urea and Guanidine Hydrochloride Denaturation of Ribonuclease, Lysozyme, α-Chymotrypsin, and b-Lactoglobulin. *Journal of Biological Chemistry, 249*(17), 5388–5393, doi: 10.1016/S0021-9258(20)79739-5.

Griggs, M. A. (1921). The Alkaline Hydrolysis of Casein. *Journal of Industrial & Engineering Chemistry, 13*(11), 1027–1028, doi: 10.1021/ie50143a032.

Grimsley, G. R., & Pace, C. N. (2004). Spectrophotometric determination of protein concentration. *Current Protocols in Protein Science, Chapter 3*, Unit 3.1, doi: 10.1002/0471140864.ps0301s33.

Grote, K.-H., Bender, B., & Göhlich, D. (Eds.) (2018). *Dubbel - Taschenbuch für den Maschinenbau* (25th edn). Berlin, Germany: Springer Vieweg.

Gu, B., Adjiman, C. S., & Xu, X. Y. (2017). The effect of feed spacer geometry on membrane performance and concentration polarisation based on 3D CFD simulations. *Journal of Membrane Science, 527*, 78–91, doi: 10.1016/j.memsci.2016.12.058.

Gupta, B. B., Blanpain-Avet, P., & Jaffrin, M. Y. (1992). Permeate flux enhancement by pressure and flow pulsations in microfiltration with mineral membranes. *Journal of Membrane Science, 70*(2-3), 257–266, doi: 10.1016/0376-7388(92)80111-V.

Habenicht, G. (2008). *Kleben: Grundlagen, Technologien, Anwendungen* (6th edn, VDI-Buch). Berlin, Heidelberg: Springer Berlin Heidelberg.

Hadzismajlovic, D. E., & Bertram, C. D. (1998). Flux enhancement in laminar crossflow microfiltration using a collapsible-tube pulsation generator. *Journal of Membrane Science, 142*(2), 173–189, doi: 10.1016/S0376-7388(97)00319-0.

Hadzismajlovic, D. E., & Bertram, C. D. (1999). Flux enhancement in turbulent crossflow microfiltration of yeast using a collapsible-tube pulsation generator. *Journal of Membrane Science, 163*(1), 123–134, doi: 10.1016/S0376-7388(99)00161-1.

Han, Q., Lay, H. T., Li, W., & Chew, J. W. (2021). Effect of initial particle deposition rate on cake formation during dead-end microfiltration. *Journal of Membrane Science, 618*, 118672, doi: 10.1016/j.memsci.2020.118672.

Han, Q., Li, W., Trinh, T. an, Fane, A. G., & Chew, J. W. (2018a). Effect of the surface charge of monodisperse particulate foulants on cake formation. *Journal of Membrane Science, 548*, 108–116, doi: 10.1016/j.memsci.2017.11.017.

Han, Z., Terashima, M., Liu, B., & Yasui, H. (2018b). CFD investigation of the effect of the feed spacer on hydrodynamics in spiral wound membrane modules. *Mathematical and Computational Applications, 23*(4), 80, doi: 10.3390/mca23040080.

Hargrove, S. C., & Ilias, S. (1999). Flux Enhancement using Flow Reversal in Ultrafiltration. *Separation Science and Technology, 34*(6-7), 1319–1331, doi: 10.1080/01496399908951095.

Hargrove, S. C., Parthasarathy, H., & Ilias, S. (2003). Flux Enhancement in Cross-Flow Membrane Filtration by Flow Reversal: A Case Study on Ultrafiltration of BSA. *Separation Science and Technology, 38*(12-13), 3133–3144, doi: 10.1081/SS-120022590.

Hartinger, M., Heidebrecht, H.-J., Schiffer, S., Dumpler, J., & Kulozik, U. (2019a). Milk protein fractionation by means of spiral-wound microfiltration membranes: effect of the pressure adjustment mode and temperature on flux and protein permeation. *Foods, 8*(6), doi: 10.3390/foods8060180.

Hartinger, M., Heidebrecht, H.-J., Schiffer, S., Dumpler, J., & Kulozik, U. (2019b). Technical concepts for the investigation of spatial effects in spiral-wound microfiltration membranes. *Membranes, 9*(7), doi: 10.3390/membranes9070080.

Hartinger, M., Napiwotzki, J., Schmid, E.-M., Hoffmann, D., Kurz, F., & Kulozik, U. (2020a). Influence of spacer design and module geometry on the filtration performance during skim milk microfiltration with flat sheet and spiral-wound membranes. *Membranes, 10*(4), doi: 10.3390/membranes10040057.

Hartinger, M., Napiwotzki, J., Schmid, E.-M., Kurz, F., & Kulozik, U. (2020b). Semi-quantitative, spatially resolved analysis of protein deposit layers on membrane surfaces. *MethodsX, 7*, 100780, doi: 10.1016/j.mex.2019.100780.

Hartinger, M., Schiffer, S., Heidebrecht, H.-J., Dumpler, J., & Kulozik, U. (2019c). Investigation on the spatial filtration performance in spiral-wound membranes – Influence and length-dependent adjustment of the transmembrane pressure. *Journal of Membrane Science, 591*, 117311, doi: 10.1016/j.memsci.2019.117311.

Hartinger, M., Schiffer, S., Heidebrecht, H.-J., Dumpler, J., & Kulozik, U. (2020c). Milk protein fractionation by custom-made prototypes of spiral-wound microfiltration membranes operated at extreme crossflow velocities. *Journal of Membrane Science, 605*, 118110, doi: 10.1016/j.memsci.2020.118110.

Hashim, N. A., Liu, Y., & Li, K. (2011). Stability of PVDF hollow fibre membranes in sodium hydroxide aqueous solution. *Chemical Engineering Science, 66*(8), 1565–1575, doi: 10.1016/j.ces.2010.12.019.

Hashino, M., Hirami, K., Ishigami, T., Ohmukai, Y., Maruyama, T., Kubota, N., et al. (2011). Effect of kinds of membrane materials on membrane fouling with BSA. *Journal of Membrane Science, 384*(1-2), 157–165, doi: 10.1016/j.memsci.2011.09.015.

Heidebrecht, H.-J., & Kulozik, U. (2019). Fractionation of casein micelles and minor proteins by microfiltration in diafiltration mode. Study of the transmission and yield of the immunoglobulins IgG, IgA and IgM. *International Dairy Journal, 93*, 1–10, doi: 10.1016/j.idairyj.2019.01.009.

Hennion, M.-C. (1999). Solid-phase extraction: method development, sorbents, and coupling with liquid chromatography. *Journal of Chromatography. A, 856*(1-2), 3–54, doi: 10.1016/S0021-9673(99)00832-8.

Ho, C. C., & Zydney, A. L. (2000). A Combined Pore Blockage and Cake Filtration Model for Protein Fouling during Microfiltration. *Journal of colloid and interface science, 232*(2), 389–399, doi: 10.1006/jcis.2000.7231.

Holt, C. (2004). An equilibrium thermodynamic model of the sequestration of calcium phosphate by casein micelles and its application to the calculation of the partition of salts in milk. *European biophysics journal : EBJ, 33*(5), 421–434, doi: 10.1007/s00249-003-0377-9.

Holt, C., Carver, J. A., Ecroyd, H., & Thorn, D. C. (2013). Invited review: Caseins and the casein micelle: their biological functions, structures, and behavior in foods. *Journal of Dairy Science, 96*(10), 6127–6146, doi: 10.3168/jds.2013-6831.

Holzmüller, W., & Kulozik, U. (2016). Protein quantification by means of a stain-free SDS-PAGE technology without the need for analytical standards: Verification and validation of the method. *Journal of Food Composition and Analysis, 48*, 128–134, doi: 10.1016/j.jfca.2016.03.003.

Horne, D. S. (2003). Casein micelles as hard spheres: limitations of the model in acidified gel formation. *Colloids and Surfaces A: Physicochemical and Engineering Aspects, 213*(2-3), 255–263, doi: 10.1016/S0927-7757(02)00518-6.

Horne, D. S. (2020). Casein micelle structure and stability. In *Milk proteins* (pp. 213–250). Cambridge: Elsevier.

Horne, D. S., & Dalgleish, D. G. (1980). Electrostatic interaction and the kinetics of protein aggregation: αs1-casein. *International Journal of Biological Macromolecules, 2*(3), 154–160, doi: 10.1016/0141-8130(80)90067-7.

Hou, Y., Wu, Z., Dai, Z., Wang, G., & Wu, G. (2017). Protein hydrolysates in animal nutrition: Industrial production, bioactive peptides, and functional significance. *Journal of animal science and biotechnology, 8*, 24, doi: 10.1186/s40104-017-0153-9.

Howell, J. A., Field, R. W., & Wu, D. (1993). Yeast cell microfiltration: Flux enhancement in baffled and pulsatile flow systems. *Journal of Membrane Science, 80*(1), 59–71, doi: 10.1016/0376-7388(93)85132-G.

Huang, J., Luo, J., Chen, X., Feng, S., & Wan, Y. (2021). New insights into effect of alkaline cleaning on fouling behavior of polyamide nanofiltration membrane for wastewater treatment. *The Science of the Total Environment, 780*, 146632, doi: 10.1016/j.scitotenv.2021.146632.

Huisman, I. H., Prádanos, P., & Hernández, A. (2000). The effect of protein–protein and protein–membrane interactions on membrane fouling in ultrafiltration. *Journal of Membrane Science, 179*(1-2), 79–90, doi: 10.1016/S0376-7388(00)00501-9.

Hurt, E. E., Adams, M. C., & Barbano, D. M. (2015). Microfiltration: Effect of channel diameter on limiting flux and serum protein removal. *Journal of Dairy Science, 98*(6), 3599–3612, doi: 10.3168/jds.2014-9225.

Igbinigun, E., Fennell, Y., Malaisamy, R., Jones, K. L., & Morris, V. (2016). Graphene oxide functionalized polyethersulfone membrane to reduce organic fouling. *Journal of Membrane Science, 514*, 518–526, doi: 10.1016/j.memsci.2016.05.024.

Ishak, A., Merkin, J. H., Nazar, R., & Pop, I. (2008). Mixed convection boundary layer flow over a permeable vertical surface with prescribed wall heat flux. *Zeitschrift für angewandte Mathematik und Physik, 59*(1), 100–123, doi: 10.1007/s00033-006-6082-7.

Jaffrin, M. Y., Gupta, B. B., & Paullier, P. (1994). Energy saving pulsatile mode cross flow filtration. *Journal of Membrane Science, 86*(3), 281–290, doi: 10.1016/0376-7388(93)E0151-9.

Jaleh, B., Etivand, E. S., Mohazzab, B. F., Nasrollahzadeh, M., & Varma, R. S. (2019). Improving Wettability: Deposition of TiO2 Nanoparticles on the O2 Plasma Activated Polypropylene Membrane. *International journal of molecular sciences, 20*(13), doi: 10.3390/ijms20133309.

Jennings, W. G., McKillop, A. A., & Luick, J. K. (1957). Circulation Cleaning. *Journal of Dairy Science, 40*(11), 1471–1479, doi: 10.3168/jds.S0022-0302(57)94658-1.

Jha, B. K., & Ajibade, A. O. (2009). Free convective flow of heat generating/absorbing fluid between vertical porous plates with periodic heat input. *International Communications in Heat and Mass Transfer, 36*(6), 624–631, doi: 10.1016/j.icheatmasstransfer.2009.03.003.

Jimenez-Lopez, A. J., Leconte, N., Dehainault, O., Geneste, C., Fromont, L., & Gésan-Guiziou, G. (2008). Role of milk constituents on critical conditions and deposit structure in

skim milk microfiltration (0.1µm). *Separation and Purification Technology, 61*(1), 33–43, doi: 10.1016/j.seppur.2007.09.023.

Jin, Y., Hengl, N., Baup, S., Pignon, F., Gondrexon, N., Sztucki, M., et al. (2014). Effects of ultrasound on cross-flow ultrafiltration of skim milk: Characterization from macro-scale to nano-scale. *Journal of Membrane Science, 470*, 205–218, doi: 10.1016/j.memsci.2014.07.043.

Kaneda, M., Lu, X., Cheng, W., Zhou, X., Bernstein, R., Zhang, W., et al. (2019). Photografting Graphene Oxide to Inert Membrane Materials to Impart Antibacterial Activity. *Environmental Science & Technology Letters, 6*(3), 141–147, doi: 10.1021/acs.estlett.9b00012.

Karabelas, A. J., Koutsou, C. P., & Sioutopoulos, D. C. (2018). Comprehensive performance assessment of spacers in spiral-wound membrane modules accounting for compressibility effects. *Journal of Membrane Science, 549*, 602–615, doi: 10.1016/j.memsci.2017.12.037.

Kasemset, S., He, Z., Miller, D. J., Freeman, B. D., & Sharma, M. M. (2016). Effect of polydopamine deposition conditions on polysulfone ultrafiltration membrane properties and threshold flux during oil/water emulsion filtration. *Polymer, 97*, 247–257, doi: 10.1016/j.polymer.2016.04.064.

Kavianipour, O., Ingram, G. D., & Vuthaluru, H. B. (2017). Investigation into the effectiveness of feed spacer configurations for reverse osmosis membrane modules using Computational Fluid Dynamics. *Journal of Membrane Science, 526*, 156–171, doi: 10.1016/j.memsci.2016.12.034.

Kazemimoghadam, M., & Mohammadi, T. (2007). Chemical cleaning of ultrafiltration membranes in the milk industry. *Desalination, 204*(1-3), 213–218, doi: 10.1016/j.desal.2006.04.030.

Kessler, H. G. (1996). *Lebensmittel- und Bioverfahrenstechnik: Molkereitechnologie* (4th edn). München: Kessler.

Kieferle, I., & Kulozik, U. (2021). Importance of process conditions in the displacement of protein concentrates from spiral-wound membrane modules. *Food and Bioproducts Processing, 126*, 51–61, doi: 10.1016/j.fbp.2020.12.002.

Kim, K.-J., & Fane, A. G. (1995). Performance evaluation of surface hydrophilized novel ultrafiltration membranes using aqueous proteins. *Journal of Membrane Science, 99*(2), 149–162, doi: 10.1016/0376-7388(94)00215-K.

Kim, K.-J., Sun, P., Chen, V., Wiley, D. E., & Fane, A. G. (1993). The cleaning of ultrafiltration membranes fouled by protein. *Journal of Membrane Science, 80*(1), 241–249, doi: 10.1016/0376-7388(93)85148-P.

Kim, Y.-B., Lee, K., & Chung, J.-H. (2002). Optimum cleaning-in-place conditions for stainless steel microfiltration membrane fouled by terephthalic acid solids. *Journal of Membrane Science, 209*(1), 233–240, doi: 10.1016/S0376-7388(02)00347-2.

Koutsou, C. P., Yiantsios, S. G., & Karabelas, A. J. (2007). Direct numerical simulation of flow in spacer-filled channels: Effect of spacer geometrical characteristics. *Journal of Membrane Science, 291*(1-2), 53–69, doi: 10.1016/j.memsci.2006.12.032.

Koutsou, C. P., Yiantsios, S. G., & Karabelas, A. J. (2009). A numerical and experimental study of mass transfer in spacer-filled channels: Effects of spacer geometrical characteristics and Schmidt number. *Journal of Membrane Science, 326*(1), 234–251, doi: 10.1016/j.memsci.2008.10.007.

Kraume, M. (2012). *Transportvorgänge in der Verfahrenstechnik: Grundlagen und apparative Umsetzungen* (2nd edn, VDI-Buch). Berlin, Heidelberg: Springer Berlin Heidelberg.

Krstić, D. M., Tekić, M. N., Carić, M. Đ., & Milanović, S. D. (2002). The effect of turbulence promoter on cross-flow microfiltration of skim milk. *Journal of Membrane Science, 208*(1-2), 303–314, doi: 10.1016/S0376-7388(02)00308-3.

Kruif, C. G. de, & Zhulina, E. B. (1996). κ-casein as a polyelectrolyte brush on the surface of casein micelles. *Colloids and Surfaces A: Physicochemical and Engineering Aspects, 117*(1-2), 151–159, doi: 10.1016/0927-7757(96)03696-5.

Kuberkar, V. T., & Davis, R. H. (1999). Effects of added yeast on protein transmission and flux in cross-flow membrane microfiltration. *Biotechnology progress, 15*(3), 472–479, doi: 10.1021/bp990023l.

Kühnl, W., Piry, A., Kaufmann, V., Grein, T., Ripperger, S., & Kulozik, U. (2010). Impact of colloidal interactions on the flux in cross-flow microfiltration of milk at different pH values: A surface energy approach. *Journal of Membrane Science, 352*(1-2), 107–115, doi: 10.1016/j.memsci.2010.02.006.

Kulozik, U., & Kersten, M. (2002a). Membrane Fractionation of Dairy Proteins by Means of Microfiltration. *Engineering in Life Sciences, 2*(9), 275–278, doi: 10.1002/1618-2863(20020910)2:9%3C275:AID-ELSC275%3E3.0.CO;2-6.

Kulozik, U., & Kersten, M. (2002b). New ways for the fractionation of dairy and minor constituents using utp-membrane technology. In Bulletin-International Dairy Federation (Ed.) (374th ed., Vol. 374, pp 37-42). Brussels, Belgium: International Dairy Federation.

Kumar, R., & Ismail, A. F. (2015). Fouling control on microfiltration/ultrafiltration membranes: Effects of morphology, hydrophilicity, and charge. *Journal of Applied Polymer Science, 132*(21), n/a-n/a, doi: 10.1002/app.42042.

Kürzl, C., Hartinger, M., Ong, P., Schopf, R., Schiffer, S., & Kulozik, U. (2023). Increasing Performance of Spiral-Wound Modules (SWMs) by Improving Stability against Axial

Pressure Drop and Utilising Pulsed Flow. *Membranes, 13*(9), 791, doi: 10.3390/membranes13090791.

Kürzl, C., & Kulozik, U. (2023a). Alternating flow direction improves chemical cleaning efficiency in hollow fibre membranes following skim milk microfiltration. *Journal of Food Engineering, 356*, 111587, doi: 10.1016/j.jfoodeng.2023.111587.

Kürzl, C., & Kulozik, U. (2023b). Comparison of the efficiency of pulsed flow membrane cleaning in hollow fibre (HFM) and spiral-wound microfiltration membranes (SWM). *Food and Bioproducts Processing*(139), 166–177, doi: 10.1016/j.fbp.2023.03.012.

Kürzl, C., & Kulozik, U. (2023c). Influence of Pulsed and Alternating Flow on the Filtration Performance during Skim Milk Microfiltration with Flat-Sheet Membranes. *Separation and Purification Technology*(321), 124234, doi: 10.1016/j.seppur.2023.124234.

Kürzl, C., Tran, T., & Kulozik, U. (2022a). Application of a pulsed crossflow to improve chemical cleaning efficiency in hollow fibre membranes following skim milk microfiltration. *Separation and Purification Technology*(302), 122123, doi: 10.1016/j.seppur.2022.122123.

Kürzl, C., Wohlschläger, H., Schiffer, S., & Kulozik, U. (2022b). Concentration, purification and quantification of milk protein residues following cleaning processes using a combination of SPE and RP-HPLC. *MethodsX*(9), 101695, doi: 10.1016/j.mex.2022.101695.

Laksono, S., El Sherbiny, I. M., Huber, S. A., & Panglisch, S. (2021). Fouling scenarios in hollow fiber membranes during mini-plant filtration tests and correlation to microalgae-loaded feed characteristics. *Chemical Engineering Journal, 420*, 127723, doi: 10.1016/j.cej.2020.127723.

Lee, H., Amy, G., Cho, J., Yoon, Y., Moon, S. H., & Kim, I. S. (2001). Cleaning strategies for flux recovery of an ultrafiltration membrane fouled by natural organic matter. *Water research, 35*(14), 3301–3308, doi: 10.1016/s0043-1354(01)00063-x.

Lee, S., & Elimelech, M. (2007). Salt cleaning of organic-fouled reverse osmosis membranes. *Water research, 41*(5), 1134–1142, doi: 10.1016/j.watres.2006.11.043.

Lehmkuhl, S., Wiese, M., Schubert, L., Held, M., Küppers, M., Wessling, M., et al. (2018). Continuous hyperpolarization with parahydrogen in a membrane reactor. *Journal of magnetic resonance (San Diego, Calif. : 1997), 291*, 8–13, doi: 10.1016/j.jmr.2018.03.012.

Lelièvre, C., Legentilhomme, P., Gaucher, C., Legrand, J., Faille, C., & Bénézech, T. (2002). Cleaning in place: effect of local wall shear stress variation on bacterial removal from stainless steel equipment. *Chemical Engineering Science, 57*(8), 1287–1297, doi: 10.1016/S0009-2509(02)00019-2.

Li, F., Meng, J., Ye, J., Yang, B., Tian, Q., & Deng, C. (2014). Surface modification of PES ultrafiltration membrane by polydopamine coating and poly(ethylene glycol) grafting: Morphology, stability, and anti-fouling. *Desalination, 344*, 422–430, doi: 10.1016/j.desal.2014.04.011.

Li, H., Bertram, C. D., & Wiley, D. E. (1998). Mechanisms by which pulsatile flow affects cross-flow microfiltration. *AIChE Journal, 44*(9), 1950–1961, doi: 10.1002/aic.690440903.

Li, Q., & Elimelech, M. (2004). Organic fouling and chemical cleaning of nanofiltration membranes: measurements and mechanisms. *Environmental science & technology, 38*(17), 4683–4693, doi: 10.1021/es0354162.

Liao, Y., Wang, R., Tian, M., Qiu, C., & Fane, A. G. (2013). Fabrication of polyvinylidene fluoride (PVDF) nanofiber membranes by electro-spinning for direct contact membrane distillation. *Journal of Membrane Science, 425-426*, 30–39, doi: 10.1016/j.memsci.2012.09.023.

Lowry, O. H., Roseborough, N. J., Farr, A. L., & Randall, R. J. (1951). Protein measurement with the Folin phenol reagent. *Journal of Biological Chemistry, 193*(1), 265–275.

Luelf, T., Bremer, C., & Wessling, M. (2016). Rope coiling spinning of curled and meandering hollow-fiber membranes. *Journal of Membrane Science, 506*, 86–94, doi: 10.1016/j.memsci.2016.01.037.

Luelf, T., Tepper, M., Breisig, H., & Wessling, M. (2017). Sinusoidal shaped hollow fibers for enhanced mass transfer. *Journal of Membrane Science, 533*, 302–308, doi: 10.1016/j.memsci.2017.03.030.

Maartens, A., Jacobs, E. P., & Swart, P. (2002). UF of pulp and paper effluent: membrane fouling-prevention and cleaning. *Journal of Membrane Science, 209*(1), 81–92, doi: 10.1016/S0376-7388(02)00266-1.

Mahon, H. I. (1966). Permeability separatory apparatus, permeability separatory membrane element, method of making the same and process utilizing the same: US Patent (US3228876A).

Makardij, A. A., Chen, X. D., & Farid, M. M. (1999). Microfiltration and ultrafiltration of milk: some aspects of fouling and cleaning. *Food and Bioproducts Processing*(2), 107–113, doi: 10.1205/096030899532394.

Matsumoto, K., Kawahara, M., & Ohya, H. (1988). Cross-flow filtration of yeast by microporous ceramic membrane with backwashing. *Journal of Fermentation Technology, 66*(2), 199–205, doi: 10.1016/0385-6380(88)90048-9.

Matzinos, P., & Álvarez, R. (2002). Effect of ionic strength on rinsing and alkaline cleaning of ultrafiltration inorganic membranes fouled with whey proteins. *Journal of Membrane Science, 208*(1-2), 23–30, doi: 10.1016/S0376-7388(02)00133-3.

Melin, T., & Rautenbach, R. (2007). *Membranverfahren: Grundlagen der Modul- und Anlagenauslegung* (3rd edn, VDI-Buch). Berlin, Heidelberg: Springer Berlin Heidelberg.

Mercadé-Prieto, R., & Chen, X. D. (2005). Caustic-induced gelation of whey deposits in the alkali cleaning of membranes. *Journal of Membrane Science, 254*(1-2), 157–167, doi: 10.1016/j.memsci.2004.12.038.

Mercadé-Prieto, R., Paterson, W. R., Dong Chen, X., & Wilson, D. I. (2008). Diffusion of NaOH into a protein gel. *Chemical Engineering Science, 63*(10), 2763–2772, doi: 10.1016/j.ces.2008.02.029.

Meyer, P., Mayer, A., & Kulozik, U. (2015). High concentration of skim milk proteins by ultrafiltration: Characterisation of a dynamic membrane system with a rotating membrane in comparison with a spiral wound membrane. *International Dairy Journal, 51*, 75–83, doi: 10.1016/j.idairyj.2015.07.010.

Mores, W. D., & Davis, R. H. (2002). Yeast foulant removal by backpulses in crossflow microfiltration. *Journal of Membrane Science, 208*(1-2), 389–404, doi: 10.1016/S0376-7388(02)00319-8.

Mores, W. D., & Davis, R. H. (2003). Yeast-Fouling Effects in Cross-Flow Microfiltration with Periodic Reverse Filtration. *Industrial & Engineering Chemistry Research, 42*(1), 130–139, doi: 10.1021/ie020421k.

Muñoz-Aguado, M. J., Wiley, D. E., & Fane, A. G. (1996). Enzymatic and detergent cleaning of a polysulfone ultrafiltration membrane fouled with BSA and whey. *Journal of Membrane Science, 117*(1-2), 175–187, doi: 10.1016/0376-7388(96)00066-X.

Neal, P. R., Li, H., Fane, A. G., & Wiley, D. E. (2003). The effect of filament orientation on critical flux and particle deposition in spacer-filled channels. *Journal of Membrane Science, 214*(2), 165–178, doi: 10.1016/S0376-7388(02)00500-8.

Ng, K. S., Dunstan, D. E., & Martin, G. J. (2018). Influence of processing temperature on flux decline during skim milk ultrafiltration. *Separation and Purification Technology, 195*, 322–331, doi: 10.1016/j.seppur.2017.12.029.

Ng, K. S., Haribabu, M., Harvie, D. J., Dunstan, D. E., & Martin, G. J. (2017). Mechanisms of flux decline in skim milk ultrafiltration: A review. *Journal of Membrane Science, 523*, 144–162, doi: 10.1016/j.memsci.2016.09.036.

Nielsen, E. B., & Schellman, J. A. (1967). The absorption spectra of simple amides and peptides. *Journal of Physical Chemistry. A, 71*(7), 2297–2304, doi: 10.1021/j100866a051.

Nigam, M. O., Bansal, B., & Chen, X. D. (2008). Fouling and cleaning of whey protein concentrate fouled ultrafiltration membranes. *Desalination, 218*(1-3), 313–322, doi: 10.1016/j.desal.2007.02.027.

Noordman, T. R., Jonge, A. de, Wesselingh, J. A., Bel, W., Dekker, M., Voorde, E., et al. (2002). Application of fluidised particles as turbulence promoters in ultrafiltration. *Journal of Membrane Science, 208*(1-2), 157–169, doi: 10.1016/S0376-7388(02)00229-6.

Olayiwola, B., & Walzel, P. (2009). Effects of in-phase oscillation of retentate and filtrate in crossflow filtration at low Reynolds number. *Journal of Membrane Science, 345*(1-2), 36–46, doi: 10.1016/j.memsci.2009.08.022.

Pace, C. N., Vajdos, F., Fee, L., Grimsley, G. R., & Gray, T. (1995). How to measure and predict the molar absorption coefficient of a protein. *Protein Science : a Publication of the Protein Society, 4*(11), 2411–2423, doi: 10.1002/pro.5560041120.

Parnham, C. S., & Davis, R. H. (1996). Protein recovery from bacterial cell debris using crossflow microfiltration with backpulsing. *Journal of Membrane Science, 118*(2), 259–268, doi: 10.1016/0376-7388(96)00108-1.

Partridge, J. A., & Furtado, M. M. (1990). Immunoperoxidase detection of whey protein soils on ultrafiltration membranes 1. *Journal of Food Protection, 53*(6), 484–488, doi: 10.4315/0362-028X-53.6.484.

Paugam, L., Delaunay, D., & Rabiller-Baudry, M. (2010). Cleaning efficiency and impact on production fluxes of oxidising disinfectants on a pes ultrafiltration membrane fouled with proteins. *Food and Bioproducts Processing, 88*(4), 425–429, doi: 10.1016/j.fbp.2010.10.005.

Pérez-Herranz, V., Guiñón, J. L., & García-Antón, J. (1999). Analysis of mass and momentum transfer in an annular electrodialysis cell in pulsed flow. *Chemical Engineering Science, 54*(11), 1667–1675, doi: 10.1016/S0009-2509(98)00537-5.

Piry, A., Kühnl, W., Grein, T., Tolkach, A., Ripperger, S., & Kulozik, U. (2008). Length dependency of flux and protein permeation in crossflow microfiltration of skimmed milk. *Journal of Membrane Science, 325*(2), 887–894.

Pollock, J., Ho, S. V., & Farid, S. S. (2013). Fed-batch and perfusion culture processes: economic, environmental, and operational feasibility under uncertainty. *Biotechnology and Bioengineering, 110*(1), 206–219, doi: 10.1002/bit.24608.

Poole, C. F., & Poole, S. K. (2002). Principles and Practice of Solid-Phase Extraction. In *Comprehensive sampling and sample preparation* (pp. 273–297): Elsevier.

Porcellato, D., Aspholm, M., Skeie, S. B., Monshaugen, M., Brendehaug, J., & Mellegård, H. (2018). Microbial diversity of consumption milk during processing and storage. *International Journal of Food Microbiology, 266*, 21–30, doi: 10.1016/j.ijfoodmicro.2017.11.004.

Porcelli, N., & Judd, S. (2010). Chemical cleaning of potable water membranes: A review. *Separation and Purification Technology, 71*(2), 137–143, doi: 10.1016/j.seppur.2009.12.007.

Puspitasari, V., Granville, A., Le-Clech, P., & Chen, V. (2010). Cleaning and ageing effect of sodium hypochlorite on polyvinylidene fluoride (PVDF) membrane. *Separation and Purification Technology, 72*(3), 301–308, doi: 10.1016/j.seppur.2010.03.001.

Qiu, T. Y., & Davies, P. A. (2015). Concentration polarization model of spiral-wound membrane modules with application to batch-mode RO desalination of brackish water. *Desalination, 368*, 36–47, doi: 10.1016/j.desal.2014.12.048.

Qu, P., Bouchoux, A., & Gésan-Guiziou, G. (2015). On the cohesive properties of casein micelles in dense systems. *Food Hydrocolloids, 43*, 753–762, doi: 10.1016/j.foodhyd.2014.08.005.

Qu, P., Gésan-Guiziou, G., & Bouchoux, A. (2012). Dead-end filtration of sponge-like colloids: The case of casein micelle. *Journal of Membrane Science, 417-418*, 10–19, doi: 10.1016/j.memsci.2012.06.003.

Rabiller-Baudry, M., Bégoin, L., Delaunay, D., Paugam, L., & Chaufer, B. (2008). A dual approach of membrane cleaning based on physico-chemistry and hydrodynamics. *Chemical Engineering and Processing: Process Intensification, 47*(3), 267–275, doi: 10.1016/j.cep.2007.01.026.

Rabiller-Baudry, M., Gésan-Guiziou, G., Roldan-Calbo, D., Beaulieu, S., & Michel, F. (2005). Limiting flux in skimmed milk ultrafiltration: impact of electrostatic repulsion due to casein micelles. *Desalination, 175*(1), 49–59, doi: 10.1016/j.desal.2004.09.022.

Rabiller-Baudry, M., Le Maux, M., Chaufer, B., & Bégoin, L. (2002). Characterisation of cleaned and fouled membrane by ATR—FTIR and EDX analysis coupled with SEM: application to UF of skimmed milk with a PES membrane. *Desalination, 146*(1-3), 123–128, doi: 10.1016/S0011-9164(02)00503-9.

Rabiller-Baudry, M., Loulergue, P., Girard, J., El Mansour El Jastimi, M., Bouzin, A., Le Gallic, M., et al. (2021). Consequences of membrane aging on real or misleading evaluation of membrane cleaning by flux measurements. *Separation and Purification Technology, 259*, 118044, doi: 10.1016/j.seppur.2020.118044.

Rabiller-Baudry, M., Paugam, L., Bégoin, L., Delaunay, D., Fernandez-Cruz, M., Phina-Ziebin, C., et al. (2006). Alkaline cleaning of PES membranes used in skimmed milk ultrafiltration: from reactor to spiral-wound module via a plate-and-frame module. *Desalination, 191*(1-3), 334–343, doi: 10.1016/j.desal.2005.07.028.

Redkar, S., Kuberkar, V., & Davis, R. H. (1996). Modeling of concentration polarization and depolarization with high-frequency backpulsing. *Journal of Membrane Science, 121*(2), 229–242, doi: 10.1016/S0376-7388(96)00179-2.

Regula, C., Carretier, E., Wyart, Y., Gésan-Guiziou, G., Vincent, A., Boudot, D., et al. (2014). Chemical cleaning/disinfection and ageing of organic UF membranes: a review. *Water research, 56*, 325–365, doi: 10.1016/j.watres.2014.02.050.

Rehan, Z. A., Gzara, L., Khan, S. B., Alamry, K. A., El-Shahawi, M. S., Albeirutty, M. H., et al. (2016). Synthesis and Characterization of Silver Nanoparticles-Filled Polyethersulfone Membranes for Antibacterial and Anti-Biofouling Application. *Recent patents on nanotechnology, 10*(3), 231–251, doi: 10.2174/1872210510666160429145228.

Richardson, E. G., & Tyler, E. (1929). The transverse velocity gradient near the mouths of pipes in which an alternating or continuous flow of air is established. *Proceedings of the Physical Society, 42*(1), 1–15, doi: 10.1088/0959-5309/42/1/302.

Ripperger, S., & Altmann, J. (2002). Crossflow microfiltration – state of the art. *Separation and Purification Technology, 26*(1), 19–31, doi: 10.1016/S1383-5866(01)00113-7.

Ripperger, S., & Grein, T. (2007). Filtrationsverfahren mit Membranen und ihre Modellierung. *Chemie Ingenieur Technik, 79*(11), 1765–1776, doi: 10.1002/cite.200700150.

Roche, J., & Royer, C. A. (2018). Lessons from pressure denaturation of proteins. *Journal of the Royal Society, Interface, 15*(147), doi: 10.1098/rsif.2018.0244.

Rodgers, V. G., & Sparks, R. E. (1992). Effect of transmembrane pressure pulsing on concentration polarization. *Journal of Membrane Science, 68*(1-2), 149–168, doi: 10.1016/0376-7388(92)80158-g.

Roth, H., Alders, M., Luelf, T., Emonds, S., Mueller, S. I., Tepper, M., et al. (2019). Chemistry in a spinneret — Sinusoidal-shaped composite hollow fiber membranes. *Journal of Membrane Science, 585*, 115–125, doi: 10.1016/j.memsci.2019.05.029.

Rott, N. (1990). Note on the History of the Reynolds Number. *Annual Review of Fluid Mechanics, 22*(1), 1–12, doi: 10.1146/annurev.fl.22.010190.000245.

Rouaix, S., Causserand, C., & Aimar, P. (2006). Experimental study of the effects of hypochlorite on polysulfone membrane properties. *Journal of Membrane Science, 277*(1-2), 137–147, doi: 10.1016/j.memsci.2005.10.040.

Samuelsson, G., Dejmek, P., Trägårdh, G., & Paulsson, M. (1997). Minimizing whey protein retention in cross-flow microfiltration of skim milk. *International Dairy Journal, 7*(4), 237–242, doi: 10.1016/S0958-6946(97)00009-5.

Saxena, A., Tripathi, B. P., Kumar, M., & Shahi, V. K. (2009). Membrane-based techniques for the separation and purification of proteins: an overview. *Advances in Colloid and Interface Science, 145*(1-2), 1–22, doi: 10.1016/j.cis.2008.07.004.

Schiffer, S., Hartinger, M., Matyssek, A., & Kulozik, U. (2020). On the reversibility of deposit formation in low temperature milk microfiltration with ceramic membranes depending on mode of adjustment of transmembrane pressure and wall shear stress. *Separation and Purification Technology, 247*, 116962, doi: 10.1016/j.seppur.2020.116962.

Schiffer, S., & Kulozik, U. (2020). Effect of temperature-dependent bacterial growth during milk protein fractionation by means of 0.1 µM microfiltration on the length of possible production cycle times. *Membranes, 10*(11), 326, doi: 10.3390/membranes10110326.

Schiffer, S., Matyssek, A., Hartinger, M., Bolduan, P., Mund, P., & Kulozik, U. (2021). Effects of selective layer properties of ceramic multi-channel microfiltration membranes on the milk protein fractionation. *Separation and Purification Technology, 259*, 118050, doi: 10.1016/j.seppur.2020.118050.

Schlichting, H., & Gersten, K. (2006). *Grenzschicht-Theorie* (10th edn). Heidelberg: Springer.

Schopf, R. (2022). *Control of deposit layer formation for optimized milk protein fractionation by microfiltration hollow fiber membranes* .

Schopf, R., Desch, F., Schmitz, R., Arar, D., & Kulozik, U. (2022). Effect of flow channel number in multi-channel tubular ceramic microfiltration membranes on flux and small protein transmission in milk protein fractionation. *Journal of Membrane Science, 644*, 120153, doi: 10.1016/j.memsci.2021.120153.

Schopf, R., & Kulozik, U. (2021). Impact of feed concentration on milk protein fractionation by hollow fiber microfiltration membranes in diafiltration mode. *Separation and Purification Technology, 276*, 119278, doi: 10.1016/j.seppur.2021.119278.

Schopf, R., Schmidt, F., & Kulozik, U. (2021a). Impact of hollow fiber membrane length on the milk protein fractionation. *Journal of Membrane Science, 620*, 118834, doi: 10.1016/J.MEMSCI.2020.118834.

Schopf, R., Schmidt, F., Linner, J., & Kulozik, U. (2021b). Comparative assessment of tubular ceramic, spiral wound, and hollow fiber membrane microfiltration Module Systems for Milk Protein Fractionation. *Foods, 10*(4), 692, doi: 10.3390/foods10040692.

Schopf, R., Schork, N., Amling, E., Nirschl, H., Guthausen, G., & Kulozik, U. (2020). Structural Characterisation of Deposit Layer during Milk Protein Microfiltration by Means of In-Situ MRI and Compositional Analysis. *Membranes, 10*(4), doi: 10.3390/membranes10040059.

Schwinge, J., Neal, P. R., Wiley, D. E., Fletcher, D. F., & Fane, A. G. (2004). Spiral wound modules and spacers. *Journal of Membrane Science, 242*(1-2), 129–153, doi: 10.1016/j.memsci.2003.09.031.

Schwinge, J., Wiley, D. E., & Fletcher, D. F. (2002). A CFD study of unsteady flow in narrow spacer-filled channels for spiral-wound membrane modules. *Desalination, 146*(1-3), 195–201, doi: 10.1016/S0011-9164(02)00470-8.

Schwinge, J., Wiley, D. E., & Fletcher, D. F. (2003). Simulation of unsteady flow and vortex shedding for narrow spacer-filled channels. *Industrial & Engineering Chemistry Research, 42*(20), 4962–4977, doi: 10.1021/ie030211n.

Scopes, R. K. (1974). Measurement of protein by spectrophotometry at 205 nm. *Analytical Biochemistry, 59*(1), 277–282, doi: 10.1016/0003-2697(74)90034-7.

Seale, B., Bremer, P., Flint, S. H., Brooks, J., & Palmer, J. (2015). Overview of the Problems Resulting from Biofilm Contamination in the Dairy Industry. In K. H. Teh, S. H. Flint, J.

Brooks, & G. Knight (Eds.), *Biofilms in the Dairy Industry* (pp. 49–64). Chichester, UK: John Wiley & Sons, Ltd.

Sharma, M. M., Chamoun, H., Sarma, D. R., & Schechter, R. S. (1992). Factors controlling the hydrodynamic detachment of particles from surfaces. *Journal of colloid and interface science, 149*(1), 121–134, doi: 10.1016/0021-9797%2892%2990398-6.

Shojaefar, M. H., Noorpoor, A. R., Avanesians, A., & Ghaffarpou, M. (2005). Numerical investigation of flow control by suction and injection on a subsonic airfoil. *American Journal of Applied Sciences, 2*(10), 1474–1480, doi: 10.3844/AJASSP.2005.1474.1480.

Shorrock, C. J., & Bird, M. R. (1998). Membrane Cleaning: Chemically Enhanced Removal of Deposits Formed During Yeast Cell Harvesting. *Food and Bioproducts Processing, 76*(1), 30–38, doi: 10.1205/096030898531729.

Singh, A. K. (1984). Stokes problem for a porous vertical plate with heat sinks by finite difference method. *Astrophysics and Space Science, 103*(2), 241–248, doi: 10.1007/BF00653740.

Siow, K. S., Britcher, L., Kumar, S., & Griesser, H. J. (2006). Plasma Methods for the Generation of Chemically Reactive Surfaces for Biomolecule Immobilization and Cell Colonization - A Review. *Plasma Processes and Polymers, 3*(6-7), 392–418, doi: 10.1002/ppap.200600021.

Smith, P. K., Krohn, R. I., Hermanson, G. T., Mallia, A. K., Gartner, F. H., Provenzano, M. D., et al. (1985). Measurement of protein using bicinchoninic acid. *Analytical Biochemistry, 150*(1), 76–85.

Spiazzi, E., Lenoir, J., & Grangeon, A. (1993). A new generator of unsteady-state flow regime in tubular membranes as an anti-fouling technique: A hydrodynamic approach. *Journal of Membrane Science, 80*(1), 49–57, doi: 10.1016/0376-7388(93)85131-F.

Springer, F., Ghidossi, R., Carretier, E., Veyret, D., Dhaler, D., & Moulin, P. (2010). Study of the Effect of Geometry on Wall Shear Stress and Permeate Flux for Ceramic Membranes: CFD and Experimental Approaches. *Engineering Applications of Computational Fluid Mechanics, 4*(1), 17–28, doi: 10.1080/19942060.2010.11015296.

Steinhauer, T., Kulozik, U., & Gebhardt, R. (2014). Structure of milk protein deposits formed by casein micelles and β-lactoglobulin during frontal microfiltration. *Journal of Membrane Science, 468*, 126–132, doi: 10.1016/j.memsci.2014.05.027.

Swaisgood, H. E. (2003). Chemistry of the caseins. In P. F. Fox & P. L. H. McSweeney (Eds.), *Advanced Dairy Chemistry-1 Proteins*: *Part A / Part B* (3rd ed., pp. 139–201, Springer eBook Collection). Boston, MA: Springer.

Tepper, M., Eminoglu, Y., Mehling, N., Walorski, J., Roth, H., & Wessling, M. (2022). Rotation-in-a-Spinneret integrates static mixers inside hollow fiber membranes. *Journal of Membrane Science, 656*, 120599, doi: 10.1016/j.memsci.2022.120599.

Tolkach, A., & Kulozik, U. (2007). Reaction kinetic pathway of reversible and irreversible thermal denaturation of β-lactoglobulin. *Le Lait, 87*(4-5), 301–315, doi: 10.1051/lait:2007012.

Töpel, A. (2016). *Chemie und Physik der Milch: Naturstoff, Rohstoff, Lebensmittel* (4th edn). Hamburg: Behr's Verlag.

Toro-Sierra, J., Tolkach, A., & Kulozik, U. (2013). Fractionation of α-Lactalbumin and β-Lactoglobulin from Whey Protein Isolate Using Selective Thermal Aggregation, an Optimized Membrane Separation Procedure and Resolubilization Techniques at Pilot Plant Scale. *Food and Bioprocess Technology, 6*(4), 1032–1043, doi: 10.1007/s11947-011-0732-2.

Trägårdh, G. (1989). Membrane cleaning. *Desalination, 71*(3), 325–335, doi: 10.1016/0011-9164(89)85033-7.

Väisänen, P., Bird, M. R., & Nyström, M. (2002). Treatment of UF membranes with simple and formulated cleaning agents. *Food and Bioproducts Processing, 80*(2), 98–108, doi: 10.1205/09603080252938735.

van der Bruggen, B. (2018). Microfiltration, ultrafiltration, nanofiltration, reverse osmosis, and forward osmosis. In *Fundamental Modelling of Membrane Systems* (pp. 25–70): Elsevier.

van Oss, C. J. (1993). Acid—base interfacial interactions in aqueous media. *Colloids and Surfaces A: Physicochemical and Engineering Aspects, 78*, 1–49, doi: 10.1016/0927-7757(93)80308-2.

van Oss, C. J. (2006). *Interfacial forces in aqueous media* (2nd edn). Boca Raton, Fla.: CRC Taylor & Francis.

van Reis, R., & Zydney, A. L. (2007). Bioprocess membrane technology. *Journal of Membrane Science, 297*(1-2), 16–50, doi: 10.1016/j.memsci.2007.02.045.

Verwey, E. J. W., & Overbeek, J. T. G. (1948). Theory of the stability of lyophobic colloids: The Interaction of Sol Particles Having an Electric Double Layer. *The Journal of physical and colloid chemistry, 51*(3), 631–636, doi: 10.1021/j150453a001.

Visser, J. (1970). Measurement of the force of adhesion between submicron carbon-black particles and a cellulose film in aqueous solution. *Journal of colloid and interface science, 34*(1), 26–31, doi: 10.1016/0021-9797(70)90254-7.

Visvanathan, C., & Aim, R. B. (1989). Application of an Electric Field for the Reduction of Particle and Colloidal Membrane Fouling in Crossflow Microfiltration. *Separation Science and Technology, 24*(5-6), 383–398, doi: 10.1080/01496398908049776.

Wakeman, R. J. (1998). Electrically Enhanced Microfiltration of Albumin Suspensions. *Food and Bioproducts Processing, 76*(1), 53–59, doi: 10.1205/096030898531756.

Walstra, P. (1999). *Dairy Technology* : CRC Press.

Walstra, P., & Jenness, R. (1984). *Dairy chemistry and physics* (A Wiley-Interscience publication). New York: Wiley.

Wang, J., Chen, X., Reis, R., Chen, Z., Milne, N., Winther-Jensen, B., et al. (2018). Plasma Modification and Synthesis of Membrane Materials-A Mechanistic Review. *Membranes, 8*(3), doi: 10.3390/membranes8030056.

Weidemann, C., Vogt, S., & Nirschl, H. (2014). Cleaning of filter media by pulsed flow – Establishment of dimensionless operation numbers describing the cleaning result. *Journal of Food Engineering, 132*, 29–38, doi: 10.1016/j.jfoodeng.2014.02.005.

Weinberger, M. E., Andlinger, D. J., & Kulozik, U. (2021). A novel approach for characterisation of stabilising bonds in milk protein deposit layers on microfiltration membranes. *International Dairy Journal, 118*, 105044, doi: 10.1016/j.idairyj.2021.105044.

Weinberger, M. E., & Kulozik, U. (2021a). Effect of low-frequency pulsatile crossflow microfiltration on flux and protein transmission in milk protein fractionation. *Separation Science and Technology, 56*(6), 1112–1127, doi: 10.1080/01496395.2020.1749080.

Weinberger, M. E., & Kulozik, U. (2021b). On the effect of flow reversal during crossflow microfiltration of a cell and protein mixture. *Food and Bioproducts Processing, 129*, 24–33, doi: 10.1016/j.fbp.2021.07.001.

Weinberger, M. E., & Kulozik, U. (2021c). Pulsatile crossflow improves microfiltration fractionation of cells and proteins. *Journal of Membrane Science, 629*, 119295, doi: 10.1016/j.memsci.2021.119295.

Weinberger, M. E., & Kulozik, U. (2022). Understanding the fouling mitigation mechanisms of alternating crossflow during cell-protein fractionation by microfiltration. *Food and Bioproducts Processing, 131*, 136–143, doi: 10.1016/j.fbp.2021.11.003.

Wemsy Diagne, N., Rabiller-Baudry, M., & Paugam, L. (2013). On the actual cleanability of polyethersulfone membrane fouled by proteins at critical or limiting flux. *Journal of Membrane Science, 425-426*, 40–47, doi: 10.1016/j.memsci.2012.09.001.

Whitaker, R., Sherman, J. M., & Sharp, P. F. (1927). Effect of Temperature on the Viscosity Of Skimmilk. *Journal of Dairy Science, 10*(4), 361–371, doi: 10.3168/jds.S0022-0302(27)93852-1.

Wiese, M., Nir, O., Wypysek, D., Pokern, L., & Wessling, M. (2019). Fouling minimization at membranes having a 3D surface topology with microgels as soft model colloids. *Journal of Membrane Science, 569*, 7–16, doi: 10.1016/j.memsci.2018.09.058.

Wiles, P. G., Gray, I. K., & Kissling, R. C. (1998). Routine analysis of proteins by Kjeldahl and Dumas methods: review and interlaboratory study using dairy products. *Journal of AOAC International, 81*(3), 620–632.

Winzeler, H. B., & Belfort, G. (1993). Enhanced performance for pressure-driven membrane processes: the argument for fluid instabilities. *Journal of Membrane Science, 80*(1), 35–47, doi: 10.1016/0376-7388(93)85130-O.

Wu, J., Cheng, L., Li, C., Cao, R., Chen, C., Cao, M., et al. (2017). Experimental Study of Nonlinear Flow in Micropores Under Low Pressure Gradient. *Transport in Porous Media, 119*(1), 247–265, doi: 10.1007/s11242-017-0882-4.

Xu, Q., Pearce, G. K., & Field, R. W. (2017). Pressure driven inside feed (PDI) hollow fibre filtration: Optimizing the geometry and operating parameters. *Journal of Membrane Science, 537*, 323–336, doi: 10.1016/j.memsci.2017.05.010.

Yadav, K., & Morison, K. R. (2010). Effects of hypochlorite exposure on flux through polyethersulphone ultrafiltration membranes. *Food and Bioproducts Processing, 88*(4), 419–424, doi: 10.1016/j.fbp.2010.09.005.

Yamamoto, K., Kobayashi, K., Endo, K., Miyasaka, T., Mochizuki, S., Kohori, F., et al. (2005). Hollow-fiber blood-dialysis membranes: superoxide generation, permeation, and dismutation measured by chemiluminescence. *Journal of artificial organs : the official journal of the Japanese Society for Artificial Organs, 8*(4), 257–262, doi: 10.1007/s10047-005-0315-y.

Yang, J., Kjellberg, K., Jensen, B. B. B., Nordkvist, M., Gernaey, K. V., & Krühne, U. (2019). Investigation of the cleaning of egg yolk deposits from tank surfaces using continuous and pulsed flows. *Food and Bioproducts Processing, 113*, 154–167, doi: 10.1016/j.fbp.2018.10.007.

Yeo, A., & Fane, A. G. (2005). Performance of individual fibers in a submerged hollow fiber bundle. *Water science and technology : a journal of the International Association on Water Pollution Research, 51*(6-7), 165–172.

Yin, Y., Zhao, Y., Li, C., & Wang, R. (2023). Fabrication of polyamide hollow fiber nanofiltration membrane with intensified positive surface charge density via a secondary interfacial polymerization. *Journal of Membrane Science, 682*, 121778, doi: 10.1016/j.memsci.2023.121778.

Zhang, G. J., Liu, Z. Z., Song, L. F., Hu, J. Y., Ong, S. L., & Ng, W. J. (2004). One-step cleaning method for flux recovery of an ultrafiltration membrane fouled by banknote printing works wastewater. *Desalination, 170*(3), 271–280, doi: 10.1016/j.desa1.2004.02.101.

Zhao, T. S., & Cheng, P. (1996). Experimental studies on the onset of turbulence and frictional losses in an oscillatory turbulent pipe flow. *International Journal of Heat and Fluid Flow, 17*(4), 356–362, doi: 10.1016/0142-727X(95)00108-3.

Zulewska, J., & Barbano, D. M. (2013). Influence of casein on flux and passage of serum proteins during microfiltration using polymeric spiral-wound membranes at 50°C. *Journal of Dairy Science, 96*(4), 2048–2060, doi: 10.3168/jds.2012-6032.

Zydney, A. L., & Colton, C. K. (1986). A Concentration Polarisation Model for the Filtrate Flux in Cross-Flow Microfiltration of Particulate Suspensions. *Chemical Engineering Communications, 47*(1-3), 1–21, doi: 10.1080/00986448608911751.

Appendix

Peer reviewed publications (included in this thesis)

Kürzl, C., & Kulozik, U. (2023a). Alternating flow direction improves chemical cleaning efficiency in hollow fibre membranes following skim milk microfiltration. Journal of Food Engineering, 356, 111587, doi: 10.1016/j.jfoodeng.2023.111587.

Kürzl, C., & Kulozik, U. (2023b). Comparison of the efficiency of pulsed flow membrane cleaning in hollow fibre (HFM) and spiral-wound microfiltration membranes (SWM). Food and Bioproducts Processing (139), 166–177, doi: 10.1016/j.fbp.2023.03.012.

Kürzl, C., & Kulozik, U. (2023c). Influence of Pulsed and Alternating Flow on the Filtration Performance during Skim Milk Microfiltration with Flat-Sheet Membranes. Separation and Purification Technology (321), 124234, doi: 10.1016/j.seppur.2023.124234.

Kürzl, C., Hartinger, M., Ong, P., Schopf, R., Schiffer, S., & Kulozik, U. (2023). Increasing Performance of Spiral-Wound Modules (SWMs) by Improving Stability against Axial Pressure Drop and Utilising Pulsed Flow. Membranes, 13(9), 791, doi: 10.3390/membranes13090791.

Kürzl, C., Tran, T., & Kulozik, U. (2022). Application of a pulsed crossflow to improve chemical cleaning efficiency in hollow fibre membranes following skim milk microfiltration. Separation and Purification Technology (302), 122123, doi: 10.1016/j.seppur.2022.122123.

Kürzl, C., Wohlschläger, H., Schiffer, S., & Kulozik, U. (2022). Concentration, purification and quantification of milk protein residues following cleaning processes using a combination of SPE and RP-HPLC. MethodsX (9), 101695, doi: 10.1016/j.mex.2022.101695.

Non-reviewed publications

Kürzl, C. (2019). Einfluss kleinster Produktrückstände auf den Wasserflux bei der Membranfiltration. *Milchwissenschaftliche Forschung Weihenstephan, Jahresbericht 2019.*

Kürzl, C. (2020). Einfluss von Kreislauf bzw. Durchlauf von Reinigungsmitteln auf die Reinigung von Mikrofiltrationsmembranen. *Milchwissenschaftliche Forschung Weihenstephan, Jahresbericht 2020.*

Kürzl, C. (2021). Einfluss des Reinigungserfolges auf die Filtrationsperformance und mikrobielle Vorbelastung bei der Mikrofiltration von Magermilch. *Milchwissenschaftliche Forschung Weihenstephan, Jahresbericht 2021.*

Kürzl, C. (2022). Einsatz pulsierender und alternierender Strömung beim Cleaning-in-Place (CIP) von Membranen. *Milchwissenschaftliche Forschung Weihenstephan, Jahresbericht 2022.*

Oral presentations[8]

Kürzl, C. and Kulozik, U. (2021). Einsatz pulsierender Strömung für die Membranreinigung. Jahrestreffen der ProcessNet-Fachgruppe Membrantechnik, Online, February 04-05.

Kürzl, C. and Kulozik, U. (2021). Application of pulsating flow for cleaning-in-place (CIP) of membranes. Weihenstephaner Milchwirtschaftliche Herbsttagung, Freising, Germany, October 07-08.

Kürzl, C. and Kulozik, U. (2022). Mit IGF ressourceneffizient filtrieren und reinigen: Einsatz pulsierender und alternierender Strömung am Beispiel der Magermilch-Mikrofiltration (AiF 57EWN). Vortragsreihe Highlights der FEI-Gemeinschaftsforschung, Online, May 17.

Kürzl, C. and Kulozik, U. (2022). Membranreinigung mit pulsierenden Strömungen. Tagung der Arbeitskreise der technischen Sachverständigen/Amtsingenieure und der Beratungsinhenieure und Architekten für das Molkereiwesen, Wald, Germany, October 27.

Kürzl, C. and Kulozik, U. (2023). Improving the Efficiency and Sustainability of Membrane Filtration and Cleaning Processes using Pulsed Flow. 13th International Congress on Membranes and Membrane Processes, Chiba, Japan, July 9-14.

Kürzl, C. and Kulozik, U. (2023). Mikrofiltration von Milch: Reinigung von Membranen mittels pulsierender Strömung. Weihenstephaner Milchwirtschaftliche Herbsttagung, Freising, Germany, October 12-13.

[8] The presenting author is underlined

Poster presentations[9]

Kürzl, C. and Kulozik, U. (2022). Einsatz pulsierender und alternierender Strömung bei der Membranreinigung. Jahrestreffen der ProcessNet-Fachgruppe Lebensmittelverfahrenstechnik, Frankfurt, March 10-11.

Kürzl, C. and Kulozik, U. (2022). Application of a Pulsed Crossflow to improve Filtration Performance and Cleaning Efficiency in Membranes. 5th Food Structure and Functionality Symposium, Cork, September 18-21.

Kürzl, C. and Kulozik, U. (2022). Application of Alternative Flow Types to improve Filtration Performance and Cleaning Efficiency in Membranes. Weihenstephaner Milchwirtschaftliche Herbsttagung, Freising, October 13

[9] The presenting author is underlined